THESIS ON NATURAL AND EXACT SCIENCES B100

Neuronal Activity-Dependent Transcription Factors and Regulation of Human *BDNF* Gene

PRIIT PRUUNSILD

TUT PRESS

TALLINN UNIVERSITY OF TECHNOLOGY
Faculty of Science
Department of Gene Technology

Dissertation was accepted for the defence of the degree of Doctor of Philosophy in Natural and Exact Sciences on November 26, 2010.

Supervisor: **Prof. Tõnis Timmusk, PhD**

Department of Gene Technology,
Tallinn University of Technology, Estonia

Opponents: **Prof. Noel J Buckley, PhD**

Institute of Psychiatry, Centre for the Cellular Basis of Behaviour,
James Black Centre, King's College London, the United Kingdom

Senior researcher Arnold Kristjuhan, PhD

Institute of Molecular and Cell Biology,
Faculty of Science and Technology, University of Tartu, Estonia

Defence of the thesis: January 7, 2011

Declaration:
Hereby I declare that this doctoral thesis, my original investigation and achievement, submitted for the doctoral degree at Tallinn University of Technology has not been submitted for any academic degree.

/Priit Pruunsild/

This dissertation was supported by European Social Fund.

ISSN 1406-4723
ISBN 978-9949-23-047-1

LOODUS- JA TÄPPISTEADUSED B100

Närvitalitlusest sõltuvad transkriptsioonifaktorid ja inimese *BDNF* geeni avaldumise regulatsioon

PRIIT PRUUNSILD

TTÜ KIRJASTUS

CONTENTS

INTRODUCTION

The fate and shape of neurons is to a great extent regulated by the nerve growth factor family of neurotrophins that have trophic effects on certain subpopulations of neurons during development. One of the neurotrophins, brain-derived neurotrophic factor (BDNF), has been found to have fundamental roles also in adult brain physiology in regulating synaptic transmission and plasticity. Accordingly, *BDNF* has widespread expression in the mammalian nervous system and its mRNA and protein levels rise dramatically in postnatal development. An important driving force of postnatal brain development is sensory experience, i.e. neuronal activity, which mediates fine-tuning of adaptive functions of the brain, for example learning and memory, through structural and functional refinement of neuronal circuits. Neuronal activity-responsive transcription is a significant component in these processes and recent studies have established that approximately 300 genes are activity-regulated in neurons. *BDNF* is one of them and activity-dependent transcription of *BDNF* has been shown to be essential for the development of proper cortical inhibitory network. Therefore, signaling between the synapse and the nucleus of a neuron, exemplified by coupling of neuronal activity and transcription, is fundamental in BDNF biology. Although a lot of studies have been conducted on the synaptic activity-dependent regulation of *BDNF* transcription in rodents, less is known about human *BDNF* regulation. Knowledge about human *BDNF* regulation would be of great importance however, since dysregulation of *BDNF* expression has been associated with a number of neuropsychiatric disorders. In addition, several protein families besides the conventional neuronal activity-regulated transcription factors have been recently implicated in activity-dependent transcription, but their role in *BDNF* expression has not been reported.

OUTLINE OF THE THESIS

In the first part of the thesis I will review the literature about the functions of BDNF in the nervous system. Then, I will focus more specifically on the neuronal activity-mediated roles of BDNF that will be followed by summary of the regulation of rodent *BDNF* transcription by neuronal activity. Lastly, an overview of Ca^{2+}-dependent transcription factors is given.

In the second part I will present the results of the research that was undertaken to complete the thesis. First, the structures, alternative splicing and expression of the human and mouse Ca^{2+}-regulated transcription factor *KCNIP* and *NFAT* gene families are described (Publications I and III). Second, the structure, splicing and expression of the human *BDNF* gene is characterized (Publication II). Third, the *cis*-elements and transcription factors involved in human *BDNF* transcriptional activation by neuronal activity are described (Publication IV and manuscript). And last, the results of the analyses of KCNIP and NFAT factors in Ca^{2+}-regulated transcription of *BDNF* are presented (Publication V and manuscript).

ORIGINAL PUBLICATIONS

I Pruunsild P, Timmusk T. (2005)
Structure, alternative splicing, and expression of the human and mouse *KCNIP* gene family.
Genomics, Nov;86(5):581-93

II Pruunsild P*, Kazantseva A*, Aid T, Palm K, Timmusk T. (2007)
Dissecting the human *BDNF* locus: bidirectional transcription, complex splicing, and multiple promoters.
Genomics, Sep;90(3):397-406

III Vihma H*, **Pruunsild P***, Timmusk T. (2008)
Alternative splicing and expression of human and mouse *NFAT* genes.
Genomics, Nov;92(5):279-91

IV Koppel I, Aid-Pavlidis T, Jaanson K, Sepp M, **Pruunsild P**[#], Palm K, Timmusk T. (2009)
Tissue-specific and neural activity-regulated expression of human *BDNF* gene in BAC transgenic mice.
BMC Neurosci. 2009 Jun 25;10:68

V Vashishta A, Habas A, **Pruunsild P**[#], Zheng JJ, Timmusk T, Hetman M. (2009)
Nuclear factor of activated T-cells isoform c4 (NFATc4/NFAT3) as a mediator of antiapoptotic transcription in NMDA receptor-stimulated cortical neurons.
J Neurosci. 2009 Dec 2;29(48):15331-40

MANUSCRIPT

Pruunsild P, Sepp M, Orav E, Koppel I, Timmusk T.
Identification of *cis*-elements and transcription factors regulating neuronal activity-dependent transcription of human *BDNF* gene

*equal contribution
[#] partial involvement

ABBREVIATIONS

AMPA α-amino-3-hydroxyl-5-methyl-4-isoxazole-propionate
antiBDNF antisense *BDNF* gene/transcript
AP1 activator protein 1
ARNT aryl hydrocarbon receptor nuclear translocator
ATF activating transcription factor
BAC bacterial artificial chromosome
BDNF brain derived neurotrophic factor
bHLH basic helix-loop-helix
BRG1 brahma-related gene 1
bZip basic leucine zipper
CA hippocampal subfield *cornu ammonis*
CAT chloramphenicol acetyltransferase
CaMK Ca^{2+}/calmodulin-dependent protein kinase
cAMP cyclic adenosine monophosphate
CaRE Ca^{2+} response element
CaRF Ca^{2+} response factor
CBP CREB binding protein
CCAT Ca^{2+} channel associated transcription regulator
cDNA complementary DNA
C/EBPβ CCAAT/enhancer-binding protein beta
ChIP chromatin immunoprecipitation
CpG cytosine-phosphate-guanine
CRE cAMP/Ca^{2+}-response element
CREB cAMP/Ca^{2+}-response element binding protein
CREST Ca^{2+}-responsive transactivator
CNS central nervous system
delTAD deletion of TAD
DIV days *in vitro*
DNA deoxyribonucleic acid
DRE downstream regulatory element
DREAM downstream regulatory element antagonist modulator
EMSA electrophoretic mobility shift assay
ER endoplasmatic reticulum
EGR early growth response
ERK extracellular signal regulated kinase
GABA gamma-aminobutyric acid
Gadd45 growth arrest and DNA damage-inducible 45
GFP green fluorescent protein
hBDNF human BDNF
HD Huntington's disease
HDAC histone deacetylase
IP_3 inositol trisphosphate

JNK Jun N-terminal kinase
kDa kilodalton
KA kainic acid
KChIP potassium channel interacting protein
KCNIP potassium channel interacting protein
LIM Lin11-Isl1-Mec3 domain
L-LTP late-phase LTP
LTD long term depression
LTP long term potentiation
MADS MCM1-AGAMOUS-DEFICIENS-SRF domain
MAPK mitogen activated protein kinase
mBDNF mouse BDNF
MeCP methyl CpG binding protein
MEF myocyte-specific enhancer factor
Met methionine
mRNA messenger RNA
NFAT nuclear factor of activated T-cells
NFATc cytoplasmic NFAT
NFkB nuclear factor kappa B
NGF nerve growth factor
NMDA N-methyl-D-aspartic acid
NPAS neuronal PAS domain protein
NRSE neuron-restrictive silencer element
NRSF neuron-restrictive silencing factor
NTR neurotrophin receptor
p promoter
PAS Per-Arnt-Sim domain
PasRE bHLH-PAS factor response element
PC prohormone convertase
PCR polymerase chain reaction
PI3K phosphatidylinositol-3-kinase
PK protein kinase
PLCγ1 phospholipase Cγ1
PNS peripheral nervous system
RACE rapid amplification of cDNA ends
rBDNF rat BDNF
RHD Rel homology domain
rodBDNF rodent BDNF
RNA ribonucleic acid
RSK ribosomal s6 kinase
RT-qPCR quantitative real-time RT-PCR
RT-PCR reverse transcriptase PCR
Ser serine
shRNA short hairpin RNA

SNP single nucleotide polymorphism
SRE serum response element
SRF serum response factor
SVZ subventricular zone
TAD transcription activation domain
TCF ternary complex factor
TGN trans-Golgi network
trkB tropomyosin-related kinase receptor B
UBE USF binding element
USF upstream stimulatory factor
UTR untranslated region
VGCC voltage-gated Ca^{2+} channel
WT wild type

1. Introduction to BDNF biology

Brain-derived neurotrophic factor (BDNF, Barde et al., 1982) belongs to the nerve growth factor (NGF) family of structurally related molecules named neurotrophins. Other members of the neurotrophin family in mammals include the founding member NGF (Levi-Montalcini and Hamburger, 1951), neurotrophin-3 (NT-3, Maisonpierre et al., 1990) and neurotrophin-4/5 (NT-4/5, Hallbook et al., 1991). Each neurotrophin possesses a distinct profile of growth-promoting and survival effects on subpopulations of neurons in the central and peripheral nervous systems (CNS and PNS; Bibel and Barde, 2000). During development, BDNF supports the survival and differentiation of selected neuronal populations, participates in axonal growth and pathfinding and modulates dendritic growth and morphology (Binder and Scharfman, 2004). In adult, BDNF is one of the major regulators of activity-dependent neurotransmission and plasticity (Poo, 2001).

1.1 Structure and expression of *BDNF* gene

The structure of the *BDNF* gene has been thoroughly studied in rodents (Timmusk et al., 1993; Liu et al., 2006; Aid et al., 2007). The rat *BDNF* gene was first described to have four promoters driving expression of transcripts containing different 5' exons (Timmusk et al., 1993). Recently the mouse and rat *BDNF* (m*BDNF* and r*BDNF*) gene structures were updated, however. A number of newly discovered exons were described and altogether the rodent *BDNF* (rod*BDNF*) genes were shown to have nine separate promoters upstream of eight untranslated 5' exons and a 3' exon that encodes the mature BDNF protein (Aid et al., 2007). The *BDNF* gene is localized to chromosome 2 or 3 in mouse or rat, respectively (Maisonpierre et al., 1991; Liu et al., 2006). The human *BDNF* (h*BDNF*) has also been shown to consist of multiple 5′ non-coding exons and one coding exon, which give rise to alternatively spliced transcripts (Aoyama et al., 2001; Fang et al., 2003; Liu et al., 2005; Fig. 1). The human *BDNF* gene has been described to have seven non-coding exons and one coding exon (Liu et al., 2005) and is localized to chromosome 11 (Maisonpierre et al., 1991).

In mammals, *BDNF* has widespread expression with significant postnatal rise in mRNA and protein levels (Maisonpierre et al., 1990; Maisonpierre et al., 1991; Conner et al., 1997; Katoh-Semba et al., 1997). During development, *BDNF* expression is more abundant in the nervous system compared to other tissues and its levels are dramatically increased in the brain postnatally (Katoh-Semba et al., 1997). In the adult nervous system, *BDNF* displays a wide distribution pattern, with the highest levels of mRNA and protein in the hippocampus, amygdala, cerebral cortex, and hypothalamus. *BDNF* mRNA expression is mostly confined to neurons and there are only a few brain areas where *BDNF* transcripts are not

detected (Ernfors et al., 1990; Hofer et al., 1990; Phillips et al., 1990; Timmusk et al., 1994a; Conner et al., 1997; Katoh-Semba et al., 1997; Webster et al., 2006). *BDNF* expression in adult tissues is detectable also outside of the CNS. Lower *BDNF* mRNA levels than in the hippocampus have been detected in the thymus, liver, spleen, heart, and lung (Ernfors et al., 1990; Maisonpierre et al., 1990; Maisonpierre et al., 1991; Yamamoto et al., 1996; Katoh-Semba et al., 1997).

1.2 BDNF synthesis, release and signaling

As described above, each promoter of the *BDNF* gene drives transcription of mRNAs with different untranslated 5' exons (Timmusk et al., 1993; Liu et al., 2006; Aid et al., 2007; Fig. 1). In addition, *BDNF* mRNAs are polyadenylated at one of the two alternative polyadenylation sites in its 3' untranslated region (UTR) leading to distinct populations of *BDNF* mRNAs with either short 3' UTR or with long 3' UTR (Timmusk et al., 1993). It has been shown that the short 3' UTR mRNAs of *BDNF* are restricted to soma, but the long 3' UTR *BDNF* mRNAs are in addition localized into dendrites of neurons (An et al., 2008). Therefore, translation of BDNF protein takes place in the cell soma, but is possible also in dendrites (Lessmann et al., 2003; An et al., 2008).

BDNF protein is initially produced as a precursor protein (pre-proBDNF) with a signal peptide (pre-region), a pro-region that contains an N-linked glycosylation site and a pair of basic amino acids recognized by processing enzymes (Chao and Bothwell, 2002; Fig. 1). The signal peptide directs sequestration of the newly formed BDNF polypeptide into the endoplasmatic reticulum (ER) where the pre-region is cleaved by signal peptidase to form proBDNF (32 kDa; Halban and Irminger, 1994). Then, homodimerization of proBDNF peptides occurs and two alternative routes of processing could be used: a) proBDNF enters the constitutive secretory pathway and is cleaved by furin or furin-like endoproteases to produce mature BDNF (14 kDa) in the trans-Golgi network (TGN); or b) proBDNF enters the regulated secretory pathway where it is either cleaved by prohormone convertase PC1 or PC2 in immature secretory vesicles after budding from the TGN to produce mature BDNF, or not cleaved and stored for secretion as proBDNF (Seidah et al., 1996; Mowla et al., 1999; Mowla et al., 2001). It has been shown that in cells that have both the constitutive and regulated secretory pathway, for example in neurons, the majority of proBDNF avoids furin cleavage and is sorted into the regulated secretory pathway (Mowla et al., 1999). This is mediated by interaction of the pro-domain with sortilin and is dependent on a specific sorting motif in the mature BDNF domain that interacts with carboxypeptidase E and directs proBDNF into the regulated pathway vesicles (Chen et al., 2005b; Lou et al., 2005).

BDNF protein within the CNS neurons is stored in vesicles in the soma as well as in neuronal processes and anterograde transport along both axons and dendrites has been reported (Fawcett et al., 1998; Hartmann et al., 2001; Lessmann et al., 2003). For example, axonal transport of BDNF to presynaptic terminals of striatal

afferents in cortical neurons (Altar et al., 1997) and dendritic transport of BDNF to postsynaptic structures in hippocampal neurons has been demonstrated (Hartmann et al., 2001). In accordance to the localization of BDNF containing vesicles in dendrites and axons, both pre- and postsynaptic secretion of BDNF is possible (Hartmann et al., 2001; Kohara et al., 2001). Diffusion of secretory vesicles towards the plasma membrane and exocytosis of BDNF is considered to be relatively slow compared to the extremely fast fusion of neurotransmitter-containing vesicles with the plasma membrane, although both processes are critically dependent on neuronal activity and Ca^{2+} influx (Lessmann et al., 2003). At first it was reported that BDNF release is dependent on intracellular Ca^{2+} stores and extracellular Ca^{2+} is dispensable (Griesbeck et al., 1999). However, postsynaptic BDNF release in glutamatergic synapses needs extracellular Ca^{2+} influx because it has been shown to be dependent on AMPA and NMDA type of glutamate receptors and could be mediated also by direct activation of postsynaptic voltage-gated Ca^{2+} channels (VGCC) (Hartmann et al., 2001). Nevertheless, neuronal activity is needed also for presynaptic BDNF exocytosis (Kohara et al., 2001) and Ca^{2+}-induced Ca^{2+} release and inositol trisphosphate (IP_3)-mediated Ca^{2+} release from ER are involved in BDNF secretion (Griesbeck et al., 1999; Canossa et al., 2001; Balkowiec and Katz, 2002).

BDNF is secreted in two forms from cultured cells – as mature BDNF or as proBDNF that has retained the pro-region (Mowla et al., 1999; Mowla et al., 2001; Egan et al., 2003). Distinct functions for mature and proBDNF have been demonstrated, indicating that both the mature and the pro-form of BDNF could be physiologically significant (Lee et al., 2001; Teng et al., 2005). However, proBDNF functions could be limited since it is cleaved by the extracellular protease plasmin or matrix metalloproteinases after exotcytosis to produce mature BDNF (Pang et al., 2004). Moreover, recently two studies have reported contradictory results on proBDNF secretion from cells *in vivo* in the CNS, leaving open the question whether *in vivo* only mature BDNF or both, mature and proBDNF, are physiologically relevant (Matsumoto et al., 2008; Yang et al., 2009).

BDNF binds with high affinity to the tropomyosin-related kinase receptor trkB that is a member of the receptor tyrosine kinase family. In addition, all neurotrophins, including BDNF, bind with low affinity to the neurotrophin receptor p75NTR that belongs to the tumor necrosis factor superfamily (Meakin and Shooter, 1992). BDNF binding to the trkB receptor results in receptor dimerization and kinase activation that promotes signaling by creating phosphorylated docking sites for adaptor proteins that couple the receptor to the mitogen activated protein kinase (MAPK)/extracellular signal regulated kinase (ERK) pathway, the phosphatidylinositol-3-kinase (PI3K)/Akt kinase pathway and phospholipase Cγ1 (PLCγ1) activity. The consequences of these pathways in brief are: a) MAPK/ERK initiated signaling regulates neuronal differentiation; b) PI3K/Akt initiated pathways differ between neuronal subpopulations, but in general, result in promotion of cell survival; and c) PLCγ1 activation leads to release of Ca^{2+} from the ER and consequently modulates many functions related to neuronal activity

(Patapoutian and Reichardt, 2001). Responsiveness of the full length trkB receptor to BDNF could be inhibited by naturally occurring truncated trkB isoforms trkBT1 and trkBT2 that lack the kinase domain (Eide et al., 1996; Fryer et al., 1997). Furthermore, a recent study has added complexity to the regulation of BDNF signaling by demonstrating that 36 different receptor isoforms could be synthesized from the human *trkB* gene (Luberg et al., 2010).

p75NTR receptor elicits biologic actions distinct from those of the trk receptors and most notably, neurotrophin binding to p75NTR has been found to induce apoptosis through recruitment of several cytoplasmatic interactors that activate Jun N-terminal kinase (JNK), p53 and proteases of the caspase family (Dechant and Barde, 2002). Interestingly, whereas mature BDNF induces trkB phosphorylation, proBDNF does not. Instead, proBDNF binds preferably p75NTR and its coreceptor sortilin and initiates signaling events that lead to cell death (Teng et al., 2005).

Trk-signaling is activated locally within distal neuronal processes, but includes also retrograde transport of intact neurotrophin-trk complexes to the neuronal cell body (DiStefano et al., 1992; Ginty and Segal, 2002). For BDNF it has been shown that both trkB and also p75NTR can mediate this retrograde transport (von Bartheld et al., 1996). The BDNF-trkB complexes have been shown to be moved from neurites to the cell body by dynein motor machinery mediated vesicular trafficking (Watson et al., 1999; Yano et al., 2001).

1.3 Functions of BDNF signaling

BDNF signaling has central roles in brain development and physiology in mammals and consequently it influences cognitive functions and behavior. BDNF was first described to support survival of embryonic sensory neurons (Barde et al., 1982). Accordingly, studies using *BDNF* knock-out mice showed that during development BDNF is dispensable for motor neurons, but is required for survival of certain sensory neuron populations in the PNS (Ernfors et al., 1994; Jones et al., 1994). The fact that most homozygote *BDNF* mutants died within two days after birth underscores the importance of BDNF signaling. However, it also restricts the possibilities to study the roles of BDNF in the adult CNS *in vivo*. Thus, hints about BDNF functions in the adult brain came from studies with cultured CNS neurons and hippocampal slices demonstrating that BDNF is a neuronal activity-dependent survival factor for cortical neurons (Ghosh et al., 1994) and is required for normal synaptic activity in the hippocampus, including long term potentiation (LTP), which is an established cellular model for learning and memory (Kang and Schuman, 1995; Patterson et al., 1996). Shortly afterwards, first roles for BDNF in the CNS *in vivo* were revealed though, when it was demonstrated that BDNF is involved in neural network patterning by regulating survival and differentiation of CNS neurons during postnatal development (Schwartz et al., 1997; Schwartz et al., 1998). Since then, a lot of research has been concentrating on the molecular mechanisms related to neuronal activity-dependent and BDNF-regulated synaptic plasticity in the CNS. These functions are more specifically discussed in the next

section of the thesis. Here, in the following paragraphs, I shall rather give a general overview of the pleiotropic roles of BDNF signaling.

As mentioned, the predominant function of BDNF by signaling through trkB is supporting the survival of subpopulations of sensory neurons in the PNS and hippocampal and cortical neurons in the CNS (Barde et al., 1982; Ernfors et al., 1994; Jones et al., 1994; Minichiello and Klein, 1996; Schwartz et al., 1997). On the other hand, induction of apoptosis through BDNF binding to p75NTR has also been demonstrated to be essential: BDNF signaling via p75NTR regulates death of certain sympathetic neurons in the PNS during development (Bamji et al., 1998).

In addition to regulating survival, BDNF controls growth and differentiation of neurons. Growth of peripheral nerves *in vivo* is partly dependent on BDNF (Tucker et al., 2001). However, other neurotrophins are involved in this function and the precise role of BDNF remains to be elucidated. In the CNS, both regulation of axonal elaboration (Cabelli et al., 1995; Cohen-Cory and Fraser, 1995) and dendritic growth are dynamically regulated by BDNF (McAllister et al., 1997). Recently it was shown that BDNF promotes the postnatal growth of striatal neurons and their dendrites in particular (Rauskolb et al., 2010).

BDNF could be involved also in potentiating neurogenesis in the adult subventricular zone (SVZ) since intraventricular infusion or virus-mediated overexpression of BDNF in the adult rat brain increases neurogenesis (Zigova et al., 1998; Benraiss et al., 2001). Moreover, endogenous BDNF-producing endothelial cells have been suggested to supply the support for newly generated neurons in the SVZ (Leventhal et al., 1999).

Concurrently with acting at cellular level, BDNF has systemic roles in the brain that influence behavioral and cognitive functions. BDNF is involved in development and function of the serotonergic system in the adult CNS and therefore, is important for regulation of mood and food intake. Heterozygous *BDNF* knock-out mice have behavioral characteristics linked to dysfunction of serotonin pathways such as aggressiveness and hyperphagia (Lyons et al., 1999; Kernie et al., 2000). Conditional deletion of the *BDNF* gene in postnatal brain leads to hyperactivity, anxiety and obesity (Rios et al., 2001). And furthermore, a single nucleotide polymorphism (SNP) in the h*BDNF* gene, substituting the amino acid valine at position 66 in BDNF to methionine (66Met), may be a risk factor for eating and anxiety disorders, major depression and bipolar disorder (Ribases et al., 2003; Jiang et al., 2005; McIntosh et al., 2007; Soliman et al., 2010). However, association between the 66Met allele and susceptibility to these complex disorders has been questioned and could be influenced by haplotype, ethnicity and gender (Nakata et al., 2003; Petryshen et al., 2010; Verhagen et al., 2010).

BDNF has a role also in the dopaminergic system as BDNF-trkB signaling has been implicated in addictive behavior upon cocaine use. During cocaine use BDNF expression and release is induced in nucleus accumbens neurons (Graham et al., 2007) and after cocaine withdrawal, BDNF expression levels rise in the ventral tegmental area (Pu et al., 2006). It has been suggested that elevated BDNF levels elicit drug craving by potentiating synapses in the mesolimbic dopamine pathway

for cue-associated activity (Pu et al., 2006; Graham et al., 2007). Essential role for BDNF in dopamine signaling has been demonstrated also in aversive social experience-dependent stress (Berton et al., 2006).

Normal BDNF expression and signaling through trkB are required for learning and memory because: a) heterozygous *BDNF* knock-out mice have learning deficits (Linnarsson et al., 1997), b) mice lacking postnatal forebrain-specific trkB have deficient LTP at hippocampal synapses (Minichiello et al., 1999), and c) there is a rapid and selective induction of *BDNF* expression during hippocampus-dependent contextual learning in rats (Hall et al., 2000).

Also, BDNF signaling has been associated with neuropathic pain (Coull et al., 2005) and behavioral responses to nociceptive pain (Kerr et al., 1999; Pezet et al., 2002).

BDNF dysregulation has been implicated in neurodegenerative diseases and correspondingly, reductions in BDNF levels in the hippocampus, substantia nigra and striatum in Alzheimer's, Parkinson's and Huntington's disease (HD), respectively, have been documented (Phillips et al., 1991; Howells et al., 2000; Zuccato et al., 2001). Of these diseases, the most compelling link with BDNF has been proposed for HD. It has been shown that mutant huntingtin causes a neuron-restrictive silencing factor (NRSF)-dependent decrease in *BDNF* gene transcription (Zuccato et al., 2003) and a deficit in BDNF protein vesicular transport (Gauthier et al., 2004), which lead to loss of trophic support for striatal neurons that die in Huntington's disease. Even so, the role of decreased BDNF levels in the progression of HD is likely a part of a bigger functional impact of NSRF dysregulation because expression of many NRSF target genes has been found to be affected in HD (Zuccato et al., 2007; Buckley et al., 2010).

And lastly, seizure-induced increase in hippocampal BDNF levels has been proposed to have a central role in epilepsy (Gall et al., 1991; Jankowsky and Patterson, 2001). In agreement with results in rodents (Isackson et al., 1991), epileptic activity-dependent increase in BDNF levels has been described in humans (Takahashi et al., 1999).

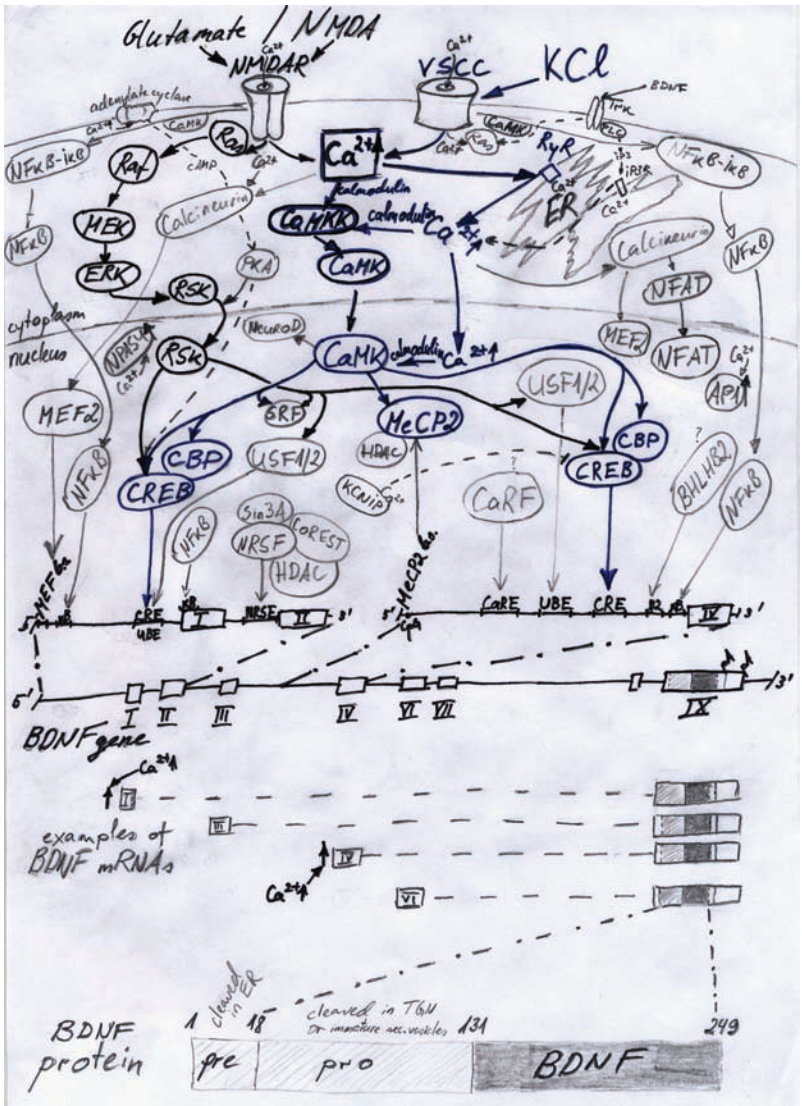

Figure 1. Genomic structure of the human *BDNF* gene and signal transduction networks mediating neuronal activity-dependent *BDNF* expression. Neuronal activity elicits Ca^{2+} influx through neurotransmitter receptors or voltage-gated Ca^{2+} channels and leads to activation of Ca^{2+} -regulated signaling pathways. These pathways converge on transcription factor proteins in the nucleus and lead to their activation through posttranslational modifications or regulate transcription factors in the cytoplasm thereby controlling their nuclear translocation. In addition, neuronal activity up-regulates several genes that encode transcription factors, which in turn promote transcription. The main signaling route that impacts neuronal activity-dependent *BDNF* transcription is colored dark blue. *BDNF* exons are shown as boxes and their numbers are indicated by roman numerals; introns are shown as lines. Open boxes represent untranslated exons, filled boxes correspond to the sequences coding for BDNF protein. Promoter regions with *cis*-regulatory elements described for the rodent *BDNF* are magnified. Only some examples of mRNAs transcribed from the *BDNF* gene are shown. The pre-pro sequence and mature *BDNF* are depicted as light and dark gray, respectively. For details, see text.

2. Neuronal activity and BDNF

2.1 Neuronal activity-dependent function of BDNF

The major role of BDNF in neuronal activity-dependent functions is to adjust and transform synaptic connections in the brain and thereby regulate adaptive responses critical for brain development and cognition. This conclusion has been drawn from a large body of research including the following. In brief, BDNF was proposed to have a role in activity-dependent modulation of synaptic connections in the visual cortex (Castren et al., 1992) and was shown to regulate the function of developing synapses (Lohof et al., 1993). Then, BDNF was demonstrated to elicit LTP in the adult hippocampus (Kang and Schuman, 1995) and it was postulated that BDNF regulates synaptic efficacy (Thoenen, 1995). Moreover, it has been demonstrated that BDNF is required for normal synaptic activity in the hippocampus (Korte et al., 1996; Patterson et al., 1996) and that both LTP and long term depression (LTD) are coupled to corresponding changes in synaptic secretion of BDNF (Aicardi et al., 2004). Therefore, by now, with a myriad of results also from other studies, it is well accepted that BDNF signaling regulates neuronal activity-dependent synaptic plasticity (Schinder and Poo, 2000; Poo, 2001; Lu, 2003; Bramham and Messaoudi, 2005).

Developing visual cortex has been a good model for studying activity-dependent functions of BDNF. Based on the knowledge that visual deprivation during the critical period of visual cortex development affects segregation of synaptic connections and the finding that *BDNF* mRNA levels are rapidly regulated by sensory input in the visual cortex, BDNF was suggested to play a role in neuronal activity-dependent refinement of synaptic connections (Castren et al., 1992). By now it has been shown that activity-dependent control of axonal branching and growth, remodeling of synaptic connections (Cabelli et al., 1995; Cabelli et al., 1997) and, eventually, maturation of cortical inhibition in the visual cortex during the critical period of development, is regulated by BDNF (Huang et al., 1999a). These findings have led to the understanding that BDNF acts as a synaptic morphogen that regulates the formation and structural modification of synaptic contacts in an activity-dependent manner (Poo, 2001).

Additionally, BDNF-trkB signaling is required for sufficient postsynaptic stimulation to enhance synaptic activity to a long-lasting form (Korte et al., 1996; Patterson et al., 1996). *BDNF* knock-out mouse hippocampal synapses fail to exhibit late-phase LTP (L-LTP) that requires synthesis of new proteins (Korte et al., 1998). Moreover, homozygous *trkB* mutants show impaired LTP (Minichiello et al., 1999) and treatment of hippocampal slices from wild-type mice with trkB antibodies prevents L-LTP in particular (Korte et al., 1998). The understanding that BDNF is not a housekeeping factor, but regulates synaptic function, is supported also by the finding that *BDNF* expression in the hippocampus is selectively elevated during contextual learning in rats (Hall et al., 2000).

The primary role for BDNF in synapse development and induction of LTP was first described to be enhancement of presynaptic transmitter release by presynaptic trkB signaling (Lohof et al., 1993; Stoop and Poo, 1996; Li et al., 1998). More specifically, trkB signaling was suggested to be involved in mobilizing and docking of synaptic neurotransmitter containing vesicles to presynaptic active zones since *BDNF* knock-out mouse hippocampal synaptosomes contain significantly lower levels of synaptophysin and synaptobrevin than the wild type mouse synaptosomes (Pozzo-Miller et al., 1999). Consequently, it was postulated that potentiation of synapses by BDNF occurs presynaptically (Schinder and Poo, 2000). Intriguingly however, another mechanism how BDNF-trkB signaling leads to functional synaptic modification has been suggested by studies showing that BDNF itself acts as a potent endogenous excitatory molecule in the mammalian CNS by inducing neuronal depolarization through trkB-mediated sodium channel activation (Kafitz et al., 1999; Blum et al., 2002). In the light of this finding, it is noteworthy that BDNF-dependent and sodium channel coupled LTP has been shown to be induced exclusively by postsynaptic trkB signaling within dendritic spines of hippocampal synapses and is generated only when paired with afferent neuronal activity (Kovalchuk et al., 2002). It can be concluded that according to this latter model, BDNF signaling enhances synaptic connections postsynaptically upon sufficient presynaptic input. This could be a widespread means of action since BDNF-induced neuronal excitation has been found in many types of neurons in the CNS (Kafitz et al., 1999; Blum et al., 2002). Regardless of the mechanism, whether BDNF is released pre- or postsynaptically, or both, is not clear (Hartmann et al., 2001; Kohara et al., 2001; Bramham and Messaoudi, 2005). Furthermore, synapse activity regulation by BDNF could be even more complex as secretion of BDNF is not only regulated by excitatory stimuli, but also by autocrine or paracrine trkB activation (Canossa et al., 2001; Balkowiec and Katz, 2002) and BDNF could be re-secreted after endocytosis by either the secreting cell itself or the target cell (Lessmann et al., 2003).

Regulation of synaptic plasticity by BDNF is tightly controlled by neuronal activity. As discussed above, neuronal activity is required for BDNF secretion (Griesbeck et al., 1999; Hartmann et al., 2001; Balkowiec and Katz, 2002). The fact that the 66Met containing hBDNF activity-dependent secretion is reduced and as a result affects human memory, emphasizes the importance of secretion regulation (Egan et al., 2003). In addition, neuronal activity facilitates movement of trkB receptors to the cell surface enhancing responsiveness of neurons to BDNF (Meyer-Franke et al., 1998; Du et al., 2000).

BDNF-dependent LTP has been shown to include local protein synthesis at synapses (Kang and Schuman, 1996). The mRNAs that are translated at synapses comprise also *BDNF* and *trkB* transcripts. Thus, regulation of BDNF signaling occurs also at mRNA level. Both *BDNF* and *trkB* mRNAs are targeted to dendrites in a neuronal activity-dependent manner and are translated in dendrites in response to activity (Tongiorgi et al., 1997). Furthermore, *BDNF* as well as *trkB* mRNA localization into dendrites is under the control of BDNF-trkB singaling (Righi et

al., 2000). Both 5' and 3' UTRs of *BDNF* mRNAs have been shown to regulate trafficking of *BDNF* transcripts into dendrites or retention into the cell soma (An et al., 2008; Chiaruttini et al., 2008). Exon VI and exon II containing *BDNF* mRNAs have been found to localize more to dendrites upon neuronal activity whereas exon I and IV transcripts exhibit somatic localization (Chiaruttini et al., 2008). The short 3' UTR mRNAs of *BDNF* are restricted to soma, but the long 3' UTR mRNAs are in addition localized into dendrites (An et al., 2008). Also, the Val66Met SNP site in the BDNF pro-region coding mRNA sequence has been implicated in dendritic trafficking of *BDNF* mRNA and therefore, impaired subcellular localization of the 66Met variant *BDNF* mRNAs has been linked to the pathophysiology of neuropsychiatric disorders associated with the 66Met allele (Chiaruttini et al., 2009). Recently it was demonstrated that the *BDNF* long 3' UTR mRNAs, which are localized into dendrites, undergo neuronal activity-dependent translation that contributes to trkB activation *in vivo*, suggesting a molecular mechanism for achieving local regulation of activity-induced BDNF-dependent synaptic plasticity (Lau et al., 2010).

2.2 Regulation of *BDNF* transcription

Regulation of *BDNF* transcription is a major contributor to the functions described above. The level of *BDNF* mRNA increases markedly in response to neuronal activity and transcriptional regulation of *BDNF* has been used as a model for neuronal activity-responsive gene expression (Greer and Greenberg, 2008). Therefore, regulation of rodent *BDNF* transcription has been relatively well characterized.

Various stimuli regulate *BDNF* expression levels in neurons. Kainic acid (KA) treatment (Zafra et al., 1990), electrical stimulation resulting in epileptogenesis (Ernfors et al., 1991), lesion-induced recurrent limbic seizures (Isackson et al., 1991), electrical stimulation inducing LTP (Patterson et al., 1992; Castren et al., 1993), ischemic and hypoglycemic insults (Lindvall et al., 1992), application of KCl to the cortical surface (Kokaia et al., 1993), exposure to light as sensory input (Castren et al., 1992), mechanical stimulation of mystacial whiskers (Rocamora et al., 1996), BDNF-trkB signaling (Yasuda et al., 2007), enriched environment (Falkenberg et al., 1992; Young et al., 1999) and physical activity (Neeper et al., 1996) all increase neuronal activity in the brain and have been shown to induce *BDNF* mRNA expression. On the other hand, treatments or conditions that reduce neuronal activity, for example inhibition of neuronal activity by gamma-aminobutyric acid (GABA) (Berninger et al., 1995), monocular deprivation (Bozzi et al., 1995), immobilization stress (Smith et al., 1995) and Alzheimer's disease (Phillips et al., 1991), have been demonstrated to decrease *BDNF* mRNA levels. Furthermore, expression of *BDNF* undergoes circadian oscillation, mirroring variations in physiological activity (Bova et al., 1998).

The molecular dissection of rod*BDNF* transcription regulation started with the study describing the gene structure of the rat *BDNF* gene, showing that alternative

usage of promoters enables exon- and tissue-specific and seizure-induced regulation of *BDNF* expression (Timmusk et al., 1993). Then it was shown that the *BDNF* promoters are differentially regulated by activation of different subtypes of glutamate receptors (Metsis et al., 1993). Also, activation of VGCCs was found to be necessary for neuronal activity-dependent *BDNF* expression in cortical neurons, indicating that Ca^{2+} influx is crucial for induction of *BDNF* transcription (Ghosh et al., 1994).

The first *cis*-elements and transcription factors regulating *BDNF* neuronal activity-dependent transcription were identified for *BDNF* promoter IV (pIV). Activity-induced Ca^{2+} influx and activation of Ca^{2+}/calmodulin-dependent protein kinase (CaMK) IV was shown to result in cAMP/Ca^{2+}-response element binding protein CREB-dependent up-regulation of *BDNF* exon IV transcription via CREB binding to a cAMP/Ca^{2+}-response element (CRE) in *BDNF* promoter IV (Shieh et al., 1998; Tao et al., 1998; Fig. 1). Ca^{2+} response factor (CaRF) binding to a CaRE element in promoter IV was suggested to assure Ca^{2+} influx signal specificity to the induction and to be responsible for the specific activation of this promoter in neurons (Tao et al., 2002; Fig. 1). Also, upstream stimulatory factors (USFs) binding to an E-box element (USF binding element, UBE) in promoter IV (Chen et al., 2003a) and methyl CpG binding protein (MeCP) 2 binding to specific methylated CpG-s in *BDNF* promoter IV, were shown to be involved in the up-regulation (Chen et al., 2003b; Martinowich et al., 2003; Fig. 1). Additionally, basic helix-loop-helix protein B2 (BHLHB2) and nuclear factor kappa B (NFkB) have been shown to modulate promoter IV neuronal activity-dependent regulation by binding the respective *cis*-elements in pIV (Jiang et al., 2008; Fig. 1).

Transcription of the rodent *BDNF* exon I is also induced by neuronal activity (Timmusk et al., 1993). CREB and USF-s contribute to the Ca^{2+}-mediated activation of *BDNF* promoter I by binding overlapping CRE and UBE elements, respectively (Tabuchi et al., 2002; Fig. 1). Also, NFkB, through binding two pairs of NFkB response elements in *BDNF* promoter I region (Lubin et al., 2007; Fig. 1), and myocyte-specific enhancer factor (MEF) 2D, via binding a distally located enhancer element (Flavell et al., 2008; Fig. 1), have been implicated in mediating the neuronal activity-dependent induction of *BDNF* exon I transcription. Indirect evidence suggests that MEF2D could regulate also *BDNF* pIV (Hong et al., 2008) and neuronal PAS domain protein 4 (NPAS4) could regulate *BDNF* promoter I and IV (Lin et al., 2008), because both of the proteins have been shown to bind promoter I and IV regions of mouse *BDNF*. However, the binding site of MEF2D in pIV and the binding sites of NPAS4 in promoters I and IV were not specified and their contribution to the induction of the respective promoters was not analyzed.

BDNF expression is regulated by the zinc-finger protein NRSF binding a neuron-restrictive silencer element (NRSE) in promoter II (Palm et al., 1998; Timmusk et al., 1999; Fig. 1). NRSF recruits transcriptional co-repressors mSin3A and CoREST that interact with several proteins, including HDACs, to regulate transcription (Andres et al., 1999; Huang et al., 1999b; Roopra et al., 2000). It has

been shown that the *BDNF* NRSE is involved in the repression of basal and kainic acid-induced transcription from *BDNF* promoters I and II in neurons, indicating that it has a role in modulating activity-dependent expression of *BDNF in vivo* (Timmusk et al., 1999).

Very little is known of regulation of other *BDNF* exons. Yet, *BDNF* exon VI expression has been found to be potentially regulated by transcription factors CCAAT/enhancer-binding protein beta (C/EBPβ) and Sp1 and could be activated by CaMKII and the MAPK/ERK pathway (Takeuchi et al., 2002; Park et al., 2006).

2.3 Neuronal activity-regulated transcription factors

Neuronal activity could be abridged to rise in Ca^{2+} concentration that serves as a molecular messenger directly or indirectly regulating almost all activity-dependent processes throughout the nervous system (Berridge, 1998; Augustine et al., 2003). Ca^{2+}-dependent transcription is frequently used as a synonym for neuronal activity-dependent transcription and the *cis*-elements and transcription factors involved are commonly referred as Ca^{2+}-dependent elements or factors, respectively. In the following chapters an overview of the Ca^{2+}-regulated factors involved in neuronal activity-dependent transcription is given. For several of the proteins, rodent *BDNF* has been the model target gene or the first target gene to be identified.

2.3.1 Phosphorylation-regulated activation

Extracellular stimulation can lead to rapid transcriptional induction of gene expression (Greenberg and Ziff, 1984; Morgan and Curran, 1986). CREB binding to the *cis*-element CRE, first described as a cAMP signaling dependent transcription regulation system (Montminy and Bilezikjian, 1987), is one of the best characterized mechanisms mediating such processes, including Ca^{2+}-dependent transcription regulation in neurons. CREB belongs to the mammalian activating transcription factor (ATF)/CREB family of basic leucine zipper (bZip) transcription factors, which bind to the consensus DNA recognition sequence TGACGTCA, designated the CRE element (Lonze and Ginty, 2002). Ca^{2+} influx induces phosphorylation of DNA-bound CREB at Ser133 that is followed by phospho-Ser133-dependent recruitment of the co-activator CREB binding protein (CBP), which in turn stimulates rapid transcriptional activation (Gonzalez and Montminy, 1989; Sheng et al., 1990; Chrivia et al., 1993). There are two predominant extracellular Ca^{2+} entry routes in neurons - through VGCCs and through ionotropic glutamate receptors. As non-NMDA receptor activation results in Ca^{2+} influx indirectly via VGCCs and NMDA receptor activation results in Ca^{2+} influx directly through the NMDA channel itself (Lerea et al., 1992), the NMDA receptors are the major contributors to Ca^{2+} concentration rise through glutamate receptors (Bading et al., 1995). Both, Ca^{2+} entry via VGCCs and NMDA receptors, activate CaMK and MAPK/ERK signaling. However, when CREB-dependent

transcription in neurons is considered, the results of VGCC and NMDA receptor activation are different (Bading et al., 1993). MAPK/ERK signaling is activated in the immediate vicinity of either NMDA receptors or VGCCs and the signal propagates to the nucleus, where CREB is phosphotylated at Ser133 by the ribosomal s6 kinase (RSK) 2, independent of global increases in Ca^{2+} concentration (Xia et al., 1996; Dolmetsch et al., 2001; Hardingham et al., 2001a). Interestingly, MAPK/ERK *per se* does not activate CREB-mediated transcription (Chawla et al., 1998). The reason is that CREB-dependent transcription in neurons requires an increase in nuclear Ca^{2+} concentration, Ca^{2+} binding to nuclear calmodulin and activation of CaMKIV, which is achieved predominantly by Ca^{2+} entry through VGCCs (Hardingham et al., 1997; Chawla et al., 1998). Thus, only Ca^{2+} flux through VGCCs potently stimulates CREB-mediated transcription (Bading et al., 1993). Like MAPK/ERK signaling, CaMKIV posphorylates CREB at Ser133 (Bito et al., 1996) and as a result, both pathways lead to phosphorylated Ser133-dependent CBP reqruitment (Chrivia et al., 1993). Even so, effective stimulation of CREB-dependent transcription in neurons requires CREB phosphorylation at Ser142 and Ser143 in addition to Ser133 and phosphorylation of the signal-regulated transcription activation domain of CBP, processes that are both selectively induced by nuclear Ca^{2+} and CaMKIV (Chawla et al., 1998; Kornhauser et al., 2002). Therefore, the mode of Ca^{2+} entry differentially controls CREB-dependent transcription in neurons as VGCCs activity triggers a far more robust CREB-mediated transcriptional response than Ca^{2+} entry through NMDA receptors (Hardingham et al., 1999). Hence, CREB-mediated transcription is induced by Ca^{2+} influx through NMDA receptors only when Ca^{2+}-induced Ca^{2+} release from intracellular stores promotes Ca^{2+} wave propagation into the nucleus (Hardingham et al., 2001b). Alternatively, CREB-dependent transcription is activated by nuclear CaMKIV by both Ca^{2+} entry through VGCCs and NMDA receptors via translocation of Ca^{2+}/CaM into the nucleus, whereas repeated Ca^{2+} signaling causes significantly faster and less specifically VGCC-dependent CREB activation (Deisseroth et al., 1998; Mermelstein et al., 2001). In any case, the role of MAPK/ERK signaling might be prolonging transcriptionally active state of CREB, because MAPK/ERK pathway could affect CREB phosphorylation after the initial activation of CREB by CaMKIV (Hardingham et al., 2001a; Wu et al., 2001).

CREB-mediated expression of *BDNF* likely follows the mechanisms of CREB-dependent transcription in neurons. The importance of the CREB/CRE system in *BDNF* promoter IV regulation is accentuated by the fact that knock-in mutation of the CRE element in *BDNF* pIV almost blocks m*BDNF* promoter IV activity-responsiveness *in vivo* (Hong et al., 2008).

The other major neuronal activity-dependent and phosphorylation-activated transcription regulation system consists of the serum response factor (SRF) that belongs to the MADS-box family of transcription factors and the A/T-rich consensus serum response *cis*-element $CC(A/T)_2A(A/T)_3GG$ named SRE (Pipes et al., 2006). It was first characterized to regulate the promoter of the proto-oncogene c-fos. SRF was found to bind SRE in conjunction with ternary complex factor

(TCF) subfamily of Ets proteins, most notably Elk1 (Greenberg et al., 1987; Treisman, 1987; Shaw et al., 1989; Posern and Treisman, 2006). Studies on c-fos gene regulation have shown that Ca^{2+}-dependent phosphorylation of SRF by CaMKs and MAPK/ERK signaling at serine 103 facilitates formation of the ternary complex on SRE (Shaw et al., 1989; Bading et al., 1993; Rivera et al., 1993; Misra et al., 1994). Additionally, actin modulates signal transduction to SRF (Posern et al., 2002) and several cofactors contribute to the transcriptional response (Posern and Treisman, 2006). In contrast to *BDNF* pIV, the c-fos promoter contains both CRE and SRE elements and is inducible in neurons by both Ca^{2+} influx via VGCCs and NMDA receptors since SRE-dependent transcription of c-fos does not need nuclear Ca^{2+} signaling (Bading et al., 1993).

MeCP2-controlled transcription is also a phosphorylation mediated and activity-dependent gene regulation mechanism in neurons. MeCP2 belongs to the family of methyl-CpG binding domain proteins (Hendrich and Bird, 1998) and binds DNA that contains one or more symmetrically methylated CpGs (Nan et al., 1993). In general, it mediates transcriptional repression by recruiting histone deacetylases (Nan et al., 1997). MeCP2 has widespread expression in mammalian cells (Meehan et al., 1992), but its expression levels rise specifically in neurons during postnatal development (Balmer et al., 2003). Mutations in MeCP2 cause the progressive neurodevelopmental disorder Rett syndrome (Amir et al., 1999). Also, both MeCP2 deficiency and overexpression lead to neurodevelopmental abnormalities, indicating that MeCP2 levels must be tightly regulated in neurons for normal brain function (Tudor et al., 2002; Collins et al., 2004). Impairment of MeCP2-regulated *BDNF* expression has been suggested to be involved in the pathology of Rett syndrome. MeCP2 has been shown to bind specific methylated CpGs on *BDNF* promoter IV, recruit histone deacetylases and repress transcription, whereas neuronal activity has been found to trigger neuron-specific phosphorylation and release of MeCP2 from the promoter, allowing activity-dependent induction of *BDNF* expression in cultured neurons (Chen et al., 2003b; Martinowich et al., 2003; Zhou et al., 2006). The role of MeCP2 on *BDNF* promoter IV was the first characterization of neuronal activity-dependent gene transcription regulation by DNA methylation-mediated chromatin remodeling. Although MeCP2 was described to act as a repressor on *BDNF* promoter, MeCP2 knock-out mice have decreased levels of *BDNF* (Chang et al., 2006). Thus, MeCP2-mediated control over gene expression in neurons, including *BDNF* regulation, is likely to be more complex. Accordingly, MeCP2 has been shown to function both as a repressor and activator of transcription in brain and intriguingly, MeCP2 has been proposed to be an activator of *BDNF in vivo* (Chahrour et al., 2008). Furthermore, recently it was shown that MeCP2 is a neuron-specific genome-wide regulator of chromatin structure instead of being a gene-specific transcription factor (Skene et al., 2010). Whatever the mechanism of MeCP2 is in the regulation of transcription, DNA methylation seems to play a role in *BDNF* expression. A growth arrest and DNA damage-inducible 45 (Gadd45) family protein that relieves epigenetic gene silencing by erasing methylation marks, has been shown to be up-regulated

following electroconvulsive treatment (Ploski et al., 2006) and has been demonstrated to be required for activity-induced DNA demethylation of specific promoters, including *BDNF* promoter IX, in neurons (Ma et al., 2009). Specifically, modulation of neurogenesis in the adult brain has been described to be associated with binding of Gadd45β to *BDNF* promoter IX, demethylation of the promoter and activation of *BDNF* promoter IX-dependent transcription after electroconvulsive treatment (Ma et al., 2009).

Regulation of basic helix-loop-helix (bHLH) proteins by neuronal activity is less studied, but most probably involves activation of these proteins by phosphorylation. USF1 and USF2 are DNA E-box motif (CANNTG) binding bHLH transcription factors (Murre et al., 1989) that are ubiquitously, yet with different ratios to each other, expressed in mammals (Sirito et al., 1994). USF proteins are essential in embryonic development as USF1 and USF2 double mutant mice die during embryogenesis (Sirito et al., 1998). USF single knock-out mice are viable, but including other phenotypic features, the USF2-null mice are prone to spontaneous epileptic seizures, indicating a role for USF-s in brain function (Sirito et al., 1998). Neuronal activity-dependent transcription of rat *BDNF* exon I and IV mRNAs was the first Ca^{2+} signal-mediated function to be described for USF-s in neurons (Tabuchi et al., 2002; Chen et al., 2003a). Since then, other important roles for USF proteins in brain development and function, for example up-regulation of the K^+/Cl^- cotransporter 2 isoform b in the developing brain (Markkanen et al., 2008) and neuron-specific expression regulation of calcitonin gene-related peptide in trigeminal ganglion neurons (Park and Russo, 2008), have been characterized. Although not directly shown in neurons, transcriptional activation by the USF proteins depends strongly on the core promoter context (Luo and Sawadogo, 1996) and is stimulated by phosphorylation of the USF-s by the MAPK/ERK pathway kinases or protein kinase C (PKC) (Galibert et al., 2001; Chen et al., 2005a). Another bHLH factor, BHLHB2 (Rossner et al., 1997), has been implicated in *BDNF* regulation by directly binding an E-box element in *BDNF* pIV (Jiang et al., 2008) or possibly by interacting with the USF proteins and inhibiting their function (Dhar and Taneja, 2001). In addition, the roles of bHLH proteins have been extensively studied in neurogenesis (Lee, 1997) and among other results, it has been found that neuronal activity modulates the function of the bHLH transcription factors NeuroD and NeuroD2 via CaMKII and CaMKIV activation, respectively. CaMKII-NeuroD pathway regulates activity-dependent dendritic growth (Gaudilliere et al., 2004) and CaMKIV-NeuroD2 pathway regulates synaptic maturation of the thalamocortical connections (Ince-Dunn et al., 2006).

NFkB activity protects neurons against excitotoxic cell death (Yu et al., 1999) and has been suggested to be involved in neuronal activity-dependent gene expression (Meberg et al., 1996; Suzuki et al., 1997; Freudenthal and Romano, 2000). NFkB represents a group of structurally related and evolutionarily conserved proteins, with five members in mammals, which share the Rel homology DNA binding domain (RHD) that binds the consensus sequence GGGG(C/T)NNCC(C/T) (Ghosh et al., 1998). NFkB-dependent transcriptional

control follows the mechanism where inhibitory IkB factor is associated with NFkB in the cytoplasm without a stimulus and target gene transcription is induced when NFkB is released from IkB upon an activating signal, including Ca^{2+} influx, and translocated into the nucleus (Baeuerle and Baltimore, 1988). Because NFkB could be activated at synapses and transported to the nucleus independent of both Ca^{2+} wave propagation and activation of kinase-mediated signaling pathways, the NFkB system of synapse-to-nucleus signaling is different from the mechanisms described above. Indeed, NFkB is activated locally upon synaptic stimulation through phosphorylation by CaMKII and transported retrogradely from neuronal processes to the nucleus, where it induces gene transcription (Wellmann et al., 2001; Meffert et al., 2003). *BDNF* could be one of the target genes for NFkB as change in NFkB subunit composition bound to *BDNF* promoter I following kainate-induced seizures in rat brain has been described (Lubin et al., 2007) and enhanced recruitment of NFkB to *BDNF* promoter IV in cultured hippocampal neurons after NMDA receptor activation has been suggested (Jiang et al., 2008). NFkB-mediated regulation of activity-dependent transcription could be modulated by MAPK/ERK, PI3K and AMP-activated protein kinase activity (Lubin et al., 2005; Yoon et al., 2008).

Very little is known of the transcriptional mechanisms of CaRF, a protein with no homology with other transcription factors. It has been speculated that it is phosphorylated (Tao et al., 2002), but this has not been shown. However, CaRF is regulated in a Ca^{2+}- and neuron-selective manner and has been suggested to confer neuron-specificity to activity-dependent transcription as has been shown for the regulation of *BDNF* (Tao et al., 2002). In addition to *BDNF*, it potentially regulates also other genes that are involved in the organization and function of neural circuits underlying learning and memory (McDowell et al., 2010; Pfenning et al., 2010).

2.3.2 Phosphorylation and dephosphorylation-regulated activation

The mechanisms of Ca^{2+}-dependent activation of the myocyte enhancer factor-2 (MEF2) family proteins were first described in myocytes and were found to include both phosphorylation and dephosphorylation. The four MEF2 proteins, MEF2A-D, belong to the MADS-box family of transcription factors along with SRF and bind the consensus DNA sequence $CTA(A/T)_4TAG$ (Pipes et al., 2006). They repress target gene transcription through chromatin remodeling by recruiting class II histone deacetylases (HDACs) to MEF2 target genes (Lu et al., 2000). It has been established in myocytes that upon Ca^{2+} release through IP_3 receptors, HDACs are phosphorylated by Ca^{2+}-activated CaMKII and exported from the nucleus allowing derepression of MEF2-regulated transcription (McKinsey et al., 2000; Backs et al., 2006; Wu et al., 2006). In addition to CaMKII, HDAC phosphorylation and nuclear export is enhanced by PKC (Vega et al., 2004). Regulation of MEF2-dependent gene expression in neurons is probably similar to the mechanisms described in myocytes. However, in neurons, additional regulatory steps are p38 mitogen-activated protein kinase (p38 MAPK)-dependent phosphorylation of MEF2 (Mao

et al., 1999) or dephosphorylation of MEF2 by CaM-dependent serine/threonine protein phosphatase calcineurin (Mao and Wiedmann, 1999). Ca^{2+} influx via VGCCs induces p38 MAPK-dependent phosphorylation of MEF2C and activation of MEF-dependent transcription in cerebellar granule neurons (Mao et al., 1999) and Ca^{2+} influx into hippocampal neurons, both through VGCCs and NMDA receptors, activates calcineurin, which dephosphorylates MEF2A and stimulates MEF2-dependent transcription (Flavell et al., 2006; Shalizi et al., 2006). MEF-mediated activity-dependent transcription in neurons supports newly differentiated neuron survival (Mao et al., 1999) and controls excitatory synapse development (Flavell et al., 2006; Shalizi et al., 2006; Flavell et al., 2008). As mentioned before, a MEF2 binding site located upstream of *BDNF* pI regulates *BDNF* transcription (Flavell et al., 2008). However, it has been speculated that there are several distinct MEF2 binding sites in the *BDNF* locus (Flavell and Greenberg, 2008) and MEF2D binding in the region of *BDNF* promoter IV has been documented (Hong et al., 2008).

2.3.3 Dephosphorylation-regulated activation

Nuclear factor of activated T cells (NFAT) is a family of four Ca^{2+}-regulated (NFATc1-c4) transcription factors and one osmotic tension-regulated (NFAT5) transcription factor that are evolutionarily related to the Rel/NFkB proteins and bind the consensus DNA sequence (T/A)GGAAA(A/T)N (Graef et al., 2001). NFAT proteins interact with each other or with partner transcription factors like activator protein 1 (AP1) complex forming proteins (Jain et al., 1992), GATA4 (Molkentin et al., 1998) and MEF2 (Blaeser et al., 2000) to activate transcription. NFAT-dependent transcription is repressed through NFAT phosphorylation by various kinases, such as casein kinase 1 (Okamura et al., 2004), glycogen synthase kinase 3 (Beals et al., 1997; Okamura et al., 2004), p38 MAPK (Gomez del Arco et al., 2000) and Jun N-terminal kinase (Chow et al., 1997). Upon Ca^{2+} influx the NFATs are dephosphorylated by calcineurin and translocated into the nucleus allowing NFAT-dependent induction of transcription (Hogan et al., 2003). NFAT proteins regulate gene transcription in various developing and adult tissues. Their role has been most extensively described in the immune system, in the thymus, spleen, and peripheral blood lymphocytes, but NFAT-dependent transcription has been found to have a role also in other organ systems and tissues, including the CNS (Crabtree and Olson, 2002; Hill-Eubanks et al., 2003; Nguyen and Di Giovanni, 2008). In cultured hippocampal neurons, calcineurin-dependent NFATc4-driven transcription is induced by activation of VGCCs as well as NMDA receptors (Graef et al., 1999). BDNF-TrkB singnaling mediated PKC activity and IP_3-dependent release of Ca^{2+} from intracellular stores, have also been found to induce calcineurin and NFAT-dependent transcription (Groth and Mermelstein, 2003). It has been found that the function of NFAT-mediated transcription in the developing CNS is regulation of axonal growth (Graef et al., 2003). Also,

destabilization of NFAT-dependent regulatory mechanisms has been proposed to cause some of the neurobiological features of Down syndrome (Arron et al., 2006).

2.3.4 Ca^{2+}-regulated CREB or CBP interacting transcriptional co-activators

Some of the factors that have been described to induce transcription in response to neuronal activity are not sequence specific DNA binding transcription factors, but instead, modulate the function of CREB or CBP, or both. First, the LIM domain-only 4 (LMO4)-mediated transcriptional activity is induced by CaMKIV-dependent formation of a protein complex containing CREB, LMO4 and LIM domain binding factor CLIM (Kashani et al., 2006). The activity of this complex is important for patterning of thalamocortical connections during development (Kashani et al., 2006) and neuron survival after stroke (Schock et al., 2008). Second, high mobility group box protein TOX3 that regulates nucleosome structure (Travers, 2003), has been found to associate with the CREB-CBP complex upon neuronal activity and augment CRE-mediated transcription (Yuan et al., 2009). And third, Ca^{2+}-responsive transactivator (CREST)-regulated transcription involves activity-induced and calcineurin-mediated HDAC1 release from transcription activator BRG1 and subsequent CREST-dependent CBP recruitment to BRG1 (Aizawa et al., 2004; Qiu and Ghosh, 2008). The latter has been shown to regulate neuron morphogenesis (Aizawa et al., 2004).

2.3.5 Regulation by direct Ca^{2+} binding

A completely different means of transcription regulation by neuronal activity was proposed when the mechanism of action of the transcriptional repressor DREAM (downstream regulatory element antagonist modulator) was described. DREAM was shown to bind a DNA element with a core consensus sequence identical to the CRE half site (GTCA), designated DRE (downstream regulatory element), downstream of the transcription start site of the prodynorphin gene and repress transcription (Carrion et al., 1999). It was demonstrated that when nuclear Ca^{2+} concentration is elevated, DREAM binds Ca^{2+}, is unbound from the DRE and allows transcriptional activation of prodynorphin (Carrion et al., 1999). This was the first demonstration of gene expression induction through direct Ca^{2+} binding by a transcription factor. DREAM, also named KCNIP3, belongs to the EF-hand motif containing potassium channel-interacting protein (KCNIP) family of four Ca^{2+} binding proteins, KCNIP1-4, which have been implicated in the modulation of A-type potassium channels (An et al., 2000) and in the regulation of presenilin processing by γ-secretase (Buxbaum et al., 1998) in addition to transcriptional regulation. The *KCNIP* genes are highly similar but encode unique N-terminal sequences, which could have importance in the diverse roles described for the KCNIP proteins (Holmqvist et al., 2001). However, *in vivo* studies have presented conflicting results about the functions of KCNIPs. Most importantly, two *KCNIP3* knock-out mice have been developed, which show different phenotypes. The first

study on *KCNIP3* knock-out mice demonstrated that these mice have elevated levels of prodynorphin mRNA and dynorphin A peptides in the spinal cord, indicating that *KCNIP3* is a transcriptional repressor *in vivo* (Cheng et al., 2002). Intriguingly, these mice had no impairment of Kv4 channels and they did not have detectable differences in presenilin processing. In contrast, the other study for which the *KCNIP3* knock-out mice were developed, showed that there are no changes in prodynorphin expression (Lilliehook et al., 2003). Instead, long-term potentiation and presenilin processing are altered, which indicates an *in vivo* role for KCNIP3 in modulating the A-type potassium channels and γ-secretase function, respectively. Regardless of these discordances, KCNIP3 as a transcription factor has been studied in more detail. It has been shown that KCNIP3 interacts with CREB and Ca^{2+}-dependent breakdown of this interaction could be a regulatory step in CREB-dependent transcription (Ledo et al., 2002). Notably, one study has suggested KCNIP3 to be involved in the regulation of CREB-dependent *BDNF* exon IV mRNA expression (Fontan-Lozano et al., 2009). In addition, KCNIP3-mediated derepression of transcription could be modulated by cAMP-dependent interaction of a bZIP family transcription factor alphaCREM (cAMP responsive element modulator) with KCNIP3, which prevents binding of KCNIP3 to the DRE (Ledo et al., 2000).

2.3.6 Neuronal activity-dependently expressed transcription factors

Activity-dependent transcription could be regulated by factors expression of which is induced by neuronal activity. This allows a delayed transcriptional response compared to the immediate response caused by signaling pathways activated instantly by Ca^{2+} influx. The best characterized neuronal activity-induced transcription factor genes include the proto-oncogenes c-fos, c-jun, junB, Fra1 and Fra2 encoding the AP1 complex forming proteins of the bZIP family (Morgan et al., 1987; Saffen et al., 1988) and Egr1 and Egr3 of the early growth response (EGR) family (Sukhatme et al., 1988; O'Donovan et al., 1998). Neuronal activity-dependent rise in the levels of the AP1 complexes is accompanied by increase in DNA binding activity to the AP1 recognition sequence TGA(C/G)TCA and the CRE element, which are bound with high and low affinity, respectively, by AP1 heterodimers (Sonnenberg et al., 1989b; Sonnenberg et al., 1989a). The EGR family members contain a highly conserved DNA-binding domain composed of three zinc-finger motifs that recognize a nine-bp G/C rich sequence (O'Donovan et al., 1999). The possibilities for the transcriptional program launched by these proteins is versatile as the AP1 proteins can interact with each other, with related bZIP proteins and with structurally unrelated transcription factors, including the EGRs, to produce different, yet highly sequence-specific, transcription regulatory complexes (Chinenov and Kerppola, 2001; Levkovitz and Baraban, 2002).

Recently, neuronal activity-induced genes in cultured hippocampal and cortical neurons were identified (Lin et al., 2008; Zhang et al., 2009). In addition to the previously described transcription factors, some other genes involved in

transcription regulation were noted to be distinctly strongly induced by Ca^{2+} signaling. For example: (1) the ATF/CREB family member ATF3, homodimer of which acts as a transcriptional repressor (Hai and Hartman, 2001); (2) the aforementioned Gadd45β that relieves epigenetic gene silencing by erasing methylation marks from DNA, including from *BDNF* promoter IX (Ma et al., 2009); (3) the bHLH-PAS protein family member NPAS4 that: a) is selectively expressed in neuronal tissues and forms heterodimeric transcription activation complexes with the bHLH-PAS family member aryl hydrocarbon receptor nuclear translocator (ARNT) 2 (Ooe et al., 2004), b) is induced by KCl depolarization *in vivo* (Hester et al., 2007), and c) regulates inhibitory synapse development (Lin et al., 2008); and (4) the steroid nuclear hormone receptor family NR4A1/Nur77/ NGFIB orphan nuclear receptor subfamily member Nur77 that regulates cell survival (Suzuki et al., 2003; Moll et al., 2006).

2.3.7 An exception?

Fascinatingly, the VGCCs themselves can directly regulate transcription. It has been shown that a C-terminal fragment of an L-type VGCC, named Ca^{2+} channel associated transcription regulator (CCAT) translocates to the nucleus and regulates transcription (Gomez-Ospina et al., 2006). CCAT-dependent transcriptional response is negatively regulated by Ca^{2+}-signaling as the CCAT is translocated out of the nucleus upon both activation of the VGCCs and the NMDA receptors (Gomez-Ospina et al., 2006).

AIM OF THE THESIS

Factors involved in neuronal activity-dependent transcription are regulated by different mechanisms, mirroring distinct requirements for gene expression programs activated in response to Ca^{2+}-elevating stimuli in neurons. Whether all of the different means of Ca^{2+}-dependent regulation impact *BDNF* transcription is unknown. However, one of the reasons for the complexity of the *BDNF* gene structure might be to allow that. In the light of this hypothesis, activity-dependent transcription factors that have not been reported to regulate *BDNF* should be tested for a role in *BDNF* transcription. Moreover, in parallel with efforts to gain insight into possible novel players in *BDNF* activity-dependent transcription, it is important to re-examine the knowledge about *BDNF* regulation obtained from rodents, on human *BDNF* transcription, since dysregulation of *BDNF* expression has been associated with a number of neuropsychiatric disorders.

The aim of this study was twofold:

a) to describe the expression and gene structures of Ca^{2+}-regulated transcription factor family genes the functions of which have been poorly characterized in neurons; and
b) to determine the *cis*-elements and transcription factors involved in neuronal activity-dependent activation of human *BDNF* transcription.

The following was undertaken:

- the structures, alternative splicing and expression of the human and mouse Ca^{2+}-regulated transcription factor *KCNIP* and *NFAT* gene families were characterized;
- the human *BDNF* gene structure and expression was described;
- detailed analysis of human *BDNF* transcriptional activation by neuronal activity was performed.

MATERIALS AND METHODS

I used the following methods during the study:

- Bioinformatic analyses of gene and mRNA sequences (publications I-V and manuscript)
- Cloning (publications I-V and manuscript)
- Mutagenesis (publication V and manuscript)
- RNA isolation, cDNA synthesis and RT-PCR (publications I-V and manuscript)
- 5' RACE analyses of transcription initiation sites (publication II)
- Culturing of immortalized cells (publication II)
- *in situ* hybridization (publications I, III and IV)
- Quantitative real-time RT-PCR (publications IV, V and manuscript)
- Western blotting (manuscript)
- Electrophoretic mobility shift assay (manuscript)
- Primary cortical neuron culture and transfection (publication V and manuscript)
- Analysis of genetically modified mice (publication IV and manuscript)
- Chloramphenicol acetyltransferase reporter assay (publication II)
- Luciferase reporter assay (publication V and manuscript)
- Chromatin immunoprecipitation (manuscript)

RESULTS AND DISCUSSION

1. Alternative splicing and expression of human and mouse *KCNIP* genes (publication I)

Considering the contradictory data about the functions of the KCNIP proteins obtained from the *KCNIP3* knock-outs (Cheng et al., 2002; Lilliehook et al., 2003) and the finding that KCNIPs have unique N-termini that could have functional significance (Holmqvist et al., 2001), it is important to elucidate the gene structures, alternative splicing and coding potentials of the alternative transcripts of the *KCNIP* genes. In addition, the expression pattern of the *KCNIP*s in the brain is of interest, when their potential role in transcriptional regulation of activity-induced genes, such as *BDNF*, is analyzed.

We studied the structures of the human and mouse *KCNIP1-4* genes and analyzed the expression of *KCNIP* alternative transcripts in human and mouse with RT-PCR. Also, by using *in situ* hybridization, we studied the cellular distribution of *KCNIP* expression in the mouse CNS.

We identified a novel 5′ exon, exon Ia, in addition to the previously described 5′ exon, exon Ib (An et al., 2000; Boland et al., 2003), in both human and mouse *KCNIP1*. Both *KCNIP1* transcripts, with exon Ia and exon Ib, were predominantly expressed in the nervous system.

Our results revealed five different transcripts for *KCNIP2:* (1) *KCNIP2-Ia,* containing 5′ exon Ia and exons IIa and IIb (KChIP2a, Ohya et al., 2001); (2) *KCNIP2-IaΔIIb,* containing 5′ exon Ia and exon IIa (KChIP2b, An et al., 2000); (3) *KCNIP2-IaΔIIab* containing 5′ exon Ia and lacking exons IIa and IIb (KChIP2c, Ohya et al., 2001); (4) *KCNIP2-IbΔIIab,* containing 5′ exon Ib and lacking exons IIa and IIb (KChIP2g, Decher et al., 2004); and (5) *KCNIP2-IcΔIIab,* containing 5′ exon Ic and lacking exons IIa and IIb. Using RT-PCR analyses we detected all five of these *KCNIP2* transcripts in human and all except *KCNIP2-IcΔIIab* in mouse tissues. In both human and mouse, *KCNIP2-Ia* was strongly expressed in the brain except in the cerebellum, where *KCNIP2-Ia* was not detected. *KCNIP2-IaΔIIb* was moderately or weakly expressed in the human brain, heart, spinal cord, thymus, and trachea. In mouse, the levels of *KCNIP2-IaΔIIb* were high in the heart. *KCNIP2-IaΔIIab* levels were high in the human heart and thymus. In mouse, high levels of *KCNIP2-IbΔIIab* were seen in several brain regions and in the testis. In human, *KCNIP2-IcΔIIab* was expressed in several non-neural tissues, particularly in the heart and testis. We did not detect *KCNIP2-IcΔIIab* expression in the nervous system.

We identified two predominant transcripts for *KCNIP3:* (1) *KCNIP3-Ia,* containing the previously described 5′ exon, named here exon Ia, and exon II (KChIP3, An et al., 2000), also named *DREAM* (Carrion et al., 1999) and *calsenilin* (Buxbaum et al., 1998), and (2) *KCNIP3-IbΔII,* containing a novel 5′ exon Ib and lacking exon II. RT-PCR analyses showed that *KCNIP3* transcripts with exon Ia and the novel exon Ib are differentially expressed in mouse and

human tissues, with *KCNIP3-Ia* having the predominant expression in the nervous system. It has been reported that in mouse *KCNIP3* transcripts with protein coding regions differing by 4 nucleotides due to alternative usage of a splice acceptor site downstream of the conventional 3′ splice site of intron I , inside exon II, are generated (Spreafico et al., 2001). The authors named these reading frames the DREAM frame and the calsenilin frame, speculating that this alternative splicing and subsequent differences in the translated proteins would be the cause for the different functions observed for KCNIP3 (Spreafico et al., 2001). We found that this transcript, which we have named *KCNIP3-IaΔ4nII*, is indeed present in mouse tissues, but its levels are almost 10-fold lower than *KCNIP3-Ia* levels. However, we could not detect *KCNIP3-IaΔ4nII* in human. We conclude that in human the KCNIP3 proteins cannot have different functions due to the respective alternative splicing described for mouse.

Our results revealed six predominant transcripts for human *KCNIP4*: (1) *KCNIP4-Ia*, containing the previously described 5′ exon Ia and exon II (KChIP4bl, Holmqvist et al., 2002), also named named *CALP250* (Morohashi et al., 2002); (2) *KCNIP4-IaΔII*, containing the previously described 5′ exon Ia and lacking exon II (CALP216, Morohashi et al., 2002); (3) *KCNIP4-IbΔII*, containing a novel 5′ exon, exon Ib, and lacking exon II; (4) *KCNIP4-IcΔII*, containing another novel 5′ exon, exon Ic, and lacking exon II; (5) *KCNIP4-IdΔII*, containing a previously described 5′ exon, exon Id, and lacking exon II (KChIP4a, Holmqvist et al., 2002); and (6) *KCNIP4-IeΔII*, containing yet another novel 5′ exon, exon Ie, and lacking exon II. RT-PCR analyses showed that in human and also in mouse, *KCNIP4-Ia* mRNA was predominantly expressed in the brain, where it was detected at different levels in all regions analyzed. *KCNIP4-IaΔII* was detected only in the human brain. *KCNIP4-IbΔII* and *KCNIP4-IcΔII* mRNAs were present also only in human. *KCNIP4-IbΔII* was expressed at high levels in the human brain, spinal cord, small intestine, and stomach, and *KCNIP4-IcΔII* was expressed exclusively in the kidney. *KCNIP4-IdΔII* expression was detected only in several regions of the brain and spinal cord, in human. Of the mouse brain regions analyzed, strong *KCNIP4-IdΔII* expression was detected in caudal regions, most significantly in the cerebellum. *KCNIP4-IeΔII* levels were high in the human brain and spinal cord. In mouse, *KCNIP4-IeΔII* levels were high in the brain, particularly in the ventral midbrain, cerebellum and cortex.

In order to find out whether the *KCNIP*s are expressed in the cells that enable them to regulate neuronal activity-dependent gene expression in brain, we analyzed the expression of all *KCNIP* mRNAs in adult mouse central nervous system by *in situ* hybridization. The hybridization probes for each *KCNIP* were constructed to recognize all of the major splice variants. We observed clear similarities and differences in the expression patterns of *KCNIP1-4*. Most importantly, in the cerebral cortex all the *KCNIPs* were detected in the neurons of layers II–VI. However, *KCNIP1* mRNA expression pattern could be distinguished very clearly from the patterns of other *KCNIP* mRNAs as it was detected in the scattered neurons, most possibly interneurons, of all layers of the cerebral cortex. Also,

although all *KCNIP* mRNAs were detected in the hippocampal formation, there were differences in the distribution of expression between different *KCNIPs*. *KCNIP1* was expressed in scattered interneurons, *KCNIP2* and 4 mRNAs were evenly and strongly expressed in the CA1–CA3 pyramidal layers and in the granular layer of the dentate gyrus, and *KCNIP3* mRNA was predominantly expressed in the granular layer of the dentate gyrus and with lower levels in the CA1–CA3 pyramidal layers.

Taken together, here we describe one novel alternative 5′ exon for both the human and mouse *KCNIP1* gene (exon Ia) and the human and mouse *KCNIP3* gene (exon Ib). Also, for the human *KCNIP4* we describe three novel 5′ exons (Ib, Ic, and Ie), one of which is present also in the mouse genome (exon Ie). As discussed in the overview of the literature, three different functions have been demonstrated for the KCNIP family proteins. It could be that the different N-termini of the KCNIP proteins, encoded by the alternative 5' exons, have biological significance *in vivo* by contributing to the functional specificity of different KCNIP isoforms. For example, independent functions in different cell compartments, in the nucleus and the cell membranes, could be achieved by targeting of the protein within the cell using the N-terminus as a signal. In general, the N-termini of the KCNIP family proteins share no homology with each other. As an exception, we describe here that the novel exon Ia in the human *KCNIP1* gene and the novel exon Ib in the human *KCNIP4* gene, are homologous. Remarkably, there are several positively charged lysine and arginine residues in the N-termini encoded by these splice variants, indicating that the respective protein isoforms might comprise a nuclear localization signal (NLS). This provides further support for the suggestion that one of the means how the different functions of the KCNIPs might be accomplished, is through subcellular targeting of the proteins. In the light of our *in situ* hybridization results, all of the KCNIPs could theoretically regulate activity-dependent transcription as their expression is high in the cortex and hippocampus, structures where most prominent neuronal activity-regulated induction of gene expression takes place. However, because of the novel putative NLS sequences, isofoms of KCNIP1 and KCNIP4, encoded by transcript *KCNIP1-IaΔII* and a human-specific transcript *KCNIP4-IbΔII*, respectively, are particularly good candidates for having a function as an activity-dependent regulator of gene expression in addition to KCNIP3 as the previously described prototype transcription factor of the KCNIP family. When *BDNF* regulation is considered, however, KCNIP1 is unlikely to be of significance, since it is expressed in inhibitory interneurons, cells where *BDNF* is not expressed, throughout the forebrain.

2. Expression, structure and alternative splicing of the human and mouse *NFAT* genes (publication III)

NFATc4 has been implicated in neuronal activity-dependent gene transcription (Graef et al., 1999). Whether other NFAT family members contribute to this

function is unclear. To provide basis for answering this question, we decided to comprehensively describe the expression of the Ca^{2+}-regulated members of the *NFAT* gene family, with the emphasis on their expression in the brain. For that, expression of different NFAT isoforms, generated by splicing or usage of alternative 5′ and 3′ exons, was studied and *in situ* hybridization analysis of *NFAT* gene expression in the mouse brain was performed.

Our results on the structures of the *NFAT* genes are in agreement with previous data from other groups (Imamura et al., 1998; Chuvpilo et al., 1999; Plyte et al., 2001) and add also important new data about the complex splicing and expression of this gene family. In general, there are several alternative transcripts for the *NFAT* genes, which are generated by usage of alternative 5′ and 3′ exons and alternative splicing. According to our data, human and mouse *NFATc1* and *NFATc2*, and mouse *NFATc3* and *NFATc4*, have two alternative 5′exons. In human we detected six alternative 5′exons for *NFATc3* and seven alternative 5′ exons for *NFATc4*. Our results also showed that in both human and mouse, *NFATc1* and *NFATc3* have two alternative 3′ exons and *NFATc4* has one 3′ exon. For *NFATc2* we detected one 3′ exon in human, but three alternative 3′ exons in mouse. In addition, alternative splicing is used for all *NFAT* genes and in combination with the usage of alternative 5′ and 3′ exons , this could theoretically lead to 8 different protein isoforms of NFATc1, 6 different isoforms of both NFATc2 and NFATc3, and 24 different isoforms of NFATc4 in human. Regardless of the complex usage of 5' and 3' exons and splicing, the *NFAT* genes are very similar in their central region, which encodes the DNA-binding Rel homology domain, where there is almost no splicing. This indicates that splicing and usage of 5' and 3' exons probably does not influence NFAT DNA binding properties. However, as both the different N- and C-termini of the NFATs have previously been shown to contain transcription activation domains (TAD-s) that convey different transactivation potential (Rao et al., 1997; Imamura et al., 1998), we suggest that usage of alternative 5' and 3' exons and alternative splicing of the *NFAT*s might give flexibility to transcription activation potency of the NFAT proteins.

In previous studies only *NFATc4* expression has been characterized in more detail in adult nervous system and cultured primary neurons (Ranger et al., 1998; Graef et al., 1999; Bradley et al., 2005; Groth et al., 2007), giving the notion that NFATc4 might be the most abundant and the most important NFAT factor expressed in the nervous system. However, our *in situ* hybridization results showed that *NFATc2*, not *NFATc4*, is the predominant *NFAT* expressed in adult mouse brain. The highest *NFATc2* mRNA levels were detected in the pyramidal cell layer of the CA1–CA3 regions of the hippocampus, in the Purkinje and granule cell layers of the cerebellum, olfactory bulb, hypothalamus and thalamus. Conversely, we show that *NFATc4* is indeed expressed in brain, but at lower levels compared to the other *NFAT*s. Moderate expression was detected only in the cerebellar, olfactory bulb, and dentate gyrus granule cells and in the mitral cells of the olfactory bulb. On the other hand, according to our PCR analysis of *NFAT*

expression during mouse brain development, *NFATc4* was more abundantly expressed in the earlier stages of development and the expression levels decreased during later stages. Therefore, NFATc4 function might be especially important in the developing brain.

Before this study, *NFATc3* expression in the brain had been demonstrated only in the hypothalamus and striatum and in certain cell lines of neuronal origin (Asai et al., 2004; Jayanthi et al., 2005). We describe *NFATc3* expression in the cerebellar granule cells, in Purkinje cells and, to a lesser extent, in the granule cells of the dentate gyrus and olfactory bulb in mouse brain. Thus, our data indicate that *NFATc2* and *NFATc3* could significantly contribute to brain development and physiology. Accordingly, results of *NFAT* knock-out studies have drawn attention to this beforehand. Whereas mice with the combination of *NFATc2*, *NFATc3*, and *NFATc4* mutations have a complete defect of midline crossing of the commissural neurons in response to netrins (Graef et al., 2003), *NFAT* single-knock-out mice, have less significant neuronal defects (Graef et al., 2001; Crabtree and Olson, 2002). This indicates that all, NFATc2, c3 and c4, have important roles in the nervous sytem.

To date, there were no indications of *NFATc1* expression in the brain. Surprisingly, we found that *NFATc1* is also expressed in mouse brain. *NFATc1* had the highest expression levels in the granular and glomerular cell layers of the olfactory bulb and moderate expression was seen in the cerebellar granule cells.

These results demonstrate that, in principle, all of the NFATs could potentially participate in the regulation of neuronal activity-dependent gene regulation because, although with different patterns, all *NFAT*s are expressed in brain. However, they also argue that *NFATc4*, which has previously described to be the major contributor to neuronal gene regulation by NFATs, is in fact less abundant in brain than *NFATc2*. The role of NFATc4 in neuronal activity-dependent gene transcription has been shown in cultured neurons though (Graef et al., 1999) and our results demonstrate that the expression levels of *NFATc4* peak at postnatal day 1 in the mouse brain. Therefore, NFATc4 is a suitable candidate for the regulation of activity-dependent gene expression in developing brain. However, it is likely that other NFATs, and NFATc2 in particular, could take over the function later in development.

3. Characterization of the gene structure and expression of human *BDNF* (publications II and IV)

Only partial description of the h*BDNF* gene has been given thus far. Expression of the alternative transcripts of human *BDNF* has been studied in only a few brain regions and has not been investigated in human non-neural tissues (Aoyama et al., 2001; Liu et al., 2005). Therefore, we decided to thoroughly analyze the structure of the h*BDNF* gene, to characterize the expression of alternatively spliced *BDNF* mRNAs in different human tissues and brain regions, and to identify and study the activities of alternative human *BDNF* promoters.

To re-examine the human *BDNF* gene structure and to identify mRNAs transcribed from the gene, *in silico* analysis of the human *BDNF* transcripts, 5′ rapid amplification of cDNA ends (5′RACE), and RT -PCR analyses of *BDNF* expression on total RNAs from adult human frontal cerebral cortex, medulla and hippocampus, were performed. The structures of the h*BDNF* gene and transcripts determined in this study are in good agreement with the results obtained for the rat and mouse *BDNF* genes (Aid et al., 2007) and, in general, follow the pattern where different 5' exons are spliced to a single 3' coding exon. Our analysis showed that the human *BDNF* gene spans ~70 kb and consists of 11 exons, whereas exons II, III, IV, V, Vh, VI, and VIIIh are untranslated exons and translation of the transcripts containing these exons starts from the ATG positioned in exon IX. Exons I, VII, and VIII contain in-frame ATG codons that could be used as translation start sites. In addition, we identified alternative splice donor sites in exons II, V, and VI and found that transcripts that use exon IX as the 5' transcript (IX-5') could be either alternatively spliced to comprise different regions or combinations of regions of exon IX (IXa, IXb, IXc, and IXd) or not subjected to internal splicing and contain all the regions of exon IX. Interestingly, there are two human-specific exons, designated here Vh and VIIIh. Moreover, in contrast to the rodent gene, there are exons that are detected exclusively as internal exons without a transcription start site and are present only in transcripts with a certain 5' exon. For example, h*BDNF* exon VIII was not detected in any transcript other than the ones starting with exon V, pointing to a possible functional regulation between the usage of a certain promoter and subsequent splicing. Independent of the 5′ exon usage, two separate polyadenylation signals in exon IX can be utilized in *BDNF* transcripts. In addition, it has been reported that natural antisense transcripts are transcribed from the human *BDNF* gene locus (Liu et al., 2005). We analyzed the exon-intron structure of this non-coding gene that is not present in rodents and, most importantly, found that exons 5 and 6 of *antiBDNF* overlap with the *BDNF* coding exon.

We analyzed the splicing of the human *BDNF* and *antiBDNF* pre-mRNAs and expression of consequent alternative mRNAs in detail by RT-PCR in 22 different adult human tissues. Altogether, the results indicate that transcripts containing *BDNF* exons II, III, IV, V, and VII are predominantly brain-specific and transcripts containing exons I and Vh are, in addition to brain, expressed in certain peripheral tissues. Transcripts containing exons VI and IXabcd show a wide pattern of expression. *antiBDNF* transcripts are present at different levels in almost all human tissues analyzed and certain alternative transcripts of *antiBDNF* are expressed in a tissue-specific manner.

Expression analysis of human *BDNF* and *antiBDNF* transcripts in 30 different adult brain regions was performed by RT-PCR. The results showed that all *BDNF* transcripts are expressed at high levels in the mammillary body, pons, hippocampus, frontal cortex, colliculi, and olfactory tract, whereas in other brain regions the alternative transcripts show differential expression. *antiBDNF* transcripts were expressed in all studied brain structures at similar levels.

Previous work has shown that *BDNF* is expressed predominantly in neurons (Ernfors et al., 1990; Phillips et al., 1990; Timmusk et al., 1994a; Conner et al., 1997; Webster et al., 2006). However, some studies have identified *BDNF* expression also in astrocytes (Zafra et al., 1992; Condorelli et al., 1994), microglia (Elkabes et al., 1996), and oligodendrocytes (Dai et al., 2003), both *in vivo* and *in vitro*. To verify that h*BDNF* is expressed in neurons, we analyzed the expression of *BDNF* in the human hippocampus using *in situ* hybridization. In agreement with earlier findings, our results showed that the highest levels of h*BDNF* mRNA is present in the granule neurons of the dentate gyrus, whereas other hippocampal regions have relatively weaker expression in pyramidal neurons. On the other hand, we also report here, with the results of RT-PCR analyses, that at least some of the alternatively spliced human *BDNF* mRNAs, particularly the IXabcd transcripts, are present *in vivo* in the corpus callosum and optic nerve, which contain mostly oligodendroglial cells and axonal projections. This suggests that *BDNF* expression is, in addition to neurons, possible also in glial cells in human.

Gene expression in eukaryotes is a highly coordinated process involving regulation at many different levels, among which the regulation of transcription is one of the most important. The promoter regions regulating human *BDNF* transcription have not been analyzed, however. Thus, hypothesizing that a functional promoter precedes each of the identified 5′ exon of h*BDNF* and that there is a promoter upstream of *antiBDNF* exon 1, the activities of nine potential promoter regions within the h*BDNF* gene and the region upstream of exon 1 of *antiBDNF* were analyzed for transcription-promoting activity using chloramphenicol acetyltransferase (CAT) assay. The putative promoter regions, each ~0.2 – 1.3 kb in length, containing 5′ flanking genomic sequence and a part of the respective 5′UTR coding sequence, were isolated and cloned into the pBLCAT2 vector in front of the *CAT* gene. Promoter activities were analyzed in human embryonic kidney HEK293T and mouse neuroblastoma N2a cells. The results showed that all the regions upstream of the 5′ exons of the human *BDNF* gene and the region upstream of the 5′ exon of the *antiBDNF* gene were functional in activating CAT expression. Notably, h*BDNF* promoters upstream of exons III and VI and the *antiBDNF* promoter were the strongest in both cell lines. These results indicate that, as has been identified for the rat *BDNF* (Timmusk et al., 1993), usage of alternative promoters that give flexibility to the control of gene expression, could be involved in the regulation of developmental stage-specific, cell type-specific and neuronal activity-induced expression of human *BDNF*.

We showed that endogenous non-coding antisense RNAs are transcribed from the human *BDNF* gene locus and according to our data, h*BDNF* and *antiBDNF* are coexpressed in many tissues. The levels of *BDNF* mRNA do not appear to be specifically reduced in tissues that express high levels of *antiBDNF* transcripts, however. Even so, we show that in the human brain, *BDNF* and *antiBDNF* transcripts form dsRNA duplexes *in vivo*, indicating that *antiBDNF* transcripts could modulate the levels of *BDNF* mRNA or protein in human. Homologous sequences to the human *antiBDNF* exons have not been found in rodent genomes

and *antiBDNF* mRNAs are not expressed in rodents (Aid et al., 2007). Therefore, an additional regulatory step compared to the rodent *BDNF* expression is possible for human *BDNF* regulation. *antiBDNF* could have evolved during primate/hominid evolution because highly homologous sequences to human *antiBDNF* are present in the genomes of chimpanzee and rhesus monkey.

Altogether, this detailed characterization of the h*BDNF* gene locus provides the basis for studying the mechanisms of *BDNF* gene regulation in human.

4. Identification of *cis*-elements and transcription factors regulating neuronal activity-dependent human *BDNF* transcription

4.1 Neuronal activity-induced expression of human *BDNF* (publication IV and manuscript)

Activity-dependent transcription of human *BDNF* was analyzed using bacterial artificial chromosome (BAC) transgenic mice carrying 168 kb of the human *BDNF* locus. First, kainic acid (KA) treatment of the transgenic mice was used to analyze activity-dependent gene regulation *in vivo*. Second, depolarization of primary neurons from the transgenic mice with KCl treatment was used as the model of neuronal activity *in vitro*.

The expression of the h*BDNF* in the human *BDNF*-BAC mice was confirmed by RT-PCR and *in situ* hybridization to mimic endogenous mouse *BDNF* expression in most neuron populations, including neurons of the CA1-CA3 and hilar regions of the hippocampus and the cerebral cortex. This indicated that the human *BDNF*-BAC construct contains the necessary genomic regions for accurate *BDNF* expression. For analysis of neuronal activity-induced h*BDNF* expression, treatment of mice with KA was performed for 3 hours. With RT-PCR we found that both endogenous mouse *BDNF* and transgenic human *BDNF* transcripts, which contain exons I, IV and IX-5', were markedly up-regulated by KA treatment in the hippocampus and cortex. Human *BDNF* and mouse *BDNF* mRNAs containing other 5' exons were induced to a lesser extent. Additionally, *in situ* hybidization analysis was performed and marked induction of transgenic human *BDNF* mRNA by KA treatment in the pyramidal neurons of CA1-CA3 layers, in the hilar region of hippocampus and also in the layers II – VI of cerebral cortex was documented. Endogenous mouse *BDNF* was induced in the same neuronal populations, suggesting that the 168 kb h*BDNF*-BAC construct contains the regulatory elements needed for proper control over neuronal-activity induced *BDNF* transcription.

Next, in order to characterize the molecular mechanisms that govern neuronal activity-dependent expression of human *BDNF*, we decided to use depolarization of primary neuronal membranes with KCl treatment as the model, because that would make it possible to examine the responses of human *BDNF* promoters to neuronal activity by using reporter transfection experiments. We determined whether human *BDNF* expression is up-regulated in response to neuronal activity

in cultured primary cortical neurons using neurons from the transgenic mice. Primary neurons cultured 7 days *in vitro* (DIV) were treated with 25 mM KCl and the levels of the transgenic human and endogenous mouse *BDNF* mRNAs were measured by RT-qPCR. The results showed that total h*BDNF* mRNA, measured with primers detecting all of the h*BDNF* transcripts, was up-regulated in these neurons similarly to the endogenous total m*BDNF*. Next, we analyzed the up-regulation of different human *BDNF* exon-specific transcripts. Both h*BDNF* and m*BDNF* exon I and exon IV containing transcripts were the most up-regulated *BDNF* mRNAs by neuronal depolarization. With a slightly weaker rise in levels compared to mouse *BDNF* exon IV transcripts, mouse *BDNF* exon IX-5' transcripts were also induced. Interestingly however, the expression levels of m*BDNF* IX-5' transcripts were considerably more elevated than h*BDNF* IX-5'mRNA levels.

Provided that induction of both h*BDNF* and m*BDNF* exon I transcripts was particularly strong, we measured the relative abundance of exon I transcripts compared to exon IV transcripts in transgenic mouse primary neurons before and after KCl-depolarization. The results showed that h*BDNF* exon I transcripts reached to comparable levels with exon IV transcript levels upon depolarization of neurons. m*BDNF* exon I transcript levels were elevated to approximately 60% of mouse exon IV transcript levels. Also, whereas there were approximately 20-fold less mouse exon I transcripts compared to mouse exon IV transcripts in uninduced cells, the human exon I mRNAs were only 4-fold less abundant than human exon IV mRNAs. Considering this and that the r*BDNF* exon I mRNAs have been reported to constitute less than 5% of total *BDNF* mRNAs in the adult rat cortex (Timmusk et al., 1994b), whereas exon I transcripts in adult human parietal cortex have been found to be half as abundant as exon IV mRNAs (Garzon and Fahnestock, 2007), we point out that *BDNF* exon I transcripts could represent a relatively larger proportion of total *BDNF* mRNAs in human brain than in rodent brain.

Two important aspects should be considered when interpreting these results. First, we used rodent cells to study h*BDNF* regulation. Therefore, one might ask how accurately these results mirror the regulation of *BDNF* in human. Second, the results could be influenced by the fact that all regulatory sequences responsible for neuronal activity-dependent up-regulation of h*BDNF* might not be present in the BAC construct. It is recognized that differences in *cis*-regulatory elements rather than *trans*-acting factors explain many of the inter-species variations in gene regulation (Wilson and Odom, 2009). Moreover, human regulatory elements or a human chromosome have been shown to direct human-specific gene expression and transcription factor binding in transgenic mice (Prabhakar et al., 2008; Wilson et al., 2008). Therefore, we believe it is plausible to use rodent neurons as a tool for studying regulation of a human gene. On the other hand, we admit that the human *BDNF* transgene could be missing regulatory elements. For example, the antisense *BDNF* or the distal 5' region found to influence h*BDNF* expression *in vivo* (Gray et al., 2006). Nevertheless, in principle, depolarization of mouse primary neurons

activated h*BDNF* and therefore, rodent primary neurons are credible for h*BDNF* promoter studies.

4.2 *cis*-elements and transcription factors required for membrane depolarization-mediated activation of h*BDNF* in cultured neurons (manuscript)

We cloned the promoter regions of human *BDNF* major exons and the human-specific 5' exon Vh in front of luciferase reporter and analyzed their ability to induce luciferase activity in response to KCl-depolarization in rat primary neurons. Our results showed that h*BDNF* promoters I and IV, that were induced approximately 7- and 6-fold, respectively, were the most up-regulated *BDNF* promoters by KCl treatment. In addition, promoter IX was induced approximately 1.7-fold, which was statistically significant, whereas pII 1.2-fold induction was not. pVh was not induced and pVI activity was reduced upon depolarization.

These results showed that promoters I and IV of the human *BDNF* are the predominant neuronal activity-regulated promoters of the h*BDNF* gene. In addition, given that we demonstrated KA treatment-induced up-regulation of human exon IX-5' in transgenic mice carrying h*BDNF* and that KCl treatment-mediated induction of h*BDNF* pIX was statistically significant, human *BDNF* pIX could also be a substantial player in human *BDNF* activity-dependent expression. Therefore, we next transfected plasmid constructs containing the wild-type or several activity-responsive *cis*-element mutant *BDNF* promoters I, IV or IX in front of the luciferase reporter gene into primary rat neurons and studied the induction of the luciferase activity by KCl-treatment.

For h*BDNF* promoter I we determined that mutation in the CRE-like element orthologous to the CRE-like element reported to contribute to the activity-mediated activation of rat *BDNF* pI (Tabuchi et al., 2002), does not significantly affect the induction of h*BDNF* promoter I. Instead, a novel asymmetric E-box-like element is the activity-responsive *cis*-element in this promoter.

For h*BDNF* promoter IV we established that mutation in the CRE element orthologous to the CRE described for the r*BDNF* pIV (Shieh et al., 1998; Tao et al., 1998) almost abolishes the depolarization-induced up-regulation of h*BDNF* pIV activity. Mutation in the *cis*-element orthologous to the rat pIV UBE element reduces induction and the contribution of the element orthologous to the rat pIV CaRE is not significant. In addition, we determined that mutation in a novel E-box-like element similar to the asymmetric E-box-like element we identified in human *BDNF* pI significantly decreases the induction of pIV. This indicates that in h*BDNF* promoter IV, the E-box-like element is also needed for responsiveness to neuronal activity. The mutation in the binding site for NFkB does not affect KCl-mediated induction of pIV and the effect of the mutation in the binding site for BHLHB2 had an opposite effect compared to the results obtained by Jiang et al. for the rat pIV (Jiang et al., 2008). In addition, we tested whether a site identical to the consensus binding site for the transcription factors of the NFAT family in human

BDNF promoter IV is involved in KCl treatment mediated up-regulation of pIV activity. We found that mutating this element does not significantly lower the induction of human *BDNF* promoter IV.

For h*BDNF* pIX we found that the inducible region contains a CRE-like element and again an asymmetric E-box-like element, which are partially overlapping and activity-responsive.

Collectively, these data showed that the most important *cis*-regulatory elements required for the KCl treatment induced up-regulation of h*BDNF* promoters are: a) the novel asymmetric E-box element in pI; b) CRE, UBE and the novel asymmetric E-box element in pIV; and c) CRE and the novel asymmetric E-box element in pIX.

The transcription factors binding the regions responsible for the induction of h*BDNF* promoters were determined by electrophoretic mobility shift assays (EMSA). First, with all of the three separate promoter probes containing the asymmetric E-box-like element we detected a strong signal of mobility shift only when lysates from neurons treated 2h with KCl were used. Such asymmetric E-box-like elements have been shown to bind bHLH-PAS factors (Ooe et al., 2004). Moreover, Ooe et al. have shown that bHLH-PAS factor ARNT2-NPAS4 dimers bind with the highest affinity to the sequence identical to the one we mapped in human *BDNF* pI (Ooe et al., 2004). Therefore we used ARNT2 and NPAS4 antibodies in the assays and determined that all of the E-box-like elements were bound by ARNT2-NPAS4 dimers. We named these elements PasREs (for bHLH-PAS factor response element). The CRE and CRE-like elements in promoters I, IV and IX and the UBE element in promoter IV were confirmed to bind CREB and USF proteins, respectively.

Next, we performed transient transfection experiments with h*BDNF* promoter-luciferase constructs and ARNT2, NPAS4, USF and CREB expression constructs to confirm the results obtained with EMSA. The strongest increase in KCl-induced promoter I activity was obtained when ARNT2 and NPAS4 together were overexpressed. Results with CREB overexperssion showed that CREB did not enhance induction of pI. CREB enhanced basal levels of *BDNF* pI activity only when fused to the viral transcription activation domain VP16, indicating that CREB binds to h*BDNF* pI, but most probably does not regulate its neuronal activity-dependent induction. Basal promoter activities were weakly enhanced and KCl-induced levels were slightly reduced in USF overexpressing neurons, suggesting that the USF proteins are also not involved in h*BDNF* pI activity-dependent regulation. To answer the question whether the predominant role of ARNT2 and NPAS4 in inducing neuronal activity-dependent up-regulation of *BDNF* pI is human-specific, we analyzed the effect of CREB and ARNT2-NPAS4 overexpression on the rat *BDNF* pI promoter. Our experiments demonstrated that excess of CREB in primary neurons was sufficient to significantly enhance only the basal activity, but not KCl-induced activity of r*BDNF* pI. With ARNT2 and NPAS4 overexpression, on the other hand, there was strong increase in r*BDNF* pI activity both in uninduced and KCl-treated neurons compared to the control pRC

transfected cells. Moreover, the data of Tabuchi et al. shows that deletion of the CRE-like element in r*BDNF* pI decreases the basal activity of the promoter, whereas deletion of a region upstream of the CRE specifically reduces fold induction of r*BDNF* pI upon depolarization (Tabuchi et al., 2002). Thus, CREB or a related factor is regulating the basal activity of *BDNF* pI, but the transcription factors contributing most significantly to the activity-induced activation of *BDNF* pI are bHLH-PAS proteins ARNT2 and NPAS4 that bind the novel activity regulated *cis*-element named PasRE here. This result is supported by previous studies that have shown that: a) a region upstream of the CRE-like element is involved in activity-dependent regulation of rat pI (Tabuchi et al., 2002); b) NPAS4 binds DNA in the pI region of m*BDNF* (Lin et al., 2008); c) NPAS4 forms a heterodimer preferably with ARNT2 in brain (Ooe et al., 2009); and d) ARNT2-NPAS4 dimer has the highest affinity to a DNA sequence identical to the PasRE element in h*BDNF* pI (Ooe et al., 2004). Moreover, m*BDNF* levels are reduced in NPAS4 knock-out mice (Lin et al., 2008).

The results with h*BDNF* promoter IV showed that, USF-VP16 overexpression elevated uninduced as well as KCl-induced levels of human *BDNF* promoter IV-driven luciferase activity in primary neurons. These effects were lost when the UBE mutated h*BDNF* pIV-luciferase construct was used. KCl-induction of h*BDNF* pIV was significantly enhanced by overexpression of CREB and VP16-CREB overexpression enhanced both uninduced and depolarization-induced h*BDNF* pIV activity. All these effects were lost when CRE mutated pIV was used. When ARNT2 and NPAS4 were overexpressed together, promoter IV activity measured from uninduced neurons as well as pIV activity measured from KCl-induced neurons was significantly higher than the respective activities obtained from mock-transfected cells. Again, ARNT2-NPAS4 overexpression did not enhance PasRE mutated h*BDNF* pIV activity.

Experiments with human *BDNF* pIX showed that overexpression of CREB enhanced the induction and overexpression of VP16-CREB enhanced both the uninduced and induced levels of h*BDNF* pIX driven luciferase activity. Overexpression of NPAS4 with ARNT2 enhanced the induced promoter IX-dependent luciferase levels.

Altogether the results show that: a) KCl-mediated activation of h*BDNF* pI in cortical neurons is dependent on the novel *cis*-regulatory element PasRE and bHLH-PAS transcription factor ARNT2-NPAS4 dimer that binds the PasRE; b) CREB, ARNT2-NPAS4 and USF bind to CRE, PasRE and UBE elements in the h*BDNF* pIV, respectively, and are the central factors required for activation of h*BDNF* pIV by KCl-mediated membrane depolarization; and c) activation of human *BDNF* pIX is mediated by ARNT2-NPAS4 and CREB binding to the PasRE and CRE-like elements in h*BDNF* promoter IX, respectively.

In addition to the mutation analyses described above, we studied the induction kinetics of WT and CRE or PasRE mutated h*BDNF* pIV and determined that the CRE element in h*BDNF* pIV is fundamental for initiating transcription by neuronal depolarization and the PasRE element is necessary for enhancing further the

transcriptional activity driven by human *BDNF* pIV. We concluded this since the CRE mutation in pIV almost abolished induction, but mutation of the PasRE element allowed h*BDNF* pIV activation with identical kinetics compared to the WT promoter and significant decrease in induction was detected only after 3h of KCl treatment. These results are in accordance with the finding that CRE mutation in the m*BDNF* pIV loses its inducibility *in vivo* (Hong et al., 2008) and with the data presented by Lin et al. that the NPAS4 protein, shown here to bind *BDNF* PasREs as a heterodimer with ARNT2, is produced in primary cultured neurons after depolarization of neuronal membranes (Lin et al., 2008). Moreover, we found that EMSA shift by ARNT2-NPAS4 heterodimer was detectable only with lysates of depolarized neurons. Interestingly, the predominant rise of both human and mouse *BDNF* exon I transcript levels took place later after KCl addition than the major rise in *BDNF* exon IV transcript levels as was shown here using primary neurons from h*BDNF*-BAC mice. This supports the finding that NPAS4 accumulation is needed for induction of pI. pIV, on the other hand, is induced by CREB as an immediate-early promoter.

4.3 Involvement of endogenous PasRE elements in the regulation of *BDNF* expression (manuscript)

Since all *cis*-elements except the novel PasREs that we have described here for human *BDNF* promoters have been shown before to be important for rod*BDNF* activity-dependent induction, we chose to validate the role of the PasRE elements also at the level of endogenous rodent *BDNF* regulation. For that, we used overexpression of delTAD-ARNT2 and delTAD-NPAS4 constructs which are devoid of the transcription activation domains and have the ability to compete with the endogenous bHLH-PAS factors by binding to PasRE elements and interfere with activity-regulated *BDNF* transcription. We electroporated delTAD-ARNT2 and delTAD-NPAS4 expression constructs or a control GFP construct into rat primary neurons using Amaxa nucleofection and treated the cells at 5 DIV with 25 mM KCl. RT-qPCR results showed that the up-regulation of r*BDNF* exon I, IV and IX-5' mRNAs in the delTAD-ARNT2 and delTAD-NPAS4 expressing cells was considerably weaker than in GFP electroporated cells, suggesting that the full induction of activity-responsive transcription of endogenous r*BDNF* exon I, IV and IX-5' mRNAs is to a great extent dependent on bHLH-PAS transcription factors ARNT2 and NPAS4 binding the PasRE elements. Interestingly, the activity-regulated *cis*-elements described here for the human pIX are not conserved in rodents. However, we found that induction of endogenous rat exon IX-5' transcription was partly dependent on bHLH-PAS factors. This is conceivable though, because only one-third of transcription factor binding events take place on an aligned site in an orthologous promoter between human and mouse (Odom et al., 2007) suggesting another PasRE location in rod*BDNF* pIX.

Next, we performed chromatin immunoprecipitation (ChIP) experiments to demonstrate that ARNT2-NPAS4 and CREB bind to PasRE and CRE elements,

respectively, on endogenous *BDNF* promoters in human cells. For that, either constructs coding for ARNT2-V5 or NPAS4-V5 alone or together with NPAS4 or ARNT2 coding constructs, respectively, or CREB1-V5 coding construct, were transfected into HEK293 cells and ChIP with anti-V5 antibody was performed. We observed strong binding of ARNT2-V5 and NPAS4-V5 on h*BDNF* pI and pIV only when the V5-tagged proteins were expressed together with NPAS4 and ARNT2, respectively, supporting the data that ARNT2 and NPAS4 bind DNA as a dimer. CREB1-V5 was also significantly enriched on h*BDNF* pI and IV. None of the V5-tagged proteins were bound to pIX or the unrelated negative control region.

By overexpressing VP16-CREB1, ARNT2, NPAS4 or ARNT2 together with NPAS4 in HEK239 cells and measuring endogenous h*BDNF* mRNA expression by RT-qPCR, we observerd strongly elevated h*BDNF* exon I and IV transcript levels upon ARNT2-NPAS4 co-transfection and VP16-CREB1 transfection. Notably, VP16-CREB1 induced human *BDNF* exon IV transcription relatively more than exon I transcription, when the effect of ARNT2-NPAS4 on the respective transcripts is considered. In accordance with the results of the ChIP and EMSA experiments, only weak up-regulation was detected for h*BDNF* exon IX-5' transcripts, most probably due to much weaker binding of CREB and ARNT2-NPAS4 to promoter IX. Taken together, our results imply that transcription factors ARNT2, NPAS4 and CREB bind h*BDNF* promoters I and IV in chromatin context and enhance transcription of endogenous h*BDNF*. Also, these experiments suggest that ARNT2-NPAS4 dimer binds and induces endogenous h*BDNF* pI relatively more than pIV and CREB, on the other hand, binds and induces endogenous human *BDNF* pIV relatively more than pI.

Finally, we performed ChIP experiments with anti-ARNT2 and anti-CREB1 ab-s and human postmortem parietal cortex samples to analyze whether ARNT2 and CREB1 bind h*BDNF* promoters in the human brain *in vivo*. We detected significant enrichment of ARNT2 on h*BDNF* pIV and pI. CREB1 was significantly enriched only on h*BDNF* pIV and not on h*BDNF* pI. Thus, ARNT2 binds h*BDNF* pI and pIV and CREB1 binds h*BDNF* pIV in the human parietal cortex *in vivo*, which strongly supports our previous results showing that ARNT2 and NPAS4 regulate h*BDNF* exon I and exon IV and CREB regulates h*BDNF* exon IV neuronal activity-dependent transcription (Fig. 2). The *in vivo* role of the novel PasRE elements in *BDNF* promoters described here is especially noteworthy in the light of the knowledge that ARNT2 is a key transcription factor in the hippocampus, where it is potentially crucial for synaptic plasticity (Valen et al., 2009), and both ARNT2 as well as NPAS4 are neuroprotective transcription factors (Drutel et al., 1999; Hester et al., 2007; Zhang et al., 2009) that could be good therapeutic targets in treatment of diseases and disorders with altered *BDNF* expression.

4.4 Do the KCNIP and NFAT proteins regulate neuronal activity-dependent *BDNF* transcription? (publication V and manuscript)

One study has suggested that KCNIP3 is involved in the regulation of CREB-dependent mouse *BDNF* exon IV mRNA expression by repressing CREB-mediated transcription in a Ca^{2+}-regulated manner (Fontan-Lozano et al., 2009). We tested whether KCNIP factors are involved in CREB-dependent transcription in our experimental setup based on *BDNF* promoter transfection into primary cultured neurons. Our luciferase experiments with overexpressed WT as well as Ca^{2+}-insensitive EF-hand mutant KCNIP3 or with other KCNIP family members, including those that we found to contain the NLS in their N-terminus, did not reveal statistically significant changes in human promoter IV induction upon KCl treatment. However, in the study where KCNIP3 involvement was demonstrated, another experimental system based on light deprivation *in vivo* was used and compared to WT mice only a slight increase in light induced *BDNF* exon IV transcript levels in *KCNIP3* knock-out mice was documented (Fontan-Lozano et al., 2009). This indicates that in our luciferase assay-based experiment these changes might be below the detection limit. As CREB-dependent transcription is not activated in cultured neurons by the other major means of extracellular Ca^{2+} enrty, via the NMDA receptors (Bading et al., 1993; Hardingham et al., 1997), we did not test for the possibility of Ca^{2+} influx route-specific role for the KCNIPs. We conclude that in cultured cortical neurons, CREB-dependent regulation of human *BDNF* pIV is not significantly affected by the KCNIP proteins and suggest that the KCNIP proteins are not among the major regulators of neuronal activity-mediated transcription of h*BDNF*, but could rather possess a modulatory role.

I have described above that we did not detect involvement of the h*BDNF* pIV NFAT consensus *cis*-element in KCl treatment-mediated up-regulation of pIV activity. Since NFAT-driven transcription is induced by activation of both VGCCs as well as NMDA receptors in cultured neurons (Graef et al., 1999), we tested the possibility that NFAT regulates pIV in an NMDA receptor activity-dependent manner. Compared with the WT promoter, human *BDNF* pIV with mutation in the conserved NFAT binding site had diminished responsiveness to NMDA receptor stimulation by 10 μM NMDA in cultured rat primary cortical neurons. This result suggests that the NFATs might contribute to activation of human *BDNF* promoter IV by NMDA receptor activation. To determine which of the NFATs is regulated by NMDA receptor activation and mediates NMDA receptor-induced *BDNF* pIV up-regulation, we studied *NFAT* mRNA expression in cultured cortical neurons. By RT-PCR mRNAs for all *NFAT* genes, *NFATc1-c4*, were detected. However, I have characterized above that there are significant temporal differences in relative abundance of *NFAT* mRNAs during mouse brain development *in vivo*. Specifically, although *NFATc2* is the predominantly expressed *NFAT* in the adult mouse brain, according to our RT-qPCR data, expression levels of *NFATc3* and *NFATc4* in particular, peak at postnatal day 1 in the brain. Furthermore, neuronal activity-dependent NFAT-mediated gene transcription has been shown in cultured neurons

to be mediated by NFATc4 (Graef et al., 1999). Thus, we focused our studies on NFATc4. We used transfection of constructs encoding shRNAs targeting NFATc4 to determine that NFATc4 mediates NFAT-driven *BDNF* transcription in cultured cortical neurons. NFATc4 knockdown reduced basal mRNA levels of endogenous *BDNF* to 60% of the levels in neurons transfected with the control shRNA construct. In addition, we analyzed the effect of NFATc4 overexpression and NFATc4 shRNA mediated knocknown on NMDA receptor-mediated activation of *BDNF* pIV and found that *BDNF* promoter IV induction was significantly enhanced and reduced, respectively. These results indicate that NFATc4 contributes to activation of human *BDNF* pIV and add NFATc4 to the list of activity-dependent transcriptional regulators of *BDNF* (Fig. 2). Because the consensus NFAT binding cis-element in the *BDNF* is adjacent to a consensus site for a potential NFAT partner, MEF2, we hypothesize that NFATc4 interacts with MEF2D to regulate *BDNF* transcription. Although the exact MEF2D binding site has not been identified in *BDNF* pIV, MEF2D has been shown to bind promoter IV of mouse *BDNF* by ChIP (Hong et al., 2008) providing support to this suggestion.

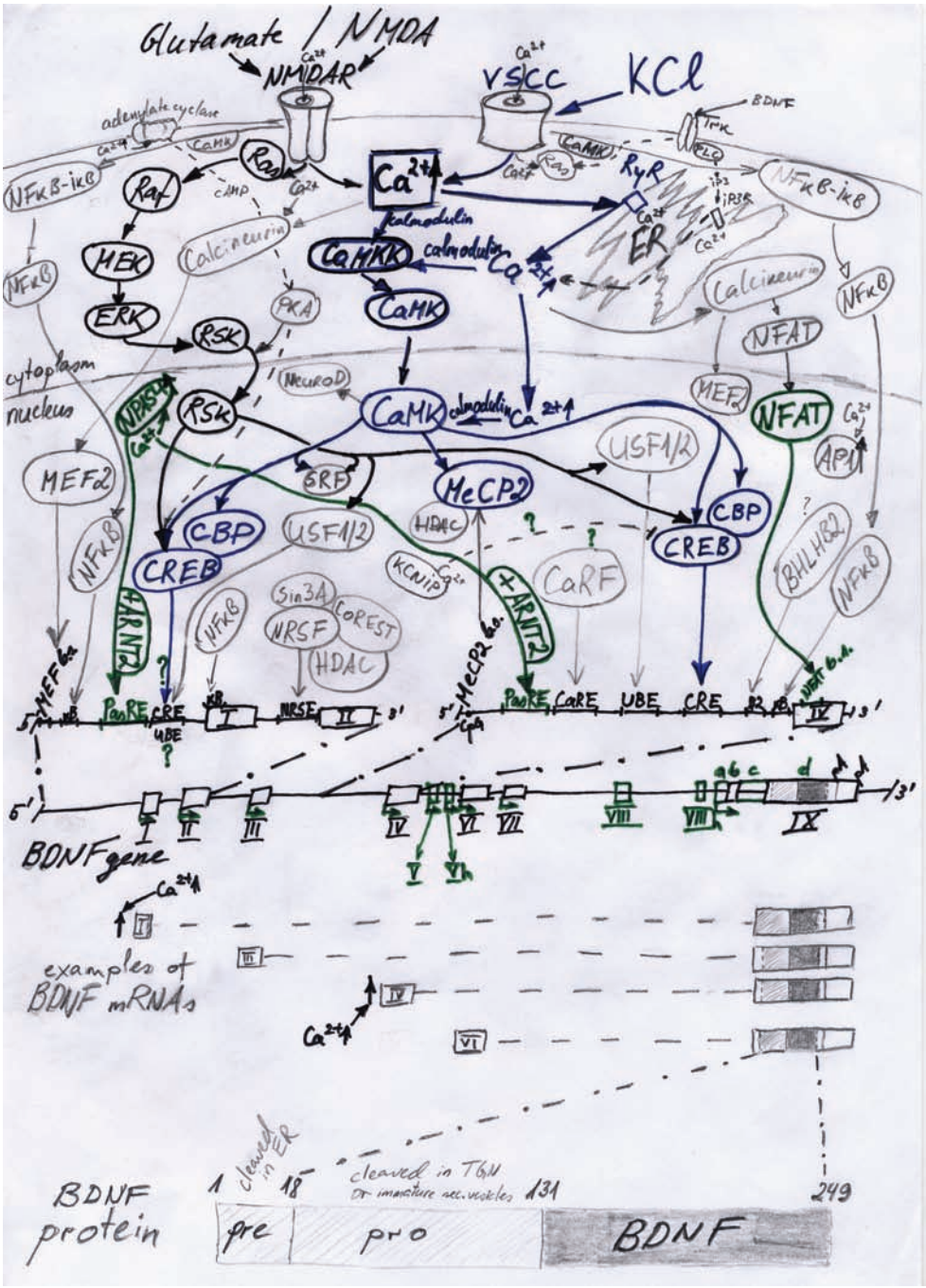

Figure 2. Genomic structure of the human *BDNF* gene and signal transduction networks mediating neuronal activity-dependent *BDNF* expression. To Figure 1 of the thesis the main novel findings of this study are added and highlighted in green. For details, see text.

CONCLUSIONS

1. Alternatively spliced *KCNIP* mRNAs are expressed differentially and could contribute to the diversity of functions of the KCNIP proteins.
2. Alternative transcripts for the *NFAT* genes are generated predominantly by usage of alternative 5′ and 3′ exons. All *NFAT* mRNAs are expressed in the neurons of the mouse brain with specific patterns for each *NFAT*.
3. The human *BDNF* gene contains 11 exons and nine functional promoters. The 3′ exon encodes all or most of the protein depending on the 5′ exon used. The human *BDNF* contains two more exons than the rodent *BDNF*.
4. Human *BDNF* transcripts containing exons II, III, IV, V, and VII are mostly brain-specific, whereas other *BDNF* mRNAs are also expressed at variable levels in non-neural tissues.
5. Endogenous non-coding antisense RNAs are transcribed from the human *BDNF* gene locus. Human *BDNF* and *antiBDNF* transcripts form RNA duplexes in adult human brain *in vivo*.
6. Exon I, IV and IX-5' transcripts of human *BDNF* are the most up-regulated human *BDNF* mRNAs by kainic acid treatment in transgenic human *BDNF*-BAC mouse brain and exon I and IV transcripts of human *BDNF* are the most up-regulated human *BDNF* mRNAs by depolarization of primary cortical neurons.
7. Activity-regulated induction of human *BDNF* promoter I depends primarily on a novel PasRE element; activity-regulated induction of human *BDNF* promoter IV depends predominantly on CRE, PasRE and UBE elements; and activation of human *BDNF* pIX is mediated by PasRE and CRE-like elements.
8. The CRE element in human *BDNF* promoter IV is fundamental for initiating transcription by neuronal depolarization from promoter IV and the PasRE element in promoter IV is necessary for enhancing further the promoter IV-driven transcriptional activity.
9. The novel PasRE elements in promoter I and promoter IV are conserved in human and rodents and are bound by bHLH-PAS transcription factor ARNT2-NPAS4 heterodimers
10. Membrane depolarization-induced activation of human *BDNF* promoter IV is not significantly affected by the KCNIP proteins in cultured cortical neurons.
11. NFATc4 contributes to induction of human *BDNF* promoter IV in an NMDA receptor activity-dependent manner.

REFERENCES

Aicardi G, Argilli E, Cappello S, Santi S, Riccio M, Thoenen H, Canossa M (2004) Induction of long-term potentiation and depression is reflected by corresponding changes in secretion of endogenous brain-derived neurotrophic factor. Proc Natl Acad Sci U S A 101:15788-15792.

Aid T, Kazantseva A, Piirsoo M, Palm K, Timmusk T (2007) Mouse and rat BDNF gene structure and expression revisited. J Neurosci Res 85:525-535.

Aizawa H, Hu SC, Bobb K, Balakrishnan K, Ince G, Gurevich I, Cowan M, Ghosh A (2004) Dendrite development regulated by CREST, a calcium-regulated transcriptional activator. Science 303:197-202.

Altar CA, Cai N, Bliven T, Juhasz M, Conner JM, Acheson AL, Lindsay RM, Wiegand SJ (1997) Anterograde transport of brain-derived neurotrophic factor and its role in the brain. Nature 389:856-860.

Amir RE, Van den Veyver IB, Wan M, Tran CQ, Francke U, Zoghbi HY (1999) Rett syndrome is caused by mutations in X-linked MECP2, encoding methyl-CpG-binding protein 2. Nat Genet 23:185-188.

An JJ, Gharami K, Liao GY, Woo NH, Lau AG, Vanevski F, Torre ER, Jones KR, Feng Y, Lu B, Xu B (2008) Distinct role of long 3' UTR BDNF mRNA in spine morphology and synaptic plasticity in hippocampal neurons. Cell 134:175-187.

An WF, Bowlby MR, Betty M, Cao J, Ling HP, Mendoza G, Hinson JW, Mattsson KI, Strassle BW, Trimmer JS, Rhodes KJ (2000) Modulation of A-type potassium channels by a family of calcium sensors. Nature 403:553-556.

Andres ME, Burger C, Peral-Rubio MJ, Battaglioli E, Anderson ME, Grimes J, Dallman J, Ballas N, Mandel G (1999) CoREST: a functional corepressor required for regulation of neural-specific gene expression. Proc Natl Acad Sci U S A 96:9873-9878.

Aoyama M, Asai K, Shishikura T, Kawamoto T, Miyachi T, Yokoi T, Togari H, Wada Y, Kato T, Nakagawara A (2001) Human neuroblastomas with unfavorable biologies express high levels of brain-derived neurotrophic factor mRNA and a variety of its variants. Cancer Lett 164:51-60.

Arron JR, Winslow MM, Polleri A, Chang CP, Wu H, Gao X, Neilson JR, Chen L, Heit JJ, Kim SK, Yamasaki N, Miyakawa T, Francke U, Graef IA, Crabtree GR (2006) NFAT dysregulation by increased dosage of DSCR1 and DYRK1A on chromosome 21. Nature 441:595-600.

Asai M, Iwasaki Y, Yoshida M, Mutsuga-Nakayama N, Arima H, Ito M, Takano K, Oiso Y (2004) Nuclear factor of activated T cells (NFAT) is involved in the depolarization-induced activation of growth hormone-releasing hormone gene transcription in vitro. Mol Endocrinol 18:3011-3019.

Augustine GJ, Santamaria F, Tanaka K (2003) Local calcium signaling in neurons. Neuron 40:331-346.

Backs J, Song K, Bezprozvannaya S, Chang S, Olson EN (2006) CaM kinase II selectively signals to histone deacetylase 4 during cardiomyocyte hypertrophy. J Clin Invest 116:1853-1864.

Bading H, Ginty DD, Greenberg ME (1993) Regulation of gene expression in hippocampal neurons by distinct calcium signaling pathways. Science 260:181-186.

Bading H, Segal MM, Sucher NJ, Dudek H, Lipton SA, Greenberg ME (1995) N-methyl-D-aspartate receptors are critical for mediating the effects of glutamate on intracellular calcium concentration and immediate early gene expression in cultured hippocampal neurons. Neuroscience 64:653-664.

Baeuerle PA, Baltimore D (1988) I kappa B: a specific inhibitor of the NF-kappa B transcription factor. Science 242:540-546.

Balkowiec A, Katz DM (2002) Cellular mechanisms regulating activity-dependent release of native brain-derived neurotrophic factor from hippocampal neurons. J Neurosci 22:10399-10407.

Balmer D, Goldstine J, Rao YM, LaSalle JM (2003) Elevated methyl-CpG-binding protein 2 expression is acquired during postnatal human brain development and is correlated with alternative polyadenylation. J Mol Med 81:61-68.

Bamji SX, Majdan M, Pozniak CD, Belliveau DJ, Aloyz R, Kohn J, Causing CG, Miller FD (1998) The p75 neurotrophin receptor mediates neuronal apoptosis and is essential for naturally occurring sympathetic neuron death. J Cell Biol 140:911-923.

Barde YA, Edgar D, Thoenen H (1982) Purification of a new neurotrophic factor from mammalian brain. Embo J 1:549-553.

Beals CR, Sheridan CM, Turck CW, Gardner P, Crabtree GR (1997) Nuclear export of NF-ATc enhanced by glycogen synthase kinase-3. Science 275:1930-1934.

Benraiss A, Chmielnicki E, Lerner K, Roh D, Goldman SA (2001) Adenoviral brain-derived neurotrophic factor induces both neostriatal and olfactory neuronal recruitment from endogenous progenitor cells in the adult forebrain. J Neurosci 21:6718-6731.

Berninger B, Marty S, Zafra F, da Penha Berzaghi M, Thoenen H, Lindholm D (1995) GABAergic stimulation switches from enhancing to repressing BDNF expression in rat hippocampal neurons during maturation in vitro. Development 121:2327-2335.

Berridge MJ (1998) Neuronal calcium signaling. Neuron 21:13-26.

Berton O, McClung CA, Dileone RJ, Krishnan V, Renthal W, Russo SJ, Graham D, Tsankova NM, Bolanos CA, Rios M, Monteggia LM, Self DW, Nestler EJ (2006) Essential role of BDNF in the mesolimbic dopamine pathway in social defeat stress. Science 311:864-868.

Bibel M, Barde YA (2000) Neurotrophins: key regulators of cell fate and cell shape in the vertebrate nervous system. Genes Dev 14:2919-2937.

Binder DK, Scharfman HE (2004) Brain-derived neurotrophic factor. Growth Factors 22:123-131.

Bito H, Deisseroth K, Tsien RW (1996) CREB phosphorylation and dephosphorylation: a Ca(2+)- and stimulus duration-dependent switch for hippocampal gene expression. Cell 87:1203-1214.
Blaeser F, Ho N, Prywes R, Chatila TA (2000) Ca(2+)-dependent gene expression mediated by MEF2 transcription factors. J Biol Chem 275:197-209.
Blum R, Kafitz KW, Konnerth A (2002) Neurotrophin-evoked depolarization requires the sodium channel Na(V)1.9. Nature 419:687-693.
Boland LM, Jiang M, Lee SY, Fahrenkrug SC, Harnett MT, O'Grady SM (2003) Functional properties of a brain-specific NH2-terminally spliced modulator of Kv4 channels. Am J Physiol Cell Physiol 285:C161-170.
Bozzi Y, Pizzorusso T, Cremisi F, Rossi FM, Barsacchi G, Maffei L (1995) Monocular deprivation decreases the expression of messenger RNA for brain-derived neurotrophic factor in the rat visual cortex. Neuroscience 69:1133-1144.
Bova R, Micheli MR, Qualadrucci P, Zucconi GG (1998) BDNF and trkB mRNAs oscillate in rat brain during the light-dark cycle. Brain Res Mol Brain Res 57:321-324.
Bradley KC, Groth RD, Mermelstein PG (2005) Immunolocalization of NFATc4 in the adult mouse brain. J Neurosci Res 82:762-770.
Bramham CR, Messaoudi E (2005) BDNF function in adult synaptic plasticity: the synaptic consolidation hypothesis. Prog Neurobiol 76:99-125.
Buckley NJ, Johnson R, Zuccato C, Bithell A, Cattaneo E (2010) The role of REST in transcriptional and epigenetic dysregulation in Huntington's disease. Neurobiol Dis 39:28-39.
Buxbaum JD, Choi EK, Luo Y, Lilliehook C, Crowley AC, Merriam DE, Wasco W (1998) Calsenilin: a calcium-binding protein that interacts with the presenilins and regulates the levels of a presenilin fragment. Nat Med 4:1177-1181.
Cabelli RJ, Hohn A, Shatz CJ (1995) Inhibition of ocular dominance column formation by infusion of NT-4/5 or BDNF. Science 267:1662-1666.
Cabelli RJ, Shelton DL, Segal RA, Shatz CJ (1997) Blockade of endogenous ligands of trkB inhibits formation of ocular dominance columns. Neuron 19:63-76.
Canossa M, Gartner A, Campana G, Inagaki N, Thoenen H (2001) Regulated secretion of neurotrophins by metabotropic glutamate group I (mGluRI) and Trk receptor activation is mediated via phospholipase C signalling pathways. Embo J 20:1640-1650.
Carrion AM, Link WA, Ledo F, Mellstrom B, Naranjo JR (1999) DREAM is a Ca2+-regulated transcriptional repressor. Nature 398:80-84.
Castren E, Zafra F, Thoenen H, Lindholm D (1992) Light regulates expression of brain-derived neurotrophic factor mRNA in rat visual cortex. Proc Natl Acad Sci U S A 89:9444-9448.
Castren E, Pitkanen M, Sirvio J, Parsadanian A, Lindholm D, Thoenen H, Riekkinen PJ (1993) The induction of LTP increases BDNF and NGF

mRNA but decreases NT-3 mRNA in the dentate gyrus. Neuroreport 4:895-898.
Chahrour M, Jung SY, Shaw C, Zhou X, Wong ST, Qin J, Zoghbi HY (2008) MeCP2, a key contributor to neurological disease, activates and represses transcription. Science 320:1224-1229.
Chang Q, Khare G, Dani V, Nelson S, Jaenisch R (2006) The disease progression of Mecp2 mutant mice is affected by the level of BDNF expression. Neuron 49:341-348.
Chao MV, Bothwell M (2002) Neurotrophins: to cleave or not to cleave. Neuron 33:9-12.
Chawla S, Hardingham GE, Quinn DR, Bading H (1998) CBP: a signal-regulated transcriptional coactivator controlled by nuclear calcium and CaM kinase IV. Science 281:1505-1509.
Chen J, Malcolm T, Estable MC, Roeder RG, Sadowski I (2005a) TFII-I regulates induction of chromosomally integrated human immunodeficiency virus type 1 long terminal repeat in cooperation with USF. J Virol 79:4396-4406.
Chen ZY, Ieraci A, Teng H, Dall H, Meng CX, Herrera DG, Nykjaer A, Hempstead BL, Lee FS (2005b) Sortilin controls intracellular sorting of brain-derived neurotrophic factor to the regulated secretory pathway. J Neurosci 25:6156-6166.
Chen WG, West AE, Tao X, Corfas G, Szentirmay MN, Sawadogo M, Vinson C, Greenberg ME (2003a) Upstream stimulatory factors are mediators of Ca2+-responsive transcription in neurons. J Neurosci 23:2572-2581.
Chen WG, Chang Q, Lin Y, Meissner A, West AE, Griffith EC, Jaenisch R, Greenberg ME (2003b) Derepression of BDNF transcription involves calcium-dependent phosphorylation of MeCP2. Science 302:885-889.
Cheng HY, Pitcher GM, Laviolette SR, Whishaw IQ, Tong KI, Kockeritz LK, Wada T, Joza NA, Crackower M, Goncalves J, Sarosi I, Woodgett JR, Oliveira-dos-Santos AJ, Ikura M, van der Kooy D, Salter MW, Penninger JM (2002) DREAM is a critical transcriptional repressor for pain modulation. Cell 108:31-43.
Chiaruttini C, Sonego M, Baj G, Simonato M, Tongiorgi E (2008) BDNF mRNA splice variants display activity-dependent targeting to distinct hippocampal laminae. Mol Cell Neurosci 37:11-19.
Chiaruttini C, Vicario A, Li Z, Baj G, Braiuca P, Wu Y, Lee FS, Gardossi L, Baraban JM, Tongiorgi E (2009) Dendritic trafficking of BDNF mRNA is mediated by translin and blocked by the G196A (Val66Met) mutation. Proc Natl Acad Sci U S A 106:16481-16486.
Chinenov Y, Kerppola TK (2001) Close encounters of many kinds: Fos-Jun interactions that mediate transcription regulatory specificity. Oncogene 20:2438-2452.

Chow CW, Rincon M, Cavanagh J, Dickens M, Davis RJ (1997) Nuclear accumulation of NFAT4 opposed by the JNK signal transduction pathway. Science 278:1638-1641.

Chrivia JC, Kwok RP, Lamb N, Hagiwara M, Montminy MR, Goodman RH (1993) Phosphorylated CREB binds specifically to the nuclear protein CBP. Nature 365:855-859.

Chuvpilo S, Zimmer M, Kerstan A, Glockner J, Avots A, Escher C, Fischer C, Inashkina I, Jankevics E, Berberich-Siebelt F, Schmitt E, Serfling E (1999) Alternative polyadenylation events contribute to the induction of NF-ATc in effector T cells. Immunity 10:261-269.

Cohen-Cory S, Fraser SE (1995) Effects of brain-derived neurotrophic factor on optic axon branching and remodelling in vivo. Nature 378:192-196.

Collins AL, Levenson JM, Vilaythong AP, Richman R, Armstrong DL, Noebels JL, David Sweatt J, Zoghbi HY (2004) Mild overexpression of MeCP2 causes a progressive neurological disorder in mice. Hum Mol Genet 13:2679-2689.

Condorelli DF, Dell'Albani P, Mudo G, Timmusk T, Belluardo N (1994) Expression of neurotrophins and their receptors in primary astroglial cultures: induction by cyclic AMP-elevating agents. J Neurochem 63:509-516.

Conner JM, Lauterborn JC, Yan Q, Gall CM, Varon S (1997) Distribution of brain-derived neurotrophic factor (BDNF) protein and mRNA in the normal adult rat CNS: evidence for anterograde axonal transport. J Neurosci 17:2295-2313.

Coull JA, Beggs S, Boudreau D, Boivin D, Tsuda M, Inoue K, Gravel C, Salter MW, De Koninck Y (2005) BDNF from microglia causes the shift in neuronal anion gradient underlying neuropathic pain. Nature 438:1017-1021.

Crabtree GR, Olson EN (2002) NFAT signaling: choreographing the social lives of cells. Cell 109 Suppl:S67-79.

Dai X, Lercher LD, Clinton PM, Du Y, Livingston DL, Vieira C, Yang L, Shen MM, Dreyfus CF (2003) The trophic role of oligodendrocytes in the basal forebrain. J Neurosci 23:5846-5853.

Dechant G, Barde YA (2002) The neurotrophin receptor p75(NTR): novel functions and implications for diseases of the nervous system. Nat Neurosci 5:1131-1136.

Decher N, Barth AS, Gonzalez T, Steinmeyer K, Sanguinetti MC (2004) Novel KChIP2 isoforms increase functional diversity of transient outward potassium currents. J Physiol 557:761-772.

Deisseroth K, Heist EK, Tsien RW (1998) Translocation of calmodulin to the nucleus supports CREB phosphorylation in hippocampal neurons. Nature 392:198-202.

Dhar M, Taneja R (2001) Cross-regulatory interaction between Stra13 and USF results in functional antagonism. Oncogene 20:4750-4756.

DiStefano PS, Friedman B, Radziejewski C, Alexander C, Boland P, Schick CM, Lindsay RM, Wiegand SJ (1992) The neurotrophins BDNF, NT-3, and NGF display distinct patterns of retrograde axonal transport in peripheral and central neurons. Neuron 8:983-993.

Dolmetsch RE, Pajvani U, Fife K, Spotts JM, Greenberg ME (2001) Signaling to the nucleus by an L-type calcium channel-calmodulin complex through the MAP kinase pathway. Science 294:333-339.

Drutel G, Heron A, Kathmann M, Gros C, Mace S, Plotkine M, Schwartz JC, Arrang JM (1999) ARNT2, a transcription factor for brain neuron survival? Eur J Neurosci 11:1545-1553.

Du J, Feng L, Yang F, Lu B (2000) Activity- and Ca(2+)-dependent modulation of surface expression of brain-derived neurotrophic factor receptors in hippocampal neurons. J Cell Biol 150:1423-1434.

Egan MF, Kojima M, Callicott JH, Goldberg TE, Kolachana BS, Bertolino A, Zaitsev E, Gold B, Goldman D, Dean M, Lu B, Weinberger DR (2003) The BDNF val66met polymorphism affects activity-dependent secretion of BDNF and human memory and hippocampal function. Cell 112:257-269.

Eide FF, Vining ER, Eide BL, Zang K, Wang XY, Reichardt LF (1996) Naturally occurring truncated trkB receptors have dominant inhibitory effects on brain-derived neurotrophic factor signaling. J Neurosci 16:3123-3129.

Elkabes S, DiCicco-Bloom EM, Black IB (1996) Brain microglia/macrophages express neurotrophins that selectively regulate microglial proliferation and function. J Neurosci 16:2508-2521.

Ernfors P, Lee KF, Jaenisch R (1994) Mice lacking brain-derived neurotrophic factor develop with sensory deficits. Nature 368:147-150.

Ernfors P, Wetmore C, Olson L, Persson H (1990) Identification of cells in rat brain and peripheral tissues expressing mRNA for members of the nerve growth factor family. Neuron 5:511-526.

Ernfors P, Bengzon J, Kokaia Z, Persson H, Lindvall O (1991) Increased levels of messenger RNAs for neurotrophic factors in the brain during kindling epileptogenesis. Neuron 7:165-176.

Falkenberg T, Mohammed AK, Henriksson B, Persson H, Winblad B, Lindefors N (1992) Increased expression of brain-derived neurotrophic factor mRNA in rat hippocampus is associated with improved spatial memory and enriched environment. Neurosci Lett 138:153-156.

Fang H, Chartier J, Sodja C, Desbois A, Ribecco-Lutkiewicz M, Walker PR, Sikorska M (2003) Transcriptional activation of the human brain-derived neurotrophic factor gene promoter III by dopamine signaling in NT2/N neurons. J Biol Chem 278:26401-26409.

Fawcett JP, Bamji SX, Causing CG, Aloyz R, Ase AR, Reader TA, McLean JH, Miller FD (1998) Functional evidence that BDNF is an anterograde neuronal trophic factor in the CNS. J Neurosci 18:2808-2821.

Flavell SW, Greenberg ME (2008) Signaling mechanisms linking neuronal activity to gene expression and plasticity of the nervous system. Annu Rev Neurosci 31:563-590.

Flavell SW, Kim TK, Gray JM, Harmin DA, Hemberg M, Hong EJ, Markenscoff-Papadimitriou E, Bear DM, Greenberg ME (2008) Genome-wide analysis of MEF2 transcriptional program reveals synaptic target genes and neuronal activity-dependent polyadenylation site selection. Neuron 60:1022-1038.

Flavell SW, Cowan CW, Kim TK, Greer PL, Lin Y, Paradis S, Griffith EC, Hu LS, Chen C, Greenberg ME (2006) Activity-dependent regulation of MEF2 transcription factors suppresses excitatory synapse number. Science 311:1008-1012.

Fontan-Lozano A, Romero-Granados R, del-Pozo-Martin Y, Suarez-Pereira I, Delgado-Garcia JM, Penninger JM, Carrion AM (2009) Lack of DREAM protein enhances learning and memory and slows brain aging. Curr Biol 19:54-60.

Freudenthal R, Romano A (2000) Participation of Rel/NF-kappaB transcription factors in long-term memory in the crab Chasmagnathus. Brain Res 855:274-281.

Fryer RH, Kaplan DR, Kromer LF (1997) Truncated trkB receptors on nonneuronal cells inhibit BDNF-induced neurite outgrowth in vitro. Exp Neurol 148:616-627.

Galibert MD, Carreira S, Goding CR (2001) The Usf-1 transcription factor is a novel target for the stress-responsive p38 kinase and mediates UV-induced Tyrosinase expression. Embo J 20:5022-5031.

Gall C, Lauterborn J, Bundman M, Murray K, Isackson P (1991) Seizures and the regulation of neurotrophic factor and neuropeptide gene expression in brain. Epilepsy Res Suppl 4:225-245.

Garzon DJ, Fahnestock M (2007) Oligomeric amyloid decreases basal levels of brain-derived neurotrophic factor (BDNF) mRNA via specific downregulation of BDNF transcripts IV and V in differentiated human neuroblastoma cells. J Neurosci 27:2628-2635.

Gaudilliere B, Konishi Y, de la Iglesia N, Yao G, Bonni A (2004) A CaMKII-NeuroD signaling pathway specifies dendritic morphogenesis. Neuron 41:229-241.

Gauthier LR, Charrin BC, Borrell-Pages M, Dompierre JP, Rangone H, Cordelieres FP, De Mey J, MacDonald ME, Lessmann V, Humbert S, Saudou F (2004) Huntingtin controls neurotrophic support and survival of neurons by enhancing BDNF vesicular transport along microtubules. Cell 118:127-138.

Ghosh A, Carnahan J, Greenberg ME (1994) Requirement for BDNF in activity-dependent survival of cortical neurons. Science 263:1618-1623.

Ghosh S, May MJ, Kopp EB (1998) NF-kappa B and Rel proteins: evolutionarily conserved mediators of immune responses. Annu Rev Immunol 16:225-260.

Ginty DD, Segal RA (2002) Retrograde neurotrophin signaling: Trk-ing along the axon. Curr Opin Neurobiol 12:268-274.

Gomez-Ospina N, Tsuruta F, Barreto-Chang O, Hu L, Dolmetsch R (2006) The C terminus of the L-type voltage-gated calcium channel Ca(V)1.2 encodes a transcription factor. Cell 127:591-606.

Gomez del Arco P, Martinez-Martinez S, Maldonado JL, Ortega-Perez I, Redondo JM (2000) A role for the p38 MAP kinase pathway in the nuclear shuttling of NFATp. J Biol Chem 275:13872-13878.

Gonzalez GA, Montminy MR (1989) Cyclic AMP stimulates somatostatin gene transcription by phosphorylation of CREB at serine 133. Cell 59:675-680.

Graef IA, Gastier JM, Francke U, Crabtree GR (2001) Evolutionary relationships among Rel domains indicate functional diversification by recombination. Proc Natl Acad Sci U S A 98:5740-5745.

Graef IA, Mermelstein PG, Stankunas K, Neilson JR, Deisseroth K, Tsien RW, Crabtree GR (1999) L-type calcium channels and GSK-3 regulate the activity of NF-ATc4 in hippocampal neurons. Nature 401:703-708.

Graef IA, Wang F, Charron F, Chen L, Neilson J, Tessier-Lavigne M, Crabtree GR (2003) Neurotrophins and netrins require calcineurin/NFAT signaling to stimulate outgrowth of embryonic axons. Cell 113:657-670.

Graham DL, Edwards S, Bachtell RK, DiLeone RJ, Rios M, Self DW (2007) Dynamic BDNF activity in nucleus accumbens with cocaine use increases self-administration and relapse. Nat Neurosci 10:1029-1037.

Gray J, Yeo GS, Cox JJ, Morton J, Adlam AL, Keogh JM, Yanovski JA, El Gharbawy A, Han JC, Tung YC, Hodges JR, Raymond FL, O'Rahilly S, Farooqi IS (2006) Hyperphagia, severe obesity, impaired cognitive function, and hyperactivity associated with functional loss of one copy of the brain-derived neurotrophic factor (BDNF) gene. Diabetes 55:3366-3371.

Greenberg ME, Ziff EB (1984) Stimulation of 3T3 cells induces transcription of the c-fos proto-oncogene. Nature 311:433-438.

Greenberg ME, Siegfried Z, Ziff EB (1987) Mutation of the c-fos gene dyad symmetry element inhibits serum inducibility of transcription in vivo and the nuclear regulatory factor binding in vitro. Mol Cell Biol 7:1217-1225.

Greer PL, Greenberg ME (2008) From synapse to nucleus: calcium-dependent gene transcription in the control of synapse development and function. Neuron 59:846-860.

Griesbeck O, Canossa M, Campana G, Gartner A, Hoener MC, Nawa H, Kolbeck R, Thoenen H (1999) Are there differences between the secretion characteristics of NGF and BDNF? Implications for the modulatory role of neurotrophins in activity-dependent neuronal plasticity. Microsc Res Tech 45:262-275.

Groth RD, Mermelstein PG (2003) Brain-derived neurotrophic factor activation of NFAT (nuclear factor of activated T-cells)-dependent transcription: a role for the transcription factor NFATc4 in neurotrophin-mediated gene expression. J Neurosci 23:8125-8134.

Groth RD, Coicou LG, Mermelstein PG, Seybold VS (2007) Neurotrophin activation of NFAT-dependent transcription contributes to the regulation of pro-nociceptive genes. J Neurochem 102:1162-1174.

Hai T, Hartman MG (2001) The molecular biology and nomenclature of the activating transcription factor/cAMP responsive element binding family of transcription factors: activating transcription factor proteins and homeostasis. Gene 273:1-11.

Halban PA, Irminger JC (1994) Sorting and processing of secretory proteins. Biochem J 299 (Pt 1):1-18.

Hall J, Thomas KL, Everitt BJ (2000) Rapid and selective induction of BDNF expression in the hippocampus during contextual learning. Nat Neurosci 3:533-535.

Hallbook F, Ibanez CF, Persson H (1991) Evolutionary studies of the nerve growth factor family reveal a novel member abundantly expressed in Xenopus ovary. Neuron 6:845-858.

Hardingham GE, Arnold FJ, Bading H (2001a) A calcium microdomain near NMDA receptors: on switch for ERK-dependent synapse-to-nucleus communication. Nat Neurosci 4:565-566.

Hardingham GE, Arnold FJ, Bading H (2001b) Nuclear calcium signaling controls CREB-mediated gene expression triggered by synaptic activity. Nat Neurosci 4:261-267.

Hardingham GE, Chawla S, Johnson CM, Bading H (1997) Distinct functions of nuclear and cytoplasmic calcium in the control of gene expression. Nature 385:260-265.

Hardingham GE, Chawla S, Cruzalegui FH, Bading H (1999) Control of recruitment and transcription-activating function of CBP determines gene regulation by NMDA receptors and L-type calcium channels. Neuron 22:789-798.

Hartmann M, Heumann R, Lessmann V (2001) Synaptic secretion of BDNF after high-frequency stimulation of glutamatergic synapses. Embo J 20:5887-5897.

Hendrich B, Bird A (1998) Identification and characterization of a family of mammalian methyl-CpG binding proteins. Mol Cell Biol 18:6538-6547.

Hester I, McKee S, Pelletier P, Thompson C, Storbeck C, Mears A, Schulz JB, Hakim AA, Sabourin LA (2007) Transient expression of Nxf, a bHLH-PAS transactivator induced by neuronal preconditioning, confers neuroprotection in cultured cells. Brain Res 1135:1-11.

Hill-Eubanks DC, Gomez MF, Stevenson AS, Nelson MT (2003) NFAT regulation in smooth muscle. Trends Cardiovasc Med 13:56-62.

Hofer M, Pagliusi SR, Hohn A, Leibrock J, Barde YA (1990) Regional distribution of brain-derived neurotrophic factor mRNA in the adult mouse brain. Embo J 9:2459-2464.
Hogan PG, Chen L, Nardone J, Rao A (2003) Transcriptional regulation by calcium, calcineurin, and NFAT. Genes Dev 17:2205-2232.
Holmqvist MH, Cao J, Knoppers MH, Jurman ME, Distefano PS, Rhodes KJ, Xie Y, An WF (2001) Kinetic modulation of Kv4-mediated A-current by arachidonic acid is dependent on potassium channel interacting proteins. J Neurosci 21:4154-4161.
Holmqvist MH, Cao J, Hernandez-Pineda R, Jacobson MD, Carroll KI, Sung MA, Betty M, Ge P, Gilbride KJ, Brown ME, Jurman ME, Lawson D, Silos-Santiago I, Xie Y, Covarrubias M, Rhodes KJ, Distefano PS, An WF (2002) Elimination of fast inactivation in Kv4 A-type potassium channels by an auxiliary subunit domain. Proc Natl Acad Sci U S A 99:1035-1040.
Hong EJ, McCord AE, Greenberg ME (2008) A biological function for the neuronal activity-dependent component of Bdnf transcription in the development of cortical inhibition. Neuron 60:610-624.
Howells DW, Porritt MJ, Wong JY, Batchelor PE, Kalnins R, Hughes AJ, Donnan GA (2000) Reduced BDNF mRNA expression in the Parkinson's disease substantia nigra. Exp Neurol 166:127-135.
Huang ZJ, Kirkwood A, Pizzorusso T, Porciatti V, Morales B, Bear MF, Maffei L, Tonegawa S (1999a) BDNF regulates the maturation of inhibition and the critical period of plasticity in mouse visual cortex. Cell 98:739-755.
Huang Y, Myers SJ, Dingledine R (1999b) Transcriptional repression by REST: recruitment of Sin3A and histone deacetylase to neuronal genes. Nat Neurosci 2:867-872.
Imamura R, Masuda ES, Naito Y, Imai S, Fujino T, Takano T, Arai K, Arai N (1998) Carboxyl-terminal 15-amino acid sequence of NFATx1 is possibly created by tissue-specific splicing and is essential for transactivation activity in T cells. J Immunol 161:3455-3463.
Ince-Dunn G, Hall BJ, Hu SC, Ripley B, Huganir RL, Olson JM, Tapscott SJ, Ghosh A (2006) Regulation of thalamocortical patterning and synaptic maturation by NeuroD2. Neuron 49:683-695.
Isackson PJ, Huntsman MM, Murray KD, Gall CM (1991) BDNF mRNA expression is increased in adult rat forebrain after limbic seizures: temporal patterns of induction distinct from NGF. Neuron 6:937-948.
Jain J, McCaffrey PG, Valge-Archer VE, Rao A (1992) Nuclear factor of activated T cells contains Fos and Jun. Nature 356:801-804.
Jankowsky JL, Patterson PH (2001) The role of cytokines and growth factors in seizures and their sequelae. Prog Neurobiol 63:125-149.
Jayanthi S, Deng X, Ladenheim B, McCoy MT, Cluster A, Cai NS, Cadet JL (2005) Calcineurin/NFAT-induced up-regulation of the Fas ligand/Fas death pathway is involved in methamphetamine-induced neuronal apoptosis. Proc Natl Acad Sci U S A 102:868-873.

Jiang X, Xu K, Hoberman J, Tian F, Marko AJ, Waheed JF, Harris CR, Marini AM, Enoch MA, Lipsky RH (2005) BDNF variation and mood disorders: a novel functional promoter polymorphism and Val66Met are associated with anxiety but have opposing effects. Neuropsychopharmacology 30:1353-1361.

Jiang X, Tian F, Du Y, Copeland NG, Jenkins NA, Tessarollo L, Wu X, Pan H, Hu XZ, Xu K, Kenney H, Egan SE, Turley H, Harris AL, Marini AM, Lipsky RH (2008) BHLHB2 controls Bdnf promoter 4 activity and neuronal excitability. J Neurosci 28:1118-1130.

Jones KR, Farinas I, Backus C, Reichardt LF (1994) Targeted disruption of the BDNF gene perturbs brain and sensory neuron development but not motor neuron development. Cell 76:989-999.

Kafitz KW, Rose CR, Thoenen H, Konnerth A (1999) Neurotrophin-evoked rapid excitation through TrkB receptors. Nature 401:918-921.

Kang H, Schuman EM (1995) Long-lasting neurotrophin-induced enhancement of synaptic transmission in the adult hippocampus. Science 267:1658-1662.

Kang H, Schuman EM (1996) A requirement for local protein synthesis in neurotrophin-induced hippocampal synaptic plasticity. Science 273:1402-1406.

Kashani AH, Qiu Z, Jurata L, Lee SK, Pfaff S, Goebbels S, Nave KA, Ghosh A (2006) Calcium activation of the LMO4 transcription complex and its role in the patterning of thalamocortical connections. J Neurosci 26:8398-8408.

Katoh-Semba R, Takeuchi IK, Semba R, Kato K (1997) Distribution of brain-derived neurotrophic factor in rats and its changes with development in the brain. J Neurochem 69:34-42.

Kernie SG, Liebl DJ, Parada LF (2000) BDNF regulates eating behavior and locomotor activity in mice. Embo J 19:1290-1300.

Kerr BJ, Bradbury EJ, Bennett DL, Trivedi PM, Dassan P, French J, Shelton DB, McMahon SB, Thompson SW (1999) Brain-derived neurotrophic factor modulates nociceptive sensory inputs and NMDA-evoked responses in the rat spinal cord. J Neurosci 19:5138-5148.

Kohara K, Kitamura A, Morishima M, Tsumoto T (2001) Activity-dependent transfer of brain-derived neurotrophic factor to postsynaptic neurons. Science 291:2419-2423.

Kokaia Z, Gido G, Ringstedt T, Bengzon J, Kokaia M, Siesjo BK, Persson H, Lindvall O (1993) Rapid increase of BDNF mRNA levels in cortical neurons following spreading depression: regulation by glutamatergic mechanisms independent of seizure activity. Brain Res Mol Brain Res 19:277-286.

Kornhauser JM, Cowan CW, Shaywitz AJ, Dolmetsch RE, Griffith EC, Hu LS, Haddad C, Xia Z, Greenberg ME (2002) CREB transcriptional activity in neurons is regulated by multiple, calcium-specific phosphorylation events. Neuron 34:221-233.

Korte M, Kang H, Bonhoeffer T, Schuman E (1998) A role for BDNF in the late-phase of hippocampal long-term potentiation. Neuropharmacology 37:553-559.

Korte M, Griesbeck O, Gravel C, Carroll P, Staiger V, Thoenen H, Bonhoeffer T (1996) Virus-mediated gene transfer into hippocampal CA1 region restores long-term potentiation in brain-derived neurotrophic factor mutant mice. Proc Natl Acad Sci U S A 93:12547-12552.

Kovalchuk Y, Hanse E, Kafitz KW, Konnerth A (2002) Postsynaptic Induction of BDNF-Mediated Long-Term Potentiation. Science 295:1729-1734.

Lau AG, Irier HA, Gu J, Tian D, Ku L, Liu G, Xia M, Fritsch B, Zheng JQ, Dingledine R, Xu B, Lu B, Feng Y (2010) Distinct 3'UTRs differentially regulate activity-dependent translation of brain-derived neurotrophic factor (BDNF). Proc Natl Acad Sci U S A 107:15945-15950.

Ledo F, Kremer L, Mellstrom B, Naranjo JR (2002) Ca2+-dependent block of CREB-CBP transcription by repressor DREAM. Embo J 21:4583-4592.

Ledo F, Carrion AM, Link WA, Mellstrom B, Naranjo JR (2000) DREAM-alphaCREM interaction via leucine-charged domains derepresses downstream regulatory element-dependent transcription. Mol Cell Biol 20:9120-9126.

Lee JE (1997) Basic helix-loop-helix genes in neural development. Curr Opin Neurobiol 7:13-20.

Lee R, Kermani P, Teng KK, Hempstead BL (2001) Regulation of cell survival by secreted proneurotrophins. Science 294:1945-1948.

Lerea LS, Butler LS, McNamara JO (1992) NMDA and non-NMDA receptor-mediated increase of c-fos mRNA in dentate gyrus neurons involves calcium influx via different routes. J Neurosci 12:2973-2981.

Lessmann V, Gottmann K, Malcangio M (2003) Neurotrophin secretion: current facts and future prospects. Prog Neurobiol 69:341-374.

Leventhal C, Rafii S, Rafii D, Shahar A, Goldman SA (1999) Endothelial trophic support of neuronal production and recruitment from the adult mammalian subependyma. Mol Cell Neurosci 13:450-464.

Levi-Montalcini R, Hamburger V (1951) Selective growth stimulating effects of mouse sarcoma on the sensory and sympathetic nervous system of the chick embryo. J Exp Zool 116:321-361.

Levkovitz Y, Baraban JM (2002) A dominant negative Egr inhibitor blocks nerve growth factor-induced neurite outgrowth by suppressing c-Jun activation: role of an Egr/c-Jun complex. J Neurosci 22:3845-3854.

Li YX, Xu Y, Ju D, Lester HA, Davidson N, Schuman EM (1998) Expression of a dominant negative TrkB receptor, T1, reveals a requirement for presynaptic signaling in BDNF-induced synaptic potentiation in cultured hippocampal neurons. Proc Natl Acad Sci U S A 95:10884-10889.

Lilliehook C, Bozdagi O, Yao J, Gomez-Ramirez M, Zaidi NF, Wasco W, Gandy S, Santucci AC, Haroutunian V, Huntley GW, Buxbaum JD (2003) Altered

Abeta formation and long-term potentiation in a calsenilin knock-out. J Neurosci 23:9097-9106.
Lin Y, Bloodgood BL, Hauser JL, Lapan AD, Koon AC, Kim TK, Hu LS, Malik AN, Greenberg ME (2008) Activity-dependent regulation of inhibitory synapse development by Npas4. Nature 455:1198-1204.
Lindvall O, Ernfors P, Bengzon J, Kokaia Z, Smith ML, Siesjo BK, Persson H (1992) Differential regulation of mRNAs for nerve growth factor, brain-derived neurotrophic factor, and neurotrophin 3 in the adult rat brain following cerebral ischemia and hypoglycemic coma. Proc Natl Acad Sci U S A 89:648-652.
Linnarsson S, Bjorklund A, Ernfors P (1997) Learning deficit in BDNF mutant mice. Eur J Neurosci 9:2581-2587.
Liu QR, Lu L, Zhu XG, Gong JP, Shaham Y, Uhl GR (2006) Rodent BDNF genes, novel promoters, novel splice variants, and regulation by cocaine. Brain Res 1067:1-12.
Liu QR, Walther D, Drgon T, Polesskaya O, Lesnick TG, Strain KJ, de Andrade M, Bower JH, Maraganore DM, Uhl GR (2005) Human brain derived neurotrophic factor (BDNF) genes, splicing patterns, and assessments of associations with substance abuse and Parkinson's Disease. Am J Med Genet B Neuropsychiatr Genet 134B:93-103.
Lohof AM, Ip NY, Poo MM (1993) Potentiation of developing neuromuscular synapses by the neurotrophins NT-3 and BDNF. Nature 363:350-353.
Lonze BE, Ginty DD (2002) Function and regulation of CREB family transcription factors in the nervous system. Neuron 35:605-623.
Lou H, Kim SK, Zaitsev E, Snell CR, Lu B, Loh YP (2005) Sorting and activity-dependent secretion of BDNF require interaction of a specific motif with the sorting receptor carboxypeptidase e. Neuron 45:245-255.
Lu B (2003) BDNF and activity-dependent synaptic modulation. Learn Mem 10:86-98.
Lu J, McKinsey TA, Zhang CL, Olson EN (2000) Regulation of skeletal myogenesis by association of the MEF2 transcription factor with class II histone deacetylases. Mol Cell 6:233-244.
Luberg K, Wong J, Weickert CS, Timmusk T (2010) Human TrkB gene: novel alternative transcripts, protein isoforms and expression pattern in the prefrontal cerebral cortex during postnatal development. J Neurochem 113:952-964.
Lubin FD, Johnston LD, Sweatt JD, Anderson AE (2005) Kainate mediates nuclear factor-kappa B activation in hippocampus via phosphatidylinositol-3 kinase and extracellular signal-regulated protein kinase. Neuroscience 133:969-981.
Lubin FD, Ren Y, Xu X, Anderson AE (2007) Nuclear factor-kappa B regulates seizure threshold and gene transcription following convulsant stimulation. J Neurochem 103:1381-1395.

Luo X, Sawadogo M (1996) Functional domains of the transcription factor USF2: atypical nuclear localization signals and context-dependent transcriptional activation domains. Mol Cell Biol 16:1367-1375.
Lyons WE, Mamounas LA, Ricaurte GA, Coppola V, Reid SW, Bora SH, Wihler C, Koliatsos VE, Tessarollo L (1999) Brain-derived neurotrophic factor-deficient mice develop aggressiveness and hyperphagia in conjunction with brain serotonergic abnormalities. Proc Natl Acad Sci U S A 96:15239-15244.
Ma DK, Jang MH, Guo JU, Kitabatake Y, Chang ML, Pow-Anpongkul N, Flavell RA, Lu B, Ming GL, Song H (2009) Neuronal activity-induced Gadd45b promotes epigenetic DNA demethylation and adult neurogenesis. Science 323:1074-1077.
Maisonpierre PC, Belluscio L, Squinto S, Ip NY, Furth ME, Lindsay RM, Yancopoulos GD (1990) Neurotrophin-3: a neurotrophic factor related to NGF and BDNF. Science 247:1446-1451.
Maisonpierre PC, Le Beau MM, Espinosa R, 3rd, Ip NY, Belluscio L, de la Monte SM, Squinto S, Furth ME, Yancopoulos GD (1991) Human and rat brain-derived neurotrophic factor and neurotrophin-3: gene structures, distributions, and chromosomal localizations. Genomics 10:558-568.
Mao Z, Wiedmann M (1999) Calcineurin enhances MEF2 DNA binding activity in calcium-dependent survival of cerebellar granule neurons. J Biol Chem 274:31102-31107.
Mao Z, Bonni A, Xia F, Nadal-Vicens M, Greenberg ME (1999) Neuronal activity-dependent cell survival mediated by transcription factor MEF2. Science 286:785-790.
Markkanen M, Uvarov P, Airaksinen MS (2008) Role of upstream stimulating factors in the transcriptional regulation of the neuron-specific K-Cl cotransporter KCC2. Brain Res 1236:8-15.
Martinowich K, Hattori D, Wu H, Fouse S, He F, Hu Y, Fan G, Sun YE (2003) DNA methylation-related chromatin remodeling in activity-dependent BDNF gene regulation. Science 302:890-893.
Matsumoto T, Rauskolb S, Polack M, Klose J, Kolbeck R, Korte M, Barde YA (2008) Biosynthesis and processing of endogenous BDNF: CNS neurons store and secrete BDNF, not pro-BDNF. Nat Neurosci 11:131-133.
McAllister AK, Katz LC, Lo DC (1997) Opposing roles for endogenous BDNF and NT-3 in regulating cortical dendritic growth. Neuron 18:767-778.
McDowell KA, Hutchinson AN, Wong-Goodrich SJ, Presby MM, Su D, Rodriguiz RM, Law KC, Williams CL, Wetsel WC, West AE (2010) Reduced cortical BDNF expression and aberrant memory in Carf knock-out mice. J Neurosci 30:7453-7465.
McIntosh AM, Moorhead TW, McKirdy J, Sussmann JE, Hall J, Johnstone EC, Lawrie SM (2007) Temporal grey matter reductions in bipolar disorder are associated with the BDNF Val66Met polymorphism. Mol Psychiatry 12:902-903.

McKinsey TA, Zhang CL, Lu J, Olson EN (2000) Signal-dependent nuclear export of a histone deacetylase regulates muscle differentiation. Nature 408:106-111.
Meakin SO, Shooter EM (1992) The nerve growth factor family of receptors. Trends Neurosci 15:323-331.
Meberg PJ, Kinney WR, Valcourt EG, Routtenberg A (1996) Gene expression of the transcription factor NF-kappa B in hippocampus: regulation by synaptic activity. Brain Res Mol Brain Res 38:179-190.
Meehan RR, Lewis JD, Bird AP (1992) Characterization of MeCP2, a vertebrate DNA binding protein with affinity for methylated DNA. Nucleic Acids Res 20:5085-5092.
Meffert MK, Chang JM, Wiltgen BJ, Fanselow MS, Baltimore D (2003) NF-kappa B functions in synaptic signaling and behavior. Nat Neurosci 6:1072-1078.
Mermelstein PG, Deisseroth K, Dasgupta N, Isaksen AL, Tsien RW (2001) Calmodulin priming: nuclear translocation of a calmodulin complex and the memory of prior neuronal activity. Proc Natl Acad Sci U S A 98:15342-15347.
Metsis M, Timmusk T, Arenas E, Persson H (1993) Differential usage of multiple brain-derived neurotrophic factor promoters in the rat brain following neuronal activation. Proc Natl Acad Sci U S A 90:8802-8806.
Meyer-Franke A, Wilkinson GA, Kruttgen A, Hu M, Munro E, Hanson MG, Jr., Reichardt LF, Barres BA (1998) Depolarization and cAMP elevation rapidly recruit TrkB to the plasma membrane of CNS neurons. Neuron 21:681-693.
Minichiello L, Klein R (1996) TrkB and TrkC neurotrophin receptors cooperate in promoting survival of hippocampal and cerebellar granule neurons. Genes Dev 10:2849-2858.
Minichiello L, Korte M, Wolfer D, Kuhn R, Unsicker K, Cestari V, Rossi-Arnaud C, Lipp HP, Bonhoeffer T, Klein R (1999) Essential role for TrkB receptors in hippocampus-mediated learning. Neuron 24:401-414.
Misra RP, Bonni A, Miranti CK, Rivera VM, Sheng M, Greenberg ME (1994) L-type voltage-sensitive calcium channel activation stimulates gene expression by a serum response factor-dependent pathway. J Biol Chem 269:25483-25493.
Molkentin JD, Lu JR, Antos CL, Markham B, Richardson J, Robbins J, Grant SR, Olson EN (1998) A calcineurin-dependent transcriptional pathway for cardiac hypertrophy. Cell 93:215-228.
Moll UM, Marchenko N, Zhang XK (2006) p53 and Nur77/TR3 - transcription factors that directly target mitochondria for cell death induction. Oncogene 25:4725-4743.
Montminy MR, Bilezikjian LM (1987) Binding of a nuclear protein to the cyclic-AMP response element of the somatostatin gene. Nature 328:175-178.
Morgan JI, Curran T (1986) Role of ion flux in the control of c-fos expression. Nature 322:552-555.

Morgan JI, Cohen DR, Hempstead JL, Curran T (1987) Mapping patterns of c-fos expression in the central nervous system after seizure. Science 237:192-197.

Morohashi Y, Hatano N, Ohya S, Takikawa R, Watabiki T, Takasugi N, Imaizumi Y, Tomita T, Iwatsubo T (2002) Molecular cloning and characterization of CALP/KChIP4, a novel EF-hand protein interacting with presenilin 2 and voltage-gated potassium channel subunit Kv4. J Biol Chem 277:14965-14975.

Mowla SJ, Farhadi HF, Pareek S, Atwal JK, Morris SJ, Seidah NG, Murphy RA (2001) Biosynthesis and post-translational processing of the precursor to brain-derived neurotrophic factor. J Biol Chem 276:12660-12666.

Mowla SJ, Pareek S, Farhadi HF, Petrecca K, Fawcett JP, Seidah NG, Morris SJ, Sossin WS, Murphy RA (1999) Differential sorting of nerve growth factor and brain-derived neurotrophic factor in hippocampal neurons. J Neurosci 19:2069-2080.

Murre C, McCaw PS, Vaessin H, Caudy M, Jan LY, Jan YN, Cabrera CV, Buskin JN, Hauschka SD, Lassar AB, et al. (1989) Interactions between heterologous helix-loop-helix proteins generate complexes that bind specifically to a common DNA sequence. Cell 58:537-544.

Nakata K, Ujike H, Sakai A, Uchida N, Nomura A, Imamura T, Katsu T, Tanaka Y, Hamamura T, Kuroda S (2003) Association study of the brain-derived neurotrophic factor (BDNF) gene with bipolar disorder. Neurosci Lett 337:17-20.

Nan X, Meehan RR, Bird A (1993) Dissection of the methyl-CpG binding domain from the chromosomal protein MeCP2. Nucleic Acids Res 21:4886-4892.

Nan X, Campoy FJ, Bird A (1997) MeCP2 is a transcriptional repressor with abundant binding sites in genomic chromatin. Cell 88:471-481.

Neeper SA, Gomez-Pinilla F, Choi J, Cotman CW (1996) Physical activity increases mRNA for brain-derived neurotrophic factor and nerve growth factor in rat brain. Brain Res 726:49-56.

Nguyen T, Di Giovanni S (2008) NFAT signaling in neural development and axon growth. Int J Dev Neurosci 26:141-145.

O'Donovan KJ, Wilkens EP, Baraban JM (1998) Sequential expression of Egr-1 and Egr-3 in hippocampal granule cells following electroconvulsive stimulation. J Neurochem 70:1241-1248.

O'Donovan KJ, Tourtellotte WG, Millbrandt J, Baraban JM (1999) The EGR family of transcription-regulatory factors: progress at the interface of molecular and systems neuroscience. Trends Neurosci 22:167-173.

Odom DT, Dowell RD, Jacobsen ES, Gordon W, Danford TW, MacIsaac KD, Rolfe PA, Conboy CM, Gifford DK, Fraenkel E (2007) Tissue-specific transcriptional regulation has diverged significantly between human and mouse. Nat Genet 39:730-732.

Ohya S, Morohashi Y, Muraki K, Tomita T, Watanabe M, Iwatsubo T, Imaizumi Y (2001) Molecular cloning and expression of the novel splice variants of

K(+) channel-interacting protein 2. Biochem Biophys Res Commun 282:96-102.
Okamura H, Garcia-Rodriguez C, Martinson H, Qin J, Virshup DM, Rao A (2004) A conserved docking motif for CK1 binding controls the nuclear localization of NFAT1. Mol Cell Biol 24:4184-4195.
Ooe N, Saito K, Kaneko H (2009) Characterization of functional heterodimer partners in brain for a bHLH-PAS factor NXF. Biochim Biophys Acta 1789:192-197.
Ooe N, Saito K, Mikami N, Nakatuka I, Kaneko H (2004) Identification of a novel basic helix-loop-helix-PAS factor, NXF, reveals a Sim2 competitive, positive regulatory role in dendritic-cytoskeleton modulator drebrin gene expression. Mol Cell Biol 24:608-616.
Palm K, Belluardo N, Metsis M, Timmusk T (1998) Neuronal expression of zinc finger transcription factor REST/NRSF/XBR gene. J Neurosci 18:1280-1296.
Pang PT, Teng HK, Zaitsev E, Woo NT, Sakata K, Zhen S, Teng KK, Yung WH, Hempstead BL, Lu B (2004) Cleavage of proBDNF by tPA/plasmin is essential for long-term hippocampal plasticity. Science 306:487-491.
Park KY, Russo AF (2008) Control of the calcitonin gene-related peptide enhancer by upstream stimulatory factor in trigeminal ganglion neurons. J Biol Chem 283:5441-5451.
Park SY, Lee JY, Choi JY, Park MJ, Kim DS (2006) Nerve growth factor activates brain-derived neurotrophic factor promoter IV via extracellular signal-regulated protein kinase 1/2 in PC12 cells. Mol Cells 21:237-243.
Patapoutian A, Reichardt LF (2001) Trk receptors: mediators of neurotrophin action. Curr Opin Neurobiol 11:272-280.
Patterson SL, Grover LM, Schwartzkroin PA, Bothwell M (1992) Neurotrophin expression in rat hippocampal slices: a stimulus paradigm inducing LTP in CA1 evokes increases in BDNF and NT-3 mRNAs. Neuron 9:1081-1088.
Patterson SL, Abel T, Deuel TA, Martin KC, Rose JC, Kandel ER (1996) Recombinant BDNF rescues deficits in basal synaptic transmission and hippocampal LTP in BDNF knockout mice. Neuron 16:1137-1145.
Pezet S, Malcangio M, Lever IJ, Perkinton MS, Thompson SW, Williams RJ, McMahon SB (2002) Noxious stimulation induces Trk receptor and downstream ERK phosphorylation in spinal dorsal horn. Mol Cell Neurosci 21:684-695.
Petryshen TL, Sabeti PC, Aldinger KA, Fry B, Fan JB, Schaffner SF, Waggoner SG, Tahl AR, Sklar P (2010) Population genetic study of the brain-derived neurotrophic factor (BDNF) gene. Mol Psychiatry 15:810-815.
Pfenning AR, Kim TK, Spotts JM, Hemberg M, Su D, West AE (2010) Genome-wide identification of calcium-response factor (CaRF) binding sites predicts a role in regulation of neuronal signaling pathways. PLoS One 5:e10870.

Phillips HS, Hains JM, Laramee GR, Rosenthal A, Winslow JW (1990) Widespread expression of BDNF but not NT3 by target areas of basal forebrain cholinergic neurons. Science 250:290-294.
Phillips HS, Hains JM, Armanini M, Laramee GR, Johnson SA, Winslow JW (1991) BDNF mRNA is decreased in the hippocampus of individuals with Alzheimer's disease. Neuron 7:695-702.
Pipes GC, Creemers EE, Olson EN (2006) The myocardin family of transcriptional coactivators: versatile regulators of cell growth, migration, and myogenesis. Genes Dev 20:1545-1556.
Ploski JE, Newton SS, Duman RS (2006) Electroconvulsive seizure-induced gene expression profile of the hippocampus dentate gyrus granule cell layer. J Neurochem 99:1122-1132.
Plyte S, Boncristiano M, Fattori E, Galvagni F, Paccani SR, Majolini MB, Oliviero S, Ciliberto G, Telford JL, Baldari CT (2001) Identification and characterization of a novel nuclear factor of activated T-cells-1 isoform expressed in mouse brain. J Biol Chem 276:14350-14358.
Poo MM (2001) Neurotrophins as synaptic modulators. Nat Rev Neurosci 2:24-32.
Posern G, Treisman R (2006) Actin' together: serum response factor, its cofactors and the link to signal transduction. Trends Cell Biol 16:588-596.
Posern G, Sotiropoulos A, Treisman R (2002) Mutant actins demonstrate a role for unpolymerized actin in control of transcription by serum response factor. Mol Biol Cell 13:4167-4178.
Pozzo-Miller LD, Gottschalk W, Zhang L, McDermott K, Du J, Gopalakrishnan R, Oho C, Sheng ZH, Lu B (1999) Impairments in high-frequency transmission, synaptic vesicle docking, and synaptic protein distribution in the hippocampus of BDNF knockout mice. J Neurosci 19:4972-4983.
Prabhakar S, Visel A, Akiyama JA, Shoukry M, Lewis KD, Holt A, Plajzer-Frick I, Morrison H, Fitzpatrick DR, Afzal V, Pennacchio LA, Rubin EM, Noonan JP (2008) Human-specific gain of function in a developmental enhancer. Science 321:1346-1350.
Pu L, Liu QS, Poo MM (2006) BDNF-dependent synaptic sensitization in midbrain dopamine neurons after cocaine withdrawal. Nat Neurosci 9:605-607.
Qiu Z, Ghosh A (2008) A calcium-dependent switch in a CREST-BRG1 complex regulates activity-dependent gene expression. Neuron 60:775-787.
Ranger AM, Grusby MJ, Hodge MR, Gravallese EM, de la Brousse FC, Hoey T, Mickanin C, Baldwin HS, Glimcher LH (1998) The transcription factor NF-ATc is essential for cardiac valve formation. Nature 392:186-190.
Rao A, Luo C, Hogan PG (1997) Transcription factors of the NFAT family: regulation and function. Annu Rev Immunol 15:707-747.
Rauskolb S, Zagrebelsky M, Dreznjak A, Deogracias R, Matsumoto T, Wiese S, Erne B, Sendtner M, Schaeren-Wiemers N, Korte M, Barde YA (2010) Global deprivation of brain-derived neurotrophic factor in the CNS reveals an area-specific requirement for dendritic growth. J Neurosci 30:1739-1749.

Ribases M, Gratacos M, Armengol L, de Cid R, Badia A, Jimenez L, Solano R, Vallejo J, Fernandez F, Estivill X (2003) Met66 in the brain-derived neurotrophic factor (BDNF) precursor is associated with anorexia nervosa restrictive type. Mol Psychiatry 8:745-751.

Righi M, Tongiorgi E, Cattaneo A (2000) Brain-derived neurotrophic factor (BDNF) induces dendritic targeting of BDNF and tyrosine kinase B mRNAs in hippocampal neurons through a phosphatidylinositol-3 kinase-dependent pathway. J Neurosci 20:3165-3174.

Rios M, Fan G, Fekete C, Kelly J, Bates B, Kuehn R, Lechan RM, Jaenisch R (2001) Conditional deletion of brain-derived neurotrophic factor in the postnatal brain leads to obesity and hyperactivity. Mol Endocrinol 15:1748-1757.

Rivera VM, Miranti CK, Misra RP, Ginty DD, Chen RH, Blenis J, Greenberg ME (1993) A growth factor-induced kinase phosphorylates the serum response factor at a site that regulates its DNA-binding activity. Mol Cell Biol 13:6260-6273.

Rocamora N, Welker E, Pascual M, Soriano E (1996) Upregulation of BDNF mRNA expression in the barrel cortex of adult mice after sensory stimulation. J Neurosci 16:4411-4419.

Roopra A, Sharling L, Wood IC, Briggs T, Bachfischer U, Paquette AJ, Buckley NJ (2000) Transcriptional repression by neuron-restrictive silencer factor is mediated via the Sin3-histone deacetylase complex. Mol Cell Biol 20:2147-2157.

Rossner MJ, Dorr J, Gass P, Schwab MH, Nave KA (1997) SHARPs: mammalian enhancer-of-split- and hairy-related proteins coupled to neuronal stimulation. Mol Cell Neurosci 10:460-475.

Saffen DW, Cole AJ, Worley PF, Christy BA, Ryder K, Baraban JM (1988) Convulsant-induced increase in transcription factor messenger RNAs in rat brain. Proc Natl Acad Sci U S A 85:7795-7799.

Schinder AF, Poo M (2000) The neurotrophin hypothesis for synaptic plasticity. Trends Neurosci 23:639-645.

Schock SC, Xu J, Duquette PM, Qin Z, Lewandowski AJ, Rai PS, Thompson CS, Seifert EL, Harper ME, Chen HH (2008) Rescue of neurons from ischemic injury by peroxisome proliferator-activated receptor-gamma requires a novel essential cofactor LMO4. J Neurosci 28:12433-12444.

Schwartz PM, Levy RL, Borghesani PR, Segal RA (1998) Cerebellar pathology in BDNF -/- mice: the classic view of neurotrophins is changing. Mol Psychiatry 3:116-120.

Schwartz PM, Borghesani PR, Levy RL, Pomeroy SL, Segal RA (1997) Abnormal cerebellar development and foliation in BDNF-/- mice reveals a role for neurotrophins in CNS patterning. Neuron 19:269-281.

Seidah NG, Benjannet S, Pareek S, Chretien M, Murphy RA (1996) Cellular processing of the neurotrophin precursors of NT3 and BDNF by the mammalian proprotein convertases. FEBS Lett 379:247-250.

Shalizi A, Gaudilliere B, Yuan Z, Stegmuller J, Shirogane T, Ge Q, Tan Y, Schulman B, Harper JW, Bonni A (2006) A calcium-regulated MEF2 sumoylation switch controls postsynaptic differentiation. Science 311:1012-1017.

Shaw PE, Schroter H, Nordheim A (1989) The ability of a ternary complex to form over the serum response element correlates with serum inducibility of the human c-fos promoter. Cell 56:563-572.

Sheng M, McFadden G, Greenberg ME (1990) Membrane depolarization and calcium induce c-fos transcription via phosphorylation of transcription factor CREB. Neuron 4:571-582.

Shieh PB, Hu SC, Bobb K, Timmusk T, Ghosh A (1998) Identification of a signaling pathway involved in calcium regulation of BDNF expression. Neuron 20:727-740.

Sirito M, Lin Q, Maity T, Sawadogo M (1994) Ubiquitous expression of the 43- and 44-kDa forms of transcription factor USF in mammalian cells. Nucleic Acids Res 22:427-433.

Sirito M, Lin Q, Deng JM, Behringer RR, Sawadogo M (1998) Overlapping roles and asymmetrical cross-regulation of the USF proteins in mice. Proc Natl Acad Sci U S A 95:3758-3763.

Skene PJ, Illingworth RS, Webb S, Kerr AR, James KD, Turner DJ, Andrews R, Bird AP (2010) Neuronal MeCP2 is expressed at near histone-octamer levels and globally alters the chromatin state. Mol Cell 37:457-468.

Smith MA, Makino S, Kvetnansky R, Post RM (1995) Stress and glucocorticoids affect the expression of brain-derived neurotrophic factor and neurotrophin-3 mRNAs in the hippocampus. J Neurosci 15:1768-1777.

Soliman F, Glatt CE, Bath KG, Levita L, Jones RM, Pattwell SS, Jing D, Tottenham N, Amso D, Somerville LH, Voss HU, Glover G, Ballon DJ, Liston C, Teslovich T, Van Kempen T, Lee FS, Casey BJ (2010) A genetic variant BDNF polymorphism alters extinction learning in both mouse and human. Science 327:863-866.

Sonnenberg JL, Rauscher FJ, 3rd, Morgan JI, Curran T (1989a) Regulation of proenkephalin by Fos and Jun. Science 246:1622-1625.

Sonnenberg JL, Mitchelmore C, Macgregor-Leon PF, Hempstead J, Morgan JI, Curran T (1989b) Glutamate receptor agonists increase the expression of Fos, Fra, and AP-1 DNA binding activity in the mammalian brain. J Neurosci Res 24:72-80.

Spreafico F, Barski JJ, Farina C, Meyer M (2001) Mouse DREAM/calsenilin/KChIP3: gene structure, coding potential, and expression. Mol Cell Neurosci 17:1-16.

Stoop R, Poo MM (1996) Synaptic modulation by neurotrophic factors: differential and synergistic effects of brain-derived neurotrophic factor and ciliary neurotrophic factor. J Neurosci 16:3256-3264.

Sukhatme VP, Cao XM, Chang LC, Tsai-Morris CH, Stamenkovich D, Ferreira PC, Cohen DR, Edwards SA, Shows TB, Curran T, et al. (1988) A zinc

finger-encoding gene coregulated with c-fos during growth and differentiation, and after cellular depolarization. Cell 53:37-43.
Suzuki S, Suzuki N, Mirtsos C, Horacek T, Lye E, Noh SK, Ho A, Bouchard D, Mak TW, Yeh WC (2003) Nur77 as a survival factor in tumor necrosis factor signaling. Proc Natl Acad Sci U S A 100:8276-8280.
Suzuki T, Mitake S, Okumura-Noji K, Yang JP, Fujii T, Okamoto T (1997) Presence of NF-kappaB-like and IkappaB-like immunoreactivities in postsynaptic densities. Neuroreport 8:2931-2935.
Tabuchi A, Sakaya H, Kisukeda T, Fushiki H, Tsuda M (2002) Involvement of an upstream stimulatory factor as well as cAMP-responsive element-binding protein in the activation of brain-derived neurotrophic factor gene promoter I. J Biol Chem 277:35920-35931.
Takahashi M, Hayashi S, Kakita A, Wakabayashi K, Fukuda M, Kameyama S, Tanaka R, Takahashi H, Nawa H (1999) Patients with temporal lobe epilepsy show an increase in brain-derived neurotrophic factor protein and its correlation with neuropeptide Y. Brain Res 818:579-582.
Takeuchi Y, Miyamoto E, Fukunaga K (2002) Analysis on the promoter region of exon IV brain-derived neurotrophic factor in NG108-15 cells. J Neurochem 83:67-79.
Tao X, Finkbeiner S, Arnold DB, Shaywitz AJ, Greenberg ME (1998) Ca2+ influx regulates BDNF transcription by a CREB family transcription factor-dependent mechanism. Neuron 20:709-726.
Tao X, West AE, Chen WG, Corfas G, Greenberg ME (2002) A calcium-responsive transcription factor, CaRF, that regulates neuronal activity-dependent expression of BDNF. Neuron 33:383-395.
Teng HK, Teng KK, Lee R, Wright S, Tevar S, Almeida RD, Kermani P, Torkin R, Chen ZY, Lee FS, Kraemer RT, Nykjaer A, Hempstead BL (2005) ProBDNF induces neuronal apoptosis via activation of a receptor complex of p75NTR and sortilin. J Neurosci 25:5455-5463.
Thoenen H (1995) Neurotrophins and neuronal plasticity. Science 270:593-598.
Timmusk T, Persson H, Metsis M (1994a) Analysis of transcriptional initiation and translatability of brain-derived neurotrophic factor mRNAs in the rat brain. Neurosci Lett 177:27-31.
Timmusk T, Belluardo N, Persson H, Metsis M (1994b) Developmental regulation of brain-derived neurotrophic factor messenger RNAs transcribed from different promoters in the rat brain. Neuroscience 60:287-291.
Timmusk T, Palm K, Lendahl U, Metsis M (1999) Brain-derived neurotrophic factor expression in vivo is under the control of neuron-restrictive silencer element. J Biol Chem 274:1078-1084.
Timmusk T, Palm K, Metsis M, Reintam T, Paalme V, Saarma M, Persson H (1993) Multiple promoters direct tissue-specific expression of the rat BDNF gene. Neuron 10:475-489.

Tongiorgi E, Righi M, Cattaneo A (1997) Activity-dependent dendritic targeting of BDNF and TrkB mRNAs in hippocampal neurons. J Neurosci 17:9492-9505.
Travers AA (2003) Priming the nucleosome: a role for HMGB proteins? EMBO Rep 4:131-136.
Treisman R (1987) Identification and purification of a polypeptide that binds to the c-fos serum response element. Embo J 6:2711-2717.
Tucker KL, Meyer M, Barde YA (2001) Neurotrophins are required for nerve growth during development. Nat Neurosci 4:29-37.
Tudor M, Akbarian S, Chen RZ, Jaenisch R (2002) Transcriptional profiling of a mouse model for Rett syndrome reveals subtle transcriptional changes in the brain. Proc Natl Acad Sci U S A 99:15536-15541.
Valen E, Pascarella G, Chalk A, Maeda N, Kojima M, Kawazu C, Murata M, Nishiyori H, Lazarevic D, Motti D, Marstrand TT, Tang MH, Zhao X, Krogh A, Winther O, Arakawa T, Kawai J, Wells C, Daub C, Harbers M, Hayashizaki Y, Gustincich S, Sandelin A, Carninci P (2009) Genome-wide detection and analysis of hippocampus core promoters using DeepCAGE. Genome Res 19:255-265.
Watson FL, Heerssen HM, Moheban DB, Lin MZ, Sauvageot CM, Bhattacharyya A, Pomeroy SL, Segal RA (1999) Rapid nuclear responses to target-derived neurotrophins require retrograde transport of ligand-receptor complex. J Neurosci 19:7889-7900.
Webster MJ, Herman MM, Kleinman JE, Shannon Weickert C (2006) BDNF and trkB mRNA expression in the hippocampus and temporal cortex during the human lifespan. Gene Expr Patterns 6:941-951.
Vega RB, Harrison BC, Meadows E, Roberts CR, Papst PJ, Olson EN, McKinsey TA (2004) Protein kinases C and D mediate agonist-dependent cardiac hypertrophy through nuclear export of histone deacetylase 5. Mol Cell Biol 24:8374-8385.
Wellmann H, Kaltschmidt B, Kaltschmidt C (2001) Retrograde transport of transcription factor NF-kappa B in living neurons. J Biol Chem 276:11821-11829.
Verhagen M, van der Meij A, van Deurzen PA, Janzing JG, Arias-Vasquez A, Buitelaar JK, Franke B (2010) Meta-analysis of the BDNF Val66Met polymorphism in major depressive disorder: effects of gender and ethnicity. Mol Psychiatry 15:260-271.
Wilson MD, Odom DT (2009) Evolution of transcriptional control in mammals. Curr Opin Genet Dev 19:579-585.
Wilson MD, Barbosa-Morais NL, Schmidt D, Conboy CM, Vanes L, Tybulewicz VL, Fisher EM, Tavare S, Odom DT (2008) Species-specific transcription in mice carrying human chromosome 21. Science 322:434-438.
von Bartheld CS, Williams R, Lefcort F, Clary DO, Reichardt LF, Bothwell M (1996) Retrograde transport of neurotrophins from the eye to the brain in

chick embryos: roles of the p75NTR and trkB receptors. J Neurosci 16:2995-3008.
Wu GY, Deisseroth K, Tsien RW (2001) Activity-dependent CREB phosphorylation: convergence of a fast, sensitive calmodulin kinase pathway and a slow, less sensitive mitogen-activated protein kinase pathway. Proc Natl Acad Sci U S A 98:2808-2813.
Wu X, Zhang T, Bossuyt J, Li X, McKinsey TA, Dedman JR, Olson EN, Chen J, Brown JH, Bers DM (2006) Local InsP3-dependent perinuclear Ca2+ signaling in cardiac myocyte excitation-transcription coupling. J Clin Invest 116:675-682.
Xia Z, Dudek H, Miranti CK, Greenberg ME (1996) Calcium influx via the NMDA receptor induces immediate early gene transcription by a MAP kinase/ERK-dependent mechanism. J Neurosci 16:5425-5436.
Yamamoto M, Sobue G, Yamamoto K, Terao S, Mitsuma T (1996) Expression of mRNAs for neurotrophic factors (NGF, BDNF, NT-3, and GDNF) and their receptors (p75NGFR, trkA, trkB, and trkC) in the adult human peripheral nervous system and nonneural tissues. Neurochem Res 21:929-938.
Yang J, Siao CJ, Nagappan G, Marinic T, Jing D, McGrath K, Chen ZY, Mark W, Tessarollo L, Lee FS, Lu B, Hempstead BL (2009) Neuronal release of proBDNF. Nat Neurosci 12:113-115.
Yano H, Lee FS, Kong H, Chuang J, Arevalo J, Perez P, Sung C, Chao MV (2001) Association of Trk neurotrophin receptors with components of the cytoplasmic dynein motor. J Neurosci 21:RC125.
Yasuda M, Fukuchi M, Tabuchi A, Kawahara M, Tsuneki H, Azuma Y, Chiba Y, Tsuda M (2007) Robust stimulation of TrkB induces delayed increases in BDNF and Arc mRNA expressions in cultured rat cortical neurons via distinct mechanisms. J Neurochem 103:626-636.
Yoon H, Oh YT, Lee JY, Choi JH, Lee JH, Baik HH, Kim SS, Choe W, Yoon KS, Ha J, Kang I (2008) Activation of AMP-activated protein kinase by kainic acid mediates brain-derived neurotrophic factor expression through a NF-kappaB dependent mechanism in C6 glioma cells. Biochem Biophys Res Commun 371:495-500.
Young D, Lawlor PA, Leone P, Dragunow M, During MJ (1999) Environmental enrichment inhibits spontaneous apoptosis, prevents seizures and is neuroprotective. Nat Med 5:448-453.
Yu Z, Zhou D, Bruce-Keller AJ, Kindy MS, Mattson MP (1999) Lack of the p50 subunit of nuclear factor-kappaB increases the vulnerability of hippocampal neurons to excitotoxic injury. J Neurosci 19:8856-8865.
Yuan SH, Qiu Z, Ghosh A (2009) TOX3 regulates calcium-dependent transcription in neurons. Proc Natl Acad Sci U S A 106:2909-2914.
Zafra F, Hengerer B, Leibrock J, Thoenen H, Lindholm D (1990) Activity dependent regulation of BDNF and NGF mRNAs in the rat hippocampus is mediated by non-NMDA glutamate receptors. Embo J 9:3545-3550.

Zafra F, Lindholm D, Castren E, Hartikka J, Thoenen H (1992) Regulation of brain-derived neurotrophic factor and nerve growth factor mRNA in primary cultures of hippocampal neurons and astrocytes. J Neurosci 12:4793-4799.

Zhang SJ, Zou M, Lu L, Lau D, Ditzel DA, Delucinge-Vivier C, Aso Y, Descombes P, Bading H (2009) Nuclear calcium signaling controls expression of a large gene pool: identification of a gene program for acquired neuroprotection induced by synaptic activity. PLoS Genet 5:e1000604.

Zhou Z, Hong EJ, Cohen S, Zhao WN, Ho HY, Schmidt L, Chen WG, Lin Y, Savner E, Griffith EC, Hu L, Steen JA, Weitz CJ, Greenberg ME (2006) Brain-specific phosphorylation of MeCP2 regulates activity-dependent Bdnf transcription, dendritic growth, and spine maturation. Neuron 52:255-269.

Zigova T, Pencea V, Wiegand SJ, Luskin MB (1998) Intraventricular administration of BDNF increases the number of newly generated neurons in the adult olfactory bulb. Mol Cell Neurosci 11:234-245.

Zuccato C, Belyaev N, Conforti P, Ooi L, Tartari M, Papadimou E, MacDonald M, Fossale E, Zeitlin S, Buckley N, Cattaneo E (2007) Widespread disruption of repressor element-1 silencing transcription factor/neuron-restrictive silencer factor occupancy at its target genes in Huntington's disease. J Neurosci 27:6972-6983.

Zuccato C, Tartari M, Crotti A, Goffredo D, Valenza M, Conti L, Cataudella T, Leavitt BR, Hayden MR, Timmusk T, Rigamonti D, Cattaneo E (2003) Huntingtin interacts with REST/NRSF to modulate the transcription of NRSE-controlled neuronal genes. Nat Genet 35:76-83.

Zuccato C, Ciammola A, Rigamonti D, Leavitt BR, Goffredo D, Conti L, MacDonald ME, Friedlander RM, Silani V, Hayden MR, Timmusk T, Sipione S, Cattaneo E (2001) Loss of huntingtin-mediated BDNF gene transcription in Huntington's disease. Science 293:493-498.

ACKNOWLEDGEMENTS

This work was completed in Department of Gene Technology at Tallinn University of Technology, Estonia.

I would like to express sincere appreciation to my supervisor professor Tõnis Timmusk for leading my way in science and being the driving force and support to my efforts for the past 7 years.

I am indebted to all of the lecturers at the Department of Gene Technology for sharing their knowledge.

I thank professor Madis Metsis for critically reading the manuscript of the thesis.

Many thanks to Indrek Koppel, Mari Sepp, Karin Tamm, Marko Piirsoo, Richard Tamme, Epp Väli, Tamara Aid-Pavlidis, Anna Kazantseva, Anne Kaljas, Anželika Sarapuu, Hanna Vihma, Martin Kask, Kaur Jaanson, Kaja Kannike, Ave Eesmaa, Grete Rullinkov, Helen Verev, Ester Orav, Madis Jaagura, Elina Aleksejeva, Mirjam Luhakooder, Ingrid Lekk, Kati Taal and Rahel Park for being kind, joyful and ready-to-lend-a-hand labmates.

I thank all the co-authors of my publications: people from the Neuro lab at GTI, Kaia Palm from Protobios and people from the lab of Michal Hetman at Kentucky Spinal Cord Injury Research Center.

I am thankful to my first supervisors, Rita Hõrak, Maia Kivisaar and Heili Ilves at University of Tartu, for teaching me the fundamental skills in the lab that were of great help to me in my further studies.

My fairly unique thanks go to Mari, who has been particularly helpful in the maturation of this thesis in several ways.

Most importantly, I am grateful to my mother and father, Pille, Tom and Jenna for creating such a supporting environment.

ABSTRACT

Brain-derived neurotrophic factor (BDNF) has been found to have fundamental roles in development and physiology of the nervous system. Neuronal-activity is the central factor in the regulation of *BDNF* expression and a number of Ca^{2+}-dependent transcription factors have been shown to regulate rodent *BDNF* transcription. However, several protein families besides the conventional neuronal activity-regulated factors have been recently implicated in Ca^{2+}-dependent transcription, but their role in *BDNF* regulation has not been reported. Moreover, regulation of human *BDNF* transcription has not been well characterized, although knowledge about human *BDNF* regulation would be of great importance since dysregulation of *BDNF* expression has been associated with a number of neuropsychiatric disorders. In the light of this, it is important to study regulation of human *BDNF* transcription and to test whether the activity-dependent transcription factors that have not been reported to regulate *BDNF*, are involved in *BDNF* expression. In this thesis I describe the research that was undertaken to: a) characterize the expression and gene structures of Ca^{2+}-regulated transcription factor family genes the functions of which have been poorly characterized in neurons, and b) specify the *cis*-elements and transcription factors involved in neuronal activity-dependent induction of human *BDNF* transcription.

Characterization of the structures, alternative splicing and expression of the human and mouse Ca^{2+}-regulated transcription factor *KCNIP* and *NFAT* gene families showed that alternatively spliced *KCNIP* and *NFAT* mRNAs are expressed in brain with specific patterns for different transcripts. Description of the gene structure and expression of human *BDNF* revealed that it contains two more exons than the rodent *BDNF*, having 11 exons and nine functional promoters. In addition, endogenous non-coding antisense RNAs are transcribed from the human *BDNF* gene locus. Detailed analysis of human *BDNF* transcriptional activation by neuronal activity established that exon I and IV transcripts of human *BDNF* are the most up-regulated human *BDNF* mRNAs by neuronal activity. Activity-regulated induction of human *BDNF* promoter I depends primarily on a novel PasRE element, activity-regulated induction of promoter IV depends predominantly on CRE, PasRE and UBE elements and activity-regulated induction of human *BDNF* promoter IX depends primarily on PasRE and CRE-like elements. In addition, the novel PasRE elements in promoters I and IV are conserved in human and rodents and are bound by bHLH-PAS transcription factor ARNT2-NPAS4 heterodimers. Finally, analysis of the role of KCNIP and NFAT factors in Ca^{2+}-regulated transcription of *BDNF* showed that the KCNIP proteins do not affect *BDNF* induction, whereas NFATc4 contributes to induction of human *BDNF* promoter IV in an NMDA receptor activity-dependent manner. Overall, this study adds novel *cis*-elements and *trans*-factors, namely the PasRE and NFAT binding elements and NPAS4, ARNT2 and NFATc4 proteins, to the list of activity-dependent transcriptional regulators of *BDNF*.

KOKKUVÕTE

Närvirakud sõltuvad suurel määral närvikasvuteguritest, mis toetavad nende eluspüsimist organismi arengu käigus. Üks närvikasvuteguritest, ajust pärinev neurotroofne tegur BDNF, omab väga olulist rolli ka täiskasvanud närvisüsteemi füsioloogias, kusjuures selle rolli korraldamisel on üheks kõige tähtsamaks teguriks *BDNF*i avaldumist üles timmiv* närvitalitlus. Roti ja hiire *BDNF* geeni avaldumise uurimisel on tuvastatud, et *BDNF*i transkriptsiooni timmivad mitmed erinevad Ca^{2+}-sõltuvad transkriptsioonitegurid. Lisaks hästi uuritud närvitalitlusest sõltuvatele valkudele, mis juhivad *BDNF*i geeni avaldumist, timmivad Ca^{2+}-sõltuvat geenide avaldumist närvisüsteemis veel mitmed valguperekonnad, kuid nende rolli *BDNF*i avaldumises pole siiani selgitatud. Põhjalikult pole uuritud ka inimese *BDNF* geeni timmimist, kuigi see oleks vägagi oluline, sest normist kõrvalekaldeid *BDNF*i avaldumises on täheldatud mitmete neuropsühhiaatriliste häirete puhul. Just seetõttu on inimese *BDNF*i geeni avaldumise timmimise uurimine tähtis. Sealjuures tuleks katsetada, kas need transkriptsioonitegurid, mille puhul on kirjeldatud närvitalitlusest sõltuv aktiivsus, aga pole näidatud osalust *BDNF*i avaldumises, timmivad *BDNF*i. Käesolevas teoses kirjeldan uurimistöid, mida teostati selleks, et a) selgitada närvirakkudes vähe uuritud Ca^{2+}-timmitavate transkriptsioonitegurite perekondade geenide struktuure ja avaldumist ja b) teha kindalks DNA järjestused ja transkriptsioonitegurid, mis osalevad närvitalitlusest sõltuvas inimese *BDNF* geeni avaldumise ülestimmimises.

Ca^{2+}-timmitavate transkriptsioonitegurite *KCNIP* ja *NFAT* geenide ehituste, alternatiivse splaissingu ja avaldumise kirjeldamine näitas, et iga alternatiivselt splaissitud *KCNIP* ja *NFAT* mRNA avaldub ajus eripäraselt. Inimese *BDNF* geeni ehituse ja avaldumise uurimisega tehti kindalks, et inimese *BDNF*i geenis on kaks eksonit enam kui roti või hiire *BDNF* geenis. Inimese *BDNF* sisaldab 11 eksonit ja üheksat promootorit. Lisaks transkribeeritakse inimeses *BDNF* geeniga vastassuunalisi valku mitte-avaldavaid mRNAsid. Inimese *BDNF* geeni närvitalitlusest sõltuva avaldumise ülestimmimise üksikasjalik uurimine selgitas, et närvitalitlusest tingituna timmitakse kõige enam üles inimese *BDNF* geeni eksonit I ja IV sisaldavate transkriptide avaldumine. Inimese *BDNF* geeni promootor I talitlustingitud ülestimmimine sõltub peamiselt uudsest *cis*-elemendist PasRE, *BDNF* geeni promootor IV talitlustingitud ülestimmimine sõltub peamiselt *cis*-elementidest CRE, PasRE ja UBE ja talitlustingitud inimese *BDNF*i promootor IX ülestimmimine sõltub eeskätt CRE-sarnasest *cis*-elemendist ja PasRE *cis*-elemendist. Uudsed PasRE järjestused promootorites I ja IV on olemas ka hiire ja roti *BDNF* geenides ja nendele seonduvad bHLH-PAS trankriptsioonitegurite ARNT2 ja NPAS4 dimeerid. Takkapihta sai uuritud KCNIP ja NFAT tegurite osalust *BDNF*i Ca^{2+}-timmitud avaldumises, mis näitas, et KCNIP valgud ei timmi *BDNF*i avaldumise ülesjuhtimist, kuid NFATc4 on kaastegev inimese *BDNF*i promootor IV NMDA retseptori talitlusest sõltuval ülestimmimisel. Kokkuvõtteks märgin, et käesoleva töö tulemusel saab *BDNF* geeni närvitalitlusest sõltuva

transkriptsiooni timmijate nimistusse lisada NFAT valke siduva järjestuse, PasRE järjestused ja NFATc4 ning ARNT2 ja NPAS4 valgud.

* timmima – reguleerima

PUBLICATION I

Pruunsild P, Timmusk T. (2005)
Structure, alternative splicing, and expression of the human and mouse *KCNIP* gene family.
Genomics, Nov;86(5):581-593

Available online at www.sciencedirect.com
SCIENCE DIRECT
Genomics 86 (2005) 581 – 593
GENOMICS
www.elsevier.com/locate/ygeno

Structure, alternative splicing, and expression of the human and mouse KCNIP gene family☆

Priit Pruunsild, Tõnis Timmusk*

Department of Gene Technology, Tallinn University of Technology, Akadeemia tee 15, Tallinn 19086, Estonia
National Institute of Chemical Physics and Biophysics, Akadeemia tee 23, Tallinn 12618, Estonia

Received 14 April 2005; accepted 5 July 2005
Available online 19 August 2005

Abstract

Potassium channel-interacting proteins (KCNIPs, also named KChIPs) modulate A-type potassium channels and favor their surface expression. In addition, KCNIPs have been shown to interact with presenilins and also to function as transcriptional repressors. Here we describe the structures and alternative splicing of the human and mouse *KCNIP* genes, including novel splice variants for *KCNIP1, KCNIP3,* and *KCNIP4,* and show the expression of different *KCNIP* mRNAs in various mouse and human tissues and brain regions by RT-PCR. Furthermore, we describe the expression of *KCNIP1, KCNIP2, KCNIP3,* and *KCNIP4* mRNAs in the adult mouse brain with in situ hybridization and show that all *KCNIP* mRNAs were expressed in the neurons of the mouse brain with specific patterns for each *KCNIP.* Our results show that alternatively spliced *KCNIP* mRNAs are expressed differentially and could contribute to the diversity of functions of the KCNIP proteins.

Keywords: DREAM; Calsenilin; KChIP; Alternative splicing; Potassium channels; Transcriptional repressor; Presenilin; Nervous system

KCNIPs, potassium channel-interacting proteins, are a family of calcium binding proteins with four EF-hand motifs, which have been implicated in the modulation of A-type potassium channels [1]. They have been shown to modulate and favor the surface expression of neuronal and cardiac A-type Kv-4 channels [2,3]. Interestingly, two members of the family, KCNIP3 and KCNIP4, have been shown to interact with presenilins and to regulate the levels of presenilin fragments and have also been named calsenilin [4] and CALP [5], respectively. This knowledge of the dual activity of KCNIPs has expanded further, because KCNIP3/calsenilin was found to be also a Ca^{2+}-regulated transcriptional repressor and was named DREAM (downstream regulatory element antagonist modulator) [6]. It was shown to bind to a regulatory element downstream of the transcription start site of the prodynorphin gene (DRE) and repress the expression of prodynorphin in the absence of calcium. Putative DREs are present in many genes [7,8] and in addition to DREAM, other KCNIP family proteins have the ability to bind DRE sites in vitro and to repress transcription in transient overexpression assays [9].

The KCNIPs differ from other proteins in the family of neuronal calcium binding proteins because they contain a variable N-terminal sequence that shares no homology with other calcium-binding protein domains (reviewed in [10]). Interestingly, the N-termini among the KCNIPs themselves are also unique and share no homology [1]. It has also been found that one *KCNIP* gene can encode more than one

☆ Sequence data from this article have been deposited in the GenBank Data Libraries under Accession Nos. DQ148476, DQ148477, DQ148478, DQ148479 (Human KCNIP1 isoforms); DQ148480, DQ148481, DQ148482, DQ148483, DQ148484 (Human KCNIP2 isoforms); DQ148485, DQ148486 (Human KCNIP3 isoforms); DQ148487, DQ148488, DQ148489, DQ148490, DQ148491, DQ148492 (Human KCNIP4 isoforms); DQ148493, DQ148494, DQ148495 (Mouse KCNIP1 isoforms); DQ148496, DQ148497, DQ148498, DQ148505 (Mouse KCNIP2 isoforms); DQ148499, DQ148500 (Mouse KCNIP3 isoforms); DQ148501, DQ148502, DQ148503, DQ148504 (Mouse KCNIP4 isoforms).

* Corresponding author. Department of Gene Technology, Tallinn University of Technology, Akadeemia tee 15, Tallinn 19086, Estonia. Fax: +372 620 4401.
E-mail address: tonist@kbfi.ee (T. Timmusk).

0888-7543/$ - see front matter © 2005 Elsevier Inc. All rights reserved.
doi:10.1016/j.ygeno.2005.07.001

unique N-terminal sequence due to alternative splicing [11] or alternative usage of transcription start sites [12], which in turn could have importance in the diverse roles of the KCNIP proteins. However, the only evidence that the unique N-termini have functional significance in determining the role for KCNIP has been shown in the case of KCNIP4, which has different N-termini that cause distinct effects upon Kv4 channel modulation [12].

In addition to studies showing that KCNIPs have diverse roles in different compartments of cells, some studies have presented opposite results about the function of KCNIPs in vivo. In fact, three different *KCNIP* knockout mice have been developed so far, two of them being *KCNIP3* knockouts, which show different phenotypes. The first study on *KCNIP3* knockout mice showed that these mice had elevated levels of prodynorphin mRNA and dynorphin A peptides in the spinal cord [13]. KCNIP3 was presumed to be a transcriptional repressor modulating pain processing by repressing prodynorphin expression in vivo [13]. These mice were shown to have no impairment of Kv4 channels in the heart [13], which was expected due to KCNIP3 involvement in Kv4 channel modulation [1]. In addition, these mice did not have detectable differences in the presenilin-1 and presenilin-2 expression levels or presenilin processing compared to wild-type mice, which was expected because KCNIP3 is implicated in the proteolytic processing of presenilins [4]. In contrast, the other study for which the *KCNIP3*knockout mice were developed showed that there were no changes in dynorphin expression in the knockout mice and additionally these mice were shown to have altered long-term potentiation and presenilin processing, which indicate a role for KCNIP3 in modulating the Kv4 channels and γ-secretase function, respectively [14]. The third *KCNIP* knockout developed was the *KCNIP2* knockout in which there was no transient outward potassium current in the ventricular myocytes, which is well in accordance with *KCNIP2* expression data in the heart and proposed involvement of KCNIP2 in Kv4 channel modulation [15]. As KCNIP2 was not implicated in presenilin processing and gene transcription regulation at the time the study was conducted, there is no information about dynorphin expression or presenilin processing in *KCNIP2* knockout mice. However, recent data have shown that KCNIP2 could also be in involved in gene regulation [9].

Therefore, considering the data about the functions of the KCNIP proteins obtained from the *KCNIP3* knockouts and the finding that KCNIPs have unique N-termini that could have functional significance, it is very important to study the expression pattern of different KCNIP isoforms. Accordingly, in this study we have described the structures of the human and mouse *KCNIP1, KCNIP2, KCNIP3,* and *KCNIP4* genes. We have also analyzed alternative splicing of the *KCNIP* genes and coding potentials of the alternative transcripts. Furthermore, we have analyzed the expression of different *KCNIP1, KCNIP2, KCNIP3,* and *KCNIP4* mRNA splice variants in various mouse and human tissues and brain regions by RT-PCR and describe the expression of *KCNIP1, KCNIP2, KCNIP3*, and*KCNIP4* mRNA in the adult mouse brain with in situ hybridization.

Results

The structure of human KCNIP genes

Recent studies on *KCNIPs* have identified several alternative transcripts for each *KCNIP* [1,5,11,16], but with the exception of *KCNIP2* [17], none of the studies has thoroughly analyzed the structures and alternative splicing of the *KCNIP* genes. In this study, we characterized the exon/intron structure of human *KCNIP* genes and analyzed the alternative splicing pattern of each *KCNIP* gene in both human and mouse using bioinformatics and RT-PCR. For each *KCNIP* a search for mRNA sequences and expressed sequence tags (ESTs) was performed. Furthermore, the identified cDNAs were cloned and verified by sequencing. RT-PCR analyses were carried out for characterization of the expression pattern of the alternative transcripts of the *KCNIP* family in human and mouse. Expression of human *KCNIP* alternative transcripts was analyzed in a panel of 23 adult tissues and in 30 adult brain regions. Expression of mouse *KCNIP* transcripts was studied in 8 adult nonneural tissues, 10 adult brain regions, and 6 different developmental stages of brain.

The lengths of the four human *KCNIP* genes vary from approximately 17 kb for *KCNIP2* up to approximately 1.2 Mb for *KCNIP4* (Fig. 1A). All *KCNIP* genes have multiple unique 5′ exons and share homology in the 3′ part of the genes: the last seven exons are highly homologous and have identical lengths. The identity among the most conserved last seven exons of the *KCNIP* genes is 81% on the

Fig. 1. (A) Structures and alternative transcripts of human *KCNIP* genes. The structural organization of human *KCNIP1, KCNIP2, KCNIP3*, and *KCNIP4* exons and introns was determined by analyzing genomic and mRNA sequence data using bioinformatics and RT-PCR. Exons are shown as boxes and introns are shown as lines. Filled boxes indicate the translated regions of the exons, white boxes indicate the untranslated regions of the exons. The numbers above the exons and below the introns indicate their sizes. For the 5′ and 3′ exons the sizes of the protein coding parts are shown. Vertical dashed lines indicate putative transcription start and stop sites. Green vertical lines indicate translation start codon positions and red vertical lines indicate translation stop codon positions. Exon numbers are shown in roman characters. Only the major transcript variants for each *KCNIP* gene are shown. Asterisks mark very rarely used exons. (B) N-terminal sequences of the human KCNIP proteins. For each KCNIP exon III the first 10 amino acids encoded are shown in colored letters. The color code results from an alignment of all human full-length KCNIPs in ClustalW and the colors indicate as follows: red, identity of amino acids; green, strong similarity of amino acids; and blue, weak similarity of amino acids. The homologous N-terminal sequences of human KCNIP1 and KCNIP4 are marked with a red asterisk.

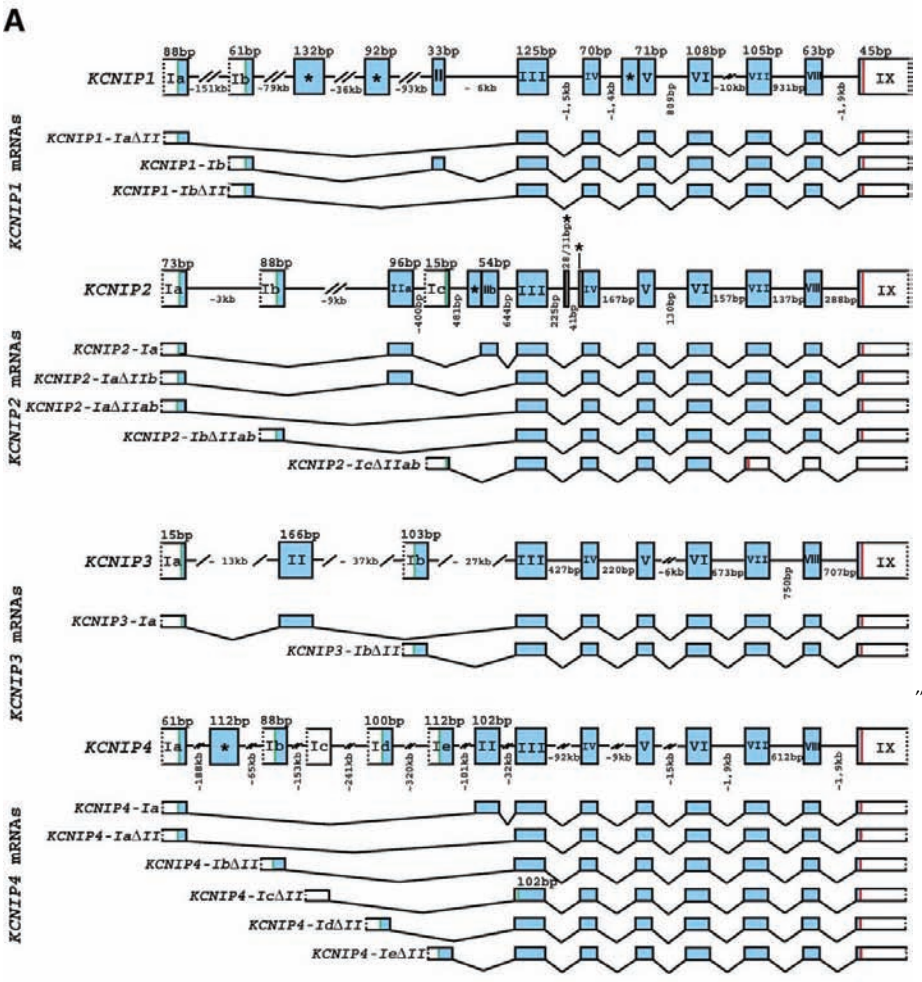
A
KCNIP1
KCNIP1 mRNAs
KCNIP1-IaΔII
KCNIP1-Ib
KCNIP1-IbΔII
KCNIP2
KCNIP2 mRNAs
KCNIP2-Ia
KCNIP2-IaΔIIb
KCNIP2-IaΔIIab
KCNIP2-IbΔIIab
KCNIP2-IcΔIIab
KCNIP3
KCNIP3 mRNAs
KCNIP3-Ia
KCNIP3-IbΔII
KCNIP4
KCNIP4 mRNAs
KCNIP4-Ia
KCNIP4-IaΔII
KCNIP4-IbΔII
KCNIP4-IcΔII
KCNIP4-IdΔII
KCNIP4-IeΔII
B
KCNIP1-IaΔII
KCNIP1-Ib
KCNIP1-IbΔII
KCNIP2-Ia
KCNIP2-IaΔIIb
KCNIP2-IaΔIIab
KCNIP2-IbΔIIab
KCNIP3-Ia
KCNIP3-IbΔII
KCNIP4-Ia
KCNIP4-IaΔII
KCNIP4-IbΔII
KCNIP4-IdΔII
KCNIP4-IeΔII

nucleotide level. The amino acid identity or strong similarity in sum of the respective regions among the KCNIP family proteins is 86%. It has been shown before that the N-termini of the KCNIP family proteins are unique and share no homology with each other [1]. However, here we describe five novel 5′ exons for the *KCNIP* family and show that two of the 5′ exons are homologous to each other. These are exon Ia in the human *KCNIP1* gene and exon Ib in the human *KCNIP4* gene. These exons are both 88 bp in length and encode 29 N-terminal amino acids for KCNIP1 and KCNIP4 isoforms.

Alternative splicing and expression of KCNIP1 in human and mouse

For both human and mouse the protein coding region of *KCNIP1* mRNA is 681 or 675 bp depending on the first exon used (Fig. 1A). We identified three predominant transcripts for *KCNIP1:* (1) *KCNIP1-IaΔII,* containing a novel 5′ exon, exon Ia, and lacking exon II; (2) *KCNIP1-Ib,* containing the previously described 5′ exon, exon Ib, and including exon II (*KChIP1b* [18]); and (3) *KCNIP1-IbΔII,* containing exon Ib and lacking exon II (*KChIP1a* [1,18]) (Fig. 1A). There is a potential translation start codon ATG 85 bp upstream of the 3′ end of exon Ia encompassed by a well-recognizable Kozak consensus sequence for translation initiation [19]. The new exon Ia encodes 29 amino acids not homologous to any other previously described N-termini of KCNIP family proteins.

In both mouse and human, *KCNIP1* transcripts with exon Ia and exon Ib were predominantly expressed in the nervous system (Figs. 2 and 3). In human, *KCNIP1-IaΔII* was expressed at high levels in the brain, spinal cord, and testis; lower levels were seen in several other tissues (Fig. 2). In the human brain high levels of *KCNIP1-IaΔII* transcripts were present in the cerebellum and pons and lower levels were detected in most other regions. In mouse, high levels of *KCNIP1-IaΔII* were observed in the olfactory bulb, cerebellum, and caudal regions of the brain; lower levels were seen in several other brain regions and in the lung and testis. In the mouse brain *KCNIP1-IaΔII* levels increased during postnatal development (Fig. 3). *KCNIP1-IbΔII* was strongly expressed in the human brain and spinal cord, low levels were seen in some other tissues (Fig. 2). In the human brain *KCNIP1-IbΔII* was expressed in all brain regions tested, although with differences in the expression levels. In mouse, the levels of *KCNIP1* transcripts with exon Ib were high in the brain (Fig. 3). Interestingly, in mouse, *KCNIP1* transcripts comprising exon Ib included or excluded exon II due to alternative splicing, whereas in human the predominant splice variant was without exon II. Also, the usage of exon II in mouse appeared to be developmentally regulated as *KCNIP1-IbΔII* was the predominant transcript in the embryonic brain but in postnatal stages transcripts including or excluding exon II were expressed with similar levels (Fig. 3).

In addition to the splice variants discussed, we cloned several human *KCNIP1* cDNAs with additional novel

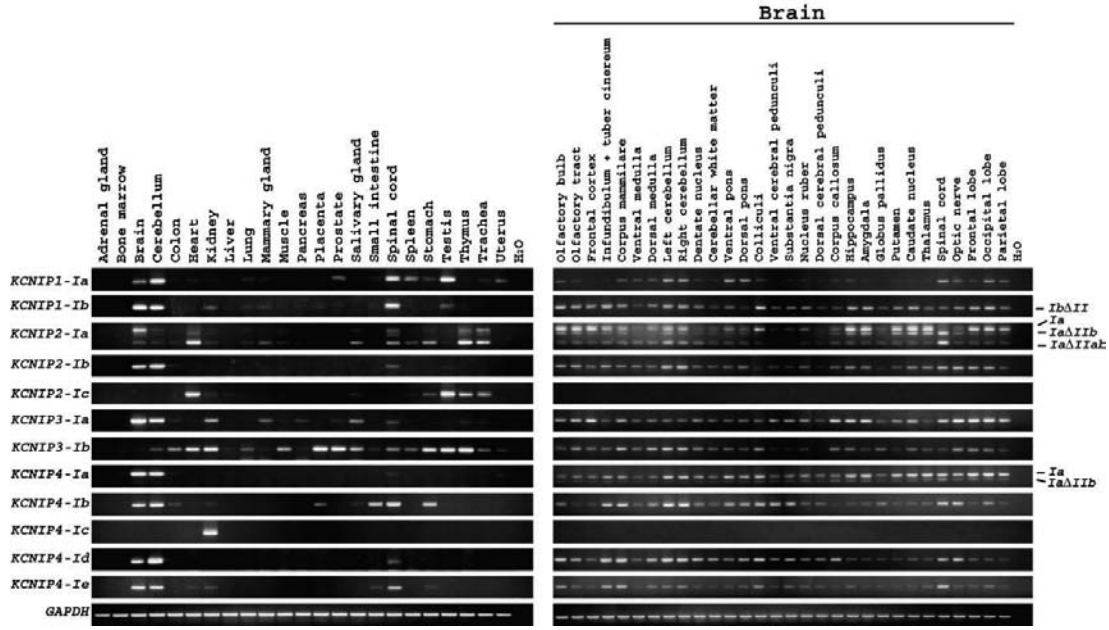

Fig. 2. Semiquantitive analysis of *KCNIP1, KCNIP2, KCNIP3, KCNIP4,* and control *GAPDH* mRNA expression by RT-PCR in various human tissues and brain regions.

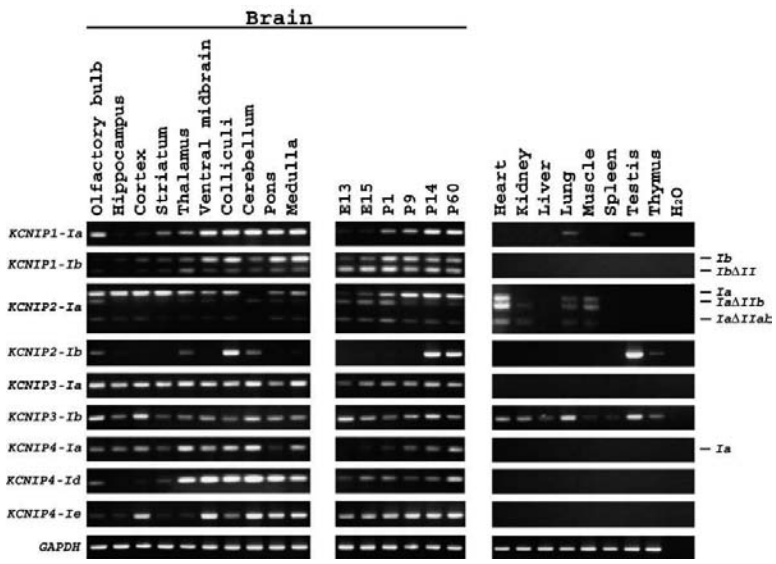

Fig. 3. Semiquantitive analysis of *KCNIP1, KCNIP2, KCNIP3, KCNIP4,* and control *GAPDH* mRNA expression by RT-PCR in various mouse brain regions, in mouse brain at the indicated developmental time points, and in various mouse tissues.

exons following exon Ib (Fig. 1A). One of these exons, 132 bp in length and located approximately 79 kb downstream of exon Ib, introduces a premature stop codon into the open reading frame (ORF) of *KCNIP1* mRNA. The second novel exon, located approximately 115 kb downstream of exon Ib, is 92 bp in length and also generates a frameshift into the mRNA, which leads to a premature stop codon in the following exon. Furthermore, we also cloned a full-length cDNA of human *KCNIP1* in which exon V is 75 bp longer at the expense of the upstream intron because a different splice acceptor site is used (Fig. 1A). This insertion, though, does not change the ORF of *KCNIP1* mRNA and does not introduce a premature stop codon and therefore encodes an additional 25 amino acids between the EF-hands 1 and 2 in KCNIP1. However, transcripts with these exons are of very low abundance as cDNAs comprising these exons were not detected by RT-PCR using RNA from different human tissues as a template. We could not find homologous sequences of the two novel exons downstream of exon Ib in the mouse *KCNIP1* genomic DNA. The 75-bp insertion upstream of exon V in mouse *KCNIP1*mRNA is also of low possibility because the potential splice site does not fit with the respective consensus sequence.

Alternative splicing and expression of KCNIP2 in human and mouse

Our results revealed five predominant transcripts for *KCNIP2:* (1) *KCNIP2-Ia,* containing 5′ exon Ia and exons IIa and IIb (*KChIP2a* [11]); (2) *KCNIP2-IaΔIIb,* containing 5′ exon Ia and exon IIa (*KChIP2b* [1]); (3) *KCNIP2-IaΔIIab* containing 5′ exon Ia and lacking exons IIa and IIb (*KChIP2c* [11]); (4) *KCNIP2-IbΔIIab,* containing 5′ exon Ib and lacking exons IIa and IIb (*KChIP2g* [17]); and (5) *KCNIP2-IcΔIIab,* containing 5′ exon Ic and lacking exons IIa and IIb (GenBank Accession No.AF367020) (Fig. 1A). Using RT-PCR analyses we detected all five of these *KCNIP2* transcripts in human and all except *KCNIP2-IcΔIIab* in mouse tissues. We also could not identify mouse *KCNIP2-IcΔIIab* cDNAs in the NCBI databases using bioinformatics.

In human, *KCNIP2-Ia* was strongly expressed in the brain; lower levels were seen in some other tissues including spinal cord, thymus, and trachea (Fig. 2). In the human brain, high levels of *KCNIP2-Ia* transcripts were expressed in the olfactory system, cerebral cortex, hippocampus, amygdala, putamen, caudate nuclei, and thalamus; lower levels were seen in most other regions studied. In adult mouse, high levels of *KCNIP2-Ia* were also observed in the rostral part of the brain—in the olfactory bulb, hippocampus, cortex, and striatum—and also in the heart (Fig. 3). Lower levels were seen in the lung and muscle and in other brain regions except the cerebellum, where *KCNIP2-Ia* was not detected. During mouse brain postnatal development *KCNIP2-Ia* levels were increased.

KCNIP2-IaΔIIb was moderately or weakly expressed in the human brain, heart, spinal cord, thymus, and trachea (Fig. 2). In the human brain *KCNIP2-IaΔIIb* was expressed in most studied regions with lower levels than *KCNIP2-Ia.* In mouse, the levels of *KCNIP2-IaΔIIb* were high in the heart; lower levels were seen in the lung, muscle, and kidney and in some regions of the brain (Fig. 3). Expression

of *KCNIP2-IaΔIIb* in the mouse brain appeared to be higher during embryonic development and lower in postnatal stages.

KCNIP2-IaΔIIab levels were high in the human heart and thymus; lower levels were seen in several other tissues (Fig. 2). In the human brain *KCNIP2-IaΔIIab* was weakly expressed in all the regions analyzed. Interestingly, in the human central nervous system *KCNIP2-Ia* was the predominant transcript of *KCNIP2* in the brain and *KCNIP2-IaΔIIab* in the spinal cord. In mouse, *KCNIP2-IaΔIIab* was weakly expressed in the heart and even less in the kidney, lung, muscle, and most of the brain regions analyzed (Fig. 3). In the mouse brain *KCNIP2-IaΔIIab* levels peaked at postnatal day 1 (P1).

Among the 23 human tissues analyzed *KCNIP2-IbΔIIab* was predominantly expressed in the brain; low levels were seen in the spinal cord (Fig. 2). *KCNIP2-IbΔIIab* was expressed in all human brain regions studied, although at different levels (Fig. 2). In mouse, high levels of *KCNIP2-IbΔIIab* were seen in several brain regions and in the testis (Fig. 3). Interestingly, in the mouse brain *KCNIP2-IbΔIIab* was expressed only during postnatal development, starting from P14 and P60.

In human, *KCNIP2-IcΔIIab* was expressed in several nonneural tissues, particularly in the heart and testis; lower levels were seen in the stomach, thymus, and trachea (Fig. 2). We did not detect *KCNIP2-IcΔIIab* expression in the nervous system.

According to bioinformatics, alternative splicing occurs also in the conserved part of human *KCNIP2* transcripts. (1) Between exons III and IV there is the possibility of three different inclusion events. Two of them, inclusion of 28-bp (GenBank Accession No.NM173342) or 31-bp (GenBank Accession No.BG819761) alternative exons, lead to frameshifts and premature stop codons in the following exon IV. The potential usage of an alternative splice site 21 bp upstream of the conventional splice site of exon IV leads to a putative protein isoform with 7 additional amino acids in front of the first EF-hand of KCNIP2 (KChIP2t [20]). (2) There is one mRNA sequence comprising exon Ic in the NCBI database with the exclusion of the 71-bp exon V. The potential amino acid sequence translated from this sequence would differ from other KCNIP2 isoforms for 69 amino acids in the N-terminus and would match the C-terminal part by 108 amino acids. (3) Exclusion of the 108-bp exon VI, which is seen only in the transcript named *KChIP2f* [17], can also occur. *KChIP2f* encodes a protein with 15 different C-terminal amino acids compared to other KCNIP2 isoforms because of intron retention between exons VIII and IX. However, we have found that all these splicing events described are very rare. We could not detect expression of these *KCNIP2* mRNAs with alternative usage or skipping of exons in the conserved coding region of *KCNIP2* mRNAs with RT-PCR (data not shown) either in human or in mouse.

Alternative splicing and expression of KCNIP3 in human and mouse

Both in human and in mouse the protein coding region of *KCNIP3* is 768 or 690 bp in length depending on the first exon used (Fig. 1A). We identified two predominant transcripts for *KCNIP3:* (1) *KCNIP3-Ia,* containing the previously described 5′ exon, named here exon Ia, and exon II (*KChIP3* [1], also named *DREAM* [6] and calsenilin [4]), and (2) *KCNIP3-IbΔII,* containing a novel 5′ exon Ib and lacking exon II (Fig. 1A). This new exon encodes an N-terminus with 34 amino acids in length that is not homologous to any other previously described KCNIP family protein N-termini.

RT-PCR analyses showed that *KCNIP3* transcripts with exon Ia and the novel exon Ib are differentially expressed in mouse and human tissues, with *KCNIP3-Ia* having predominant expression in the nervous system (Figs. 2 and 3). In human, *KCNIP3-Ia* was highly expressed in the brain; lower levels were seen in several organs including kidney, mammary and salivary gland, and spinal cord. In mouse, *KCNIP3-Ia* expression was observed only in the brain. In the human and also the mouse brain *KCNIP3-Ia* was expressed in all regions analyzed. In the mouse brain *KCNIP3-Ia* levels were upregulated during development. *KCNIP3-Ib* was expressed in most of the human and mouse tissues analyzed (Figs. 2 and 3). In both human and mouse brain, *KCNIP3-IbΔII* was widely expressed, but at lower levels than in nonneural tissues. We did not observe significant changes in the expression levels of *KCNIP3-IbΔII* in mouse brain during development.

It has been reported that in mouse alternative splicing of *KCNIP3-Ia* occurs by the usage of a splice acceptor site 4 nucleotides downstream of the conventional 3′ splice site of intron I inside exon II [16]. We found that this transcript, which we have named *KCNIP3-IaΔ4nII,* is indeed present in mouse tissues, but its levels are almost 10-fold lower than *KCNIP3-Ia* levels (data not shown). In human we could not detect *KCNIP3-IaΔ4nII* (data not shown).

Of note, in the NCBI database there is one human *KCNIP3* cDNA sequence with exon IV spliced out. We found that this would generate a frameshift in the *KCNIP3* transcript and introduce a premature stop codon in exon VII. Mouse EST and mRNA data do not reveal any splicing in the conserved coding region of the *KCNIP3* transcripts and accordingly any alternative splicing in the conserved coding part of *KCNIP3* transcripts was not detected in either human or mouse.

Alternative splicing and expression of KCNIP4 in human and mouse

Our results revealed six predominant transcripts for human *KCNIP4* (Fig. 1A): (1) *KCNIP4-Ia,* containing the previously described 5′ exon Ia and exon II (*KChIP4bl*

[21], also named $CALP_{250}$ [5]); (2) *KCNIP4-IaΔII,* containing the previously described 5′ exon Ia and lacking exon II ($CALP_{216}$ [5]); (3) *KCNIP4-IbΔII,* containing a novel 5′ exon, exon Ib, and lacking exon II; (4) *KCNIP4-IcΔII,* containing another novel 5′ exon, exon Ic, and lacking exon II; (5) *KCNIP4-IdΔII,* containing a previously described 5′ exon, exon Id, and lacking exon II (*KChIP4a* [21]); and (6) *KCNIP4-IeΔII,* containing yet another novel 5′ exon, exon Ie, and lacking exon II (Fig. 1A). The novel exons Ib and Ie contain both a putative translation start codon ATG. The novel exon Ic does not contain a potential translation start codon and therefore protein translation from this transcript could start from a putative in-frame translation start codon in exon III leading to a KCNIP4 without the variable N-terminus. Using bioinformatics, we identified exons Ia, Id, and Ie, but not Ib and Ic of the *KCNIP4* gene in the mouse genome.

RT-PCR analyses showed that in human and also in mouse, *KCNIP4-Ia* mRNA was predominantly expressed in the brain (Figs. 2 and 3). In both the human and the mouse brain *KCNIP4-Ia* was expressed at different levels in all regions analyzed. In mouse brain *KCNIP4-Ia* was expressed during postnatal development and was barely detectable in embryonic brain (Fig. 3). *KCNIP4-IaΔII* was detected only in the human brain, where low levels of the transcripts were observed in most regions (Fig. 2).

KCNIP4-IbΔII and *KCNIP4-IcΔII* mRNAs were present only in human (Fig. 2). *KCNIP4-IbΔII* was expressed at high levels in the human brain, spinal cord, small intestine, and stomach; lower levels were observed in the placenta, colon, kidney, and prostate. *KCNIP4-IcΔII* was expressed exclusively in the kidney in human.

KCNIP4-IdΔII expression was detected only in the brain and spinal cord (Figs. 2 and 3). In human *KCNIP4-IdΔII* levels were high in the brain and low in the spinal cord. In the human brain, high *KCNIP4-IdΔII* levels were observed in several regions including corpus mammillare, dorsal pons, cerebellum, colliculi, and corpus callosum; lower levels were detected in all other regions analyzed. Of the mouse brain regions analyzed, strong expression was detected in caudal regions, most significantly in the cerebellum. A modest increase in the expression levels was seen during brain development.

KCNIP4-IeΔII levels were high in the human brain and spinal cord; low levels were observed in the heart, kidney, small intestine, and stomach (Fig. 2). Of the human brain regions analyzed, *KCNIP4-IeΔII* was strongly expressed in the olfactory bulb, infundibulum, and corpus mammillare; low expression was observed in most other regions. In mouse, *KCNIP4-IeΔII* levels were high in the brain, particularly in the ventral midbrain, cerebellum, and cortex; lower levels were seen in some other regions including the pons and medulla (Fig. 3). A slight rise in the levels of *KCNIP4I-eΔII* during mouse brain development was detected.

KCNIP1, KCNIP2, KCNIP3, and KCNIP4 mRNAs are differentially expressed in the neurons of the adult mouse central and peripheral nervous system

We analyzed the expression of all *KCNIP* mRNAs in adult mouse central and peripheral nervous system by in situ hybridization. The hybridization probes for each *KCNIP*-were constructed to recognize all of the major splice variants and therefore were targeted to the conserved coding region of *KCNIP* mRNAs. To distinguish different cell types, Nissl counterstaining of the tissue sections, which allows distinction of large and weakly stained nuclei of neurons from small and strongly stained nuclei of glial cells, was used. All *KCNIP* mRNAs were expressed in the neurons of the brain with specific patterns for each *KCNIP* (Figs. 4 and 5, Supplementary Table 1).

We observed clear similarities and differences in the expression patterns of *KCNIP1, KCNIP2, KCNIP3,* and *KCNIP4.* In the olfactory system *KCNIP1* was highly expressed in the granular layer (Figs. 4A and 4E), *KCNIP2* in the granular layer and periglomerular cells (Figs. 4B and 4F), and *KCNIP3* and *KCNIP4* in the neurons of the mitral cell layer and periglomerular cells (Figs. 4C, 4D, 4G, and 4H). In the anterior olfactory nucleus *KCNIP3* mRNA levels were high, whereas *KCNIP2* and *KCNIP4* levels were moderate, and *KCNIP1* levels were low (Figs. 4A–4D).

In the cerebral cortex all the *KCNIPs* were detected in the neurons of layers II–VI (Figs. 4A–4D and 5E, 5F, 5K, 5L, 5Q, 5R, 5W, and 5X). Interestingly, the *KCNIP1* mRNA expression pattern could be distinguished very clearly from the patterns of other *KCNIP* mRNAs: *KCNIP1* mRNA was detected in the scattered neurons, most possibly interneurons, of all layers of the cerebral cortex. In the piriform cortex, a strong signal was seen for *KCNIP2, KCNIP3,* and *KCNIP4* mRNA, in contrast to *KCNIP1,* which was not seen in this brain structure (Figs. 4I–4L).

Although all *KCNIP* mRNAs were detected in the hippocampal formation, there were differences in the distribution of expression between different *KCNIPs* (Fig. 4). *KCNIP1* was expressed at high levels in scattered neurons that are most likely interneurons, around the CA regions, the dentate gyrus, and the molecular layer (Figs. 4A and 4M). *KCNIP2* mRNA was evenly and strongly expressed in the CA1–CA3 pyramidal layers and in the granular layer of the dentate gyrus (Figs. 4B and 4N). The expression pattern of *KCNIP4* in the hippocampus was similar to that of *KCNIP2,* showing high levels in the dentate gyrus, CA1, and CA2 and slightly lower levels in CA3 (Figs. 4D and 4P). *KCNIP3* mRNA was predominantly expressed in the granular layer of the dentate gyrus and with lower levels in the CA1–CA3 pyramidal layers (Figs. 4C and 4O).

The basal ganglia, caudate putamen, ventral pallidum, and accumbens showed high signal for *KCNIP1* in scattered neurons, most probably interneurons (Figs. 4A and 4I), whereas *KCNIP2* mRNA was expressed at high levels in most neurons of caudate putamen and accumbens and not in

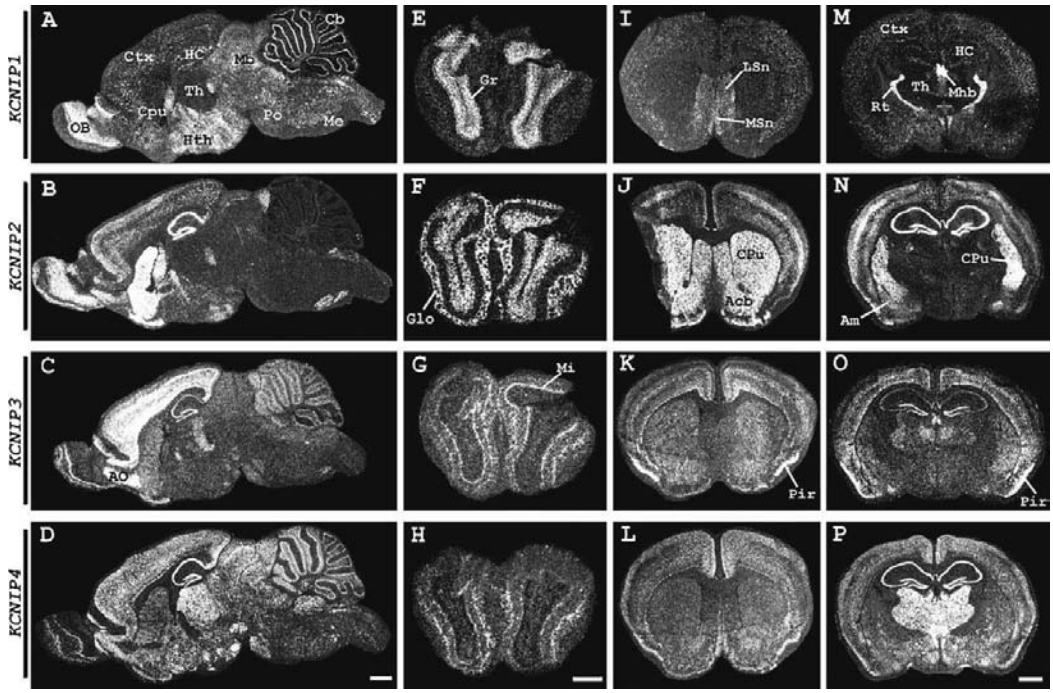

Fig. 4. In situ hybridization analysis of *KCNIP1, KCNIP2, KCNIP3,* and *KCNIP4* mRNA expression in adult mouse brain. Dark-field emulsion autoradiographs from (A, B, C, and D) sagittal sections and coronal sections from the level of the (E, F, G, and H) olfactory bulb, (I, J, K, and L) striatum, and (M, N, O, and P) thalamus are shown. The sections were hybridized with a probe for *KCNIP1* (A, E, I, and M), *KCNIP2* (B, F, J, and N), *KCNIP3* (C, G, K, and O), and *KCNIP4* (D, H, L, and P). OB, olfactory bulb; AO, anterior olfactory nucleus; Ctx, cerebral cortex; HC, hippocampus; CPu, caudate putamen (striatum); Th, thalamus; Hth, hypothalamus; Mb, midbrain; Cb, cerebellum, Po, pons; Me, medulla; Gr, granular cell layer of the olfactory bulb; Glo, glomerular cell layer of the olfactory bulb; Mi, mitral cell layer of the olfactory bulb; LSn, lateral septal nucleus; MSn, medial septal nucleus; Acb, accumbens nucleus; Am, amygdaloid nucleus; Rt, reticular thalamus, Mhb, medial habenular nucleus; Pir, piriform cortex. Scale bars, 1 mm.

ventral pallidum (Figs. 4B and 4J). For *KCNIP3* a moderate signal and for *KCNIP4* a weak signal was detected in these brain structures (Figs. 4C, 4D, 4K, and 4L). In the septum, lateral septal nuclei showed moderate and high signal for *KCNIP1* and *KCNIP2,* respectively, whereas *KCNIP3* and *KCNIP4* mRNAs were not expressed significantly in this brain structure. In the medial septum *KCNIP1* was expressed at moderate and *KCNIP2* at low levels (Figs. 4I–4L).

In the thalamus *KCNIP4* mRNA was widely expressed at high levels in most of the nuclei, whereas *KCNIP3* was moderately present predominantly in the dorsal nuclei (Figs. 4C, 4D, 4O, and 4P). In contrast, *KCNIP1* and *KCNIP2* were expressed at high and moderate levels, respectively, in the reticular thalamic nuclei and medial habenular nuclei and were not expressed in most of the other thalamic nuclei (Figs. 4A, 4B, 4M, and 4N). In the hypothalamus *KCNIP1* showed strong expression in most of the nuclei, whereas *KCNIP2, KCNIP3,* and *KCNIP4* were differentially expressed in several nuclei (Figs. 4A–4D, Supplementary Table 1). In the midbrain *KCNIP* mRNAs were expressed at moderate or low levels in the superior and inferior colliculi (Figs. 4A–4D, Supplementary Table 1).

In the cerebellum all except *KCNIP2* mRNAs were expressed (Fig. 4 and Supplementary Table 1). *KCNIP1* was expressed only in the Purkinje cell layer (Fig. 4A), *KCNIP3* in the scattered neurons of the molecular layer (Fig. 4C), and *KCNIP4* mRNA in the Purkinje cell layer and granular layer neurons (Fig. 4D). Interestingly, all the *KCNIP* mRNAs that were detected in the cerebellum shared a common feature in the expression pattern—they all were more abundant in the rostral region of the cerebellum than in the caudal region. In the pons *KCNIP3* and *KCNIP4*

Fig. 5. In situ hybridization analysis of *KCNIP1, KCNIP2, KCNIP3,* and *KCNIP4* mRNA expression in the mouse central and peripheral nervous system. Dark-field emulsion autoradiographs from horizontal sections of (A, G, M, and S) the lumbar level of P1 mouse spinal cord and its surrounding tissues and (B, H, N, and T) adult mouse lumbar level spinal cord are shown. (C, I, O, and U) Bright-field higher magnification pictures of adult mouse dorsal root ganglia showing individual neurons and glial cells. (D, J, P, and V) Dark-field emulsion autoradiographs of the same regions. (E, K, Q, and W) Bright-field higher magnification pictures of adult mouse cerebral cortex showing individual neurons and glial cells. (F, L, R, and X) Dark-field emulsion autoradiographs of the same regions. Arrows denote some positive neurons, some negative neurons are marked with asterisks. SC, spinal cord; DRG, dorsal root ganglion; DH, dorsal horn of the spinal cord; VH, ventral horn of the spinal cord. Scale bars, 500 μm for A, B, G, H, M, N, S, and T, and 20 μm for C–F, I–L, O–R, and U–X.

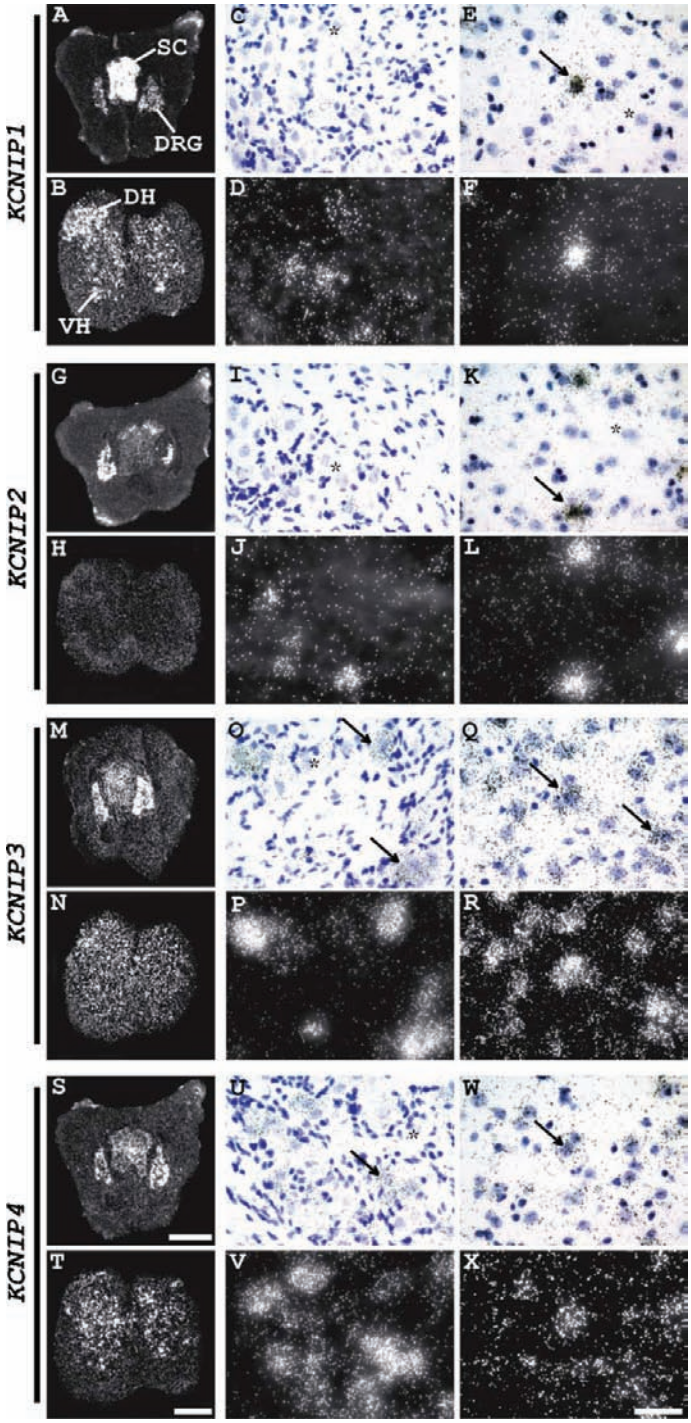
KCNIP1
KCNIP2
KCNIP3
KCNIP4
A
SC
DRG
B
DH
VH
C
D
E
F
G
H
I
J
K
L
M
N
O
P
Q
R
S
T
U
V
W
X

mRNAs were moderately expressed in the pontine nuclei (Figs. 4C and 4D). In the medulla *KCNIP* mRNAs were differentially expressed in several nuclei (Supplementary Table 1).

We also analyzed the expression of *KCNIP* mRNAs in P1 and adult mouse spinal cord and dorsal root ganglia (DRG). In the P1 mouse spinal cord neurons *KCNIP1* mRNA was expressed at high levels (Fig. 5A), *KCNIP3* and *KCNIP4* mRNA at moderate levels (Figs. 5M and 5S), and *KCNIP2* mRNA at low levels (Fig. 5G). In the P1 DRG neurons *KCNIP1* (Fig. 5A) was expressed at moderate and *KCNIP2, KCNIP3,* and *KCNIP4* (Figs. 5G, 5M, and 5S) were expressed at high levels. In the adult spinal cord all *KCNIP* mRNAs, except *KCNIP2,* were present: high levels were detected for *KCNIP1* and moderate levels for *KCNIP4* and *KCNIP3* (Figs. 5B, 5H, 5N, and 5T). In the adult DRG neurons *KCNIP3* and *KCNIP4* mRNAs were expressed at high levels in the majority of neurons (Figs. 5O, 5P, 5U, and 5V), whereas for both *KCNIP1* and *KCNIP2* moderate expression was detected in only a small subpopulation of neurons (Figs. 5C, 5D, 5I, and 5J).

Discussion

In this study we describe the structures of the human and mouse *KCNIP* genes and show that the expression of *KCNIP* genes is regulated by alternative splicing and usage of alternative 5′ exons generating transcript variants for each *KCNIP* gene that encode proteins with distinct N-termini. We found that the structures of the orthologs of human and mouse *KCNIP* genes are very similar; differences occur only in the lengths of the introns. The structures of the paralogs of *KCNIP* genes, *KCNIP1, KCNIP2, KCNIP3,* and *KCNIP4,* are also similar to each other: the unique 5′ exons are separated from clusters of homologous 3′ exons by relatively long introns, although differences occur in the overall lengths of the genes. A characteristic feature of the *KCNIP* gene family is the presence of alternative 5′ exons encoding variable N-terminal sequences. Previously it has been shown that the human, mouse, and rat *KCNIP4* genes and the human *KCNIP2* gene have two alternative 5′ exons [17,21]. In this study we describe a novel alternative 5′ exon for the human and mouse *KCNIP1* genes (exon Ia) and for the human and mouse *KCNIP3* genes (exon Ib), and for the human *KCNIP4* gene we describe three novel 5′ exons (Ib, Ic, and Ie), one of which we found also to be represented in the mouse genome (exon Ie). All these exons, except human *KCNIP4* exon Ic, encode a unique N-terminal sequence for a respective KCNIP isoform and, consequently, these isoforms could have different functions.

For the mouse *KCNIP3* gene, transcripts with protein coding regions differing by four nucleotides in length have been described [16]. The combined usage of alternative splicing acceptor sites between exon III and the preceding intron, which changes the reading frame, and possible usage of an alternative ATG as a translation start site could potentially generate four different proteins, two of which would contain the conserved EF-hands translated from the "original" *KCNIP3* reading frame. It was proposed that the different reading frames that could be used for starting protein translation would generate different N-termini in front of the four EF-hands-containing conserved domain and thus these N-termini could be the reason for the functional diversity described for KCNIP3. Thus, the authors named these reading frames the DREAM frame and the calsenilin frame [16], respectively. We compared the mouse and human *KCNIP3* sequences and found that in human the usage of both the alternative splicing acceptor site and the alternative ATG as a translation start site is possible. However, if the alternative ATG is used in human and/or the translation frame is shifted by the usage of the alternative splice acceptor site, there is a premature termination codon introduced and the transcripts would be potential candidates for nonsense mediated decay (reviewed in [22]). Accordingly, none of the human *KCNIP3* cDNAs cloned by us were missing the respective ATAG tetramer in front of exon III (data not shown). We conclude that in human the KCNIP3 proteins cannot have different functions due to the respective alternative splicing described for the mouse.

Previously it has been discussed that KCNIPs are the only family of NCS proteins that are found exclusively in mammals [10]. To date, however, there are mRNA and EST data in the databases showing that *KCNIP* family genes exist also in lower vertebrates. Using bioinformatics, we found, for example, that in the *Danio rerio* genome at least an ortholog for human *KCNIP3* exists (GenBank Accession No.BC059703), the putative protein product for which is 78% identical to human KCNIP3; in *Gallus gallus* at least an ortholog for *KCNIP2* gene exists (GenBank Accession No.NM204555), the putative protein product of which is 97% identical to human KCNIP2; and in the *Xenopus laevis* genome at least an ortholog for human *KCNIP1* exists (GenBank Accession No.BC074264), the putative protein product of which is 91% identical to human KCNIP1. Of note, we failed to identify *KCNIP* orthologs in the genomes of *Drosophila melanogaster, Ciona intestinalis,* or *Caenorhabditis elegans*. This indicates that the KCNIP family of proteins is common to vertebrates.

To date, three different functions have been implicated for the KCNIP family proteins. First, all the KCNIPs have been shown to colocalize with and modulate A-type potassium channels [1,5]. Strikingly, a KCNIP4 isoform with a different N-terminus has been shown to affect the Kv4 channels in an opposing way compared to other described KCNIP proteins, demonstrating that the variable N-termini of the KCNIPs could have functional significance [21]. Second, KCNIP3 (also named calsenilin) and KCNIP4 (CALP, for calsenilin-like protein) have been shown to have a role in presenilin function [4,5]. The fact that only KCNIP3 and KCNIP4 have been shown to interact with presenilins brings to notice the possibility that the variable N-termini have importance in

this function also. And third, KCNIP3 has been shown to be a transcription factor that binds to the DRE downstream of the transcription start site of the prodynorphin gene and represses prodynorphin expression in the absence of Ca^{2+} [6]. To date, one isoform from each KCNIP family member has been shown to bind DRE [9] and several genes have been identified that have DRE sites and are regulated by a KCNIP in vitro [7,9]. However, the KCNIP DNA binding assays have been in vitro experiments [9,23] and the only KCNIP for which the DRE site has been determined is KCNIP3 [24]. Thus, it could be that the different N-termini of the KCNIP proteins have biological significance in vivo because the N-termini could possibly contribute to the binding site specificity of the respective proteins. In light of our new findings that the KCNIPs have even more N-termini than previously considered, it is obvious to propose that the different N-termini could functionally have diverse effects on the A-type potassium channels and could modulate the interaction of KCNIP isoforms with presenilins and regulate the Ca^{2+}-dependent transcription of many genes that have DRE sites.

The three diverse functions of the KCNIPs raise a question: how is it possible that the same protein has independent functions in different cell compartments—in the nucleus and the cell membranes? The localization of KCNIPs in the cell has been analyzed in several studies and most of them have found that KCNIP proteins are localized in the cytoplasm [25–27]. However, in the case of KCNIP2 it has also been shown that it localizes in the nucleus in human ventricular myocytes [20]. The localization of KCNIP3 has been found to depend on the concentration of intracellular calcium as the increase in calcium concentration correlates with the translocation of KCNIP3 to the nucleus [28]. Whereas the cytoplasmic localization of KCNIPs and localization of them to the membranes when coexpressed with Kv4 channels [3,20] and presenilins [25] have been studied thoroughly, the localization of KCNIPs in the nucleus is less clear. The classic nuclear localization signals (NLS) are not present in the KCNIP sequences described so far. So, the identified nuclear localization of KCNIPs could be because of nuclear targeting signals different from the classical NLS, like in the β-cell homeodomain transcription factor PDX1 [29], or due to regulatory proteins that facilitate nuclear transport, like in case of hepatic glucokinase [30], for example. We have found, however, that there are two human KCNIP isoforms, encoded by *KCNIP1* mRNA with exon Ia and *KCNIP4* mRNA with exon Ib, which have homologous N-termini. The identity and strong similarity in sum is 80% between these N-termini. Remarkably, there are several positively charged lysine and arginine residues in both of the N-terminal sequences, indicating that they might comprise a NLS. Taken together, it is possible that in vivo the unique N-termini of the KCNIP isoforms have a role in determining the localization and function of the protein in the cell.

In this study we also describe the expression of *KCNIP* mRNA in the adult mouse brain with in situ hybridization. In general, the results are well in accordance with the KCNIP protein expression data in the adult rat brain [31] and also with the recent data about *KCNIP* mRNA localization in adult brain published during the preparation of this article [32]. Considering the possibility of different KCNIP N-termini being functionally significant [21], the generation of KCNIP isoform-specific antibodies or hybridization probes would be of great interest for characterization of the expression patterns of KCNIP isoforms with different N-termini. In conclusion, the results presented in this study provide information about the sites of *KCNIP* expression, thus enabling more accurate functional characterization of the KCNIP isoforms in future studies.

Experimental methods

Structure and expression analyses and cloning of the KCNIP genes

Human *KCNIP* gene structures and human and mouse *KCNIP* mRNAs were identified by analyzing genomic, mRNA, and EST databases using bioinformatics tools (http://www.ncbi.nlm.nih.gov and http://genome.ucsc.edu). All homology searches were performed using various BLAST tools (http://www.ncbi.nlm.nih.gov). Based on the sequence information acquired, primers (supplementary material) were designed to isolate human *KCNIP* cDNAs encoding full-length proteins, to analyze the expression of human and mouse *KCNIP* mRNAs, and to construct plasmids for mouse *KCNIP* riboprobe generation. Total RNAs from various human and mouse brain regions and mouse tissues were purified with RNAwiz (Ambion, USA) as recommended by the manufacturer and treated with DNase using the DNA-Free kit (Ambion). Human RNAs from different tissues were obtained from BD Biosciences (USA). First-strand cDNAs were synthesized with Superscript III reverse transcriptase as recommended by the manufacturer (Invitrogen, USA) using 5 μg of total RNA from different tissues.

PCRs were performed in a volume of 25 μl containing 1/50 of RT reaction as a template using the Expand High-Fidelity PCR System kit (Roche Diagnostics, Germany) for full-length cDNA amplifying and Naxo *Taq*polymerase (Naxo, Estonia) for expression analyses and riboprobe template plasmid construction, both according to the manufacturer's instructions. PCR fragments were resolved by agarose gel electrophoresis, excised from the gel, and cloned into the pcDNA3.1/V5-His-TOPO vector (Invitrogen) or into the pCRII-TOPO vector (Invitrogen). All cloned PCR fragments were sequenced.

In the RT-PCR of the *KCNIP* mRNAs, an annealing temperature of 57°C was used for all combinations of primers. The number of cycles in the PCR was 22–35 for

template cDNAs from human and mouse tissues and mouse brain regions and 33–40 for template cDNAs from human brain regions. PCR with primers specific for the ubiquitously expressed *GAPDH* (glyceraldehyde-3-phosphate dehydrogenase), 25 cycles, was performed as a control to determine the amount of template cDNA in different PCRs. Cycle numbers in RT-PCR reactions were optimized so that the PCR products were analyzed in the exponential phase of the PCR. Primers used to amplify the full-length human *KCNIP* cDNAs, to analyze the expression of human and mouse *KCNIP* mRNAs, and to generate mouse *KCNIP* riboprobe are described in the supplementary material.

In situ hybridization

DNA fragments for riboprobe generation were subcloned into pCRII-TOPO vector (Invitrogen) and cRNA probes were synthesized with the MAXIScript In Vitro Transcription Kit (Ambion) T7 or SP6 RNA polymerase, using [α-^{35}S]UTP (Amersham Biosciences, UK) for labeling. The *KCNIP* riboprobe fragments were selected to cover the parts of the *KCNIP* cDNAs that are present in all the main expressed splice variants of *KCNIP1, KCNIP2, KCNIP3,* or *KCNIP4*. Serial sagittal and coronal sections (14 μm) from fresh-frozen NMRI mouse brain were analyzed by in situ hybridization analyses following the previously described protocol [33]. Emulsion-dipped sections were developed after 3 weeks using D-19 developer (Eastman Kodak, USA), fixed (sodium fixer; Kodak), and counterstained with hematoxylin (Shandon, USA).

Acknowledgments

We thank Professor Mart Saarma (University of Helsinki) for providing the facility for in situ hybridization analyses and Svetlana Vasilieva (University of Helsinki) for technical assistance. This work was supported by the following grants to T.T.: Wellcome Trust International Senior Research Fellowship (Grant 067952), Estonian Science Foundation (Grant 5555), and Estonian Ministry of Education and Research (Grant 0222602).

Appendix A. Supplementary data

Supplementary data associated with this article can be found, in the online version, at doi:10.1016/j.ygeno.2005.07.001.

References

[1] W.F. An, M.R. Bowlby, M. Betty, J. Cao, H.P. Ling, G. Mendoza, J.W. Hinson, K.I. Mattsson, B.W. Strassle, J.S. Trimmer, K.J. Rhodes, Modulation of A-type potassium channels by a family of calcium sensors, Nature 403 (2000) 553–556.

[2] R. Bahring, J. Dannenberg, H.C. Peters, T. Leicher, O. Pongs, D. Isbrt, Conserved Kv4 N-terminal domain critical for effects of Kv channel-interacting protein 2.2 on channel expression and gating, J. Biol. Chem. 276 (2001) 23888–23894.

[3] R. Shibata, H. Misonou, C.R. Campomanes, A.E. Anderson, L.A. Schrader, L.C. Doliveira, K.I. Carroll, J.D. Sweatt, K.J. Rhodes, J.S. Trimmer, A fundamental role for KChIPs in determining the molecular properties and trafficking of Kv4.2 potassium channels, J. Biol. Chem. 278 (2003) 36445–36454.

[4] J.D. Buxbaum, E.K. Choi, Y. Luo, C. Lilliehook, A.C. Crowley, D.E. Merriam, W. Wasco, Calsenilin: a calcium-binding protein that interacts with the presenilins and regulates the levels of a presenilin fragment, Nat. Med. 4 (1998) 1177–1181.

[5] Y. Morohashi, N. Hatano, S. Ohya, R. Takikawa, T. Watabiki, N. Takasugi, Y. Imaizumi, T. Tomita, T. Iwatsubo, Molecular cloning and characterization of CALP/KChIP4, a novel EF-hand protein interacting with presenilin 2 and voltage-gated potassium channel subunit Kv4, J. Biol. Chem. 277 (2002) 14965–14975.

[6] A.M. Carrion, W.A. Link, F. Ledo, B. Mellstrom, J.R. Naranjo, DREAM is a Ca^{2+}-regulated transcriptional repressor, Nature 398 (1999) 80–84.

[7] C. Sanz, B. Mellstrom, W.A. Link, J.R. Naranjo, J.L. Fernandez-Luna, Interleukin 3-dependent activation of DREAM is involved in transcriptional silencing of the apoptotic Hrk gene in hematopoietic progenitor cells, EMBO J. 20 (2001) 2286–2292.

[8] M. Rivas, B. Mellstrom, J.R. Naranjo, P. Santisteban, Transcriptional repressor DREAM interacts with thyroid transcription factor-1 and regulates thyroglobulin gene expression, J. Biol. Chem. 279 (2004) 33114–33122.

[9] W.A. Link, F. Ledo, B. Torres, M. Palczewska, T.M. Madsen, M. Savignac, J.P. Albar, B. Mellstrom, J.R. Naranjo, Day–night changes in downstream regulatory element antagonist modulator/potassium channel interacting protein activity contribute to circadian gene expression in pineal gland, J. Neurosci. 24 (2004) 5346–5355.

[10] R.D. Burgoyne, J.L. Weiss, The neuronal calcium sensor family of Ca^{2+}-binding proteins, Biochem. J. 353 (2001) 1–12.

[11] S. Ohya, Y. Morohashi, K. Muraki, T. Tomita, M. Watanabe, T. Iwatsubo, Y. Imaizumi, Molecular cloning and expression of the novel splice variants of K(+) channel-interacting protein 2, Biochem. Biophys. Res. Commun. 282 (2001) 96–102.

[12] M.H. Holmqvist, J. Cao, M.H. Knoppers, M.E. Jurman, P.S. Distefano, K.J. Rhodes, Y. Xie, W.F. An, Kinetic modulation of Kv4-mediated A-current by arachidonic acid is dependent on potassium channel interacting proteins, J. Neurosci. 21 (2001) 4154–4161.

[13] H.Y. Cheng, G.M. Pitcher, S.R. Laviolette, I.Q. Whishaw, K.I. Tong, L.K. Kockeritz, T. Wada, N.A. Joza, M. Crackower, J. Goncalves, I. Sarosi, J.R. Woodgett, A.J. Oliveira-dos-Santos, M. Ikura, D. van der Kooy, M.W. Salter, J.M. Penninger, DREAM is a critical transcriptional repressor for pain modulation, Cell 108 (2002) 31–43.

[14] C. Lilliehook, O. Bozdagi, J. Yao, M. Gomez-Ramirez, N.F. Zaidi, W. Wasco, S. Gandy, A.C. Santucci, V. Haroutunian, G.W. Huntley, J.D. Buxbaum, Altered Abeta formation and long-term potentiation in a calsenilin knock-out, J. Neurosci. 23 (2003) 9097–9106.

[15] H.C. Kuo, C.F. Cheng, R.B. Clark, J.J. Lin, J.L. Lin, M. Hoshijima, V.T. Nguyen-Tran, Y. Gu, Y. Ikeda, P.H. Chu, J. Ross, W.R. Giles, K.R. Chien, A defect in the Kv channel-interacting protein 2 (KChIP2) gene leads to a complete loss of I(to) and confers susceptibility to ventricular tachycardia, Cell 107 (2001) 801–813.

[16] F. Spreafico, J.J. Barski, C. Farina, M. Meyer, Mouse DREAM/calsenilin/KChIP3: gene structure, coding potential, and expression, Mol. Cell. Neurosci. 17 (2001) 1–16.

[17] N. Decher, A.S. Barth, T. Gonzalez, K. Steinmeyer, M.C. Sanguinetti, Novel KChIP2 isoforms increase functional diversity of transient outward potassium currents, J. Physiol. 557 (2004) 761–772.

[18] L.M. Boland, M. Jiang, S.Y. Lee, S.C. Fahrenkrug, M.T. Harnett, S.M. O'Grady, Functional properties of a brain-specific NH2-terminally

spliced modulator of Kv4 channels, Am. J. Physiol. Cell Physiol. 285 (2003) C161–C170.

[19] M. Kozak, Compilation and analysis of sequences upstream from the translational start site in eukaryotic mRNAs, Nucleic Acids Res. 12 (1984) 857–872.

[20] I. Deschenes, D. DiSilvestre, G.J. Juang, R.C. Wu, W.F. An, G.F. Tomaselli, Regulation of Kv4.3 current by KChIP2 splice variants: a component of native cardiac I(to)? Circulation 106 (2002) 423–429.

[21] M.H. Holmqvist, J. Cao, R. Hernandez-Pineda, M.D. Jacobson, K.I. Carroll, M.A. Sung, M. Betty, P. Ge, K.J. Gilbride, M.E. Brown, M.E. Jurman, D. Lawson, I. Silos-Santiago, Y. Xie, M. Covarrubias, K.J. Rhodes, P.S. Distefano, W.F. An, Elimination of fast inactivation in Kv4 A-type potassium channels by an auxiliary subunit domain, Proc. Natl. Acad. Sci. USA 99 (2002) 1035–1040.

[22] T. Schell, A.E. Kulozik, M.W. Hentze, Integration of splicing, transport and translation to achieve mRNA quality control by the nonsense-mediated decay pathway, Genome Biol. 3 (2002) 1006.1–1006.6.

[23] M. Osawa, K.I. Tong, C. Lilliehook, W. Wasco, J.D. Buxbaum, H.Y. Cheng, J.M. Penninger, M. Ikura, J.B. Ames, Calcium-regulated DNA binding and oligomerization of the neuronal calcium-sensing protein, calsenilin/DREAM/KChIP3, J. Biol. Chem. 276 (2001) 41005–41013.

[24] F. Ledo, W.A. Link, A.M. Carrion, V. Echeverria, B. Mellstrom, J.R. Naranjo, The DREAM-DRE interaction: key nucleotides and dominant negative mutants, Biochim. Biophys. Acta 1498 (2000) 162–168.

[25] E.K. Choi, N.F. Zaidi, J.S. Miller, A.C. Crowley, D.E. Merriam, C. Lilliehook, J.D. Buxbaum, W. Wasco, Calsenilin is a substrate for caspase-3 that preferentially interacts with the familial Alzheimer's disease-associated C-terminal fragment of presenilin 2, J. Biol. Chem. 276 (2001) 19197–19204.

[26] D. Van Hoorick, A. Raes, W. Keysers, E. Mayeur, D.J. Snyders, Differential modulation of Kv4 kinetics by KCHIP1 splice variants, Mol. Cell. Neurosci. 24 (2003) 357–366.

[27] K. Takimoto, E.K. Yang, L. Conforti, Palmitoylation of KChIP splicing variants is required for efficient cell surface expression of Kv4.3 channels, J. Biol. Chem. 277 (2002) 26904–26911.

[28] N.F. Zaidi, E.E. Thomson, E.K. Choi, J.D. Buxbaum, W. Wasco, Intracellular calcium modulates the nuclear translocation of calsenilin, J. Neurochem. 89 (2004) 593–601.

[29] B. Hessabi, P. Ziegler, I. Schmidt, C. Hessabi, R. Walther, The nuclear localization signal (NLS) of PDX-1 is part of the homeo-domain and represents a novel type of NLS, Eur. J. Biochem. 263 (1999) 170–177.

[30] C. Shiota, J. Coffey, J. Grimsby, J.F. Grippo, M.A. Magnuson, Nuclear import of hepatic glucokinase depends upon glucokinase regulatory protein, whereas export is due to a nuclear export signal sequence in glucokinase, J. Biol. Chem. 274 (1999) 37125–37130.

[31] K.J. Rhodes, K.I. Carroll, M.A. Sung, L.C. Doliveira, M.M. Monaghan, S.L. Burke, B.W. Strassle, L. Buchwalder, M. Menegola, J. Cao, W.F. An, J.S. Trimmer, KChIPs and Kv4 alpha subunits as integral components of A-type potassium channels in mammalian brain, J. Neurosci. 24 (2004) 7903–7915.

[32] H. Xiong, I. Kovacs, Z. Zhang, Differential distribution of KChIPs mRNAs in adult mouse brain, Brain Res. Mol. Brain Res. 128 (2004) 103–111.

[33] T. Timmusk, K. Palm, M. Metsis, T. Reintam, V. Paalme, M. Saarma, H. Persson, Multiple promoters direct tissue-specific expression of the rat BDNF gene, Neuron 10 (1993) 475–489.

PUBLICATION II

Pruunsild P*, Kazantseva A*, Aid T, Palm K, Timmusk T. (2007)
Dissecting the human *BDNF* locus: bidirectional transcription, complex splicing, and multiple promoters.
Genomics, Sep;90(3):397-406

Available online at www.sciencedirect.com
ScienceDirect
Genomics 90 (2007) 397–406
GENOMICS
www.elsevier.com/locate/ygeno

Dissecting the human *BDNF* locus: Bidirectional transcription, complex splicing, and multiple promoters☆

Priit Pruunsild [1], Anna Kazantseva[1], Tamara Aid, Kaia Palm, Tõnis Timmusk *

Department of Gene Technology, Tallinn University of Technology, Akadeemia tee 15, Tallinn 19086, Estonia

Received 10 January 2007; accepted 14 May 2007
Available online 12 July 2007

Abstract

Brain-derived neurotrophic factor (BDNF), a member of the nerve growth factor family of neurotrophins, has central roles in the development, physiology, and pathology of the nervous system. We have elucidated the structure of the human *BDNF* gene, identified alternative transcripts, and studied their expression in adult human tissues and brain regions. In addition, the transcription initiation sites for human *BDNF* transcripts were determined and the activities of *BDNF* promoters were analyzed in transient overexpression assays. Our results show that the human *BDNF* gene has 11 exons and nine functional promoters that are used tissue and brain-region specifically. Furthermore, noncoding natural antisense RNAs that display complex splicing and expression patterns are transcribed in the *BDNF* gene locus from the *antiBDNF* gene (approved gene symbol *BDNFOS*). We show that *BDNF* and *antiBDNF* transcripts form dsRNA duplexes in the brain in vivo, suggesting an important role for *antiBDNF* in regulating *BDNF* expression in human.

Keywords: Neurotrophic factor; Brain; neuron; Alternative splicing; BDNF; Natural antisense transcript; RNA duplex; Lin-7c/Mals-3/veli3

Brain-derived neurotrophic factor (BDNF) is a member of the nerve growth factor family of neurotrophins. During development BDNF supports the survival and differentiation of selected neuronal populations of the peripheral and central nervous systems and participates in axonal growth and pathfinding and in the modulation of dendritic growth and morphology [1,2]. BDNF also has a prominent role in later stages of nervous system development and in the adult by regulating synaptic transmission and plasticity and acts as a central modulator of pain [3]. BDNF has been shown to be a modulator of synaptogenesis in vivo [4] and has a functional role in the expression of LTP in the hippocampus [5]. Data accumulated in recent years suggest that neuronal activity regulates transcription of *BDNF,* transport of *BDNF* mRNA and protein into dendrites, and secretion of BDNF protein, which are important for the formation of appropriate synaptic connections and for learning and memory during development and in adults [6]. A single-nucleotide polymorphism in the human *BDNF* gene, resulting in a valine to methionine substitution (Val66Met) in the prodomain, has been shown to lead to reduced activity-induced BDNF secretion and memory impairment [7]. BDNF signaling has been shown to be critical in several neuropsychiatric and neurodegenerative diseases [1], for example, Huntington disease [8]. These results taken together show that BDNF has numerous important roles in brain development, physiology, and pathology.

During development, BDNF protein expression is more abundant in the nervous system compared to other tissues and its levels are dramatically increased in the brain during postnatal development [9]. In the adult nervous system, *BDNF* displays a widespread distribution pattern, with the highest levels of mRNA and protein in the hippocampus, amygdala, cerebral cortex, and hypothalamus [9–12]. *BDNF* mRNA expression is mostly confined to neurons and there are only a few brain areas where *BDNF* mRNA is not detected [10–12]. *BDNF* expression in adult tissues is detectable also outside of the central nervous

☆ Sequence data from this article have been deposited in the GenBank Data Libraries under Accession Nos. EF674517 - EF674521 and EF689009 - EF689021 (human *BDNF* mRNAs), and EF689022 - EF689042 (human *antiBDNF* RNAs).

* Corresponding author. Fax: +372 620 4401.
E-mail address: tonis.timmusk@ttu.ee (T. Timmusk).
[1] These authors contributed equally to this work.

0888-7543/$ - see front matter © 2007 Elsevier Inc. All rights reserved.
doi:10.1016/j.ygeno.2007.05.004

system. Lower *BDNF* mRNA levels than in the hippocampus have been detected in the thymus, liver, spleen, heart, and lung [9,11,13,14].

The structure and regulation of the *BDNF* gene have been studied in rodents [15–17]. Mouse and rat *BDNF* genes have eight 5′ exons containing separate promoters upstream of each exon and one 3′ exon encoding the mature BDNF protein [17]. Multiple promoters determine tissue-specific expression of the *BDNF* transcripts [15,17]. The human *BDNF* has also been shown to consist of multiple 5′ noncoding exons and one coding exon, which give rise to alternatively spliced transcripts [18–20]. According to the most recent description of the organization of the human *BDNF* gene locus and alternatively spliced transcripts the human *BDNF* has seven noncoding and one coding exon [19]. Provided that only a partial description of the transcripts was given and expression of the alternative transcripts was studied in only a few brain regions and was not investigated in human nonneural tissues, we undertook the current study to analyze thoroughly the structure of the human *BDNF* gene, characterize the expression of alternatively spliced *BDNF* mRNAs in different human tissues and brain regions, and identify and study the activities of alternative human *BDNF* promoters.

Results

Structure and alternative splicing of human BDNF and antiBDNF (approved gene symbol BDNFOS)

To reexamine the human *BDNF* gene structure and identify mRNAs transcribed from the gene, in silico analysis, 5′ rapid amplification of cDNA ends (5′ RACE), and RT-PCR analyses were performed. First, all *BDNF* mRNAs and expressed sequence tags (ESTs) available at the NCBI database (http://www.ncbi.nlm.nih.gov) were analyzed. Primers designed for PCR analyses are presented in Supplementary Table 1. Total RNAs of the adult human frontal cerebral cortex, medulla, and hippocampus were used as templates in the RT-PCR. Second, to identify novel *BDNF* transcripts and to determine the transcription start sites for the human *BDNF* transcripts, 5′ RACE of human adult hippocampal and cerebellar RNA was performed using antisense primers specific for the 3′ exon and for the 5′ exons (Supplementary Table 1).

BDNF gene exon–intron boundaries and genomic locations were determined by BLAT algorithm (http://genome.ucsc.edu/cgi-bin/hgBlat) and by direct comparison of PCR-amplified sequences with genomic DNA sequence from the NCBI database (Accession No. AF411339). The designation of the human *BDNF* exons in this study is consistent with the naming of the mouse and rat *BDNF* exons described in the study by Aid et al. [17]. The exons unique to human *BDNF* are marked with the letter “h” and are named with the same number as the neighboring upstream exon. Our analysis showed that the human *BDNF* gene spans ~70 kb and consists of 11 exons (Fig. 1). *hBDNF* exons named by Liu et al. [19] are designated here as old exons. Comparison of our data with that of Liu et al. [19] shows that exons I–IV correspond to the respective old exons; exons V, Vh, VIII, and VIIIh are novel exons; exons VI and VII correspond to old exons V and VI, respectively; and exon IX variants IXb and IXd correspond to old exons VII and VIII, respectively (Fig. 2A). Nine of the exons, I, II, III, IV, V, Vh, VI, VII, and IX, can be defined as 5′ exons (Fig. 1). Cloning and sequencing of the 5′ RACE products revealed that the transcription start sites relative to the 3′ end of the respective exon are located as follows: −647 and −428 nt for exon I; −433, −423, −422, −416, −407, −400, −226, −224, −204, −200, −78, and −47 nt for exon II; −237 and −191 nt for exon III; −337, −333, −274, and −215 nt for exon IV; −82, −80, and −79 nt for exon V; −225 and −222 nt for exon Vh; −324; −323, −319, −318, and −315 nt for exon VI; and −184 nt for exon VII (Supplementary Fig. 1). We determined that human *BDNF* transcription starts also from the last exon, exon IX, −1102 nt upstream of the translation start site in this exon (Supplementary Fig. 1). No major differences in the transcription start site locations were observed when 5′ RACE products from hippocampal or cerebellar RNA were analyzed. Two exons, VIII and VIIIh, are rarely used and always in combination with exon V as the 5′ exon (Fig. 1). Exons II, III, IV, V, Vh, VI, and VIIIh are untranslated exons and translation of the transcripts containing these exons starts from the ATG positioned in exon IX (Supplementary Fig. 1). Exons I, VII, and VIII contain in-frame ATG codons that could be used as translation start sites leading to the prepro-BDNF proteins with longer N-termini (Fig. 2B).

In addition, we identified alternative splice donor sites in exons II, V, and VI (Fig. 1, Supplementary Fig. 1, and Table 2). Usage of these splice sites leads to the formation of transcripts with different 5′ UTR lengths but does not affect the coding region of *BDNF*. Characterization of the exon–intron boundary sequences showed that not all exon–intron splice junctions adhere to the GU–AG rule characteristic of eukaryotes. We found that exon VII is unique because the splice donor site used contains nucleotides GG instead of the conventional GU sequence (Supplementary Table 2). Exon IX, which encodes the BDNF protein and 3′ UTR, is subjected to internal splicing and/or transcription initiation upstream of exon IX that leads to the generation of alternative transcripts containing variants of exon IX. These exon IX variants comprise different regions or combinations of regions of exon IX that were designated “a”, “b”, “c”, and “d” (Fig. 1). Exon IX is used mostly in conjunction with the upstream exons (I–VIII, VIIIh), and in that case only the most 3′ region of exon IX, IXd, is included in the mature transcripts. On rare occasions when exon VI is the 5′ exon, alternative splicing occurs within exon IX leading to the inclusion of two regions, IXb and IXd, in the mRNAs. When transcription is initiated upstream of exon IX the transcripts are not subjected to internal splicing and contain all the regions of exon IX: IXa, IXb, IXc, and IXd. In extremely rare cases exon IX region “c” is spliced out (Fig. 1 and Supplementary Fig. 1).

Recently it was reported that natural antisense transcripts are transcribed from the human *BDNF* gene locus [19]. We analyzed the exon–intron junctions of amplified *BDNF* cDNAs and also noticed that several mRNAs are transcribed in an antisense direction compared to BDNF mRNAs. This finding was

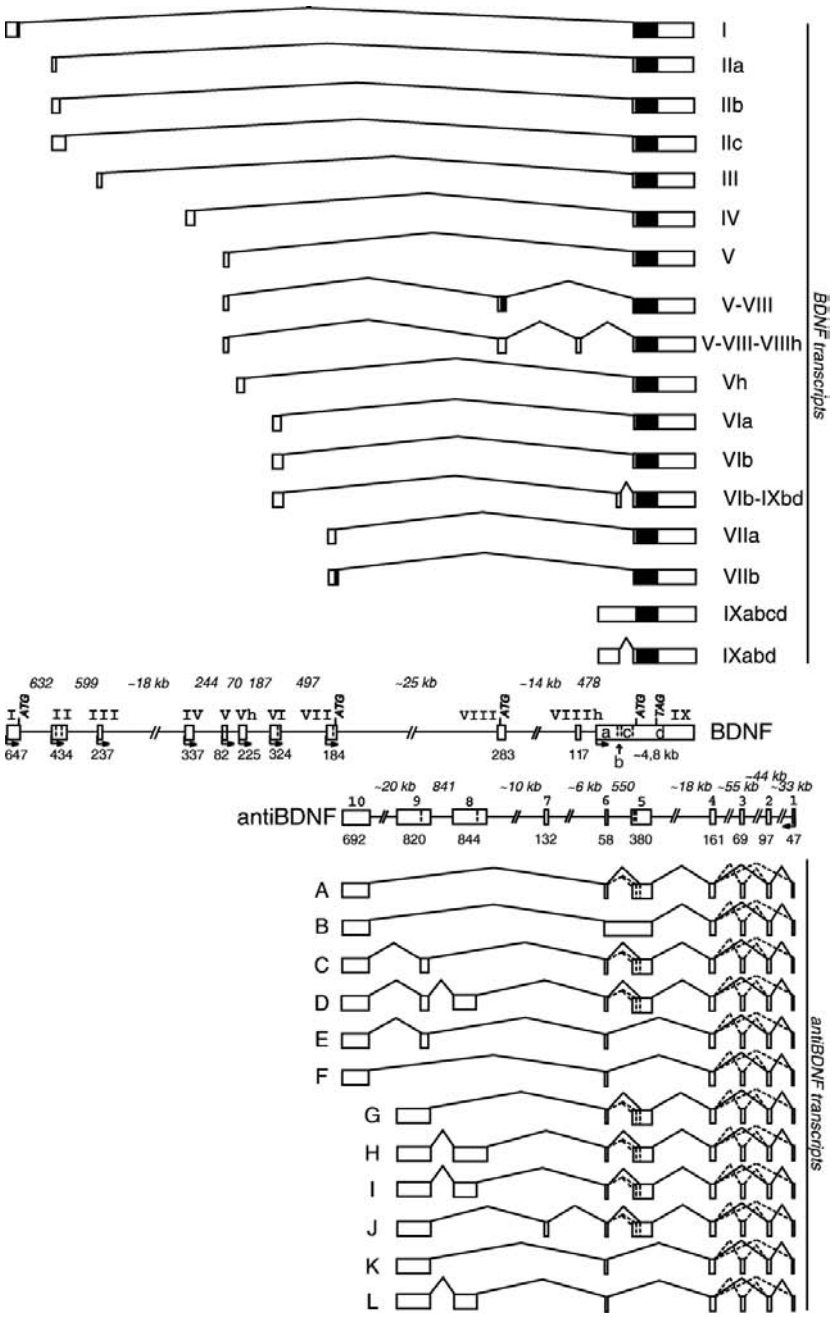

Fig. 1. Structure and alternative transcripts of the human *BDNF* (top) and *antiBDNF* (bottom) genes. The structural organization of the exons and introns was determined by analyzing genomic and mRNA sequence data using bioinformatics, RT-PCR, and 5′ RACE. Exons are shown as boxes and introns as lines. Filled boxes and open boxes indicate the translated regions of the exons and the untranslated regions of the exons, respectively. The numbers below the exons and above the introns indicate their sizes. Exon and intron sizes are in base pairs, if not indicated otherwise. Arrows indicate the transcription start sites. ATG and TAG mark the positions of the translational start and stop codons, respectively. Vertical dashed lines indicate alternative splicing sites for the respective exons. *BDNF* exon IX is divided into regions "a", "b", "c", and "d" as indicated in the box marking the position of exon IX. *BDNF* transcript names relate to the upstream exons used in front of the major 3′ exon IXd. "A"–"L" mark *antiBDNF* transcripts. Solid lines connecting the exons of transcripts represent the major splicing patterns of exons. Dashed lines connecting the exons of transcripts represent the minor splicing patterns of *antiBDNF*. Exon numbers are shown in Roman numerals for the *BDNF* gene and in Arabic numerals for the *antiBDNF* gene.

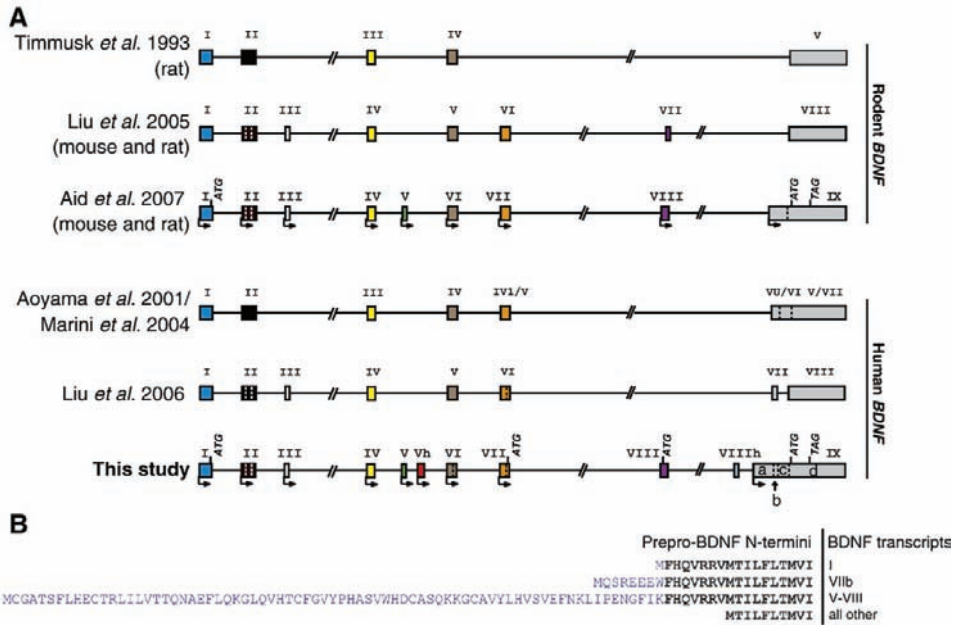

Fig. 2. (A) Comparison of the human and rodent *BDNF* gene structures proposed by different studies. Structures presented are according to Timmusk et al. [15], Liu et al. [16], Aid et al. [17], Aoyama et al. [20], Marini et al. [40], and Liu et al. [19] and the human *BDNF* gene structure determined in this study. Exons are shown as boxes and introns as lines. The identical human exons and the rodent exons homologous to the human exons are shown in the same color in all the structures. Novel exons determined by this study are in green (V), red (Vh), purple (VIII), and light blue (VIIIh). (B) Amino acid sequences of different potential prepro-BDNF N-termini. Amino acids encoded by exon IX are in black and sequences encoded by alternative 5′ exons are in blue. The transcripts encoding the respective N-termini of BDNF are listed adjacent to the N-terminal sequences.

also confirmed by orientation-specific RT-PCR and by RNase protection assay (data not shown). We named the gene and transcripts transcribed from the opposite strand of *BDNF* as *antiBDNF* (for antisense *BDNF;* part of it is described by Liu and colleagues and designated as OSBDNF—Liu et al. [19]). The *antiBDNF* gene spans ~191 kb and consists of at least 10 exons (exons 1–10) and is transcribed from one promoter as shown by our 5′ RACE analyses (Fig. 1). All intron–exon boundaries of the *antiBDNF* gene are consistent with the GU–AG consensus (Supplementary Table 2).

Exons 1–4 of the *antiBDNF* gene are located downstream of the *BDNF* gene (Fig. 1). Exon 5, 345 bp in length, overlaps regions IXc and IXd and exon 6 overlaps region IXa of the *BDNF* coding exon. Exons 7–10 of *antiBDNF* are located in the introns of *BDNF*. In silico and RT-PCR analyses showed that alternative splicing from the *antiBDNF* pre-mRNA produces more than 300 transcripts, but exon 1 of *antiBDNF* is always used as the most 5′ exon for all the transcripts. Of note, our bioinformatics analysis showed that *antiBDNF* exon 1 is in head-to-head orientation with exon 1 of *Lin-7c/Mals-3/veli3,* suggesting that a bidirectional promoter controls the expression of these genes. The majority of the *antiBDNF* alternative transcripts contain exons 5 and 6, which are complementary to the *BDNF* protein-coding exon IX. However, in several *antiBDNF* transcripts exon 5 is skipped out. In addition, exon 5 of *antiBDNF* could be spliced using three alternative splice donor sites (Fig. 1, Supplementary Fig. 2), and the lengths of exons 8 and 9 can vary because of usage of internal alternative splice acceptor sites (Fig. 1). There are no potential open reading frames in any of the identified mRNAs transcribed from the *antiBDNF* gene, suggesting that these transcripts are non-protein-coding, as proposed also by Liu et al. [19].

Expression of alternatively spliced BDNF and antiBDNF mRNAs in adult human tissues

Expression of *BDNF* and *antiBDNF* transcripts was determined by RT-PCR in 22 different adult human tissues (Fig. 3). The results showed that human *BDNF* alternative transcripts are expressed in a tissue-specific manner. The levels of the majority of the human *BDNF* transcripts were highest in the brain. However, several alternative *BDNF* mRNAs showed relatively high expression levels in nonneural tissues. For example, expression levels of transcripts containing exons VI and IXabcd were high in the heart, placenta, and prostate. Transcripts containing exons I, Vh, VI, and IXabcd were highly expressed in the testis. High levels of transcripts containing exon VI were expressed also in the lung. Several *BDNF* mRNAs were expressed at moderate or low levels in the adrenal gland (exon Vh and exon IXabcd transcripts), bone marrow (exons I, VI, and IXabcd transcripts), kidney, muscle, stomach, spinal cord (exons Vh and VI transcripts), liver (exon IXabcd transcripts), small intestine (exon VI transcripts), and trachea (exons Vh, VI, and IXabcd transcripts). Low levels of exon IXabd transcripts

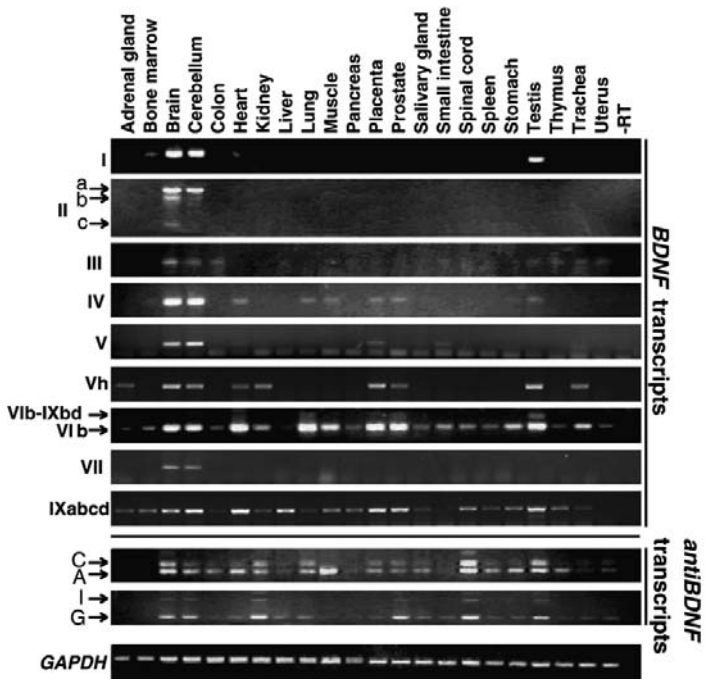

Fig. 3. Semiquantitative analysis of human *BDNF, antiBDNF,* and control *GAPDH* mRNA expression in adult human tissues by RT-PCR. Roman numerals on the left indicate the detected *BDNF* transcripts and the 5′ exon-specific primers used in combination with an antisense primer located in the *BDNF* coding region in exon IXd (Supplementary Table 1). A, C, G, and I refer to the respective *antiBDNF* transcripts shown in Fig. 1.

were observed only in some cell lines (data not shown). *BDNF* mRNAs containing exons II and VII were expressed exclusively in the brain. Altogether, the results indicate that transcripts containing exons II, III, IV, V, and VII are predominantly brain-specific. Transcripts containing exons I and Vh are, in addition to brain, expressed in certain peripheral tissues, and transcripts containing exons VI and IXabcd show a wide pattern of expression.

antiBDNF transcripts were present at different levels in almost all human tissues analyzed (Fig. 3). High expression of human *antiBDNF* transcripts was detected in the brain, kidney, spinal cord, and testis. Moderate levels of *antiBDNF* RNA were seen in the lung, prostate, salivary gland, spleen, stomach, and uterus. Low *antiBDNF* expression levels were detected in the adrenal gland, liver, placenta, small intestine, and trachea. Certain alternative transcripts of *antiBDNF* were expressed in a tissue-specific manner. For example, *antiBDNF* transcripts with exon 10 were present in the colon and muscle, whereas transcripts with exon 9 were not expressed in these tissues. Taken together, *BDNF* and *antiBDNF* expression patterns were distinct, although partially overlapping.

Expression of alternatively spliced BDNF and antiBDNF mRNAs in adult human brain regions

Expression analysis of human *BDNF* and *antiBDNF* transcripts in 30 different adult brain regions was performed by RT-PCR (Fig. 4). Several differences in the expression of alternatively spliced human *BDNF* transcripts were detected. The results showed that all *BDNF* transcripts were expressed at high levels in the corpus mammillare (mammillary body), pons, hippocampus, frontal cortex, colliculi, and olfactory tract. All *BDNF* transcripts except the ones containing exons V and VII were expressed at high levels in the cerebellum and medulla, and all transcripts but those containing exon IXabcd were expressed at high levels in the infundibulum. *BDNF* expression in the dentate nucleus, white matter of the cerebellum, substantia nigra, nucleus ruber (red nucleus), and epiphysis was very low. *BDNF* expression was also very low in the globus pallidus, striatum (caudate nucleus and putamen), and thalamus, with the exception of exon IXabcd transcripts, which were expressed at relatively high levels in these regions. In the amygdala only transcripts containing exons I, IV, and VI were expressed at high levels. In the corpus callosum only exon VI and IXabcd transcripts were detected. Notably, comparison of expression levels of individual transcripts in different brain areas indicated that *BDNF* exon II transcript levels were much higher in the cerebellum than in other brain areas. Exon IXabcd mRNAs were expressed at relatively similar levels in all brain regions, with only infundibulum having very low expression levels. Interestingly, in the brain structures that contain only glial cells and axons and do not contain neuronal cell bodies, such as corpus callosum and optic nerve, exon IXabcd transcripts were predominantly detected. Transcripts containing exons I, Vh, and VI

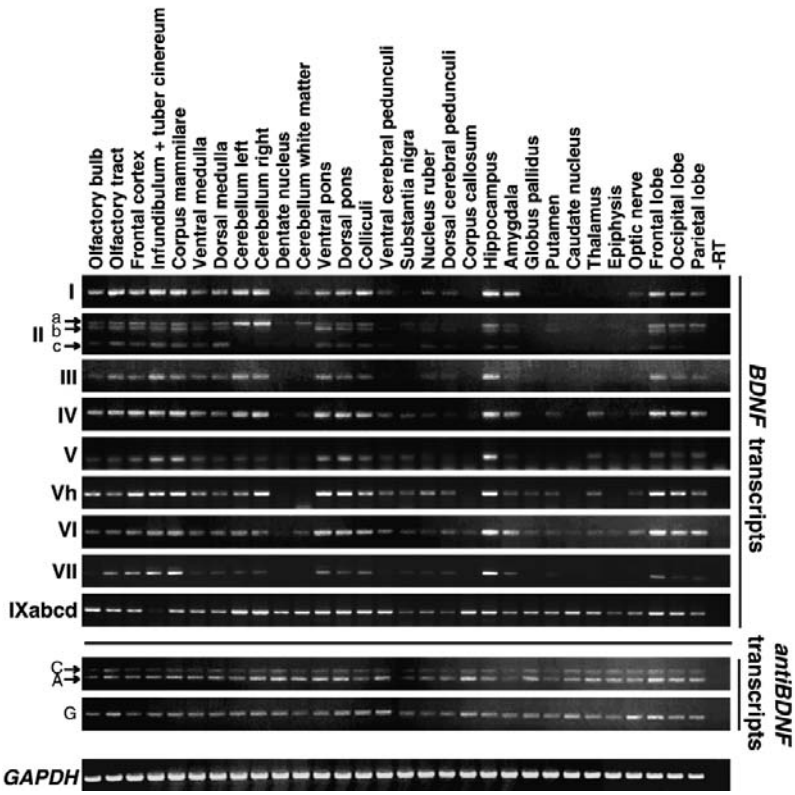

Fig. 4. Semiquantitative analysis of human *BDNF, antiBDNF,* and control *GAPDH* mRNA expression by RT-PCR in different human brain regions. Roman numerals on the left indicate the detected BDNF transcripts and the 5′-exon-specific primers used in combination with an antisense primer located in the *BDNF* coding region in exon IXd (Supplementary Table 1). A, C, and G refer to the respective *antiBDNF* transcripts shown in Fig. 1.

were also present in the optic nerve, although at low levels. *antiBDNF* transcripts were expressed in all studied brain structures at similar levels (Fig. 4).

Promoter activities of the 5′ flanking regions of human BDNF and antiBDNF upstream exons

Since the promoter regions of the human *BDNF* gene have not been analyzed previously and hypothesizing that a functional promoter precedes each of the identified 5′ exon of *BDNF* and that there is a promoter upstream of *antiBDNF* exon 1, the activities of nine potential promoter regions within the *BDNF* gene (namely the upstream sequences of exons I, II, III, IV, V, Vh, VI, VII, and IXabcd) and the region upstream of exon 1 of *antiBDNF* were analyzed for transcription-promoting activity using chloramphenicol acetyltransferase (CAT) assays. The putative promoter regions, each ~0.2–1.3 kb in length and containing a part of the respective 5′ UTR and 5′ flanking genomic sequence (Supplementary Fig. 1), were isolated and cloned into the pBLCAT2 vector in front of the *CAT* gene. The promoter constructs were transfected into human embryonic kidney HEK293T and mouse neuroblastoma N2a cells and the promoter activities were analyzed.

The results showed that all the regions upstream of the 5′ exons of the *BDNF* gene and exon 1 of the *antiBDNF* gene were functional and could activate CAT expression (Fig. 5). Thus it was concluded that the regions upstream of the 5′ exons of the *BDNF* gene and exon 1 of the *antiBDNF* gene act as separate promoters. However, the activities of the promoters varied and differences were detected also between the cell lines used. The activities of promoters upstream of exons II, V, Vh, and VII were somewhat lower compared to other promoters in N2a cells. In HEK293T cells the activities of these promoters could be detected only after longer reaction times. Other promoters showed similar activities in both of the cell lines with *BDNF* promoters upstream of exons III and VI and the *antiBDNF* promoter being the strongest in both cell lines. However, promoters upstream *BDNF* exons I, IV, and IXabcd were slightly (about twofold) more active in HEK293T cells than in N2a cells.

Human BDNF and antiBDNF transcripts form RNA duplexes in adult human brain in vivo

According to our data human *BDNF* and *antiBDNF* are co-expressed in many tissues studied. The complementary region

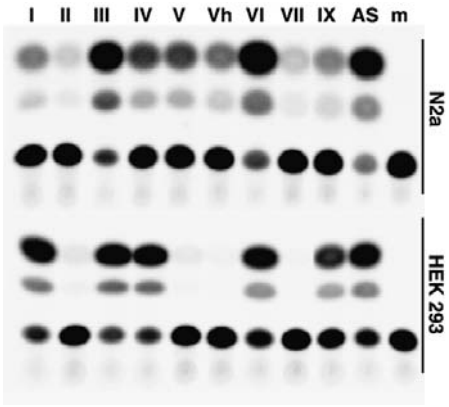

Fig. 5. Analyses of *BDNF* and *antiBDNF* promoter activities in HEK293T and N2a cells. The relative activities of the 5′ flanking regions of *BDNF* exons I, II, III, IV, V, Vh, VI, VII, and IXabcd and *antiBDNF* to promote CAT expression are shown. The promoter regions cloned in front of the *CAT* gene are shown in Supplementary Fig. 1. Note that the activities of *BDNF* promoters II, V, Vh, and VII in HEK239T cells were detectable using longer reaction times. m, mock-transfected cells, negative control.

of the majority of spliced *BDNF* and *antiBDNF* transcripts spans 222 nt or more depending on the splicing donor site used for *antiBDNF* exon 5 (Supplementary Fig. 2 and Supplementary Table 2). Based on this knowledge we hypothesized that if *antiBDNF* has a regulatory role in *BDNF* expression, the complementary RNAs might form RNA–RNA duplexes in vivo. To study this hypothesis we performed a PCR-based assay. Briefly, RNase A/T1-treated RNA from adult human cerebellum was used as a potential double-stranded RNA (dsRNA) template for cDNA synthesis and the existence of the duplexes was analyzed by PCR with primers specific for the complementary region of *BDNF* and *antiBDNF* (Supplementary Table 1). Our results showed that *BDNF*/*antiBDNF* dsRNA duplexes are present in the human brain in vivo (Fig. 6). Control experiments using a primer targeting the region of *antiBDNF* RNA outside of the complementary sequence in combination with a primer specific for the complementary region and experiments using RNA template in which the reverse transcription reaction was omitted showed that the RNA duplex-specific product was not the result of single-strand RNA (ssRNA) or genomic DNA contamination, respectively.

Discussion

Previous studies have revealed that the human *BDNF* gene consists of seven putative 5′ exons and one protein-coding exon [19,20]. However, the expression patterns of different exons have not been thoroughly studied and possible linkage of these exons to separate promoters has not been investigated. Here we show that the human *BDNF* gene, extending over 70 kb, contains 11 exons. The 3′ exon encodes all or most of the protein depending on the 5′ exon used. Independent of the 5′ exon usage, two separate polyadenylation signals in exon IX can be utilized in *BDNF* transcripts. In addition, our data showed that the human *BDNF* gene comprises nine functional promoters.

The structures of the human *BDNF* gene and transcripts determined in this study are in good agreement with the results obtained for the rat and mouse *BDNF* genes [17]. Some differences are present, though. First, human *BDNF* contains two more exons than rodent *BDNF.* Compared to the rat and mouse genes [17] there is an additional exon, exon Vh, linked to a promoter between exons V and VI. Human *BDNF* exon VIIIh, which is not linked to a separate promoter, is also not present in

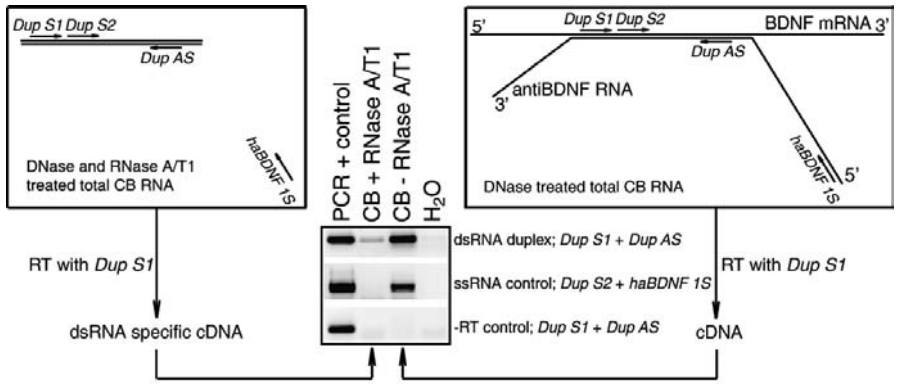

Fig. 6. *BDNF* and *antiBDNF* transcripts form dsRNA duplexes in the human brain in vivo. A schematic representation of the RNA duplex detection assay is shown. Briefly, total human cerebellar RNA was DNase treated. This RNA was divided into two—one half was treated with RNase A/T1 (box on the left) and the other was used as a −RNase control (box on the right). Both RNAs were reverse transcribed (RT) with a *BDNF*/*antiBDNF* complementary region-specific primer, Dup_S1. Subsequently these cDNAs were used as templates in PCR to detect *BDNF*/*antiBDNF* duplex with primers Dup_S1 and Dup_AS. ssRNA contamination control reaction was conducted with primers Dup_S2 and haBDNF_S1. The −RT reaction was used for detection of genomic DNA contamination using primers Dup_S1 and Dup_AS. Lines indicate RNAs, double line marks the complementary region of *BDNF* exon IXd and *antiBDNF* exon 5. Primer positions are indicated with arrows parallel with the lines and primer names are in italic. Human hippocampal cDNA synthesized using an oligo(dT) primer (PCR+control) was used as positive control for all the reactions.

rodent *BDNF*. Furthermore, cryptic splicing donor and acceptor sites are used in human exon IX leading to transcripts containing exons IXbd and IXabd. These transcripts have not been detected in rodents [17]. All this adds more complexity to the regulation of human *BDNF*. Second, in most cases, the usage of alternative promoters in the human *BDNF* gene leads to the expression of transcripts with different 5′ UTRs and with the protein-coding region in the common 3′ exon IXd. However, usage of an alternative upstream in-frame translation start site containing exon I, VII, or VIII could potentially lead to human BDNF prepro-proteins with longer N-termini. Only the translation initiation codon within exon I is characteristic of rodent *BDNF* genes, suggesting that there are more BDNF protein isoforms in human than in rodents. Third, although the transcription initiation sites are generally in good agreement with the respective regions in rodents, we identified more transcription start sites for human exons II and IV than had been reported previously for the rodent *BDNF* respective exons. Fourth, in contrast to the rodent *BDNF* genes we found that exon VIII of the human *BDNF* is not used as a 5′ exon as determined by the 5′ RACE analysis. We show that in human the rarely used exon VIII of *BDNF* is exclusively spliced to exon V. Exon V can also be spliced to exon IXd without including exon VIII. Exon VIII was not detected in any transcript other than the ones starting with exon V, pointing to a possible functional regulation between the usage of a certain promoter and subsequent splicing. Similar promoter-governed splicing regulation has been identified for the human nitric oxide synthase (*NOS1*) [21] and mouse *bcl-X* [22] genes, for example. This kind of splicing regulation is especially interesting provided the notion that exon VIII of *BDNF* contains one of the alternative ATGs that may lead to the synthesis of a prepro-BDNF protein with an alternative N-terminus.

We analyzed the splicing of the human *BDNF* pre-mRNAs and expression of consequent alternative mRNAs in detail. We found that *BDNF* transcripts containing exons II, III, IV, V, and VII are mostly brain-specific, whereas other *BDNF* mRNAs are also expressed at variable levels in nonneural tissues. Similar to the expression pattern of *BDNF* mRNAs in rodents [16,17], the most abundant transcripts in human nonneural tissues were transcripts containing exons VI and IXabcd that were expressed at high levels in several tissues, particularly heart, lung, skeletal muscle, testis, prostate, and placenta. To the best of our knowledge, these are the first data about the expression of alternatively spliced *BDNF* mRNAs in human nonneural tissues. In the human brain, expression of BDNF has been studied at the protein level using many different antibodies, the specificity of which is not always clear [23]. Fewer data are available about *BDNF* mRNA expression. In most studies on human *BDNF*, mRNA expression has been studied in only some regions of brain using postmortem tissue [23–25]. In two studies the expression of human *BDNF* mRNAs with alternative 5′ exons was examined in a few adult brain regions using RT-PCR [19,26]. Our study is the first to examine *BDNF* exon-specific mRNA levels across the whole human brain, thus adding important new data to *BDNF* expression in adult human brain. In the adult human brain, high levels of *BDNF* mRNAs were present in the hippocampus, cerebral cortex, amygdala, and cerebellum, which is similar to the previously reported data on the *BDNF* expression in rodent brain [10,11,15,27,28]. *BDNF* is expressed predominantly in neurons, although some studies have identified *BDNF* expression also in rodent astrocytes [29,30], microglia [31], and oligodendrocytes [32], both in vivo and in vitro. Here we show that some of the alternatively spliced human *BDNF* mRNAs, particularly transcripts containing exons VI and IXabcd, are present in vivo in the corpus callosum and optic nerve containing mostly oligodendroglial cells and axonal projections.

Gene expression in eukaryotes is a highly coordinated process involving regulation at many different levels, among which the regulation of transcription is one of the most important. Several types of *cis*-acting DNA sequence elements, including promoters, contribute to this process. About 18% of human genes have multiple promoters, which regulate and increase their transcriptional and translational potential [33]. Human *BDNF* promoter IV is the only promoter of the human *BDNF* gene that had been characterized so far [18]. In this study we show that *BDNF* gene expression is under the control of at least nine alternative tissue-specific promoters linked to separate 5′ exons. Alternative promoters of the *BDNF* gene could also be involved in developmental stage-specific expression and cell-type-specific expression, giving additional flexibility to the control of *BDNF* expression. Therefore, the data presented in this study show that the expression of the human *BDNF* gene is highly regulated at the level of transcription.

One of the results of our study was the characterization of endogenous noncoding antisense RNAs transcribed from the human *BDNF* gene locus. According to our data the *antiBDNF* gene consists of 10 exons and one functional promoter upstream of exon 1. We show that *antiBDNF* transcripts are expressed in almost all adult human tissues analyzed. High levels of *antiBDNF* mRNAs are present in the brain, kidney, spinal cord, and testis. Expression levels are low in adrenal gland, bone marrow, pancreas, small intestine, uterus, and some other tissues. In the adult brain, all *antiBDNF* transcripts are expressed at similar levels in all brain regions analyzed. We found that hundreds of different noncoding RNAs might be generated from the *antiBDNF* gene as a result of alternative splicing. Alternatively spliced isoform diversity is common to many eukaryotic organisms and it is particularly widely used in the nervous system [34]. Interestingly, *antiBDNF* is not present in rodents [16,17]. *antiBDNF* ESTs are also not available for chimpanzee and rhesus monkey although highly homologous sequences are present in the genomes of these animals (data not shown). All this suggests that *antiBDNF* could have evolved during primate/hominid evolution, as was proposed also by Liu et al. [19].

In this study we have shown that in the human brain *BDNF* and *antiBDNF* transcripts form dsRNA duplexes in vivo. This indicates that *antiBDNF* transcripts could have an important role in the regulation of *BDNF* expression in human. Several studies have shown that natural antisense transcripts (NATs) are involved in the regulation of gene expression in eukaryotes [35,36]. For example, NATs have been suggested to play an

important role in the regulation of several genes encoding transcription factors that are important in eye development and function in mice [37]. Characterization of overlapping transcripts in various species indicates that this form of RNA-mediated gene regulation represents a widespread phenomenon [36,38]. NATs are particularly prevalent in the nervous system where they regulate the expression of several genes [35]. In the case of human *BDNF* and *antiBDNF,* the transcripts could act as *cis*-antisense RNAs and generate siRNAs targeting one of the initial transcripts, as do the natural *cis*-siRNAs described for genes involved in salt tolerance in *Arabidopsis thaliana* [39]. Other possible regulatory functions of *antiBDNF* would be direct inhibition of *BDNF* transcription or translation and/or regulation of *BDNF* pre-mRNA splicing. Our results show that the expression of *antiBDNF* and *BDNF* transcripts in different tissues is not mutually exclusive and that the levels of *BDNF* mRNA do not appear to be specifically reduced in tissues that express high levels of *antiBDNF* transcripts. However, it is possible that the *antiBDNF* transcripts could modulate the levels of *BDNF* provided they are coexpressed in the same cell.

In conclusion, this detailed characterization of the human *BDNF* gene locus opens up insights into the mechanisms governing *BDNF* gene regulation in human.

Materials and methods

RNA isolation, RT-PCR, and cloning and sequencing of RT-PCR products

Total RNAs from 23 human tissues were obtained from Clontech. Total RNAs from postmortem adult human brain regions were isolated using the RNAwiz RNA isolation reagent and treated with DNase (Ambion, USA) according to the supplier's protocol. All experiments with human tissues were approved by the local ethical committee. Five micrograms of total RNA was reverse-transcribed to cDNA with an oligo(dT) primer (Proligo, France) and SuperScript III reverse transcriptase using the SuperScript III First-Strand Synthesis System (Invitrogen, USA). PCR amplification was carried out using HOT FIREPol DNA polymerase (Solis Biodyne, Estonia), according to the manufacturer's instructions. One-fortieth of the first-strand cDNA reaction mix was used in the PCR. The exon-specific PCR primers were designed based on the sequence of the human *BDNF* gene (NCBI Accession No. AF411339), ESTs, and mRNA sequences from GenBank. Sequences for all primers are listed in Table 1 of the supplementary material. The lengths of the PCR products using the primer hBDNF_IXbAS in combination with the following primers were hBDNF_IS, 472 bp; hBDNF_IIS, 610, 527, and 312 bp; hBDNF_IIIS, 347 bp; hBDNF_IVS, 412 bp; hBDNF_VS, 673, 556, and 273 bp; hBDNF_VhS, 340 bp; hBDNF_VIS, 494, 387, and 369 bp; hBDNF_VIIS, 429 and 328 bp; and hBDNF_IXS, 597 and 363 bp. The lengths of the longest PCR products with haBDNF_1S in combination with the following primers were haBDNF_9AS, 947 bp, and haBDNF_10AS, 1483 bp. All products from the RT-PCR were cloned into the pCRII-TOPO vector (Invitrogen) and sequenced.

Analyses of transcription start sites

The transcription start sites for the *BDNF* and *antiBDNF* transcripts were detected with 5′ RACE using the GeneRacer Kit (Invitrogen) for full-length, RNA ligase-mediated rapid amplification of 5′ cDNA ends, according to the manufacturer's instructions. Briefly, 5 μg of total RNA from human hippocampus and cerebellum was dephosphorylated and decapped. The GeneRacer RNA oligo was ligated to the decapped 5′ ends of the full-length mRNAs and reverse transcription of the mRNAs was performed. RACE-ready cDNAs were used as templates for subsequent PCR using the GeneRacer 5′ primer in combination with *BDNF* exon-specific primers (Supplementary Table 1). The PCR products were gel purified and cloned into the pCRII-TOPO (Invitrogen) vector and verified by sequencing.

BDNF promoter–CAT reporter plasmids and CAT assay

PCR was performed to amplify promoter fragments of the human *BDNF* and *antiBDNF* genes with the appropriate primers (Supplementary Table 1). Human genomic DNA was used as a template. The amplified fragments were cloned into the pBL-CAT2 plasmid upstream of the coding region of the *CAT* gene, replacing the thymidine kinase promoter, and verified by sequencing. HEK293T and N2a cells were used for the analysis of promoter activities. The cells were maintained in Dulbecco's modified Eagle's medium supplemented with 10% fetal calf serum at 37°C in a 5% CO_2 atmosphere. Transfection of cells with the promoter–CAT reporter plasmids was performed with FuGENE 6 (Roche Diagnostics, USA) according to the supplier's instructions. The transfected cells were harvested 40 h after transfection. The samples were incubated with ^{14}C-labeled chloramphenicol and acetyl-CoA and the radioactive products were separated by thin-layer chromatography silica gel (Merck, USA) and visualized by autoradiography as described before [15].

BDNF/antiBDNF RNA duplex analyses

Ten micrograms of human cerebellar RNA, isolated with RNAwiz (Ambion), was treated with DNase (Ambion Turbo DNA-*free*) for 30 min at 37°C according to the manufacturer's instructions, precipitated, and treated with RNase A/T1 (Ambion) for 30 min at 37°C in RNase buffer (300 mM NaCl, 10 mM Tris, pH 7.4, and 5 mM EDTA). The reaction was terminated with 0.4 mg/ml proteinase K (Roche) in 200 mM Tris, pH 7.4, 25 mM EDTA, and 1% SDS for 30 min at 37°C, and the dsRNA was phenol/chloroform extracted. cDNA was synthesized from this dsRNA using the *BDNF/antiBDNF* complementary region-specific primer Dup_S1 (Supplementary Table 1) with Superscript III (Invitrogen) according to the manufacturer's instructions in the presence of 5% DMSO. In subsequent RNA duplex detection PCR 1/20 of the cDNA was used along with primers specific for the *BDNF/antiBDNF* complementary region, Dup_S1 and Dup_AS (Supplementary Table 1; product size 156 bp). Primer haBDNF_1S recognizing *antiBDNF* exon 1 in combination with Dup_S2 (Supplementary Table 1; product size 490 bp) was used for detection of ssRNA contamination. In addition, a −RT reaction was used for detection of genomic DNA contamination using primers Dup_S1 and Dup_AS. All PCRs were performed as follows: 40 cycles of 94°C for 30 s, 57°C for 30 s, and 72°C for 30 s.

Acknowledgments

We thank Enn Jõeste and Liina Kiho from North Estonian Regional Hospital, Tallinn, for help in collecting tissue samples; Epp Väli for technical assistance; Richard Tamme for critically reading the manuscript; and Mart Speek for experimental advice. This work was supported by the following grants to T. T.: Wellcome Trust International Senior Research Fellowship (Grant 067952) and Estonian Ministry of Education and Research (Grant 0222602).

Appendix A. Supplementary data

Supplementary data associated with this article can be found, in the online version, at doi:10.1016/j.ygeno.2007.05.004.

References

[1] D.K. Binder, H.E. Scharfman, Brain-derived neurotrophic factor, Growth Factors 22 (2004) 123–131.
[2] M. Bibel, Y.A. Barde, Neurotrophins: key regulators of cell fate and cell shape in the vertebrate nervous system, Genes Dev. 14 (2000) 2919–2937.

[3] S. Pezet, S.B. McMahon, Neurotrophins: mediators and modulators of pain, Annu. Rev. Neurosci. 29 (2006) 507–538.
[4] B. Alsina, T. Vu, S. Cohen-Cory, Visualizing synapse formation in arborizing optic axons in vivo: dynamics and modulation by BDNF, Nat. Neurosci. 4 (2001) 1093–1101.
[5] M. Korte, P. Carroll, E. Wolf, G. Brem, H. Thoenen, T. Bonhoeffer, Hippocampal long-term potentiation is impaired in mice lacking brain-derived neurotrophic factor, Proc. Natl. Acad. Sci. USA 92 (1995) 8856–8860.
[6] B. Lu, BDNF and activity-dependent synaptic modulation, Learn. Mem. 10 (2003) 86–98.
[7] M.F. Egan, M. Kojima, J.H. Callicott, T.E. Goldberg, B.S. Kolachana, A. Bertolino, E. Zaitsev, B. Gold, D. Goldman, M. Dean, B. Lu, D.R. Weinberger, The BDNF val66met polymorphism affects activity-dependent secretion of BDNF and human memory and hippocampal function, Cell 112 (2003) 257–269.
[8] C. Zuccato, E. Cattaneo, Role of brain-derived neurotrophic factor in Huntington's disease, Prog. Neurobiol. (2007).
[9] R. Katoh-Semba, I.K. Takeuchi, R. Semba, K. Kato, Distribution of brain-derived neurotrophic factor in rats and its changes with development in the brain, J. Neurochem. 69 (1997) 34–42.
[10] J.M. Conner, J.C. Lauterborn, Q. Yan, C.M. Gall, S. Varon, Distribution of brain-derived neurotrophic factor (BDNF) protein and mRNA in the normal adult rat CNS: evidence for anterograde axonal transport, J. Neurosci. 17 (1997) 2295–2313.
[11] P. Ernfors, C. Wetmore, L. Olson, H. Persson, Identification of cells in rat brain and peripheral tissues expressing mRNA for members of the nerve growth factor family, Neuron 5 (1990) 511–526.
[12] T. Timmusk, H. Persson, M. Metsis, Analysis of transcriptional initiation and translatability of brain-derived neurotrophic factor mRNAs in the rat brain, Neurosci. Lett. 177 (1994) 27–31.
[13] P.C. Maisonpierre, M.M. Le Beau, R. Espinosa III, N.Y. Ip, L. Belluscio, S.M. de la Monte, S. Squinto, M.E. Furth, G.D. Yancopoulos, Human and rat brain-derived neurotrophic factor and neurotrophin-3: gene structures, distributions, and chromosomal localizations, Genomics 10 (1991) 558–568.
[14] P.C. Maisonpierre, L. Belluscio, B. Friedman, R.F. Alderson, S.J. Wiegand, M.E. Furth, R.M. Lindsay, G.D. Yancopoulos, NT-3, BDNF, and NGF in the developing rat nervous system: parallel as well as reciprocal patterns of expression, Neuron 5 (1990) 501–509.
[15] T. Timmusk, K. Palm, M. Metsis, T. Reintam, V. Paalme, M. Saarma, H. Persson, Multiple promoters direct tissue-specific expression of the rat BDNF gene, Neuron 10 (1993) 475–489.
[16] Q.R. Liu, L. Lu, X.G. Zhu, J.P. Gong, Y. Shaham, G.R. Uhl, Rodent BDNF genes, novel promoters, novel splice variants, and regulation by cocaine, Brain Res. 1067 (2006) 1–12.
[17] T. Aid, A. Kazantseva, M. Piirsoo, K. Palm, T. Timmusk, Mouse and rat BDNF gene structure and expression revisited, J. Neurosci. Res. 85 (2007) 525–535.
[18] H. Fang, J. Chartier, C. Sodja, A. Desbois, M. Ribecco-Lutkiewicz, P.R. Walker, M. Sikorska, Transcriptional activation of the human brain-derived neurotrophic factor gene promoter III by dopamine signaling in NT2/N neurons, J. Biol. Chem. 278 (2003) 26401–26409.
[19] Q.R. Liu, D. Walther, T. Drgon, O. Polesskaya, T.G. Lesnick, K.J. Strain, M. de Andrade, J.H. Bower, D.M. Maraganore, G.R. Uhl, Human brain derived neurotrophic factor (BDNF) genes, splicing patterns, and assessments of associations with substance abuse and Parkinson's disease, Am. J. Med. Genet. B Neuropsychiatr. Genet. 134 (2005) 93–103.
[20] M. Aoyama, K. Asai, T. Shishikura, T. Kawamoto, T. Miyachi, T. Yokoi, H. Togari, Y. Wada, T. Kato, A. Nakagawara, Human neuroblastomas with unfavorable biologies express high levels of brain-derived neurotrophic factor mRNA and a variety of its variants, Cancer Lett. 164 (2001) 51–60.
[21] Y. Wang, D.C. Newton, G.B. Robb, C.L. Kau, T.L. Miller, A.H. Cheung, A.V. Hall, S. VanDamme, J.N. Wilcox, P.A. Marsden, RNA diversity has profound effects on the translation of neuronal nitric oxide synthase, Proc. Natl. Acad. Sci. USA 96 (1999) 12150–12155.
[22] A. Pecci, L.R. Viegas, J.L. Baranao, M. Beato, Promoter choice influences alternative splicing and determines the balance of isoforms expressed from the mouse bcl-X gene, J. Biol. Chem. 276 (2001) 21062–21069.
[23] M.G. Murer, Q. Yan, R. Raisman-Vozari, Brain-derived neurotrophic factor in the control human brain, and in Alzheimer's disease and Parkinson's disease, Prog. Neurobiol. 63 (2001) 71–124.
[24] H.S. Phillips, J.M. Hains, M. Armanini, G.R. Laramee, S.A. Johnson, J.W. Winslow, BDNF mRNA is decreased in the hippocampus of individuals with Alzheimer's disease, Neuron 7 (1991) 695–702.
[25] M.J. Webster, C.S. Weickert, M.M. Herman, J.E. Kleinman, BDNF mRNA expression during postnatal development, maturation and aging of the human prefrontal cortex, Brain Res. Dev. Brain. Res. 139 (2002) 139–150.
[26] D. Garzon, G. Yu, M. Fahnestock, A new brain-derived neurotrophic factor transcript and decrease in brain-derived neurotrophic factor transcripts 1, 2 and 3 in Alzheimer's disease parietal cortex, J. Neurochem. 82 (2002) 1058–1064.
[27] S. Ceccatelli, P. Ernfors, M.J. Villar, H. Persson, T. Hokfelt, Expanded distribution of mRNA for nerve growth factor, brain-derived neurotrophic factor, and neurotrophin 3 in the rat brain after colchicine treatment, Proc. Natl. Acad. Sci. USA 88 (1991) 10352–10356.
[28] M. Hofer, S.R. Pagliusi, A. Hohn, J. Leibrock, Y.A. Barde, Regional distribution of brain-derived neurotrophic factor mRNA in the adult mouse brain, EMBO J. 9 (1990) 2459–2464.
[29] D.F. Condorelli, P. Dell'Albani, G. Mudo, T. Timmusk, N. Belluardo, Expression of neurotrophins and their receptors in primary astroglial cultures: induction by cyclic AMP-elevating agents, J. Neurochem. 63 (1994) 509–516.
[30] F. Zafra, D. Lindholm, E. Castren, J. Hartikka, H. Thoenen, Regulation of brain-derived neurotrophic factor and nerve growth factor mRNA in primary cultures of hippocampal neurons and astrocytes, J. Neurosci. 12 (1992) 4793–4799.
[31] S. Elkabes, E.M. DiCicco-Bloom, I.B. Black, Brain microglia/macrophages express neurotrophins that selectively regulate microglial proliferation and function, J. Neurosci. 16 (1996) 2508–2521.
[32] X. Dai, L.D. Lercher, P.M. Clinton, Y. Du, D.L. Livingston, C. Vieira, L. Yang, M.M. Shen, C.F. Dreyfus, The trophic role of oligodendrocytes in the basal forebrain, J. Neurosci. 23 (2003) 5846–5853.
[33] J.R. Landry, D.L. Mager, B.T. Wilhelm, Complex controls: the role of alternative promoters in mammalian genomes, Trends Genet. 19 (2003) 640–648.
[34] D. Lipscombe, Neuronal proteins custom designed by alternative splicing, Curr. Opin. Neurobiol. 15 (2005) 358–363.
[35] S. Korneev, M. O'Shea, Natural antisense RNAs in the nervous system, Rev. Neurosci. 16 (2005) 213–222.
[36] C. Vanhee-Brossollet, C. Vaquero, Do natural antisense transcripts make sense in eukaryotes? Gene 211 (1998) 1–9.
[37] G. Alfano, C. Vitiello, C. Caccioppoli, T. Caramico, A. Carola, M.J. Szego, R.R. McInnes, A. Auricchio, S. Banfi, Natural antisense transcripts associated with genes involved in eye development, Hum. Mol. Genet. 14 (2005) 913–923.
[38] C. Morey, P. Avner, Employment opportunities for non-coding RNAs, FEBS Lett. 567 (2004) 27–34.
[39] O. Borsani, J. Zhu, P.E. Verslues, R. Sunkar, J.K. Zhu, Endogenous siRNAs derived from a pair of natural cis-antisense transcripts regulate salt tolerance in Arabidopsis, Cell 123 (2005) 1279–1291.
[40] A.M. Marini, X. Jiang, X. Wu, F. Tian, D. Zhu, P. Okagaki, R.H. Lipsky, Role of brain-derived neurotrophic factor and NF-kappaB in neuronal plasticity and survival: from genes to phenotype, Restor. Neurol. Neurosci. 22 (2004) 121–130.

PUBLICATION III

Vihma H*, **Pruunsild P***, Timmusk T. (2008)
Alternative splicing and expression of human and mouse *NFAT* genes.
Genomics, Nov;92(5):279-91

Genomics 92 (2008) 279–291

Contents lists available at ScienceDirect

Genomics

journal homepage: www.elsevier.com/locate/ygeno

Alternative splicing and expression of human and mouse NFAT genes ☆

Hanna Vihma [1], Priit Pruunsild [1], Tõnis Timmusk *

Department of Gene Technology, Tallinn University of Technology, Akadeemia Tee 15, Tallinn 19086, Estonia

ARTICLE INFO

Article history:
Received 13 May 2008
Accepted 24 June 2008
Available online 26 August 2008

Keywords:
NFAT
Alternative splicing
Ca^{2+}-regulated transcription factor
Calcineurin
Neurons
Brain
Nervous system

ABSTRACT

Four members of the nuclear factor of activated T cells (NFAT) family (NFATC1, NFATC2, NFATC3, and NFATC4) are Ca^{2+}-regulated transcription factors that regulate several processes in vertebrates, including the development and function of the immune, cardiovascular, musculoskeletal, and nervous systems. Here we describe the structures and alternative splicing of the human and mouse NFAT genes, including novel splice variants for *NFATC1, NFATC2, NFATC3,* and *NFATC4,* and show the expression of different NFAT mRNAs in various mouse and human tissues and brain regions by RT-PCR. Our results show that alternatively spliced NFAT mRNAs are expressed differentially and could contribute to the diversity of functions of the NFAT proteins. Since NFAT family members are Ca^{2+}-regulated and have critical roles in neuronal gene transcription in response to electrical activity, we describe the expression of *NFATC1, NFATC2, NFATC3,* and *NFATC4* mRNAs in the adult mouse brain and in the adult human hippocampus using in situ hybridization and show that all NFAT mRNAs are expressed in the neurons of the mouse brain with specific patterns for each NFAT.

Nuclear factor of activated T cells (NFAT) is a family of transcription factors evolutionarily related to Rel/NF-κB [1]. The family consists of the Ca^{2+}-regulated members NFATC1 (NFATc, NFAT2), NFATC2 (NFATp, NFAT1), NFATC3 (NFATx, NFAT4), and NFATC4 (NFAT3) and osmotic tension-regulated NFAT5. The approved human symbols for the NFAT family members are NFATC1, NFATC2, NFATC3, NFATC4 and NFATC5 and the approved mouse symbols are Nfatc1, Nfatc2, Nfatc3, Nfatc4 and Nfatc5. The Ca^{2+}-regulated NFAT proteins consist of two conserved domains—a regulatory domain in the N-terminus and a Rel homology domain (RHD) in the C-terminus [2]. The regulatory domain consists of two conserved binding sites for the protein phosphatase calcineurin (CaN) [3,4], an extended serine-rich region, and a nuclear localization signal (NLS) [5]. The Rel homology domain binds DNA and interacts with partner proteins (also referred as NFATn) to transactivate gene transcription. The partner transcription factors include AP-1 (FOS or JUN) [6], GATA4 [7], and MEF2 [8], for example. The N- and C-terminal ends of each NFAT family protein are unique and contain transcription activation domains (TADs) [9].

The NFAT proteins exist in at least two alternative conformations—one in which the NLS is exposed and the nuclear export signal (NES) is masked or vice versa. This is achieved by dephosphorylation or phosphorylation, respectively, of serines in the regulatory domain [10]. NFATs are dephosphorylated by CaN [11] and phosphorylated by various kinases [10] such as casein kinase 1 (CSNK1A1), glycogen synthase kinase 3 (GSK3A or GSK3B), p38 MAP kinase (MAPK14), and JUN N-terminal kinase (MAPK8), [12–16]. Exposure of the NLS leads to rapid import of the NFAT proteins into the nucleus, where they bind to DNA and regulate target gene expression [17], whereas phosphorylation causes rapid relocalization out of the nucleus, terminating NFAT-dependent transcription regulation [18].

NFAT proteins regulate gene transcription in various developing and adult tissues. For example, their roles in the immune system [2], cardiovascular system [2,19], skeletal muscle [20], and nervous system [21,22] have been described. Accordingly, NFAT genes are expressed in almost all tissues. However, the expression levels and patterns for each NFAT are rather distinct [17,23]. All of the NFAT genes except *NFATC4* are strongly expressed in the immune system, in the thymus, spleen, and peripheral blood lymphocytes [23–28], but are also expressed at lower levels in other tissues. *NFATC1* has been detected in the cardiovascular and digestive systems, for example [26,29,30], and *NFATC2* expression has been detected in the testis, pancreas, placenta, and brain–in the hypothalamus, hippocampus, cerebellum, olfactory bulb, and frontal cortex [23,24,31–33]. In addition to the immune system, *NFATC3* is expressed in the skeletal and smooth muscle, kidney, and lung and in the brain, where it has been shown to be expressed in the hypothalamus and striatum [26,28,31,34,35]. *NFATC4* is more evenly expressed than the other NFAT genes and its expression

☆ Sequence data from this article have been deposited in the GenBank Data Libraries under Accession Nos. EU887559- EU887566 (Human NFATC1 transcript types); EU887573- EU887580 (Human NFATC2 transcript types); EU887605- EU887625 (Human NFATC3 transcript types); EU887632- EU887655 (Human NFATC4 transcript types); EU887567- EU887572 (Mouse Nfatc1 transcript types); EU887581- EU887604 (Mouse Nfatc2 transcript types); EU887626- EU887631 (Mouse Nfatc3 transcript types); EU887656- EU887661 (Mouse Nfatc4 transcript types).

* Corresponding author. Fax: +372 620 4401.
E-mail address: tonis.timmusk@ttu.ee (T. Timmusk).

[1] These authors contributed equally to this work.

0888-7543/$ – see front matter © 2008 Elsevier Inc. All rights reserved.
doi:10.1016/j.ygeno.2008.06.011

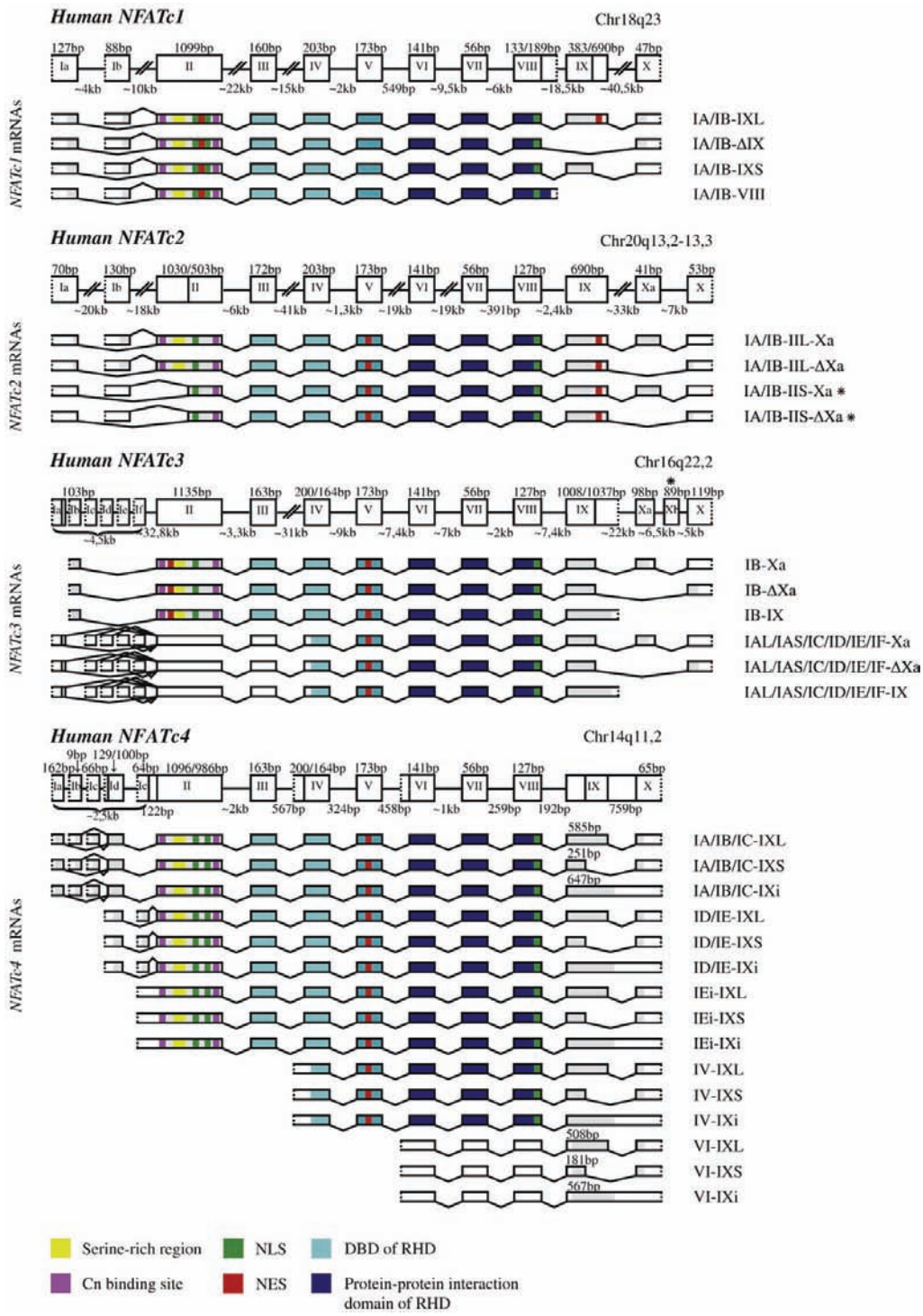
Human NFATc1
Chr18q23
127bp 88bp 1099bp 160bp 203bp 173bp 141bp 56bp 133/189bp 383/690bp 47bp
Ia Ib II III IV V VI VII VIII IX X
~4kb ~10kb ~22kb ~15kb ~2kb 549bp ~9,5kb ~6kb ~18,5kb ~40,5kb
NFATc1 mRNAs
IA/IB-IXL
IA/IB-ΔIX
IA/IB-IXS
IA/IB-VIII
Human NFATc2
Chr20q13,2-13,3
70bp 130bp 1030/503bp 172bp 203bp 173bp 141bp 56bp 127bp 690bp 41bp 53bp
Ia Ib II III IV V VI VII VIII IX Xa X
~20kb ~18kb ~6kb ~41kb ~1,3kb ~19kb ~19kb ~391bp ~2,4kb ~33kb ~7kb
NFATc2 mRNAs
IA/IB-IIL-Xa
IA/IB-IIL-ΔXa
IA/IB-IIS-Xa *
IA/IB-IIS-ΔXa *
Human NFATc3
Chr16q22,2
103bp 1135bp 163bp 200/164bp 173bp 141bp 56bp 127bp 1008/1037bp 98bp 89bp 119bp
Ia Ib Ic Id Ie If II III IV V VI VII VIII IX Xa Xb X
~4,5kb ~32,8kb ~3,3kb ~31kb ~9kb ~7,4kb ~7kb ~2kb ~7,4kb ~22kb ~6,5kb ~5kb
NFATc3 mRNAs
IB-Xa
IB-ΔXa
IB-IX
IAL/IAS/IC/ID/IE/IF-Xa
IAL/IAS/IC/ID/IE/IF-ΔXa
IAL/IAS/IC/ID/IE/IF-IX
Human NFATc4
Chr14q11,2
9bp 129/100bp
162bp 66bp 64bp 1096/986bp 163bp 200/164bp 173bp 141bp 56bp 127bp 65bp
Ia Ib Ic Id Ie II III IV V VI VII VIII IX X
~2,5kb 122bp ~2kb 567bp 324bp 458bp ~1kb 259bp 192bp 759bp
NFATc4 mRNAs
585bp
IA/IB/IC-IXL
251bp
IA/IB/IC-IXS
647bp
IA/IB/IC-IXi
ID/IE-IXL
ID/IE-IXS
ID/IE-IXi
IEi-IXL
IEi-IXS
IEi-IXi
IV-IXL
IV-IXS
IV-IXi
508bp
VI-IXL
181bp
VI-IXS
567bp
VI-IXi
Serine-rich region
NLS
DBD of RHD
Cn binding site
NES
Protein-protein interaction domain of RHD

has been detected in the placenta, lung, kidney, adipose tissue, cardiac muscle, testis, ovary, digestive system, and spinal cord and, at lower levels, in the brain—in the hippocampus, cerebellum, olfactory bulb, and various hypothalamic nuclei [19,21,23,34,36–40].

Despite this information, the expression of different NFAT isoforms generated by splicing or usage of alternative 5′ and 3′ exons has not been studied. Therefore, here we describe the structures of the human and mouse *NFATC1, NFATC2, NFATC3,* and *NFATC4* genes and analyze their alternative splicing and coding potentials. Furthermore, we have studied the expression of different *NFATC1, NFATC2, NFATC3,* and *NFATC4* mRNA splice variants in various mouse and human tissues and brain regions by RT-PCR and describe here the expression of the NFAT mRNAs in the adult mouse brain and in the adult human hippocampus using in situ hybridization.

Results

The structure of the human and mouse NFAT genes

The exon/intron structures of the human and mouse NFAT genes were characterized and the alternative splicing patterns of each NFAT gene in both human and mouse were analyzed using bioinformatics and RT-PCR. For each NFAT a search for mRNA sequences and expressed sequence tags (ESTs) was performed. RT-PCR analyses were used for the characterization of the expression patterns of the alternative transcripts in human and mouse.

The lengths of the four human NFAT genes vary from 10kb for *NFATC4* up to 170kb for *NFATC2* (Fig. 1). The NFAT genes are conserved in their central regions but are less similar in the 5′ and 3′ parts. The identity on the nucleotide level and the identity and strong similarity of the amino acids on the protein level among the most conserved part of the genes, encoded by exons V–VII, is ~ 80%. Although these exons are strongly similar, other exons are not so conserved. The identity among the full-length NFAT coding regions is ~ 50% on the nucleotide level and the amino acid identity or strong similarity in sum of the human NFAT proteins is ~ 56%.

There are several alternative transcripts for the NFAT genes, which are generated by usage of alternative 5′ and 3′ exons and alternative splicing. According to our data, human and mouse *NFATC1* and *NFATC2,* and mouse *Nfatc3* and *Nfatc4,* have two alternative 5′ exons. In human we detected six alternative 5′ exons for *NFATC3* and seven alternative 5′ exons for *NFATC4.* Our results also showed that in both human and mouse, *NFATC1* and *NFATC3* have two alternative 3′ exons and *NFATC4* has one 3′ exon. For *NFATC2* we detected one 3′ exon in human but three alternative 3′ exons in mouse. Due to these differences, the amino acid sequences within the C- and N-termini of different NFAT protein isoforms are distinct (Supplementary Figs. 1 and 2). In this study the alternative transcripts and protein isoforms have been given names according to the alternative exons used in the respective mRNAs (Fig. 1).

Alternative splicing and expression of NFATC1 in human and mouse

For both human and mouse *NFATC1,* there are two alternative 5′ exons, exons IA and IB, and two alternative 3′ exons, exons VIII and X (Fig. 1; Table 1). Also, in both human and mouse exon IX has two alternative splice variants, designated here IXL and IXS, which are generated by the usage of alternative splice donor sites. In addition, we detected a novel splice variant for human *NFATC1* lacking exon IX, indicated here as ΔIX. In human, exon IA encodes 42 amino acids (aa).

Table 1
Usage of alternative 5′ and 3′ exons and alternative splicing of human and mouse NFAT genes

Gene			Human	Mouse
NFATC1	5′ exons	IA	[24]	[41]
		IB	[29]	[42]
	3′ exons	VIII	[24]	[42]
		X	[29]	[41]
	Alternative splicing	IXL	[45]	+
		IXS	[29]	[41]
		ΔIX	+	ND
NFATC2	5′ exons	IA	+	+
		IB	[43]	[44]
	3′ exons	III	ND	+
		VIIA	ND	[33]
		X	[43]	[43]
	Alternative splicing	IIL	[43]	[43]
		IIS	+	+
		ΔII	ND	+
		XA	[43]	[43]
NFATC3	5′ exons	IAL	+	[32]
		IB	[23]	[46]
		IC	+	ND
		ID	+	ND
		IE	+	ND
		IF	+	ND
	3′ exons	IV	ND	+
		IX	[26]	ND
		X	[26]	[32]
	Alternative splicing	IAS	+	ND
		XA	[23]	[46]
		XB	[26]	ND
NFATC4	5′ exons	IA	+	ND
		IB	+	ND
		IC	+	ND
		ID	[23]	[1]
		IE	+	ND
		IV	+	ND
		VI	+	+
	3′ exon	X	[23]	[1]
	Alternative splicing	IEi	+	ND
		VIi	ND	+
		IXL	[23]	[1]
		IXS	+	ND
		IXi	+	+

+, novel transcript identified in this study; ND, not detected; references indicate studies describing the respective transcript variant.

Exon IB, located downstream from exon IA, encodes 29 aa. Transcripts that have the polyadenylation signal in exon VIII (VIII3′UTR) encode 63 aa from exon VIII, whereas transcripts containing exon X as the 3′ exon encode a C-terminal region that includes 44 aa identical to the exon VIII3′UTR isoforms in the region encoded by exon VIII, but contain an additional 245 aa or 127 aa, in the case of IXL or IXS usage, respectively. If exon IX is skipped the corresponding protein isoform lacks the 230 aa encoded by exon IXL but contains 15 C-terminal amino acids identical to the C-terminus of the exon IXL-comprising isoform. Altogether, according to our data, the possible transcript types of *NFATC1* in human are: (1) *NFATC1-IA/IB-IXL,* containing 5′ exon IA or IB, exon IXL, and 3′ exon X, having a protein coding region of 2829bp when exon IA is used or 2790bp when exon IB is used; (2) *NFATC1-IA/IB-ΔIX,* containing 5′ exon IA or IB, no exon IX, and 3′ exon X, having a protein coding region of 2139bp when exon IA is used or 2100bp when exon IB is used; (3) *NFATC1-IA/IB-IXS,* containing 5′ exon IA or IB, IXS, and 3′ exon X; exon IXS changes the open reading frame, introducing a stop codon in exon X that is 44bp upstream of the stop codon in type 1 and type 2 transcripts; the protein coding regions

Fig. 1. Structure and alternative transcripts of human NFAT genes. The structural organization of human *NFATC1, NFATC2, NFATC3,* and *NFATC4* was determined by analyzing genomic and mRNA sequence data using bioinformatics and RT-PCR. Exons are shown as boxes and introns are shown as lines. The numbers above the exons indicate the size of the protein coding part of the exon. Protein coding sequences of the mRNAs are shown as filled boxes and open boxes indicate UTRs of the mRNAs. Numbers below the introns indicate their size. Exon numbers are shown in roman characters. Asterisks mark rarely used exons and rarely transcribed mRNA variants. NES, nuclear export signal; NLS, nuclear localization signal; DBD, DNA binding domain; RHD, Rel homology domain; Cn, calcineurin A.

of *NFATC1* type 3 mRNAs are 2475bp when exon IA is used or 2436bp when exon IB is used; and (4) *NFATC1-IA/IB-VIII*, containing 5′ exon IA or IB and 3′ exon VIII; the coding region of exon VIII in type 4 transcripts is 56bp longer than in type 1, 2, and 3 transcripts; the protein coding regions are 2148bp when exon IA is used or 2109bp when exon IB is used (Fig. 1 and Supplementary Table 1). A human EST sequence corresponding to the *NFATC1* transcript lacking exon II is present in the databases; however, we did not detect it with RT-PCR and there are no references in the literature to confirm the generation of this transcript. According to our data *Nfatc1* transcripts for mouse are the same as in human, except for differences in the lengths of exons II, III, IXL, and IXS and in the length of the protein coding region of exon IB (data not shown).

In mouse, *Nfatc1* transcripts containing exon IA or exon IB were both predominantly expressed in the lung, thymus, and spleen (Fig. 2). Both alternative 3′ exon transcripts were detected in all tissues analyzed, with the levels being highest in the lung, thymus, and spleen. Exon IXS was more abundantly used than exon IXL in 3′ exon X-containing transcripts. In the adult mouse brain and during postnatal development of the brain the expression levels of transcripts containing exon IA or exon IB were similarly low (Fig. 2). In embryonic mouse brain, only *Nfatc1* transcripts comprising exon IA were expressed. In all the brain regions tested the expression levels of both of the 3′ exon transcripts were lower compared to the levels of respective mRNAs in the thymus, spleen, or lung (Fig. 2).

In human, *NFATC1* transcripts comprising exon IA were expressed more widely than transcripts comprising exon IB (Fig. 3). Both 5′ exon transcripts were highly expressed in the thymus and muscle. In addition, exon IA transcripts were expressed at high levels in the colon, small intestine, stomach, heart, uterus, testis, and thyroid and were detected also in other tissues. Exon IB mRNAs were highly expressed also in the fetal brain, cerebellum, and placenta and were undetectable in the stomach, uterus, liver, fetal liver, pancreas, salivary gland, trachea, and adrenal gland. Both 3′ exon transcripts were expressed in all the tissues analyzed, with highest levels observed in the testis, thymus, and muscle. Transcripts containing the 3′ exon X and exon IXS were expressed more predominantly than transcripts containing exon IXL or those in which exon IX was skipped. mRNAs

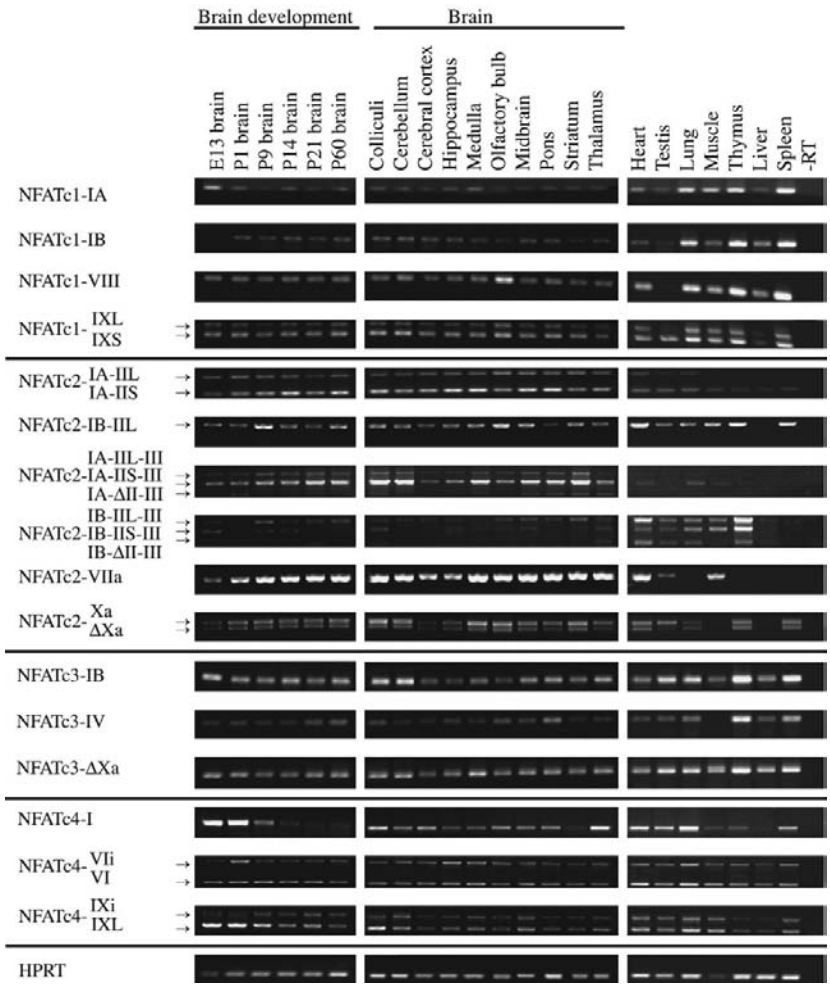

Fig. 2. Semiquantitative analysis of *Nfatc1*, *Nfatc2*, *Nfatc3*, *Nfatc4*, and control *Hprt* mRNA expression by RT-PCR in different mouse brain regions, in mouse brain at the indicated developmental time points, and in various mouse tissues.

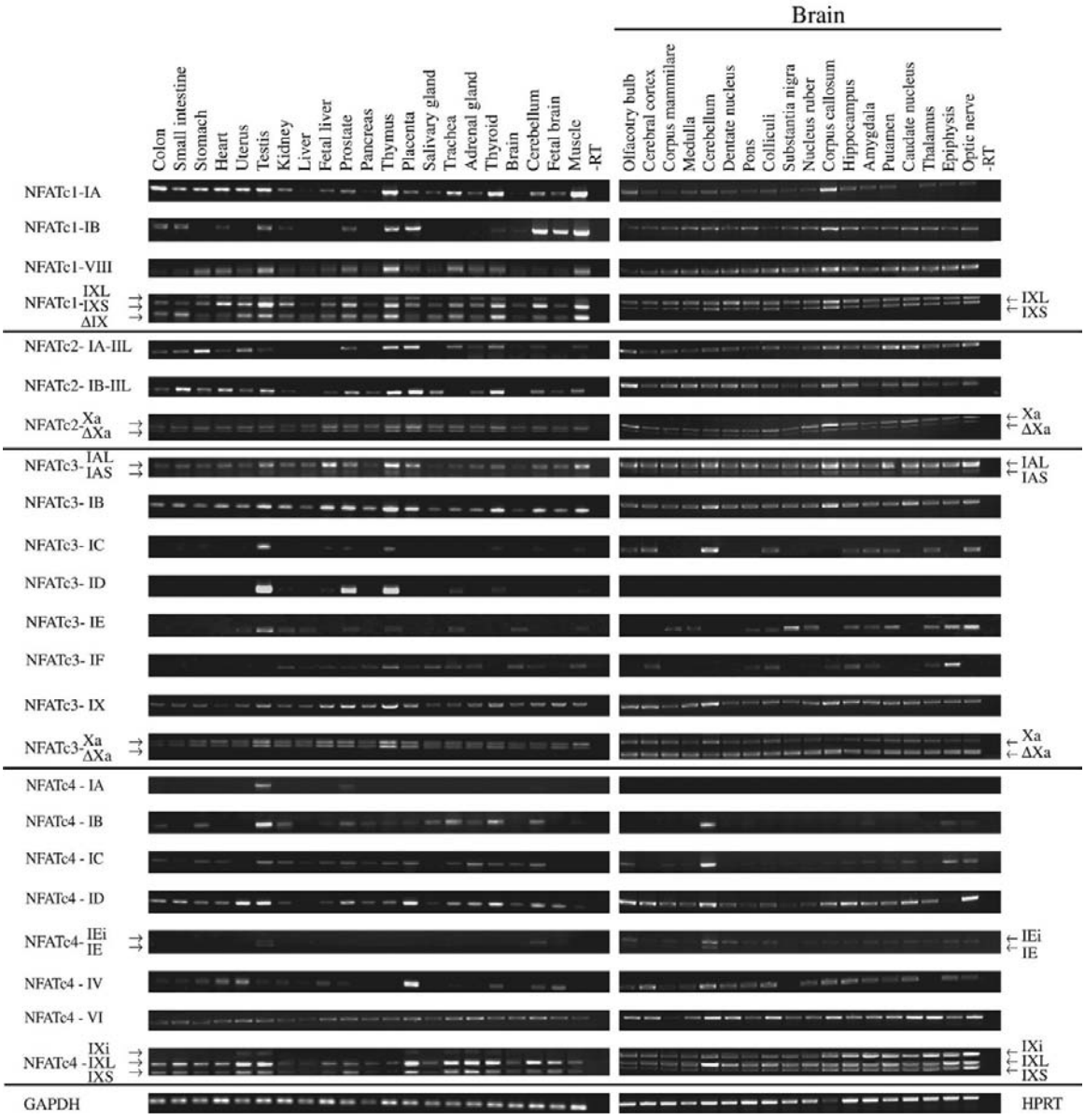

Fig. 3. Semiquantitative analysis of *NFATC1, NFATC2, NFATC3, NFATC4,* and controls *GAPDH* and *HPRT* mRNA expression by RT-PCR in various human tissues and brain regions.

with exon IXL were expressed at significantly lower levels, particularly in the small intestine, heart, liver, pancreas, salivary gland, brain, and fetal brain. Transcripts lacking exon IX or containing exon IXS were both highly and at comparable levels expressed in the thymus, thyroid, and muscle. The analysis of the expression of *NFATC1* transcripts in various human brain regions showed that transcripts comprising exon IA or exon IB were present in all regions tested, with highest levels in the corpus callosum (Fig. 3). Exon IA transcripts were expressed at relatively higher levels also in the olfactory bulb. Both of the alternative 3′ exons were also expressed in all of the regions analyzed, with the highest levels in the corpus callosum. The relative ratio of transcripts containing IXL or IXS was similar in most of the regions analyzed, except in the olfactory bulb, cerebral cortex, corpus mammilare, medulla, pons, and substantia nigra, where the expression levels of transcripts containing IXL were slightly higher. Transcripts lacking exon IX were not detected in the brain (Fig. 3).

Alternative splicing and expression of NFATC2 in human and mouse

Both human and mouse *NFATC2* contain two alternative 5′ exons, IA and IB, whereas only exon IB has been previously described (Fig. 1 and [41]). There is one 3′ exon in human, exon X, and three 3′ exons in

mouse, exons III, VIIa, and X (Table 1). Due to the usage of alternative splice acceptor sites exon II has two splice variants—IIL and IIS. Exon IIL is 1030 or 1036bp in length in human or mouse, respectively, and exon IIS is 516bp in both organisms. The shorter splice variant of exon II has not been described before. In mouse, exons IIS and IIL are both used and transcripts without exon II are also expressed, whereas in human the transcripts containing IIL are predominant and the usage of exon IIS or skipping of exon II is barely detectable. In both human and mouse exon IA encodes 23 aa and exon IB encodes 43 aa. Regardless of the 5′ exon, the translation start codon is positioned in exon II when exon IIS is used in transcripts. This leads to N-terminally truncated isoforms that are 199 and 201 aa (IA) or 219 and 221 aa (IB) shorter than the isoforms encoded by transcripts containing exon IIL in human and mouse, respectively. In both human and mouse *NFATC2* there is an additional exon compared to *NFATC1,* located upstream of exon X, named Xa here, that is either spliced in the mRNA or skipped. Usage of exon Xa leads to a translation stop codon in exon Xa. If exon Xa is not used then the translation stop codon is in exon X. This generates unique C-terminal sequences of 17 or 13 aa, for the respective NFATC2 protein isoforms. Taken together, our results showed that the possible transcript types of *NFATC2* in human are: (1) *NFATC2-IA/IB-IIL-Xa,* containing 5′ exon IA or IB, exon IIL, exon Xa, and 3′ exon X, having a protein coding region of 2703bp when exon IA is used or 2763bp when exon IB is used; (2) *NFATC2-IA/IB-IIS-Xa,* containing 5′ exon IA or IB, exon IIS, exon Xa, and 3′ exon X, having a protein coding region of 2106bp with either exon IA or exon IB; (3) *NFATC2-IA/IB-IIL-ΔXa,* containing 5′ exon IA or IB, exon IIL, and 3′ exon X and lacking exon Xa, having a protein coding region of 2715bp when exon IA is used or 2775bp when exon IB is used; (4) *NFATC2-IA/IB-IIS-ΔXa,* containing 5′ exon IA or IB, exon IIS, and 3′ exon X and lacking exon Xa, having a protein coding region of 2118bp with either exon IA or exon IB (Supplementary Table 1).

There are several differences in the mouse *Nfatc2* transcripts compared to the human ones in addition to the length of exon II. First, there are three alternative 3′ exons in mouse: exon III, exon VIIa, and exon X. The proteins encoded by transcripts using exon III or VIIa as 3′ exon lack the whole or a part of the Rel homology domain, respectively. Second, in mouse we detected *Nfatc2* transcripts lacking exon II (ΔII). Of note, according to the mouse EST and mRNA data in the NCBI databases there are transcripts in which exon V is used as the 3′ exon and transcripts with an alternative 5′ exon between exons III and IV. However, we did not detect these transcripts with PCR and there are no references to these transcripts in the literature.

Mouse *Nfatc2* transcripts containing exon IA, including transcripts with the mouse-specific 3′ exon III and transcripts with the 3′ exon VIIa, were all highly expressed in the brain, where the expression levels increased during postnatal development. In the adult mouse brain high levels were observed in the colliculi, cerebellum, medulla, olfactory bulb, and striatum (Fig. 2). Exon VIIa transcripts were highly expressed also in the heart and muscle. The levels of transcripts with exon X as the 3′ exon, either containing or lacking exon Xa, were relatively higher in the heart, testis, thymus, spleen, and brain, where they were more abundant in the colliculi, cerebellum, medulla, olfactory bulb, and striatum. Transcripts including exon IB predominantly contained exon IIL and were more broadly expressed, with relatively higher expression levels in the heart, thymus, and spleen. Transcripts containing exons IB and III3′UTR showed the highest expression levels in the heart and thymus and were very weakly expressed in the brain (Fig. 2).

In human, *NFATC2* transcripts including exon IA spliced to exon IIL were highly expressed in the stomach, uterus, thymus, placenta, trachea, and thyroid (Fig. 3). Transcripts containing exons IB and IIL were expressed highly in the small intestine, heart, testis, prostate, thymus, placenta, and thyroid. Transcripts containing IIS were hardly detectable (data not shown). Transcripts of *NFATC2* containing the 3′ exon X and either comprising or lacking exon Xa (ΔXa) were both present in all of the tissues analyzed, with exon Xa-containing transcripts being expressed at slightly higher levels. In the brain *NFATC2* was widely expressed. The expression levels were highest in the caudate putamen for exon IA and the olfactory bulb and corpus callosum for exon IB transcripts. Similar levels of exon Xa and ΔXa transcripts were expressed in almost all regions of the human brain except in the olfactory bulb, colliculi, nucleus ruber, corpus callosum, and caudate nucleus, where exon Xa transcripts were predominant (Fig. 3).

Alternative splicing and expression of NFATC3 in human and mouse

The human *NFATC3* contains six 5′ exons located within ~ 4500bp in the genome (Fig. 1), whereas in mouse there are only two alternative 5′ exons in *Nfatc3.* The human exon IB has been described before [23]. However, exons IA, IC, ID, IE, and IF are first described in this study (Table 1). Exon IB in human is homologous to exon IB in mouse and encodes 34 N-terminal amino acids of the respective proteins. Mouse 5′ exon IA is not homologous to human exon IA and encodes a unique N-terminus of 26 aa. In human, exon IB is the only 5′ exon that is a protein-coding exon. Exons IA, IC, ID, IE, and IF all lack an in-frame translation start codon and translation of *NFATC3* transcripts containing these exons could start from the ATG located in exon IV. Thus, proteins encoded by these transcripts would not contain the 485 N-terminal amino acids present in NFATC3 isoforms translated from transcripts including exon IB. Exon IA in human contains two alternative splice donor sites and the respective splice variants are named here IAL and IAS. There are two alternative 3′ exons in *NFATC3* genes: exons IX and X in human and exons IV and X in mouse. Transcripts in which exon IX is used as the 3′ exon encode proteins with 9 unique C-terminal amino acids that are not present in the proteins encoded by exon X-containing transcripts. Like in human *NFATC2* there is an alternative exon located between exon IX and exon X, designated here Xa, in both human and in mouse *NFATC3* genes. If exon Xa is used in the transcripts a stop codon is introduced. Therefore, different C-terminal sequences of 32 or 39 aa are encoded by exon X3′UTR transcripts depending on the usage or skipping, respectively, of exon Xa. Altogether, according to our data, the possible transcript types of *NFATC3* in human are: (1) *NFATC3-IB-Xa,* containing 5′ exon IB, exon Xa, and 3′ exon X, having a protein coding region of 3204bp; (2) *NFATC3-IB-ΔXa,* containing 5′ exon IB and 3′ exon X and lacking exon Xa, having a protein coding region of 3225bp; (3) *NFATC3-IB-IX,* containing 5′ exon IB and exon IX as the 3′ exon, having a protein coding region of 3135bp; (4) *NFATC3-IAL/IAS/IC/ID/IE/IF-Xa,* containing 5′ exon IAL or IAS or IC or ID or IE or IF, exon Xa, and 3′ exon X, having a protein coding region of 1767bp; (5) *NFATC3-IAL/IAS/IC/ID/IE/IF-ΔXa,* containing 5′ exon IAL or IAS or IC or ID or IE or IF and 3′ exon X and lacking exon Xa, having a protein coding region of 1788bp; and (6) *NFATC3-IAL/IAS/IC/ID/IE/IF-IX,* containing 5′ exon IAL or IAS or IC or ID or IE or IF and exon IX as the 3′ exon, having a protein coding region of 1698bp (Supplementary Table 1). Masuda et al. have described a human *NFATC3* transcript containing an additional exon upstream of exon X and downstream of exon Xa [26]. However, we were not able to detect this transcript in any of the tissues analyzed in this study.

In mouse, the expression of *Nfatc3* transcripts containing exon IB was detected in all tissues analyzed, with relatively higher levels in the testis, lung, thymus, and spleen (Fig. 2). Exon IA transcripts were barely detectable only in the testis and thymus (data not shown). *Nfatc3* transcripts containing the mouse-specific 3′ exon IV were expressed at moderate levels in the thymus and spleen. However, with the exception of muscle, low levels of this transcript were seen in all the tissues analyzed. Transcripts containing the 3′ exon X were also observed in all the tissues analyzed, with higher levels in the testis, lung, thymus, and spleen. In the mouse brain exon IB transcripts were expressed in all the regions analyzed (Fig. 2). Higher levels were seen

in the colliculi and cerebellum. During mouse brain development the levels of *Nfatc3* transcripts containing exon IB remained unchanged from embryonic day 13 (E13) up to adult, the developmental period studied here. Transcripts with 3′ exon X were expressed in all brain regions analyzed with, ΔXa transcripts being the predominant mRNAs (Fig. 2).

In human, *NFATC3* transcripts comprising exon IA or IB were more widely expressed than exon IC, ID, IE, or IF transcripts (Fig. 3). Both IA and IB transcripts were expressed at relatively higher levels in the testis, fetal liver, thymus, and muscle. In addition, exon IB was highly expressed in the prostate, placenta, thyroid, and cerebellum. IAL-containing transcripts were expressed at higher levels than IAS-containing transcripts. Transcripts containing exon IC were highly expressed in the testis. Transcripts containing exon ID had high expression in the testis, prostate, and thymus and lower expression in the kidney, liver, fetal liver, trachea, thyroid, and muscle. Exon IE was most strongly expressed in the testis and exon IF in the thymus. All the *NFATC3* 3′ exon transcript variants were expressed in all the tissues analyzed, with higher levels detected in the testis, fetal liver, prostate, thymus, and placenta. In the heart and muscle, transcripts containing exon Xa were expressed at slightly higher levels than transcripts lacking exon Xa. In the human brain, transcripts comprising exons IA and IB were expressed in all the regions analyzed, whereas exon IC transcripts were expressed only in some regions, with relatively higher levels in the cerebellum (Fig. 3). Exon ID transcripts were not detected in the human brain. Exon IE was relatively more expressed in the substantia nigra, optic nerve, and epiphysis and exon IF in the epiphysis. Expression levels of both of the alternative 3′ exons were similar in all the regions analyzed. Compared to the other brain regions exon IX transcripts were present at slightly higher levels in the olfactory bulb, cerebral cortex, cerebellum, and corpus callosum. Transcripts containing exon Xa were mostly expressed at higher levels than transcripts lacking exon Xa (Fig. 3).

Alternative splicing and expression of NFATC4 in human and mouse

Before our study, only one exon, named here exon ID, had been described as a 5′ exon in human *NFATC4* [23]. Our data show that human *NFATC4* has five 5′ exons within ~ 2.5kb of the most upstream part of the gene, named here IA, IB, IC, ID, and IE. In addition, 5′-extended exons IV and VI are also used as 5′ exons (Fig. 1 and Table 1). For mouse *Nfatc4* we identified two 5′ exons: the previously described 5′ exon, named exon I here, which is homologous to the human exon ID [26], and the 5′-extended exon VI, which has not been described before. With the usage of the 5′-extended exon VI in mouse, exclusion and retention of the intron between exons VI and VII were detected. Human exon ID and mouse exon I encode 33 aa. The human exon ID is in addition used as an internal exon: 129bp of its 3′ part are always inserted as the second exon in the transcripts starting upstream of exon ID. This is due to a cryptic splice acceptor site inside exon ID. Human *NFATC4* transcripts that use the 5′ exon IA, IB, or IC encode proteins with an additional 63, 13, or 32 aa, respectively, in their N-termini compared to the protein encoded by the transcripts containing exon ID as the 5′ exon. If exon IEi (retention of intron between exons IE and II), exon IV, or exon VI is used as the 5′ exon, the corresponding human *NFATC4* transcripts encode protein isoforms that are 70, 465, or 711 aa, respectively, shorter in their N-terminus compared to the protein encoded by the transcripts containing exon ID as the 5′ exon. Exon X is used as the 3′ exon in all mouse and human *NFATC4* mRNAs (Fig. 1). In human, there are two splice variants of exon IX, named here IXL and IXS, due to the usage of alternative splice donor sites. In addition, retention of the intron between exons IX and X leads to transcript variants indicated by IXi here. If exon IXS is used, the respective protein isoforms lack 108 aa in the C-terminal region compared to protein isoforms encoded by exon IXL-containing transcripts. IXi usage leads to protein isoforms with 20 unique amino acids in the C-terminus. In mouse, only exons IXL and IXi are used. Taken together, our results showed that the possible transcript types of *NFATC4* in human are: (1) *NFATC4-IA-IXL,* containing 5′ exon IA, exon IXL, and 3′ exon X, having a protein coding region of 2895bp; (2) *NFATC4-IA-IXS,* containing 5′ exon IA, exon IXS, and 3′ exon X, having a protein coding region of 2571bp; (3) *NFATC4-IA-IXi,* containing 5′ exon IA, exon IXi, and 3′ exon X, having a protein coding region of 2892bp; (4) *NFATC4-IB-IXL,* containing 5′ exon IB, exon IXL, and 3′ exon X, having a protein coding region of 2745bp; (5) *NFATC4-IB-IXS,* containing 5′ exon IB, exon IXS, and 3′ exon X, having a protein coding region of 2421bp; (6) *NFATC4-IB-IXi,* containing 5′ exon IB, exon IXi, and 3′ exon X, having a protein coding region of 2742bp; (7) *NFATC4-IC-IXL,* containing 5′ exon IC, exon IXL, and 3′ exon X, having a protein coding region of 2802bp; (8) *NFATC4-IC-IXS,* containing 5′ exon IC, exon IXS, and 3′ exon X, having a protein coding region of 2478bp; (9) *NFATC4-IC-IXi,* containing 5′ exon IC, exon IXi, and 3′ exon X, having a protein coding region of 2799bp; (10) *NFATC4-ID-IXL,* containing 5′ exon ID, exon IXL, and 3′ exon X, having a protein coding region of 2706bp; (11) *NFATC4-ID-IXS,* containing 5′ exon ID, exon IXS, and 3′ exon X, having a protein coding region of 2382bp; (12) *NFATC4-ID-IXi,* containing 5′ exon ID, exon IXi, and 3′ exon X, having a protein coding region of 2703bp; (13) *NFATC4-IE-IXL,* containing 5′ exon IE, exon IXL, and 3′ exon X, having a protein coding region of 2670bp; (14) *NFATC4-IE-IXS,* containing 5′ exon IE, exon IXS, and 3′ exon X, having a protein coding region of 2346bp; (15) *NFATC4-IE-IXi,* containing 5′ exon IE, exon IXi, and 3′ exon X, having a protein coding region of 2667bp; (16) *NFATC4-IEi-IXL,* containing 5′ exon IEi, exon IXL, and 3′ exon X, having a protein coding region of 2496bp; (17) *NFATC4-IEi-IXS,* containing 5′ exon IEi, exon IXS, and 3′ exon X, having a protein coding region of 2172bp; (18) *NFATC4-IEi-IXi,* containing 5′ exon IEi, exon IXi, and 3′ exon X, having a protein coding region of 2493bp; (19) *NFATC4-IV-IXL,* containing exon IV as the 5′ exon, exon IXL, and 3′ exon X, having a protein coding region of 1311bp; (20) *NFATC4-IV-IXS,* containing exon IV as the 5′ exon, exon IXS, and 3′ exon X, having a protein coding region of 987bp; (21) *NFATC4-IV-IXi,* containing exon IV as the 5′ exon, exon IXi, and 3′ exon X, having a protein coding region of 1308bp; (22) *NFATC4-VI-IXL,* containing exon VI as the 5′ exon, exon IXL, and 3′ exon X, having a protein coding region of 570bp; (23) *NFATC4-VI-IXS,* containing exon VI as the 5′ exon, exon IXS, and 3′ exon X, having a protein coding region of 246bp; and (24) *NFATC4-VI-IXi,* containing exon VI as the 5′ exon, exon IX, and 3′ exon X, having a protein coding region of 567bp (Supplementary Table 1).

Expression of mouse *Nfatc4* exon I mRNA was detected in all tissues analyzed, with higher levels in the lung, heart, testis, and spleen (Fig. 2). During brain development, the highest levels were observed at E13, the first developmental stage analyzed, and the expression decreased thereafter, reaching the lowest levels at postnatal day 14 and remaining unchanged thereafter. In the adult mouse brain the highest levels of *Nfatc4* exon I transcripts were detected in the thalamus and colliculi. Transcripts containing the extended 5′ exon VI or VIi were evenly expressed in all the peripheral tissues tested (Fig. 2). The highest expression levels of *Nfatc4* exon IXL and IXi transcripts were detected in the lung, heart, and muscle. In the brain IXL transcript levels decreased during development, while IXi transcripts were higher during postnatal development. In adult mouse brain these transcripts were most strongly expressed in the colliculi, midbrain, and cerebellum (Fig. 2).

In human, *NFATC4* transcripts comprising 5′ exons IB, IC, ID, and VI were expressed more widely than 5′ exon IA, IE, and IV transcripts (Fig. 3). Exon IA transcripts were detected only in the testis and prostate. Exon IB and IC transcripts were both expressed in several tissues, including the stomach, testis, kidney, trachea, adrenal gland, thyroid, and cerebellum. Transcripts containing exon ID were expressed in almost all tissues analyzed, with the highest levels in the small intestine, uterus, testis, prostate, placenta, thyroid, and cerebellum. Low levels of exon IE- and IEi-containing transcripts were seen only in the

testis. The 5′ exon IV transcript levels were highest in the placenta and relatively high also in the heart and uterus. Expression levels of transcripts containing exon VI as the 5′ exon were moderate in all tissues tested (Fig. 3). The 3′ exon X-containing transcripts of *NFATC4* were expressed according to the sum of the expression patterns of the 5′ exons. Highest levels were detected in the uterus, testis, placenta, trachea, adrenal gland, thyroid, and cerebellum. In most tissues, transcripts containing exon IXL were relatively more abundant than transcripts containing exon IXS. Transcripts containing the 3′ exon IX were expressed at low levels in the testis, kidney, and thymus. In the brain, all the transcript types of *NFATC4*, except exon IA transcripts, were expressed in the cerebellum (Fig. 3). In addition, high levels of 5′ exon ID, IV, and VI transcripts were detected in other brain regions: exon ID mRNAs in the olfactory bulb, hippocampus, caudate nucleus, and optic nerve; exon IV transcripts in the cerebral cortex, corpus callosum, and hippocampus; and exon VI transcripts in the olfactory bulb and cerebellum. Expression of exon X-containing transcripts, corresponding to the sum of all *NFATC4* mRNAs, was detected in all brain regions, with highest levels in the cerebellum, where exon IXL-containing transcripts were the predominant ones (Fig. 3).

In situ hybridization analyses of NFATC1, NFATC2, NFATC3, and NFATC4 expression in adult mouse brain and human hippocampus

Expression of NFAT mRNAs at the cellular level has not been studied thoroughly by in situ hybridization before. Therefore we analyzed the expression of NFAT mRNAs in adult mouse brain by in situ hybridization. The hybridization probes for each NFAT mRNA were constructed to recognize all of the major splice variants and therefore were targeted to the conserved RHD coding region of NFAT mRNAs. To distinguish different cell types, Nissl counterstaining of the tissue sections, which allows one to distinguish the large and weakly stained nuclei of neurons from the small and strongly stained nuclei of glial cells, was used. All of the NFAT mRNAs were expressed in the neurons of the brain, with specific patterns for each NFAT.

We observed similarities and differences in the expression patterns of *Nfatc1, Nfatc2, Nfatc3,* and *Nfatc4* (Figs. 4 and 5 and Supplementary Fig. 3). In the olfactory system *Nfatc1* was highly expressed in the granular layer and glomerular cell layer and *Nfatc2* in the mitral cell layer (Figs. 4 and 5). A moderate signal was detected in the glomerular and granular cell layer for *Nfatc2* (Figs. 4A, 4C, 5A, and 5D). *Nfatc3* and

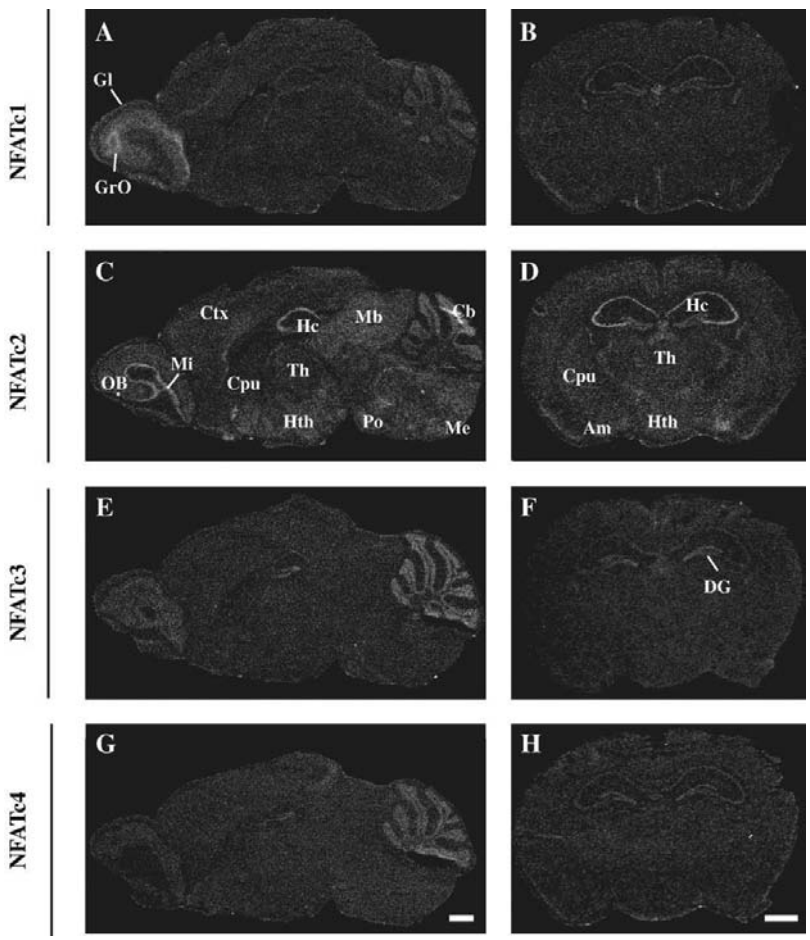

Fig. 4. In situ hybridization analysis of *Nfatc1, Nfatc2, Nfatc3,* and *Nfatc4* mRNA expression in adult mouse brain. Dark-field emulsion autoradiographs from sagittal sections (A, C, E, and G) and coronal sections at the level of thalamus (B, D, F, and H). The sections were hybridized with a probe for *Nfatc1* (A and B), *Nfatc2* (C and D), *Nfatc3* (E and F), or *Nfatc4* (G and H). Gl, glomerular layer of olfactory bulb; GrO, granular layer of olfactory bulb; OB, olfactory bulb; Mi, mitral layer of olfactory bulb; Ctx, cortex; Cpu, caudate putamen; Hc, hippocampus; Th, thalamus; Hth, hypothalamus; Mb, midbrain; Po, pons; Cb, cerebellum; Me, medulla; Am, amygdala; DG, dentate gyrus. Scale bars, 1 mm.

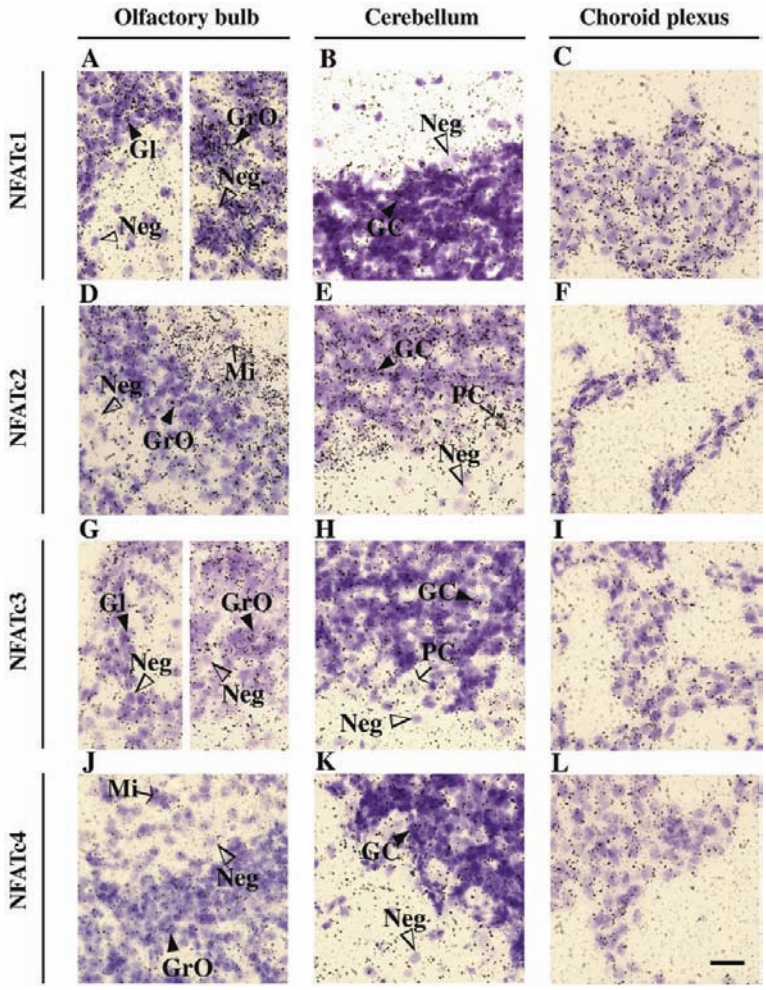

Fig. 5. In situ hybridization analysis of *Nfatc1, Nfatc2, Nfatc3,* and *Nfatc4* mRNA expression in adult mouse brain. Bright-field higher magnification pictures of the olfactory bulb (A, D, G, and J), cerebellum (B, E, H, and K), and choroid plexus (C, F, I, and L) are shown. Filled arrowheads denote some positive neurons, some negative neurons are marked with unfilled arrowheads. The sections were hybridized with a probe for *Nfatc1* (A, B, and C), *Nfatc2* (D, E, and F), *Nfatc3* (G, H, and I), or *Nfatc4* (J, K, and L). Gl, glomerular cell layer of the olfactory bulb; GrO, granular cells of the olfactory bulb; Mi, mitral cell layer, PC, Purkinje cells; GC, granular cells of the cerebellum; Neg, negative cell. Scale bar, 50 μm.

Nfatc4 were expressed at low levels in the glomerular and granular layer (Figs. 4E, 4G, 5G, and 5J). In addition, *Nfatc4* was expressed in the mitral cell layer (Figs. 4G and 5J).

In the cerebral cortex *Nfatc2* mRNA expression was detected at relatively high levels in the neurons of layers II–VI (Fig. 4C and Supplementary Figs. 3A–D). The expression levels of other NFAT family members in this brain region were below the detection limit of our in situ hybridization method. Although all NFAT mRNAs were detected in the hippocampal formation, there were differences in the distribution and level of expression between different NFAT genes. *Nfatc2* showed a strong signal in the hippocampus, particularly in the CA1–CA3 pyramidal layers, and slightly lower levels in the granular layer of the dentate gyrus (Figs. 4C and D and Supplementary Figs. 3B–D). *Nfatc3* mRNA was moderately expressed only in the granular layer of the dentate gyrus and was detected at low levels in the CA1–CA3 pyramidal layers (Figs. 4E and F). *Nfatc1* and *Nfatc4* mRNAs were expressed at evenly low levels in both the CA1–CA3 pyramidal cells and the dentate gyrus granular cells (Figs. 4A and B).

In the basal ganglia, evenly distributed moderate signal was detected for *Nfatc2* in the caudate putamen, ventral pallidum, accumbens, and septum (Fig. 4C and Supplementary Fig. 3A), whereas *Nfatc1* mRNA was expressed at moderate levels only in the region of bed nucleus of stria terminalis (data not shown). *Nfatc3* and *Nfatc4* mRNAs were not expressed significantly in these brain structures (Figs. 4E and G). In the thalamus, hypothalamus, and midbrain *Nfatc2* mRNA was widely expressed at high or moderate levels in most of the nuclei (Figs. 4C and D and Supplementary Figs. 3B and C). In contrast, signal for *Nfatc1, Nfatc3,* and *Nfatc4* was barely detectable in these structures (Figs. 4A, B, and E–H).

In the cerebellum all NFAT transcripts were expressed (Figs. 4 and 5). *Nfatc1* and *Nfatc4* were moderately expressed only in the granular neurons (Figs. 4A, 4G, 5B, and 5K), whereas *Nfatc2* and *Nfatc3* were expressed in the granular cell layer and also in the Purkinje cell layer (Figs. 4C, 4E, 5E, and 5H). In the granular layer cells the signal for *Nfatc2* and *Nfatc3* was relatively stronger than that for *Nfatc1* and *Nfatc4*. In the pons and medulla only *Nfatc2* showed moderate expression all over the region (Fig. 4C and Supplementary Figs. 3E and F).

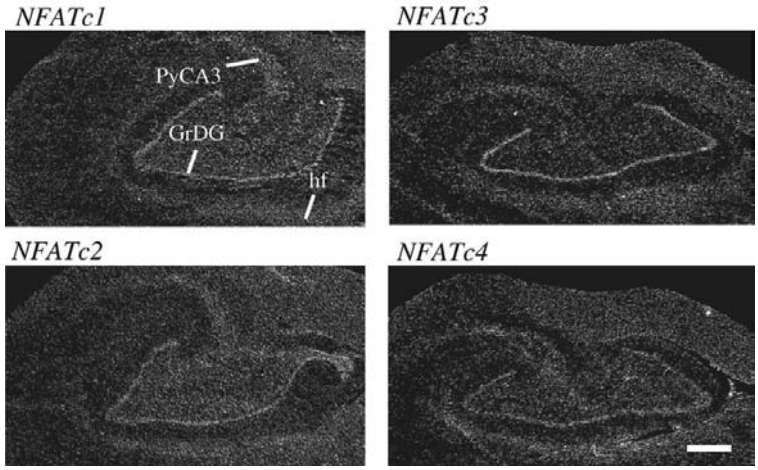

Fig. 6. In situ hybridization analysis of *NFATC1, NFATC2, NFATC3,* and *NFATC4* mRNA expression in adult human hippocampus. Dark-field emulsion autoradiographs from coronal sections at the level of hippocampus. GrDG, granular cell layer of the dentate gyrus; PyCA3, CA3 pyramidal cells; hf, hippocampal fissure. Scale bar, 1 mm.

In the choroid plexus and ependymal cells *Nfatc1* and *Nfatc2* were expressed at high levels and *Nfatc3* and *Nfatc4* at moderate levels (Figs. 5C, F, I, and L).

In the human hippocampus all four NFATs were expressed. For all NFATs stronger signal was detected in the granular layer of the dentate gyrus, in the pyramidal neurons of CA3 region, and in the hippocampal fissure (Fig. 6).

Discussion

The aim of this study was to characterize the structures, alternative splicing, and expression of the NFAT genes in human and in mouse. Our results on the structures of the NFAT genes are in agreement with previous data from other groups [28,29,33,42,43] and also add important new data about the complex splicing and expression of this gene family. NFAT genes encode proteins that are very similar in their central region, which encodes the Rel homology domain, but are clearly variable in their N- and C-terminal parts due to the less conserved 5′ and 3′ regions of the paralogs of the genes, which differ significantly in their protein-coding potencies. Here we show that the NFAT genes are even more diverse in the 5′ and 3′ regions than previously described. All NFAT genes in human and mouse have multiple alternatively used 5′ exons: according to our data human and mouse *NFATC1* and *NFATC2* and mouse *Nfatc3* and *Nfatc4* have two alternative 5′ exons; human *NFATC3* has six and *NFATC4* has seven alternative 5′ exons. We show that usage of 3′-terminal exons is also complex: human and mouse *NFATC1* and *NFATC3* genes contain two and the mouse *Nfatc2* contains three alternative 3′ exons. Human *NFATC2* and both human and mouse *NFATC4* have one 3′ exon. In addition, alternative splicing is used for all NFAT genes and in combination with the usage of alternative 5′ and 3′ exons this could theoretically lead to 8 different protein isoforms of NFATC1, 6 different isoforms of both NFATC2 and NFATC3, and 24 different isoforms of NFATC4 in human.

The alternative 5′ exons of *NFATC1* have been described before [24,29,44,45] and the results of our bioinformatic and expression studies confirm that the *NFATC1* gene has two alternative 5′ exons in both mouse and human. Also, our expression analyses are consistent with studies showing *NFATC1* expression predominantly in the immune system [23–26,46]. For *NFATC2* only one 5′ exon had been previously described [41]. Here we have identified and characterized a novel alternative 5′ exon for both human and mouse *NFATC2*. We show that in human the previously known *NFATC2* 5′ exon, exon IB, and the novel alternative 5′ exon, named here exon IA, are expressed at similar levels in most of the tissues, except in the heart, where exon IB-containing mRNAs are the predominant transcripts. In mouse though, exon IA is used predominantly in the brain and exon IB both in the brain and in nonneural tissues. In addition to the novel *NFATC2* 5′ exon we describe a novel splice variant of exon II that is conserved in human and mouse and results in a short form of exon II, named IIS here. Usage of the short variant of exon II is the predominant splicing event in mouse for transcripts starting with exon IA. However, in human, exon IIS transcripts of *NFATC2* are barely detectable. *NFATC2* exon IIS-containing transcripts encode proteins without the N-terminal CaN binding site and serine-rich region. The functions of such isoforms are yet to be elucidated.

We have shown here that human *NFATC3* and *NFATC4* contain six and five 5′ exons, respectively. The human *NFATC3* exon IB and *NFATC4* exon ID are the only 5′ exons homologous to a 5′ exon in mouse *Nfatc3* and *Nfatc4,* respectively. These homologous exons are the only 5′ exons that have been previously described for *NFATC3* and *NFATC4* [23]. In human *NFATC3* and *NFATC4* the 5′ exons are located very close to each other in the 5′ ends of the genes. The close placement of the exons leaves open the possibility that they compile one exon with multiple transcription start sites. However, bioinformatic and PCR analyses showed that the 5′ sequences of both human *NFATC3* and *NFATC4* transcripts are not overlapping and use distinct splice donor sites, indicating that they are derived from different exons. In addition, there is an alternative transcription start site in human *NFATC4* located upstream of exon IV. Usage of this transcription start site generates protein isoforms that are similar to the *NFATC3* isoforms encoded by transcripts with the novel 5′ exons IA, IC, and ID of *NFATC3,* which yield NFAT isoforms without the whole regulatory domain. The function of these proteins is unclear. However, since we found generation of such isoforms for both *NFATC3* and *NFATC4* in human, these isoforms could be important in functions yet undefined. Another interesting observation about the putative N-termini of the human *NFATC3* and *NFATC4* is that although exon IB of human *NFATC3* and exons IA, IB, IC, and ID of human *NFATC4* encode N-termini that are different comparing the whole sequence, they clearly contain a conserved stretch of 12 amino acids—[E/D]EL[E/D]FKLVFGE[E/D] (Supplementary Fig. 1). The N-termini of the NFAT proteins have previously been shown to contain TADs [17]. We suggest that the TADs of the NFAT proteins contain important motifs that probably function

similarly but have also evolved to be distinct, potentially to convey different gene regulation activities.

The 3′ regions of NFAT genes are also diverse due to alternative splicing and usage of alternative 3′ exons. For example, in human, exon IX of *NFATC1* can be alternatively spliced in three ways, leading to transcripts lacking exon IX (ΔIX), with a long variant of exon IX (IXL) or with a short variant of exon IX (IXS). ΔXI transcripts have not been described before. Similar to the N-termini of NFAT proteins, there is a conserved motif (LDQ[T/L]YLDD(VN)E[I/L]I[R/D]) in the C-terminal sequences that locates to the C-terminal TAD of the NFATC1 and NFATC2 proteins [17] (Supplementary Fig. 2). This sequence is present only in the NFATC1 isoform NFATC1-IXL, whereas it is present in all human NFATC2 isoforms (Supplementary Fig. 2). In addition, by bioinformatics we found that this conserved motif contains a putative NES (Supplementary Fig. 2). Hence the isoforms lacking the sequence may act differently compared to the isoforms containing the TAD/NES. Our expression analysis of *NFATC1* showed that splice variants with exon IXS, encoding protein isoforms lacking the conserved motif, are the most abundantly expressed transcripts.

Alternative 3′ exons of NFAT genes are used in a species-specific manner. For example, for the mouse *Nfatc2,* exon VIIa has been shown to be an alternative 3′ exon and transcripts that include this exon are expressed specifically in neurons and encode a constitutively active isoform [33]. Our expression analysis confirmed that this *Nfatc2* transcript, named here *Nfatc2IB-IIS-VIIa,* is expressed in the mouse brain. However, in human, the homolog of this *Nfatc2* transcript is not expressed. Our analysis showed that similar species-specific differences are present also for human and mouse *NFATC3.* In human, and not in mouse, exon IX is used as an alternative 3′ exon. Transcripts including this exon encode the human-specific NFATC3 protein isoform containing a C-terminal TAD with a different transactivation potential compared to other NFATC3 C-terminal TADs [28]. In this study we have shown that this transcript is expressed in all human tissues analyzed. Furthermore, we show that *Nfatc3* transcripts using exon IV as the 3′ exon encoding a protein isoform lacking most of the Rel homology domain are expressed in mouse, in most of the tissues analyzed, and not in human. These data combined show that different NFAT C-termini could potentially have functionally unique characteristics, emphasizing that although NFAT proteins may have redundancy in their functions, as can be concluded from knockout studies [47,48], the specific functions of different NFAT isoforms could have an impact on Ca^{2+}-dependent gene expression in different tissues and species depending on the isoform expressed. Species-specific splicing and usage of alternative 5′ exons have also been shown to regulate other genes, for example, splicing of the *p53* tumor suppressor gene [49] and usage of 5′ exons of the transcription factor *NR5A1* [50].

In previous studies only *NFATC4* expression has been characterized in more detail in some regions of adult nervous system and cultured primary neurons [21,35,36,38,39,51,52]. However, there is evidence that NFATC2 and NFATC3 might also have important functions in the nervous system. Mice with the combination of *Nfatc2, Nfatc3,* and *Nfatc4* mutations have a complete defect of midline crossing of the commissural neurons in response to netrins and neurons from these mice are unable to respond to neurotrophins [47], whereas NFAT single-knockout mice have lesser neuronal defects [2,19]. In addition, there is evidence that *NFATC2* and *NFATC3* are expressed in some regions of the brain—in the hypothalamus and olfactory bulb [24,31,32]. To date there are no indications of *NFATC1* expression in the brain. To find out which of the NFAT genes are expressed in the adult brain and in which cells they are expressed we analyzed expression of NFAT mRNAs in adult mouse brain using in situ hybridization. Our results showed that *Nfatc2* is broadly expressed throughout the adult mouse brain and is the predominantly expressed NFAT in the mouse brain. The highest *Nfatc2* mRNA levels were detected in the pyramidal cell layer of the CA1–CA3 regions of the hippocampus, in the Purkinje and granule cell layers of the cerebellum, olfactory bulb, hypothalamus, and thalamus. Surprisingly, we found that *Nfatc1* is also expressed in mouse brain, having the highest expression levels in the granular and glomerular cell layers of the olfactory bulb. Moderate expression was seen also in the cerebellar granule cells. This suggests that NFATC1 may have important functions in the brain in addition to the functions in the tissues described earlier by others [24,26,52]. Before this study *NFATC3* expression in the brain had been demonstrated only in the hypothalamus and striatum and in certain cell lines of neuronal origin [31,35]. Here we describe *NFATC3* expression in the cerebellar granule cells and in Purkinje cells and, to a lesser extent, in the granule cells of the dentate gyrus and olfactory bulb. Therefore, our findings are consistent with the knockout studies showing that both *NFATC2* and *NFATC3* contribute to the development and function of the nervous system [47].

Several studies have shown that *NFATC4* is expressed in the brain, giving the notion that *NFATC4* might be the most abundant NFAT expressed in the nervous system. Expression has been shown in the adult rat hippocampus using RT-PCR and in situ hybridization and in the adult mouse hippocampus using RT-PCR [21], in cultured rat striatal cells using Western blot analysis [35] and in the adult mouse striatum using immunohistochemistry [51], in adult mouse dorsal root ganglion and spinal cord using in situ hybridization [36], in cultured rat cerebellar granule cells using immunocytochemistry [38], in adult mouse hippocampus using immunohistochemistry [39], and in cultured rat hippocampal neurons using immunocytochemistry [53]. However, we detected only low levels of *Nfatc4* expression in the brain. To ensure credibility we repeated the assay twice using two different hybridization probes. We show here that *Nfatc4* is indeed expressed in the brain but at lower levels compared to the other NFATs. Moderate expression was detected only in the cerebellar, olfactory bulb, and dentate gyrus granule cells and in the mitral cells of the olfactory bulb. On the other hand, according to our PCR analysis of NFAT expression during mouse brain development, *Nfatc4* was more abundantly expressed in the earlier stages of development and the levels were decreased during later stages. Therefore, Nfatc4 function might be especially important in the developing brain. Surprisingly, our PCR results showed that *NFATC4* is relatively highly expressed in the human brain, indicating again that NFAT signaling could have species-specific features. Moreover, in situ hybridization analysis showed that in the adult human brain all NFAT genes are expressed in the CA1–CA3 pyramidal neurons and dentate gyrus granule cells.

Notably, in the human brain all the NFATs, among other regions, were expressed in the corpus callosum and optic nerve—regions of the brain containing mainly neuronal projections and glial cells. By in situ hybridization, we found that the majority of the signal in the mouse brain accumulated in certain neuronal populations, although for all NFATs, very low signal was detected all over the brain, including glial cells. Thus, it is possible that in addition to neurons, NFAT genes are also expressed in glial cells. In the human hippocampus all NFATs were expressed in the CA3 pyramidal neurons and dentate gyrus granular cell layer and also in the hippocampal fissure, which further supports the possibility that NFAT genes are expressed in both neurons and glial cells.

In conclusion, the results of this study provide comprehensive data about the structure, splicing pattern, and expression of NFAT genes in human and mouse, providing useful information for future studies aiming to elucidate the functions of different NFAT isoforms.

Materials and methods

Structure, expression analysis, and cloning of the NFAT genes

Human NFAT gene structures and human and mouse NFAT mRNAs were identified by analyzing genomic, mRNA, and EST databases using bioinformatics tools (http://www.ncbi.nlm.nih.gov and http://genome.ucsc.edu). All homology searches were performed using various BLAST

tools (http://www.ncbi.nlm.nih.gov). NESs were predicted using the software at http://www.cbs.dtu.dk/services/NetNES/ site and NLSs were predicted using software at http://wolfpsort.org/ site. Rel homology and serine-rich sequence motifs were predicted using the software at the http://expasy.org/prosite/ site. Based on the sequence information acquired, primers were designed to analyze the expression of human and mouse NFAT mRNAs and to construct plasmids for mouse and human NFAT riboprobe generation (Supplementary Table 2). Total RNAs from various human and mouse brain regions and mouse tissues were purified with RNAwiz (Ambion, USA) as recommended by the manufacturer and treated with DNase using a DNA-free kit (Ambion). Human RNAs from different tissues were obtained from BD Biosciences (USA). First-strand cDNAs were synthesized from 5 μg of total RNA with Superscript III reverse transcriptase (Invitrogen, USA) as recommended by the manufacturer. Fire polymerase, Hot-Fire polymerase (Solis Biodyne, Estonia), or the GC-Rich PCR System (Roche, Switzerland) was used in PCR for expression analyses and riboprobe template plasmid construction, all according to the manufacturer's instructions. An annealing temperature of 57°C was used for all combinations of primers. Cycle numbers were optimized so that the PCR products were analyzed in the exponential phase of the PCR. Depending on the primers used, 30–40 cycles of PCR were performed. PCR fragments were resolved by agarose gel electrophoresis. PCR with primers specific for the ubiquitously expressed glyceraldehyde-3-phosphate dehydrogenase (*GAPDH*), 25 cycles, was performed as a control to determine the amount of human template cDNA in different PCRs. For normalizing the amount of mouse template cDNA and the amount of template cDNA in the panel of human brain regions, a 30-cycle PCR with primers specific for the ubiquitously expressed hypoxanthine guanine phosphoribosyl transferase (*HPRT*) was performed. All PCRs were performed in a volume of 10 μl containing 1/80 of the reverse transcription reaction product as a template. All PCR products were verified by sequencing.

In situ hybridization

For both human and mouse the in situ hybridization probes were generated as follows. The NFAT riboprobe fragments were selected to cover the parts of the NFAT mRNAs that are present in all mainly expressed splice variants of *NFATC1, NFATC2, NFATC3,* or *NFATC4*. DNA fragments amplified for NFAT riboprobe generation (Supplementary Table 2) were excised from the gel and cloned into pSC-A PCR cloning vector (Stratagene, USA). The mouse NFAT plasmids were linearized adjacent to the 5′ ends of the cloned fragments. The hybridization probes for mouse were 519, 524, 436, and 831 nt in length for *Nfatc1, Nfatc2, Nfatc3,* and *Nfatc4,* respectively. For *Nfatc4* the template for the second assay was generated by digestion at the BglII site inside the cloned *Nfatc4* sequence and the length of the probe was 456 bp. For human in situ hybridization the plasmids with *NFATC1, NFATC2, NFAT3,* and *NFATC4* were linearized with Eco45III, NcoI, NcoI, or HindIII restriction enzyme inside the cloned sequences, respectively. The lengths of the resulting riboprobes were 697 nt for *NFATC1,* 615 nt for *NFATC2,* 876 nt for *NFATC3,* and 816 nt for *NFATC4.* cRNA probes were synthesized with a MAXIScript in vitro transcription kit (Ambion), using [α-^{35}S]UTP (Amersham Biosciences) for labeling, according to the manufacturer's instructions. Serial sagittal and coronal sections (20 μm) from fresh-frozen adult male Black 6 mouse brains and coronal sections (16 μm) from fresh-frozen adult male human hippocampus were subjected to in situ hybridization using a protocol described elsewhere by Timmusk et al. [54]. Emulsion-dipped sections were developed after 7 weeks using D-19 developer (Eastman Kodak, USA), fixed (sodium fixer; Kodak), and counterstained with hematoxylin (Shandon, USA).

Acknowledgments

We thank Enn Jõeste and Liina Kiho from North Estonian Regional Hospital, Tallinn, for help in collecting tissue samples; Epp Väli for technical assistance; and Richard Tamme and Liis Leitsalu for help in preparing cryostat sections. This work was supported by the following grants to T.T.: Wellcome Trust International Senior Research Fellowship (Grant 067952), Estonian Ministry of Education and Research (Grants 0222602 and 0140143), and Estonian Science Foundation (Grant 7257).

Appendix A. Supplementary data

Supplementary data associated with this article can be found, in the online version, at doi:10.1016/j.ygeno.2008.06.011.

References

[1] I.A. Graef, J.M. Gastier, U. Francke, G.R. Crabtree, Evolutionary relationships among Rel domains indicate functional diversification by recombination, Proc. Natl. Acad. Sci. U. S. A. 98 (2001) 5740–5745.
[2] G.R. Crabtree, E.N. Olson, NFAT signaling: choreographing the social lives of cells, Cell 109 (2002) S67–S79 (Suppl.).
[3] J. Aramburu, F. Garcia-Cozar, A. Raghavan, H. Okamura, A. Rao, P.G. Hogan, Selective inhibition of NFAT activation by a peptide spanning the calcineurin targeting site of NFAT, Mol. Cell 1 (1998) 627–637.
[4] S. Park, M. Uesugi, G.L. Verdine, A second calcineurin binding site on the NFAT regulatory domain, Proc. Natl. Acad. Sci. U. S. A. 97 (2000) 7130–7135.
[5] A. Kiani, A. Rao, J. Aramburu, Manipulating immune responses with immunosuppressive agents that target NFAT, Immunity 12 (2000) 359–372.
[6] J. Jain, P.G. McCaffrey, V.E. Valge-Archer, A. Rao, Nuclear factor of activated T cells contains Fos and Jun, Nature 356 (1992) 801–804.
[7] J.D. Molkentin, J.R. Lu, C.L. Antos, B. Markham, J. Richardson, J. Robbins, S.R. Grant, E.N. Olson, A calcineurin-dependent transcriptional pathway for cardiac hypertrophy, Cell 93 (1998) 215–228.
[8] F. Blaeser, N. Ho, R. Prywes, T.A. Chatila, Ca(2+)-dependent gene expression mediated by MEF2 transcription factors, J. Biol. Chem. 275 (2000) 197–209.
[9] C. Luo, E. Burgeon, A. Rao, Mechanisms of transactivation by nuclear factor of activated T cells-1, J. Exp. Med. 184 (1996) 141–147.
[10] H. Okamura, J. Aramburu, C. Garcia-Rodriguez, J.P. Viola, A. Raghavan, M. Tahiliani, X. Zhang, J. Qin, P.G. Hogan, A. Rao, Concerted dephosphorylation of the transcription factor NFAT1 induces a conformational switch that regulates transcriptional activity, Mol. Cell 6 (2000) 539–550.
[11] P.G. Hogan, L. Chen, J. Nardone, A. Rao, Transcriptional regulation by calcium, calcineurin, and NFAT, Genes Dev. 17 (2003) 2205–2232.
[12] C.R. Beals, C.M. Sheridan, C.W. Turck, P. Gardner, G.R. Crabtree, Nuclear export of NF-ATc enhanced by glycogen synthase kinase-3, Science 275 (1997) 1930–1934.
[13] C.W. Chow, M. Rincon, J. Cavanagh, M. Dickens, R.J. Davis, Nuclear accumulation of NFAT4 opposed by the JNK signal transduction pathway, Science 278 (1997) 1638–1641.
[14] P. Gomez del Arco, S. Martinez-Martinez, J.L. Maldonado, I. Ortega-Perez, J.M. Redondo, A role for the p38 MAP kinase pathway in the nuclear shuttling of NFATp, J. Biol. Chem. 275 (2000) 13872–13878.
[15] H. Okamura, C. Garcia-Rodriguez, H. Martinson, J. Qin, D.M. Virshup, A. Rao, A conserved docking motif for CK1 binding controls the nuclear localization of NFAT1, Mol. Cell. Biol. 24 (2004) 4184–4195.
[16] J. Zhu, F. Shibasaki, R. Price, J.C. Guillemot, T. Yano, V. Dotsch, G. Wagner, P. Ferrara, F. McKeon, Intramolecular masking of nuclear import signal on NF-AT4 by casein kinase I and MEKK1, Cell 93 (1998) 851–861.
[17] A. Rao, C. Luo, P.G. Hogan, Transcription factors of the NFAT family: regulation and function, Annu. Rev. Immunol. 15 (1997) 707–747.
[18] L.A. Timmerman, N.A. Clipstone, S.N. Ho, J.P. Northrop, G.R. Crabtree, Rapid shuttling of NF-AT in discrimination of Ca^{2+} signals and immunosuppression, Nature 383 (1996) 837–840.
[19] I.A. Graef, F. Chen, L. Chen, A. Kuo, G.R. Crabtree, Signals transduced by Ca(2+)/calcineurin and NFATc3/c4 pattern the developing vasculature, Cell 105 (2001) 863–875.
[20] D.C. Hill-Eubanks, M.F. Gomez, A.S. Stevenson, M.T. Nelson, NFAT regulation in smooth muscle, Trends Cardiovasc. Med. 13 (2003) 56–62.
[21] I.A. Graef, P.G. Mermelstein, K. Stankunas, J.R. Neilson, K. Deisseroth, R.W. Tsien, G.R. Crabtree, L-type calcium channels and GSK-3 regulate the activity of NF-ATc4 in hippocampal neurons, Nature 401 (1999) 703–708.
[22] T. Nguyen, S. Di Giovanni, NFAT signaling in neural development and axon growth, Int. J. Dev. Neurosci. 26 (2008) 141–145.
[23] T. Hoey, Y.L. Sun, K. Williamson, X. Xu, Isolation of two new members of the NF-AT gene family and functional characterization of the NF-AT proteins, Immunity 2 (1995) 461–472.
[24] J.P. Northrop, S.N. Ho, L. Chen, D.J. Thomas, L.A. Timmerman, G.P. Nolan, A. Admon, G.R. Crabtree, NF-AT components define a family of transcription factors targeted in T-cell activation, Nature 369 (1994) 497–502.
[25] G.W. Cockerill, A.G. Bert, G.R. Ryan, J.R. Gamble, M.A. Vadas, P.N. Cockerill, Regulation of granulocyte–macrophage colony-stimulating factor and E-selectin expression in endothelial cells by cyclosporin A and the T-cell transcription factor NFAT, Blood 86 (1995) 2689–2698.
[26] E.S. Masuda, Y. Naito, H. Tokumitsu, D. Campbell, F. Saito, C. Hannum, K. Arai, N. Arai, NFATx, a novel member of the nuclear factor of activated T cells family that is expressed predominantly in the thymus, Mol. Cell. Biol. 15 (1995) 2697–2706.

[27] D.Z. Wang, P.G. McCaffrey, A. Rao, The cyclosporin-sensitive transcription factor NFATp is expressed in several classes of cells in the immune system, Ann. N. Y. Acad. Sci. 766 (1995) 182–194.
[28] R. Imamura, E.S. Masuda, Y. Naito, S. Imai, T. Fujino, T. Takano, K. Arai, N. Arai, Carboxyl-terminal 15-amino acid sequence of NFATx1 is possibly created by tissue-specific splicing and is essential for transactivation activity in T cells, J. Immunol. 161 (1998) 3455–3463.
[29] J. Park, A. Takeuchi, S. Sharma, Characterization of a new isoform of the NFAT (nuclear factor of activated T cells) gene family member NFATc, J. Biol. Chem. 271 (1996) 20914–20921.
[30] J.L. de la Pompa, L.A. Timmerman, H. Takimoto, H. Yoshida, A.J. Elia, E. Samper, J. Potter, A. Wakeham, L. Marengere, B.L. Langille, et al., Role of the NF-ATc transcription factor in morphogenesis of cardiac valves and septum, Nature 392 (1998) 182–186.
[31] M. Asai, Y. Iwasaki, M. Yoshida, N. Mutsuga-Nakayama, H. Arima, M. Ito, K. Takano, Y. Oiso, Nuclear factor of activated T cells (NFAT) is involved in the depolarization-induced activation of growth hormone-releasing hormone gene transcription in vitro, Mol. Endocrinol. 18 (2004) 3011–3019.
[32] A.M. Ho, J. Jain, A. Rao, P.G. Hogan, Expression of the transcription factor NFATp in a neuronal cell line and in the murine nervous system, J. Biol. Chem. 269 (1994) 28181–28186.
[33] S. Plyte, M. Boncristiano, E. Fattori, F. Galvagni, S.R. Paccani, M.B. Majolini, S. Oliviero, G. Ciliberto, J.L. Telford, C.T. Baldari, Identification and characterization of a novel nuclear factor of activated T-cells-1 isoform expressed in mouse brain, J. Biol. Chem. 276 (2001) 14350–14358.
[34] B.J. Wilkins, L.J. De Windt, O.F. Bueno, J.C. Braz, B.J. Glascock, T.F. Kimball, J.D. Molkentin, Targeted disruption of NFATc3, but not NFATc4, reveals an intrinsic defect in calcineurin-mediated cardiac hypertrophic growth, Mol. Cell. Biol. 22 (2002) 7603–7613.
[35] S. Jayanthi, X. Deng, B. Ladenheim, M.T. McCoy, A. Cluster, N.S. Cai, J.L. Cadet, Calcineurin/NFAT-induced up-regulation of the Fas ligand/Fas death pathway is involved in methamphetamine-induced neuronal apoptosis, Proc. Natl. Acad. Sci. U. S. A. 102 (2005) 868–873.
[36] R.D. Groth, L.G. Coicou, P.G. Mermelstein, V.S. Seybold, Neurotrophin activation of NFAT-dependent transcription contributes to the regulation of pro-nociceptive genes, J. Neurochem. 102 (2007) 1162–1174.
[37] I.C. Ho, J.H. Kim, J.W. Rooney, B.M. Spiegelman, L.H. Glimcher, A potential role for the nuclear factor of activated T cells family of transcriptional regulatory proteins in adipogenesis, Proc. Natl. Acad. Sci. U. S. A. 95 (1998) 15537–15541.
[38] A.B. Benedito, M. Lehtinen, R. Massol, U.G. Lopes, T. Kirchhausen, A. Rao, A. Bonni, The transcription factor NFAT3 mediates neuronal survival, J. Biol. Chem. 280 (2005) 2818–2825.
[39] K.C. Bradley, R.D. Groth, P.G. Mermelstein, Immunolocalization of NFATc4 in the adult mouse brain, J. Neurosci. Res. 82 (2005) 762–770.
[40] V.S. Seybold, L.G. Coicou, R.D. Groth, P.G. Mermelstein, Substance P initiates NFAT-dependent gene expression in spinal neurons, J. Neurochem. 97 (2006) 397–407.
[41] C. Luo, E. Burgeon, J.A. Carew, P.G. McCaffrey, T.M. Badalian, W.S. Lane, P.G. Hogan, A. Rao, Recombinant NFAT1 (NFATp) is regulated by calcineurin in T cells and mediates transcription of several cytokine genes, Mol. Cell. Biol. 16 (1996) 3955–3966.
[42] I.A. Graef, F. Chen, G.R. Crabtree, NFAT signaling in vertebrate development, Curr. Opin. Genet. Dev. 11 (2001) 505–512.
[43] S. Chuvpilo, M. Zimmer, A. Kerstan, J. Glockner, A. Avots, C. Escher, C. Fischer, I. Inashkina, E. Jankevics, F. Berberich-Siebelt, et al., Alternative polyadenylation events contribute to the induction of NF-ATc in effector T cells, Immunity 10 (1999) 261–269.
[44] X. Li, S.N. Ho, J. Luna, J. Giacalone, D.J. Thomas, L.A. Timmerman, G.R. Crabtree, U. Francke, Cloning and chromosomal localization of the human and murine genes for the T-cell transcription factors NFATc and NFATp, Cytogenet. Cell Genet. 68 (1995) 185–191.
[45] S. Pan, N. Koyano-Nakagawa, L. Tsuruta, Y. Amasaki, T. Yokota, S. Mori, N. Arai, K. Arai, Molecular cloning and functional characterization of murine cDNA encoding transcription factor NFATc, Biochem. Biophys. Res. Commun. 240 (1997) 314–323.
[46] D.L. Weiss, J. Hural, D. Tara, L.A. Timmerman, G. Henkel, M.A. Brown, Nuclear factor of activated T cells is associated with a mast cell interleukin 4 transcription complex, Mol. Cell. Biol. 16 (1996) 228–235.
[47] I.A. Graef, F. Wang, F. Charron, L. Chen, J. Neilson, M. Tessier-Lavigne, G.R. Crabtree, Neurotrophins and netrins require calcineurin/NFAT signaling to stimulate outgrowth of embryonic axons, Cell 113 (2003) 657–670.
[48] J. Aramburu, J. Heitman, G.R. Crabtree, Calcineurin: a central controller of signalling in eukaryotes, EMBO Rep. 5 (2004) 343–348.
[49] M. Laverdiere, J. Beaudoin, A. Lavigueur, Species-specific regulation of alternative splicing in the C-terminal region of the p53 tumor suppressor gene, Nucleic Acids Res. 28 (2000) 1489–1497.
[50] R. Kimura, H. Yoshii, M. Nomura, N. Kotomura, T. Mukai, S. Ishihara, K. Ohba, T. Yanase, O. Gotoh, H. Nawata, et al., Identification of novel first exons in Ad4BP/SF-1 (NR5A1) gene and their tissue- and species-specific usage, Biochem. Biophys. Res. Commun. 278 (2000) 63–71.
[51] R.D. Groth, J.P. Weick, K.C. Bradley, J.I. Luoma, B. Aravamudan, J.R. Klug, M.J. Thomas, P.G. Mermelstein, D1 dopamine receptor activation of NFAT-mediated striatal gene expression, Eur. J. Neurosci. 27 (2008) 31–42.
[52] A.M. Ranger, M.J. Grusby, M.R. Hodge, E.M. Gravallese, F.C. de la Brousse, T. Hoey, C. Mickanin, H.S. Baldwin, L.H. Glimcher, The transcription factor NF-ATc is essential for cardiac valve formation, Nature 392 (1998) 186–190.
[53] J.L. Belfield, C. Whittaker, M.Z. Cader, S. Chawla, Differential effects of Ca^{2+} and cAMP on transcription mediated by MEF2D and cAMP-response element-binding protein in hippocampal neurons, J. Biol. Chem. 281 (2006) 27724–27732.
[54] T. Timmusk, K. Palm, M. Metsis, T. Reintam, V. Paalme, M. Saarma, H. Persson, Multiple promoters direct tissue-specific expression of the rat BDNF gene, Neuron 10 (1993) 475–489.

PUBLICATION IV

Koppel I, Aid-Pavlidis T, Jaanson K, Sepp M, **Pruunsild P**[#], Palm K, Timmusk T. (2009)
Tissue-specific and neural activity-regulated expression of human *BDNF* gene in BAC transgenic mice.
BMC Neurosci. 2009 Jun 25;10:68

BMC Neuroscience

Research article

Tissue-specific and neural activity-regulated expression of human BDNF gene in BAC transgenic mice

Indrek Koppel†, Tamara Aid-Pavlidis†, Kaur Jaanson, Mari Sepp, Priit Pruunsild, Kaia Palm and Tõnis Timmusk*

Address: Department of Gene Technology, Tallinn University of Technology, Akadeemia tee 15, 12618 Tallinn, Estonia

Email: Indrek Koppel - indrek.koppel@ttu.ee; Tamara Aid-Pavlidis - tamara.aid@gmail.com; Kaur Jaanson - kaur.jaanson@ttu.ee; Mari Sepp - mari.sepp@ttu.ee; Priit Pruunsild - priit.pruunsild@ttu.ee; Kaia Palm - kaia@protobios.com; Tõnis Timmusk* - tonis.timmusk@ttu.ee

* Corresponding author †Equal contributors

Published: 25 June 2009

BMC Neuroscience 2009, **10**:68 doi:10.1186/1471-2202-10-68

Received: 28 January 2009
Accepted: 25 June 2009

This article is available from: http://www.biomedcentral.com/1471-2202/10/68

Abstract

Background: Brain-derived neurotrophic factor (BDNF) is a small secreted protein that has important roles in the developing and adult nervous system. Altered expression or changes in the regulation of the BDNF gene have been implicated in a variety of human nervous system disorders. Although regulation of the rodent BDNF gene has been extensively investigated, *in vivo* studies regarding the human BDNF gene are largely limited to postmortem analysis. Bacterial artificial chromosome (BAC) transgenic mice harboring the human BDNF gene and its regulatory flanking sequences constitute a useful tool for studying human BDNF gene regulation and for identification of therapeutic compounds modulating BDNF expression.

Results: In this study we have generated and analyzed BAC transgenic mice carrying 168 kb of the human BDNF locus modified such that BDNF coding sequence was replaced with the sequence of a fusion protein consisting of N-terminal BDNF and the enhanced green fluorescent protein (EGFP). The human BDNF-BAC construct containing all BDNF 5' exons preceded by different promoters recapitulated the expression of endogenous BDNF mRNA in the brain and several non-neural tissues of transgenic mice. All different 5' exon-specific BDNF-EGFP alternative transcripts were expressed from the transgenic human BDNF-BAC construct, resembling the expression of endogenous BDNF. Furthermore, BDNF-EGFP mRNA was induced upon treatment with kainic acid in a promotor-specific manner, similarly to that of the endogenous mouse BDNF mRNA.

Conclusion: Genomic region covering 67 kb of human BDNF gene, 84 kb of upstream and 17 kb of downstream sequences is sufficient to drive tissue-specific and kainic acid-induced expression of the reporter gene in transgenic mice. The pattern of expression of the transgene is highly similar to BDNF gene expression in mouse and human. This is the first study to show that human BDNF gene is regulated by neural activity.

Background

Brain-derived neurotrophic factor (BDNF) [1], a member of the neurotrophin family, promotes survival and differentiation of several neuronal populations during mammalian development [2,3]. In the adult central nervous system, BDNF acts as a regulator of activity-dependent

neurotransmission and plasticity [4] and promotes survival of newborn hippocampal neurons [5]. BDNF has widespread expression in the developing and adult mammalian nervous system, its mRNA and protein levels rising dramatically in postnatal development [6-10]. In the adult, BDNF is also expressed in a number of non-neural tissues, with the highest levels of BDNF mRNA detected in thymus, heart and lung [11,12].

BDNF gene has a complex structure with multiple untranslated 5' exons alternatively spliced to one protein-coding 3' exon. The rat BDNF gene structure initially described to contain five exons [13] has been recently updated with a number of newly discovered exons for rodent [14,15] and human [16,17] BDNF. Untranslated 5' exons are linked with differentially regulated promoters directing tissue-specific expression of BDNF [13-17]. Furthermore, recently discovered BDNF antisense transcripts in human may exert additional control over BDNF transcription [16,17]. BDNF is a neural activity-dependent gene in rodents: various physiological stimuli induce its expression in neurons through excitatory neurotransmission-triggered calcium influx [18,19]. However, no data is available about activity-dependent transcription of the human BDNF gene in neurons, except one report showing that dopamine signaling increases the levels of BDNF exon IV transcripts in neuronally differentiated human embryonic teratocarcinoma NT2 cells [20].

Alterations in BDNF function have been associated with a variety of disorders of the nervous system [2]. As therapies modulating neurotrophic activity are being actively sought [21], it is of great importance to create model systems for studying the regulation of BDNF gene. BAC transgenic mice have proven useful in studying gene regulation as a) BAC clones are often long enough to contain all necessary DNA elements to recapitulate the expression patterns of endogenous genes independent of host genomic sequences flanking the transgene integration site and b) they can be easily modified with homologous recombination in *E. coli*, e.g. to introduce reporter genes under the control of promoters of interest [22]. BAC transgenes with EGFP reporter gene have been used for characterization of expression and regulatory regions of several neural genes [23-25]. Transgenic mice have been generated previously to study BDNF gene regulation *in vivo* [26,27]. Mouse lines carrying rat BDNF sequences of 10 kb range recapitulated BDNF expression only partially, suggesting that *cis*-acting regulatory elements necessary for accurate control of BDNF expression are located further away [26]. Recently, YAC-BDNF transgenic mice carrying 145 kb of human BDNF locus with BDNF coding sequence substituted for the EGFP reporter gene have been reported [27].

In this study we have generated BAC transgenic mice carrying human BDNF-EGFP fusion (hBDNF-EGFP) reporter gene under the control of 168 kb of human BDNF genomic sequences. C-terminal addition of EGFP to BDNF protein has been shown not to affect BDNF cellular localization, secretion and activation of its receptor TrkB in cultured neurons [28-30]. Therefore, to enable studying subcellular localization of the hBDNF-EGFP fusion protein *in vivo*, we specifically produced this fusion reporter gene construct. The aims of the study were to investigate a) expression of hBDNF-EGFP mRNA and protein in the brain and non-neural tissues and b) activity-dependent regulation of the hBDNF-EGFP transgene in the brain of the BAC transgenic mice.

Results

Generation of transgenic mice with 169 kb hBDNF-EGFP-BAC

A 168 kb BAC clone extending 84 kb upstream and 17 kb downstream of human BDNF gene was used to generate human BDNF-EGFP reporter transgenic mice (see Materials and Methods and Figure 1A–C). Briefly, EGFP reporter gene was inserted in-frame with BDNF coding region replacing the BDNF stop codon (Figure 1C). Resulting hBDNF-EGFP fusion protein was expected to mimic subcellular localization of endogenous BDNF, allowing fine resolution of transgene expression. hBDNF-EGFP-BAC construct was tested for integrity using PCR and restriction analysis (data not shown). Transgenic mice were generated by pronuclear injection, yielding four transgenic founders (A4, E1, E4 and C3). All founders contained one to two transgene copies as estimated by slot-blot hybridization (Figure 1D). PCR analysis of C3 genomic DNA and sequencing of the PCR products revealed tandem integration of two transgene copies and confirmed the intactness of 5' and 3' end sequences of the integrated transgene (Figure 1E). Offspring was obtained from three founders and bred for several generations to generate transgenic mouse lines E1, E4 and C3.

Expression of hBDNF-EGFP in transgenic mouse tissues

From three transgenic founder lines, C3 line showed pattern of expression of hBDNF-EGFP mRNAs that was highly similar to the expression of mouse endogenous BDNF (mBDNF) mRNA (Figure 2A). RT-PCR analysis revealed relatively high transgene expression in all brain regions of C3 mice, including cerebral cortex, hippocampus, striatum, thalamus, hypothalamus, midbrain, pons, medulla and cerebellum. In non-neural tissues, high levels of transgene mRNA were detected in testis, moderate levels in thymus and lung and low levels in skeletal muscle. BDNF mRNA is endogenously expressed in all these tissues both in mouse and human [14,16]; (Figure 2A). However, dissimilarly from mouse endogenous BDNF mRNA, hBDNF-EGFP mRNA was not detected in heart and kidney, where relatively high levels of mBDNF mRNA were detected. Low expression of hBDNF-EGFP transgene in the mouse kidney correlates with the finding that BDNF is expressed at low levels in human kidney [8,16].

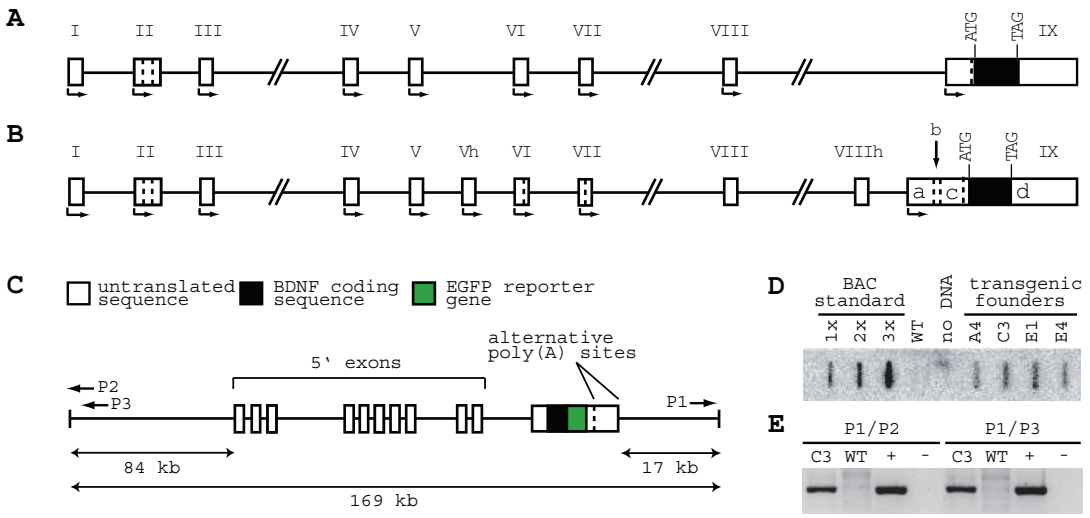

Figure 1

Schematic drawings of rodent and human BDNF genes and the BAC transgenic construct used in this study. Rodent (**A**) and human (**B**) BDNF gene structures. Rodent BDNF gene consists of a number of 5' exons (I-VIII) spliced together with a common protein-coding sequence in exon IX (transcriptional start sites are indicated with arrows). BDNF transcription can also start from exon IX introducing a unique 5' UTR sequence. Hatched lines indicate sites of alternative splicing. Although the human BDNF gene has a similar structure and splicing pattern, it has additional exons Vh and VIIIh, longer and more complexly spliced 5'UTR of exon IX. Furthermore, human BDNF exons VIII and VIIIh are not used as 5'exons, but are always spliced with exon V. For detailed description see [14,16]. (**C**) Schematic drawing of the modified BAC construct used in this study containing the human BDNF locus. EGFP reporter gene was inserted in-frame with the BDNF coding region before the BDNF stop codon creating a fused BDNF-EGFP open reading frame within 168 kb of human BDNF locus. Arrows P1-3 indicate PCR primers used for analysis of transgene integration. (**D**) Slot-blot hybridization analysis of transgene copy number in hBDNF-EGFP transgenic founder mice (A4, C3, E1 and E4). BAC standard contains hBDNF-EGFP-BAC DNA in amounts equivalent to 1–3 copies of transgene in the blotted genomic DNA. WT- wild type mouse DNA. (**E**) PCR analysis of genomic DNA from transgenic mouse line C3 with primers detecting tandem integration of hBDNF-EGFP-BAC constructs. WT – wild type mouse DNA as a negative control; (+) – circular hBDNF-EGFP-BAC DNA as a positive control; (-) – PCR without DNA as a negative control.

In E1 mice, transgene expression recapitulated that of the endogenous BDNF mRNA in thymus, lung, kidney and testis, but not in other non-neural tissues that express BDNF. In the adult brain of E1 mice, transgene mRNA expression was detected in midbrain, cerebellum, pons and medulla at levels that were lower than in the respective brain regions of C3 mice. In E4 line, hBDNF-EGFP mRNA was detected only in testis and thymus (Figure 2A).

Expression of transgenic hBDNF-EGFP mRNA was further examined in different brain regions of C3 mice since this line largely recapitulated endogenous BDNF expression and expressed the transgene at the highest levels. Quantification of hBDNF-EGFP transcripts in C3 hippocampus and cortex using ribonuclease protection assay (RPA) revealed that transgene mRNA levels were about tenfold lower than endogenous mBDNF mRNA levels (Figure 2B). Analysis of transcription from the alternative human BDNF promoters in C3 mice confirmed the expression of all transcripts with different 5' exons described to date (exons I-IXe) both in hippocampus (Figure 2C) and cerebral cortex (data not shown).

In situ hybridization of C3 mice adult brain sections revealed hBDNF-EGFP mRNA expression in the hippocampus, particularly in the pyramidal neurons of CA1 and CA3 regions and in the polymorphic neurons in the hilus of the dentate gyrus, and also in several cortical areas, including neurons of frontal, sensorimotor and piriform cortex (Figure 3, 4). Endogenous mBDNF mRNA was detected in all brain areas where hBDNF-EGFP mRNA labeling was observed. However, hBDNF-EGFP labeling was absent or below the detection limit of our *in situ* hybridization assay in several areas expressing mBDNF mRNA, e.g. claustrum, amygdala, thalamic, hypothalamic and pontine nuclei. Furthermore, *in situ* hybridization

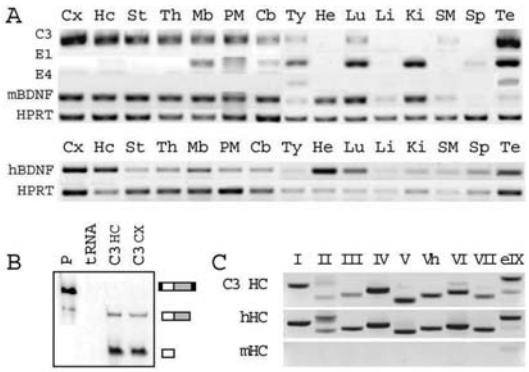

Figure 2
hBDNF-EGFP mRNA expression in tissues of three transgenic mouse lines. (**A**) RT-PCR analysis of hBDNF-EGFP mRNA expression in tissues of three transgenic BAC mouse lines – C3, E1, E4. mBDNF – mouse BDNF; hBDNF – human BDNF in human tissues; HPRT – reference gene hypoxanthine phosphoribosyltransferase. *Cx* – cortex; *Hc* – hippocampus; *St* – striatum; *Th* – thalamus; *Mb* – midbrain; *PM* – pons/medulla; *Cb* – cerebellum; *Ty* – thymus; *He* – heart; *Lu* – lung; *Li* – liver; *Ki* – kidney; *SM* – skeletal muscle; *Sp* – spleen; *Te* – testis. (**B**) Analysis of hBDNF-EGFP mRNA expression levels in C3 mouse brain by RNase protection assay. hBDNF-EGFP probe was used to determine both transgenic and endogenous BDNF mRNA levels as protein coding sequences of mouse and human BDNF share a high degree of similarity. *P* – probe without RNase; *tRNA* – yeast tRNA; *HC* – hippocampus; *CX* – cortex. On the right, black boxes denote vector-derived sequences, white boxes BDNF and gray boxes EGFP sequences. (**C**) Expression of alternative hBDNF-EGFP transcripts in C3 mouse hippocampus (HC), analyzed by RT-PCR. PCR primers used were specific for human BDNF transcripts as shown by control reactions with human (hHC) and mouse (mHC) hippocampal cDNA. eIX – transcript containing 5'-extended exon IX.

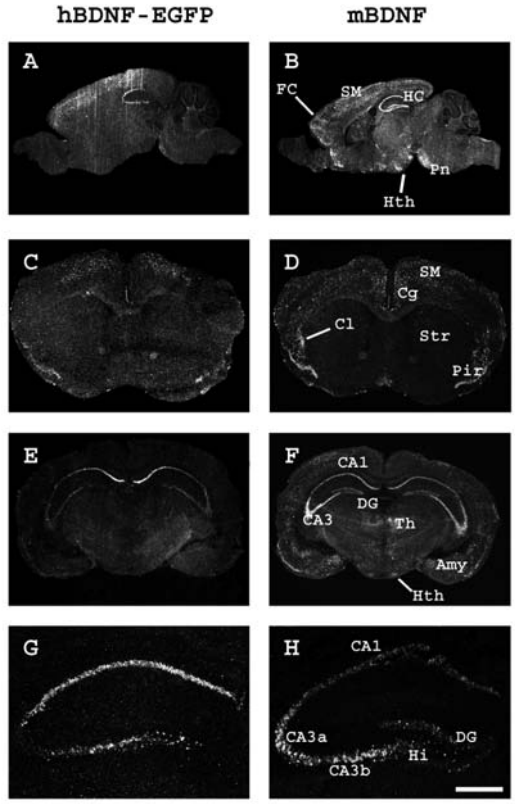

Figure 3
Overlapping patterns of BAC-driven hBDNF-EGFP and mBDNF mRNA expression in C3 mouse brain. *In situ* hybridization analysis, photoemulsion autoradiographs of 16 μm sagittal (**A**,**B**) and coronal (**C**-**H**) sections. (**C**) and (**D**) are sections taken at striatal level; (**E**) and (**F**) are sections taken at posterior hippocampal levels; (**G**) and (**H**) show enlarged hippocampal area (scale bar: 0,5 mm). *FC* – frontal cortex;*SM* – sensorimotor cortex; *HC* – hippocampus; *Pn* – pontine nuclei; *Hth* – hypothalamus; *Cg* – cingulate cortex; *Pir* – piriform cortex; *Cl* – claustrum; *Str* – striatum; *CA1*, *CA3* – hippocampal subfields; *DG* – dentate gyrus of hippocampus; *Hi* – hilar area of dentate gyrus; *Th* – thalamus; *Amy* – amygdala.

showed differential expression of hBDNF and mBDNF in cortical and hippocampal subfields. While mBDNF mRNA was expressed at high levels throughout the cerebral cortex, hBDNF-EGFP labeling was more prominent in the frontal cortex and in the sensorimotor area extending along the longitudinal fissure (Figure 3C, D and Figure 4K–N). In the hippocampus, hBDNF-EGFP labeling was observed over the CA1 and hilar subfields and part of the CA3 subfield (CA3b in Figure 3G, H and Figure 4C, D), mimicking the pattern of expression of endogenous mBDNF mRNA. On the other hand, hBDNF-EGFP mRNA was expressed at considerably lower levels in the part of CA3 subfield that showed high levels of mBDNF mRNA expression (CA3a in Figure 3G, H and Figure 4E, F). In addition, no hBDNF-EGFP labeling was detected in the granule neurons of dentate gyrus where endogenous mBDNF mRNA was highly expressed (Figure 3G, H and Figure 4I, J).

Since the BDNF gene in the transgenic construct was of human origin, we also analyzed the expression of BDNF in the human hippocampus using *in situ* hybridization. In agreement with earlier findings [31,32], our results showed that the highest levels of hBDNF mRNA were

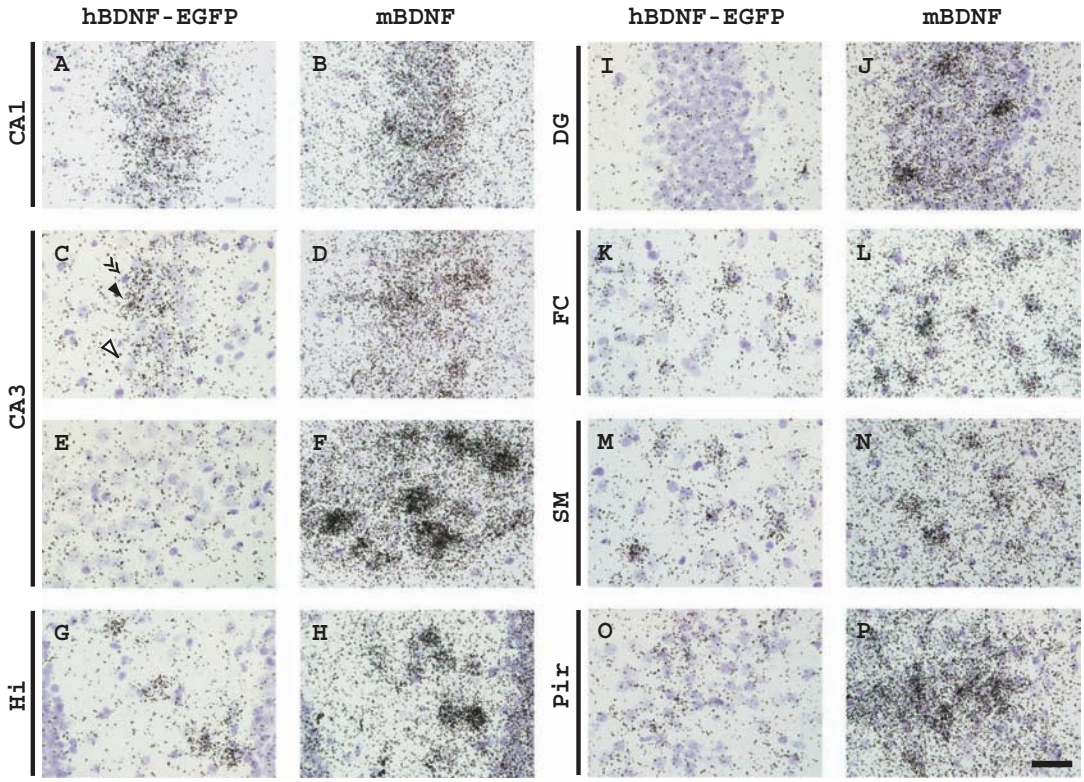

Figure 4
Cellular expression of hBDNF-EGFP mRNA in adult C3 mouse brain. *In situ* hybridization analysis, shown are bright-field autoradiographs of emulsion-dipped sections. Hybridization probes are indicated above the columns. Filled arrowhead indicates a neuron with strong labeling, empty arrowhead indicates a neuron with weak or absent labeling and double arrowheads indicate a glial cell showing no labeling. *CA1*, *CA3* – hippocampal subfields; *DG* – dentate gyrus of hippocampus; *Hi* – hilar area of dentate gyrus; *FC* – frontal cortex; *SM* – sensorimotor cortex; *Pir* – piriform cortex. Scale bar: 20 μm.

present in the granule cells of dentate gyrus, whereas other hippocampal regions showed relatively weaker expression (Figure 5). However, strong hBDNF labeling was detected over majority of CA3 and CA1 neurons using high magnification (Figure 5B, C), indicating that these areas show much weaker signal in the dark-field image partly because of the scarcity of neuronal cell bodies in the CA1 and CA3 subfields of the human hippocampus.

Next we examined expression of hBDNF-EGFP fusion protein across tissues in C3 mice. No EGFP fluorescence was observed in brain sections or cultured primary embryonic (E18) hippocampal neurons. In addition, hBDNF-EGFP protein was not detected in the hippocampus, cortex and testis by Western blot analysis with anti-EGFP or anti-BDNF antibodies (data not shown). hBDNF-EGFP open reading frame in C3 genomic DNA was analyzed for possible mutations by sequencing and was found to be intact. Together with mRNA expression data these results suggest that hBDNF-EGFP protein was either not translated in the brain and testis of C3 mice or was expressed at levels below the detection limits of our methods.

Kainic acid induces hBDNF-EGFP mRNA expression in transgenic mouse brain

Kainic acid (KA), agonist of the KA subtype ionotropic glutamate receptor, has been shown to induce BDNF mRNA levels in adult rodent hippocampus and cerebral cortex [13,19,33,34]. KA induction of transgenic hBDNF-EGFP transcripts in the hippocampus and cerebral cortex of C3 mice largely followed the induction pattern of endogenous mBDNF transcripts (Figure 6A). KA markedly

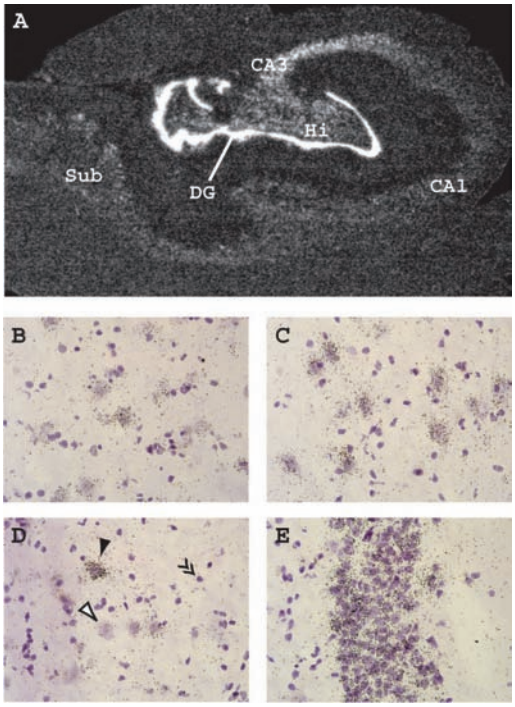

Figure 5
Expression of BDNF mRNA in the human hippocampus. (**A**) *In situ* hybridization autoradiograph of a 16 μm coronal section.*DG* – granular layer of dentate gyrus; *Hi* – hilar area of dentate gyrus; *Sub* – subiculum; *CA1*, *CA3* – hippocampal subfields. (**B-E**) High magnification bright-field photomicrographs of hematoxylin-counterstained neurons in subfields CA1 (**B**) and CA3 (**C**), the hilus (**D**) and granular layer of dentate gyrus (**E**). Filled arrowhead indicates a neuron with strong labeling, empty arrowhead indicates a neuron with weak or absent labeling and double arrowheads indicate a glial cell showing no labeling.

upregulated both endogenous mouse and transgenic hBDNF-EGFP transcripts containing exons I, IV and 5'-extended exon IX (eIX) in the hippocampus and cortex. hBDNF-EGFP and mBDNF mRNAs containing other 5' exons were induced to a lesser extent. Of note, recently described human-specific exon Vh-containing transcripts were not induced by KA in transgenic mice in the context of 169 kb hBDNF-EGFP BAC construct (Figure 6A).

Levels of BDNF transcripts showing the most robust induction by kainic acid were analyzed further using quantitative real-time RT-PCR analysis (Figure 6B). Transgenic hBDNF-EGFP exon I, exon IV and 5'-extended exon

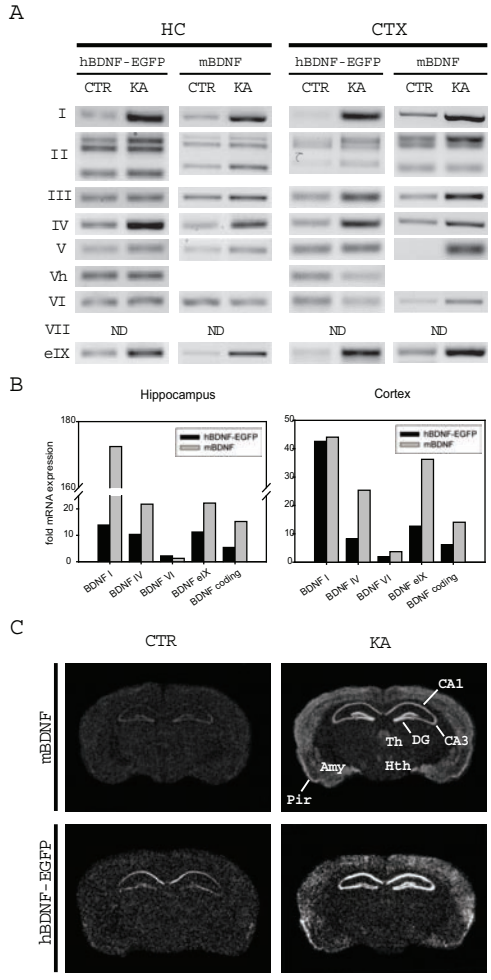

Figure 6
Kainic acid (30 mg/kg) induces transgenic hBDNF-EGFP mRNA expression in brains of C3 line transgenic mice. (**A**) Induction of alternatively spliced hBDNF-EGFP transcripts in C3 mouse hippocampus (HC) and cerebral cortex (CTX), analyzed with RT-PCR. mBDNF – mouse transcripts; ND – not determined; KA – kainic acid treated mice; CTR – control mice. Three BDNF-II bands correspond to alternatively spliced transcripts. (**B**) Quantitative real-time RT-PCR analysis of selected BDNF transcripts, normalized to HPRT1 levels and expressed as fold difference relative to mRNA levels in untreated mice. (**C**) *In situ* hybridization autoradiographs of C3 mouse coronal brain sections. *Pir* – piriform cortex; *CA1*, *CA3* – hippocampal subfields; *DG* – dentate gyrus of hippocampus; *Hi* – hilar area of dentate gyrus; *Th* – thalamus; *Hth* – hypothalamus; *Amy* – amygdala.

IX transcripts, and total hBDNF-EGFP mRNA were potently induced in both hippocampus and cortex following 3 hours of kainate treatment, similarly to respective endogenous mBDNF mRNAs. Exon VI-containing hBDNF-EGFP and endogenous mBDNF transcripts showed no induction, which is consistent with previous findings [13,14,33].

In situ hybidization analysis showed marked induction of transgenic hBDNF-EGFP mRNA by KA in the pyramidal neurons of CA1-CA3 layers, in the hilar region of hippocampus and also in the layers II – VI of cerebral cortex (Figure 6C). Importantly, kainic acid induced transgene expression also in the granular layer of dentate gyrus of hippocampus, whereas control animals did not show any detectable expression in this area. Endogenous mBDNF was induced in the same neuronal populations, suggesting that the 169 kb hBDNF-EGFP BAC construct contains all the regulatory elements that mediate kainic acid induction. We also examined expression of the hBDNF-EGFP protein in the brains of kainic acid treated C3 mice by direct EGFP fluorescence and Western blot analysis but no fusion protein was detected (data not shown).

Discussion

In this study, BAC transgenic mice carrying 168 kb of the human BDNF locus and encoding human BDNF-EGFP fusion protein were generated and analyzed. Out of three analyzed founder lines, one line (C3) largely recapitulated human BDNF mRNA expression in the brain, thymus, lung, skeletal muscle and testis. Founder line E1 mimicked human BDNF mRNA expression in some brain regions, and also in thymus, lung and kidney. Founder line E4 expressed transgene only in the thymus and testis. These results showed that although all three founder lines expressed hBDNF-EGFP mRNA at different levels, the 169 kb BAC construct, carrying 67 kb of human BDNF gene, 84 kb of 5' and 17 kb of 3' sequences, contains regulatory elements necessary for hBDNF mRNA expression in many brain regions and non-neural tissues. However, integration site-dependent expression of transgene in different founder lines suggests that the BAC construct may not contain necessary insulator elements to protect it from the influence of genomic regions flanking the transgene integration site. It has been shown for many genes that insulators can functionally isolate neighboring genes and block their interactions [35].

In several non-neural tissues, the 169 kb hBDNF-EGFP BAC recapitulated endogenous expression of both mouse and human BDNF. Transgenic mRNA was expressed in the thymus and testis in three mouse lines, expression in the lung was seen in two lines and only one line expressed hBDNF-EGFP in the kidney and skeletal muscle. All these tissues have been shown to express BDNF both in mouse and human [7,14,16]. Of note, all three founder lines expressed relatively high levels of hBDNF-EGFP in adult testis, in contrast to the very low expression levels of endogenous mBDNF in the testis. This transgene expression pattern can be explained by human origin of the BDNF gene as relatively high levels of BDNF mRNA, comparable to the levels in the brain, have been detected in the human testis [16]. In the adult human testis, expression of BDNF and its receptor TrkB has been reported in Leydig, Sertoli and germ cells [36], while in the adult mouse testis, BDNF expression has been detected in Sertoli cells and expression of its receptor TrkB in germ cells [37]. These findings indicate differences in BDNF expression between human and mouse and are further supported by the present study. On the other hand, none of the founder lines expressed hBDNF mRNA in the heart, a tissue with high levels of BDNF expression both in human and rodents [8,11,12,14]. This suggests that distinct heart-specific regulatory elements are located outside of the genomic DNA fragment that was included in the BAC construct.

Detailed analysis of hBDNF-EGFP expression in the C3 mouse brain by *in situ* hybridization showed that the transgene mimicked mBDNF expression in many neuron populations, including neurons of the CA1-CA3 and hilar regions of the hippocampus and the cerebral cortex. However, hBDNF-EGFP failed to recapitulate endogenous BDNF expression in several neuron populations, including the granule cells of dentate gyrus of hippocampus where BDNF mRNA is expressed both in human and rodents. hBDNF-EGFP expression was detected in all analyzed brain regions by RT-PCR, but not by *in situ* hybridization, indicating that transgene mRNA levels in several brain structures were below the detection limit of our *in situ* hybridization analysis.

BDNF transcription is regulated by neuronal activity through calcium-mediated pathways [18,38]. Systemic treatment of rodents with kainic acid (KA) has been used to model activity-dependent induction of BDNF mRNA in the nervous system [13,19,33,34]. Here we show that KA differentially induced alternative hBDNF-EGFP transcripts in the cortex and hippocampus (for comparison with mouse and rat see Table 1). Pronounced induction of transgenic hBDNF-EGFP transcripts containing exons I, IV, and 5'-extended exon IX (eIX), moderate induction of transcripts containing exons II, III and absence of induction of transcripts containing exon VI is consistent with the induction pattern of respective BDNF mRNAs in mouse and rat [13,14,33]. To our knowledge, this is the first time to report neural activity-dependent regulation of the human BDNF gene *in vivo*. Real-time PCR showed that total transgenic mRNA, as well as transcripts containing exons I, IV and 5'-extended exon IX were induced to a

lesser extent than the respective endogenous mBDNF mRNAs. This is consistent with earlier results reported for shorter rat BDNF transgenes [26] and could be caused by increased stability of transgenic BDNF-reporter mRNAs as compared to the mouse endogenous BDNF mRNAs. Alternatively, the absence of important regulatory elements in the transgenic construct may underlie the reduced induction of the transgene by kainic acid. *In situ* hybridization analysis of KA-treated C3 mouse brains showed induction of hBDNF-EGFP mRNAs in several neuronal populations where endogenous BDNF mRNA levels were also increased. These results show that, similarly to rodent BDNF, expression of the human BDNF gene is induced by neural activity and that regulatory elements mediating the induction are included in the 168 kb of the human BDNF locus contained in the BAC transgene. Several regulatory elements located in the rat BDNF proximal promoter IV and the transcription factors mediating activity-dependent activation of this promoter have previously been characterized [39]. Among these elements, CRE (cAMP-response element) was found to be the most important for Ca^{2+}-mediated activation of rodent BDNF promoter IV [40-42]. However, the respective regulatory elements and transcription factors responsible for the activity-dependent regulation of the human BDNF gene have not been characterized. Transgenic mice described here can be used to study the regulation of human BDNF gene *in vivo* using a variety of methods successfully applied in the studies of rodent BDNF [39].

Table 1: Regulation of human, mouse and rat BDNF exon-specific mRNAs by kainic acid in the hippocampus and cerebral cortex.

	human[1]		mouse[2]		rat[3]
exon	HC	CTX	HC	CTX	HC
I	**	**	**	**	**
II	*	*	*	*	*
III	*-	*	*	*	-
IV	**	**	**	**	**
V	*	*	*	**	**
Vh	-	-	X	X	X
VI	-	-	-	-	-
VII	ND	ND	ND	ND	**
VIII	X	X	ND	ND	*
eIX	**	**	**	**	**

- no induction; * weak induction; ** strong induction; ND – not determined; X – transcript containing this exon as the 5' exon does not exist in this organism; [1,2] based on data from the present study; [3] based on data from [14]; HC – hippocampus; CTX – cerebral cortex.

Previously, transgenic mice carrying shorter fragments of the BDNF locus have been generated and characterized [26,27]. Mice expressing the CAT reporter gene under the control of 9 kb of rat BDNF genomic sequences covering promoters I-III or promoters IV-VI showed relatively high CAT activity in most tissues and brain regions expressing endogenous BDNF mRNA. *In situ* hybridization analysis showed that these constructs carrying either BDNF promoters I-III or IV-VI were able to drive CAT mRNA expression in adult rat brain in a pattern largely overlapping with mouse BDNF mRNA expression. Nevertheless, recapitulation of endogenous BDNF expression had a number of shortcomings in these transgenes: both constructs were not expressed or were expressed at low levels in the dentate granule cells and granule cells of cerebellum; BDNF IV-VI did not mimic BDNF expression in the heart; both constructs displayed relatively high reporter activity in the striatum where rat BDNF is virtually not expressed [43]. It was assumed that these transgenic constructs lacked important regulatory elements, which could be present in a much longer gene fragment than the BAC clone used here. Although BAC transgenic mouse lines generated in this study showed improved recapitulation of expression as compared to that of the BDNF-CAT transgenic mice [26], we could not detect transgene expression in several tissues and neuron populations that express endogenous BDNF mRNA.

A recent study reported generation of human BDNF-EGFP transgenic mice using a 145 kb YAC clone including 45 kb of 5' and 33 kb of 3' flanking sequences of hBDNF gene with the protein coding sequence partially replaced with EGFP reporter gene [27]. Three out of five transgenic founder lines obtained in that study expressed transgenic mRNA in the brain and only one of these showed expression of transgenic hBDNF transcripts containing exons IV and VI in the heart. Out of three lines analyzed, EGFP fluorescence was detected in the brain of only one line, specifically in the claustrum, intermediate layer of parietal cortex, pyramidal cell layer of CA3 hippocampal subfield and a population of neurons in the granule cell layer of the dentate gyrus. However, EGFP fluorescence was not detected in other cortical neuron populations and in the CA1 region of hippocampus where rodent and also human BDNF mRNA are expressed [27]. Differences in the tissue- and neuron-specific expression of transgenic hBDNF-EGFP mRNA and protein between the study by Guillemot et al. [27] and this study can be explained with different lengths of the BDNF gene-flanking genomic regions in the transgenic constructs used: the hBDNF-BAC

Table 2: PCR primers used in this study

Primer/application	Sequence
BAC modification	
hBDNFcod_rpsL_neo_s	5' GGATAGACACTTCTTGTGTATGTACATTGACCATTAAA AGGGGAAGATAGGGCCTGGTGATGATGGCGGGATCG 3'
hBDNF_rpsL_neo_as	5'AATAGATAATTTTTGTCTCAATATAATCTAATCTATACAACATAAATCCATCAGAAGAACTCGTCAA GAAGG 3'
hBDNFcod_linker_EGFP_s	5' TAAGGATAGACACTTCTTGTGTATGTACATTGACCAT TAAAAGGGGAAGACGGGATCCACCGGTCGCCACCATGGTGAGCAAGGGCGAGGAGCTG 3'
hBDNF_EGFP_as	5' AATAGATAATTTTTGTCTCAATATAATCTAATCTATAC AACATAAATCCATTACTTGTACAGCTCGTCCATGCCGA 3'
genotyping/slot-blot hybridization/expression analysis	
hBDNF_s	GTACGTGCGGGCCCTTACCATGGATAGC
EGFP_as	TGGTGCAGATGAACTTCAGGGTCAGC
expression analysis	
mBDNF_s	GTATGTTCGGGCCCTTACTATGGATAGC
mBDNF_as	AAGTTGTGCGCAAATGACTGTTTC
HPRT1_s	CTTTGCTGACCTGCTGGATTAC
HPRT1_as	GTCCTTTTCACCAGCAAGCTTG
hBDNF_I_s	GATGCCAGTTGCTTTGTCTTCTGTAG
hBDNF_II_s	GGGCGATAGGAGTCCATTCAGCACC
hBDNF_III_s	AGTTTCGGGCGCTGGCTTAGAG
hBDNF_IV_s	GCTGCAGAACAGAAGGAGTACA
hBDNF_V_s	TCGCGTTCGCAAGCTCCGTAGTG
hBDNF_Vh_s	GGCTGGAACACCCCTCGAA
hBDNF_VI_s	GGCTTTAATGAGACACCCACCGC
hBDNF_VII_s	GAACTGAAAGGGTCTGCGACACTCT
hBDNF_IXb_s	GCTGCTAAAGTGGGAAGAAGG
hBDNF_IX_as1	GTCCTCATCCAACAGCTCTTCTATC
hBDNF_IX_as2 (with VII_s)	GAAGTGTACAAGTCCGCGTCCTTA
expression analyis (qPCR)	
EGFPq_s	CAGAAGAACGGCATCAAGGTG

Table 2: PCR primers used in this study *(Continued)*

EGFPq_as	TGGGTGCTCAGGTAGTGGTTG
hBDNFq_I_s	CAGCATCTGTTGGGGAGACGAGA
hBDNFq_IV_s	GAAGTCTTTCCCGGAGCAGCT
hBDNFq_VI_s	ATCGGAACCACGATGTGACT
hBDNFq_IXc_s	AACCTTGACCCTGCAGAATGGCCT
hBDNFq_IX_as1 (with I, IV_s)	ATGGGGGCAGCCTTCATGCA
hBDNFq_IX_as2 (with VI_s)	ACCTTGTCCTCGGATGTTTG
hBDNFq_IX_as3 (with IXc_s)	GATGGTCATCACTCTTCTCACCT
mBDNFq_I_s	TTGAAGCTTTGCGGATATTGCG
mBDNFq_IV_s	GAAATATATAGTAAGAGTCTAGAACCTTG
mBDNFq_VI_s	GCTTTGTGTGGACCCTGAGTTC
mBDNFq_IXa_s	GGACTATGCTGCTGACTTGAAAGGA
mBDNFq_IX_as1 (with I, IV, VIs)	AAGTTGCCTTGTCCGTGGAC
mBDNFq_IX_as2 (with IXa_s)	GAGTAAACGGTTTCTAAGCAAGTG
mBDNFq_coding_s	GGCCCAACGAAGAAAACCAT
mBDNFq_coding_s	AGCATCACCCGGGAAGTGT
HPRT1q_s	CAGTCCCAGCGTCGTGATTA
HPRT1q_as	AGCAAGTCTTTCAGTCCTGTC
transgene integrity	
pBACe3.6_SP6 (5'end)	TATTTAGGTGACACTATAG
rp11_5'_as (5'end)	GGACAACAGACCCAAGGAGA
rp11_3'_s (3'end)	GTAGGGTGTCTGGGTTGGTG
pBACe3.6_T7 (3'end)	TAATACGACTCACTATAGGG
transgene tandem integration	
rp11_3'_s (P1)	GTAGGGTGTCTGGGTTGGTG
pBACe_11326_s (P2)	CGGTTACGGTTGAGTAATAAATGGATG
pBACe_11365_s (P3)	GGGGCACATTTCATTACCTCTTTCTC

used in the present study contained 39 kb longer 5' and 16 kb shorter 3' genomic regions of hBDNF gene than the reported hBDNF-YAC construct [27]. In addition, part of BDNF coding sequence had been replaced with EGFP reporter gene in the hBDNF-YAC transgene [27], possibly removing *cis*-elements with regulatory function. In contrast to the present study, hBDNF-YAC transgenic mRNA expression was not analyzed in different brain regions and expression of transgenic mRNAs containing exons III, V, Vh, VII and 5'-extended exon IX was not analyzed. More detailed comparison of hBDNF-EGFP expression in the two hBDNF transgenic mouse models would allow narrowing down genomic regions containing enhancer elements for tissue-specific expression of human BDNF. For example, on the basis of current data it can be hypothesized that a *cis*-element promoting heart-specific expression of hBDNF mRNA is located within the 3' terminal 16 kb of hBDNF-YAC construct (17–33 kb downstream of the hBDNF gene; chr11:27,600,000–27,616,000; UCSC Genome Browser, Mar 2006 Assembly). Recently, a BDNF regulatory locus has been discovered 850 kb upstream of the human and mouse BDNF genes that causes obesity, cognitive impairment and hyperactivity when disrupted [44,45]. Therefore, it is possible that in addition to regulatory elements included in the hBDNF-BAC of this study and the hBDNF-YAC described before [27], others can be found hundreds of kilobases away from the BDNF gene.

EGFP reporter gene has been successfully used to visualize BAC-driven expression of neural genes in a number of studies [23-25]. In the BAC construct that was used to generate transgenic mice in the present study, EGFP reporter gene was fused C-terminally with the human BDNF coding sequence to allow detailed characterization of human BDNF expression in the nervous system. Unfortunately, we could not detect EGFP protein in the brain of C3 mice neither with fluorescence microscopy nor with Western blot analysis. This could be explained with low levels of hBDNF-EGFP protein expressed in the C3 mouse brain as transgenic hBDNF-EGFP mRNA levels were about tenfold lower than these of endogenous BDNF. It is also possible that founder mice with higher levels of BDNF-EGFP expression died during embryonic development due to overactivation of BDNF receptor TrkB. This hypothesis is supported by a study showing that embryonic overexpression of BDNF from nestin promoter results in gross abnormalities in brain architecture and perinatal death [46]. Although the hBDNF-EGFP fusion protein can be expressed in cultured cells *in vitro* [28-30], it is conceivable that it is not translated or has poor translatability and/or stability when expressed in transgenic mice *in vivo*.

Conclusion

Human genomic region covering 67 kb of the BDNF gene, 84 kb of upstream and 17 kb of downstream sequences is able to drive tissue-specific and kainic acid-induced expression of reporter gene in transgenic mice that largely overlaps with BDNF gene expression and regulation in mouse and human. This is the first study to directly show that human BDNF gene is regulated by neural activity. The BDNF-BAC transgenic mice are useful for studying the transcription regulation of human BDNF gene *in vivo*. In addition, these mice could be used for screening therapeutic agents modulating human BDNF transcription.

Methods

Generation of transgenic mice

BAC clone (RP11-651M4) containing the human BDNF locus [GenBank:AC087446.13] was purchased from Chori BACPAC Resources (USA). Red®/ET® homologous recombination in *E. coli* (Counter-Selection BAC Modification Kit, Gene Bridges GmbH, Germany) was used to delete BDNF stop codon and to insert EGFP reporter gene with the linker sequence (CGG GAT CCA CCG GTC GCC ACC) into the 3' end of BDNF. For sequences of primers used for insert synthesis see Table 2. Modified BAC was tested for the absence of rearrangements using EcoRV restriction analysis and pulsed field gel electrophoresis. Integrity of the hBDNF-EGFP reading frame was confirmed by sequencing. In order to validate the reporter activity, BAC DNA was purified using the Large Construct Purification Kit (Qiagen, USA) and transfected into COS-7 cells using DEAE-dextran mediated transfection system [47]. Five days after transfection EGFP expression and distribution in COS-7 cells was visualized using fluorescence microscopy (Eclipse 80i upright microscope, Nikon).

hEGFP-BDNF BAC DNA was purified for microinjection by alkaline lysis and linearized with PI-SceI enzyme (NEB, USA). Restriction solution was separated in low-melt agarose gel (Fermentas, Lithuania) using CHEF-DR II Pulsed Field Electrophoresis System (Bio-Rad, USA). Linearized BAC DNA was excised from the gel and purified from agarose using Gelase enzyme (NEB, USA). Transgenic mice were generated by pronuclear injection of linearized hBDNF-EGFP-BAC into CBA × C57Bl/6 mouse pronuclei in the Karolinska Center for Transgene Technologies (Sweden). Founder mice carrying the BAC transgene were identified by PCR analysis of genomic DNA. Transgene copy number was analyzed by slot-blot hybridization of genomic DNA with a [α-^{32}P]dCTP-labeled probe generated with HexaLabel DNA Labeling Kit (Fermentas, Lithuania) using pEGFP-N1 (Clontech, USA) plasmid as a template. Genomic DNA of the C3 mouse founder line was analyzed by PCR for the presence of 5' and 3' ends of the linearized transgene. Tandem insertion of transgene into the C3 line genomic DNA was analyzed by PCR with primers pBACe_11326_s or pBACe_11365_s in combination with rp11_3'_s (see Table 2) and sequencing of the PCR product. All animal experiments were performed in

agreement with the local Ethical Committee of Animal Experimentation.

Cell culture, antibodies and animal experiments

African green monkey kidney fibroblast COS-7 cells were grown in DMEM with 10% fetal calf serum and antibiotics. Primary neuronal cultures from embryonic day 18 cerebral cortex were prepared as described [48]. For Western blots and immunohistochemistry the following antibodies were used: mouse anti-GFP monoclonal antibodies (Roche Applied Science), mouse anti-GFP monoclonal antibodies (Clontech, USA); rabbit anti-BDNF (Santa Cruz Biotechnology, USA). For kainic acid treatment, adult mice weighing 20–25 g were injected intraperitoneally with 30 mg/kg of kainic acid or 1× PBS. 3 hours later mice were decapitated, hippocampus and cortex dissected, frozen on dry ice and stored at -70°C. For *in situ* hybridization whole brains were embedded in Shandon Cryomatrix™ (Thermo Fisher Scientific, USA). Four kainic acid-treated C3 mice and two control mice were used for quantitative RT-PCR analysis of total hBDNF-EGFP mRNA expression in the cerebral cortex and hippocampus. Total hBDNF-EGFP mRNA was induced 2,5–6 fold in the hippocampus of kainic acid-treated C3 mice and the mouse displaying highest induction of hBDNF-EGFP and mBDNF mRNA was analyzed further with RT-PCR for expression of exon-specific transcripts. Five kainic acid-treated C3 mice and two control mice were used for *in situ* hybridization analysis and the mouse showing highest induction of hBDNF-EGFP and mBDNF mRNA was further analyzed in more detail.

RT-PCR

Total RNA was isolated from mouse and human tissues using TRI reagent (Ambion, USA). All experiments with human tissues were approved by the local Ethical Committee for Medical Research. Two mice from each transgenic line were analyzed for tissue-specific expression of hBDNF-EGFP mRNA in brain regions and non-neural tissues and they showed identical transgene expression pattern. RNA was treated with DNase (DNA-*free*, Ambion, USA) following manufacturer's instructions and five micrograms of total RNA was used for cDNA synthesis with oligo-dT primer (Microsynth, Switzerland) and SuperScript III reverse transcriptase (Invitrogen, USA). PCR amplification was carried out with HotFire DNA polymerase (Solis Biodyne, Estonia) according to the manufacturer's instructions. Quantitative real-time PCR was performed on a LightCycler 2.0 instrument (Roche Applied Science) using qPCR Core kit for SYBR® Green I No ROX (Eurogentec, Belgium). Melting curve analysis was carried out at the end of cycling to confirm amplification of a single PCR product. All qPCR reactions were performed in triplicate and normalized to hypoxanthin phosphoribosyltransferase 1 (HPRT1) mRNA levels.

Ribonuclease protection assay

For cRNA synthesis 624 bp BDNF-EGFP fragment containing 452 bp of BDNF, 21 bp linker sequence and 151 bp of EGFP sequence was amplified with PCR from modified BAC clone RP11-651M4 and cloned into pBluescript SK+ vector (Stratagene, USA). [α-^{32}P]UTP-labeled cRNA probe was *in vitro* transcribed from linearized plasmid template using MAXIscript Kit and T3 polymerase (Ambion, USA). 10 μg of total RNA and 2.5 ×10^5 CPM of radiolabeled probe were used for RPA hybridization and the assay was performed with the RPA III Kit from Ambion as suggested by the manufacturer. The protected fragments were separated in 4% acrylamid-urea gel and detected autoradiographically using BioRad Molecular Imager FX.

In situ hybridization

cRNA probe complementary to the coding region was used to mouse BDNF mRNA and probe complementary to EGFP was used to detect hBDNF mRNA. Probes were synthesized from DNA fragments subcloned into pCR4-TOPO vector (Invitrogen, USA). [α-^{35}S]UTP-labeled probes were generated with MAXIScript In Vitro Transcription Kit (Ambion, USA) using linearized DNA template and T3 or T7 RNA polymerase. 16 μm sections of fresh-frozen C3 mouse brain were processed according to the protocol described in [13]. Slides were exposed to either BioMax MR X-ray film for one week or NTB-2 photoemulsion for 2 months, developed with D19 developer and fixed with a general-purpose fixer (all from Eastman Kodak, USA). Slides exposed to NTB-2 were counterstained with hematoxylin (Vector Laboratories Inc., USA).

Authors' contributions

IK bred and analyzed the transgenic mice, performed in situ hybridization and RT-PCR analysis. TAP prepared the BAC-BDNF-EGFP construct, carried out transfection experiments and initial characterization of the transgenic mice. KJ performed transgene integration analysis, RT-PCR experiments and contributed to the breeding of founder lines. MS performed RNase protection assay, Western blot analysis and fluorescence microscopy. PP contributed to the initial characterization of the transgenic mice, cultured embryonic neurons and performed in situ hybridization analysis of BDNF mRNA expression in human hippocampus. KP conceived and coordinated the preparation of the transgenic construct. TT conceived and coordinated the study. IK and TT co-wrote the manuscript, all authors contributed to the analysis of the results and preparation of the manuscript. All authors read and approved the final manuscript.

Acknowledgements

We thank Epp Väli for technical assistance and Enn Jõeste and Liina Kiho from North Estonian Regional Hospital, Tallinn, for collaboration. This work was supported by the following grants to TT: Wellcome Trust Inter-

national Senior Research Fellowship (Grant 067952), Estonian Ministry of Education and Research (Grant 0140143), Estonian Enterprise (Grant EU27553) and Estonian Science Foundation (Grant 7257).

References

1. Leibrock J, Lottspeich F, Hohn A, Hofer M, Hengerer B, Masiakowski P, Thoenen H, Barde YA: **Molecular cloning and expression of brain-derived neurotrophic factor.** *Nature* 1989, **341(6238):**149-152.
2. Binder DK, Scharfman HE: **Brain-derived neurotrophic factor.** *Growth Factors* 2004, **22(3):**123-131.
3. Bibel M, Barde YA: **Neurotrophins: key regulators of cell fate and cell shape in the vertebrate nervous system.** *Genes Dev* 2000, **14(23):**2919-2937.
4. Bramham CR, Messaoudi E: **BDNF function in adult synaptic plasticity: the synaptic consolidation hypothesis.** *Prog Neurobiol* 2005, **76(2):**99-125.
5. Sairanen M, Lucas G, Ernfors P, Castren M, Castren E: **Brain-derived neurotrophic factor and antidepressant drugs have different but coordinated effects on neuronal turnover, proliferation, and survival in the adult dentate gyrus.** *J Neurosci* 2005, **25(5):**1089-1094.
6. Ernfors P, Ibanez CF, Ebendal T, Olson L, Persson H: **Molecular cloning and neurotrophic activities of a protein with structural similarities to nerve growth factor: developmental and topographical expression in the brain.** *Proc Natl Acad Sci USA* 1990, **87(14):**5454-5458.
7. Maisonpierre PC, Belluscio L, Friedman B, Alderson RF, Wiegand SJ, Furth ME, Lindsay RM, Yancopoulos GD: **NT-3, BDNF, and NGF in the developing rat nervous system: parallel as well as reciprocal patterns of expression.** *Neuron* 1990, **5(4):**501-509.
8. Maisonpierre PC, Le Beau MM, Espinosa R 3rd, Ip NY, Belluscio L, de la Monte SM, Squinto S, Furth ME, Yancopoulos GD: **Human and rat brain-derived neurotrophic factor and neurotrophin-3: gene structures, distributions, and chromosomal localizations.** *Genomics* 1991, **10(3):**558-568.
9. Conner JM, Lauterborn JC, Yan Q, Gall CM, Varon S: **Distribution of brain-derived neurotrophic factor (BDNF) protein and mRNA in the normal adult rat CNS: evidence for anterograde axonal transport.** *J Neurosci* 1997, **17(7):**2295-2313.
10. Katoh-Semba R, Takeuchi IK, Semba R, Kato K: **Distribution of brain-derived neurotrophic factor in rats and its changes with development in the brain.** *J Neurochem* 1997, **69(1):**34-42.
11. Ernfors P, Wetmore C, Olson L, Persson H: **Identification of cells in rat brain and peripheral tissues expressing mRNA for members of the nerve growth factor family.** *Neuron* 1990, **5(4):**511-526.
12. Yamamoto M, Sobue G, Yamamoto K, Terao S, Mitsuma T: **Expression of mRNAs for neurotrophic factors (NGF, BDNF, NT-3, and GDNF) and their receptors (p75NGFR, trkA, trkB, and trkC) in the adult human peripheral nervous system and nonneural tissues.** *Neurochem Res* 1996, **21(8):**929-938.
13. Timmusk T, Palm K, Metsis M, Reintam T, Paalme V, Saarma M, Persson H: **Multiple promoters direct tissue-specific expression of the rat BDNF gene.** *Neuron* 1993, **10(3):**475-489.
14. Aid T, Kazantseva A, Piirsoo M, Palm K, Timmusk T: **Mouse and rat BDNF gene structure and expression revisited.** *J Neurosci Res* 2007, **85(3):**525-535.
15. Liu QR, Lu L, Zhu XG, Gong JP, Shaham Y, Uhl GR: **Rodent BDNF genes, novel promoters, novel splice variants, and regulation by cocaine.** *Brain Res* 2006, **1067(1):**1-12.
16. Pruunsild P, Kazantseva A, Aid T, Palm K, Timmusk T: **Dissecting the human BDNF locus: bidirectional transcription, complex splicing, and multiple promoters.** *Genomics* 2007, **90(3):**397-406.
17. Liu QR, Walther D, Drgon T, Polesskaya O, Lesnick TG, Strain KJ, de Andrade M, Bower JH, Maraganore DM, Uhl GR: **Human brain derived neurotrophic factor (BDNF) genes, splicing patterns, and assessments of associations with substance abuse and Parkinson's Disease.** *Am J Med Genet B Neuropsychiatr Genet* 2005, **134B(1):**93-103.
18. Flavell SW, Greenberg ME: **Signaling mechanisms linking neuronal activity to gene expression and plasticity of the nervous system.** *Annu Rev Neurosci* 2008, **31:**563-590.
19. Zafra F, Hengerer B, Leibrock J, Thoenen H, Lindholm D: **Activity dependent regulation of BDNF and NGF mRNAs in the rat hippocampus is mediated by non-NMDA glutamate receptors.** *Embo J* 1990, **9(11):**3545-3550.
20. Fang H, Chartier J, Sodja C, Desbois A, Ribecco-Lutkiewicz M, Walker PR, Sikorska M: **Transcriptional activation of the human brain-derived neurotrophic factor gene promoter III by dopamine signaling in NT2/N neurons.** *J Biol Chem* 2003, **278(29):**26401-26409.
21. Price RD, Milne SA, Sharkey J, Matsuoka N: **Advances in small molecules promoting neurotrophic function.** *Pharmacol Ther* 2007, **115(2):**292-306.
22. Heintz N: **BAC to the future: the use of bac transgenic mice for neuroscience research.** *Nat Rev Neurosci* 2001, **2(12):**861-870.
23. Gincel D, Regan MR, Jin L, Watkins AM, Bergles DE, Rothstein JD: **Analysis of cerebellar Purkinje cells using EAAT4 glutamate transporter promoter reporter in mice generated via bacterial artificial chromosome-mediated transgenesis.** *Exp Neurol* 2007, **203(1):**205-212.
24. Zeilhofer HU, Studler B, Arabadzisz D, Schweizer C, Ahmadi S, Layh B, Bosl MR, Fritschy JM: **Glycinergic neurons expressing enhanced green fluorescent protein in bacterial artificial chromosome transgenic mice.** *J Comp Neurol* 2005, **482(2):**123-141.
25. Tallini YN, Shui B, Greene KS, Deng KY, Doran R, Fisher PJ, Zipfel W, Kotlikoff MI: **BAC transgenic mice express enhanced green fluorescent protein in central and peripheral cholinergic neurons.** *Physiol Genomics* 2006, **27(3):**391-397.
26. Timmusk T, Lendahl U, Funakoshi H, Arenas E, Persson H, Metsis M: **Identification of brain-derived neurotrophic factor promoter regions mediating tissue-specific, axotomy-, and neuronal activity-induced expression in transgenic mice.** *J Cell Biol* 1995, **128(1–2):**185-199.
27. Guillemot F, Cerutti I, Auffray C, Devignes MD: **A transgenic mouse model engineered to investigate human brain-derived neurotrophic factor in vivo.** *Transgenic Res* 2007, **16(2):**223-237.
28. Haubensak W, Narz F, Heumann R, Lessmann V: **BDNF-GFP containing secretory granules are localized in the vicinity of synaptic junctions of cultured cortical neurons.** *J Cell Sci* 1998, **111(Pt 11):**1483-1493.
29. Hartmann M, Heumann R, Lessmann V: **Synaptic secretion of BDNF after high-frequency stimulation of glutamatergic synapses.** *Embo J* 2001, **20(21):**5887-5897.
30. Kojima M, Takei N, Numakawa T, Ishikawa Y, Suzuki S, Matsumoto T, Katoh-Semba R, Nawa H, Hatanaka H: **Biological characterization and optical imaging of brain-derived neurotrophic factor-green fluorescent protein suggest an activity-dependent local release of brain-derived neurotrophic factor in neurites of cultured hippocampal neurons.** *J Neurosci Res* 2001, **64(1):**1-10.
31. Phillips HS, Hains JM, Laramee GR, Rosenthal A, Winslow JW: **Widespread expression of BDNF but not NT3 by target areas of basal forebrain cholinergic neurons.** *Science* 1990, **250(4978):**290-294.
32. Webster MJ, Herman MM, Kleinman JE, Shannon Weickert C: **BDNF and trkB mRNA expression in the hippocampus and temporal cortex during the human lifespan.** *Gene Expr Patterns* 2006, **6(8):**941-951.
33. Metsis M, Timmusk T, Arenas E, Persson H: **Differential usage of multiple brain-derived neurotrophic factor promoters in the rat brain following neuronal activation.** *Proc Natl Acad Sci USA* 1993, **90(19):**8802-8806.
34. Ballarin M, Ernfors P, Lindefors N, Persson H: **Hippocampal damage and kainic acid injection induce a rapid increase in mRNA for BDNF and NGF in the rat brain.** *Exp Neurol* 1991, **114(1):**35-43.
35. Gaszner M, Felsenfeld G: **Insulators: exploiting transcriptional and epigenetic mechanisms.** *Nat Rev Genet* 2006, **7(9):**703-713.
36. Muller D, Davidoff MS, Bargheer O, Paust HJ, Pusch W, Koeva Y, Jezek D, Holstein AF, Middendorff R: **The expression of neurotrophins and their receptors in the prenatal and adult human testis: evidence for functions in Leydig cells.** *Histochem Cell Biol* 2006, **126(2):**199-211.

37. Park C, Choi WS, Kwon H, Kwon YK: **Temporal and spatial expression of neurotrophins and their receptors during male germ cell development.** *Mol Cells* 2001, **12(3):**360-367.
38. West AE, Chen WG, Dalva MB, Dolmetsch RE, Kornhauser JM, Shaywitz AJ, Takasu MA, Tao X, Greenberg ME: **Calcium regulation of neuronal gene expression.** *Proc Natl Acad Sci USA* 2001, **98(20):**11024-11031.
39. Greer PL, Greenberg ME: **From synapse to nucleus: calcium-dependent gene transcription in the control of synapse development and function.** *Neuron* 2008, **59(6):**846-860.
40. Shieh PB, Hu SC, Bobb K, Timmusk T, Ghosh A: **Identification of a signaling pathway involved in calcium regulation of BDNF expression.** *Neuron* 1998, **20(4):**727-740.
41. Tao X, Finkbeiner S, Arnold DB, Shaywitz AJ, Greenberg ME: **Ca2+ influx regulates BDNF transcription by a CREB family transcription factor-dependent mechanism.** *Neuron* 1998, **20(4):**709-726.
42. Hong EJ, McCord AE, Greenberg ME: **A biological function for the neuronal activity-dependent component of Bdnf transcription in the development of cortical inhibition.** *Neuron* 2008, **60(4):**610-624.
43. Timmusk T, Persson H, Metsis M: **Analysis of transcriptional initiation and translatability of brain-derived neurotrophic factor mRNAs in the rat brain.** *Neurosci Lett* 1994, **177(1–2):**27-31.
44. Gray J, Yeo GS, Cox JJ, Morton J, Adlam AL, Keogh JM, Yanovski JA, El Gharbawy A, Han JC, Tung YC, *et al.*: **Hyperphagia, severe obesity, impaired cognitive function, and hyperactivity associated with functional loss of one copy of the brain-derived neurotrophic factor (BDNF) gene.** *Diabetes* 2006, **55(12):**3366-3371.
45. Sha H, Xu J, Tang J, Ding J, Gong J, Ge X, Kong D, Gao X: **Disruption of a novel regulatory locus results in decreased Bdnf expression, obesity, and type 2 diabetes in mice.** *Physiol Genomics* 2007, **31(2):**252-263.
46. Ringstedt T, Linnarsson S, Wagner J, Lendahl U, Kokaia Z, Arenas E, Ernfors P, Ibanez CF: **BDNF regulates reelin expression and Cajal-Retzius cell development in the cerebral cortex.** *Neuron* 1998, **21(2):**305-315.
47. Schenborn ET, Goiffon V: **DEAE-dextran transfection of mammalian cultured cells.** *Methods Mol Biol* 2000, **130:**147-153.
48. Ahlemeyer B, Baumgart-Vogt E: **Optimized protocols for the simultaneous preparation of primary neuronal cultures of the neocortex, hippocampus and cerebellum from individual newborn (P0.5) C57Bl/6J mice.** *J Neurosci Methods* 2005, **149(2):**110-120.

PUBLICATION V

Vashishta A, Habas A, **Pruunsild P**[#], Zheng JJ, Timmusk T, Hetman M. (2009) Nuclear factor of activated T-cells isoform c4 (NFATc4/NFAT3) as a mediator of antiapoptotic transcription in NMDA receptor-stimulated cortical neurons. J Neurosci. 2009 Dec 2;29(48):15331-15340

Development/Plasticity/Repair

Nuclear Factor of Activated T-Cells Isoform c4 (NFATc4/NFAT3) as a Mediator of Antiapoptotic Transcription in NMDA Receptor-Stimulated Cortical Neurons

Aruna Vashishta,[1]* Agata Habas,[1,2]* Priit Pruunsild,[3] Jing-Juan Zheng,[1] Tõnis Timmusk,[3] and Michal Hetman[1,2]

[1]Kentucky Spinal Cord Injury Research Center and Department of Neurological Surgery and [2]Department of Pharmacology and Toxicology, University of Louisville, Louisville, Kentucky 40292, and [3]Department of Gene Technology, Tallinn University of Technology, 19086 Tallinn, Estonia

During cortical development, when NR2B subunit is the major component of the NMDA glutamate receptors (NMDARs), moderate NMDAR activity supports neuronal survival at least in part by regulating gene transcription. We report that, in cultured cortical neurons from newborn rats, the NMDARs activated the calcium-responsive transcription regulator nuclear factor of activated T cells (NFAT). Moreover, in developing rat cortex, the NFAT isoforms c3 and c4 (NFATc3 and NFATc4) were expressed at relatively higher levels at postnatal day 7 (P7) than P21, overlapping with the period of NMDAR-dependent survival. In cultured cortical neurons, NFATc3 and NFATc4 were regulated at least in part by the NR2B NMDAR. Conversely, knockdown of NFATc4 but not NFATc3 induced cortical neuron apoptosis. Likewise, NFATc4 inhibition prevented antiapoptotic neuroprotection in response to exogenous NMDA. Expression of the brain-derived neurotrophic factor (BDNF) was reduced by NFATc4 inhibition. NFATc4 regulated transcription by the NMDAR-responsive *bdnf* promoter IV. In addition, NMDAR blockers including NR2B-selective once reduced BDNF expression in P7 cortex and cultured cortical neurons. Finally, exogenous BDNF rescued from the proapoptotic effects of NFATc4 inhibition. These results identify *bdnf* as one of the target genes for the antiapoptotic signaling by NMDAR–NFATc4. Thus, the previously unrecognized NMDAR–NFATc4–BDNF pathway contributes to the survival signaling network that supports cortical development.

Introduction

In the developing nervous system, neuronal survival requires extracellular signals (Oppenheim, 1991; Snider, 1994). In the cortex, those include the excitatory neurotransmitter glutamate and the neurotrophin brain-derived neurotrophic factor (BDNF). The glutamate NMDA receptors (NMDARs) are calcium-permeable ion channels that are critical for glutamate-mediated survival (for review, see Hardingham, 2006; Hetman and Kharebava, 2006). Thus, NMDAR antagonists induced cortical neuron apoptosis when administered to rodent pups at postnatal day 7 (P7) but not P1 or P21 (Ikonomidou et al., 1999). The NMDAR are formed by two molecules of the constant NR1 subunit and two molecules of the variable NR2 subunits (Cull-Candy and Leszkiewicz, 2004). In developing forebrain neurons, NR2B is the predominant NR2 subunit and thus a major mediator of glutamate-dependent survival of cortical or hippocampal neurons (Cull-Candy and Leszkiewicz, 2004; Habas et al., 2006; Papadia et al., 2008).

Received Sept. 30, 2009; accepted Oct. 19, 2009.

This work was supported by National Institutes of Health Grants NS047341-01 and RR015576-06 (M.H.), Kentucky Spinal Cord and Head Injury Research Trust Grant 3-5 (M.H.), The Commonwealth of Kentucky Challenge for Excellence (M.H.), and Norton Healthcare (M.H.). T.T. and P.P. were supported by Estonian Ministry of Education and Research Grant 0140143, Estonian Enterprise Grant EU27553, and Estonian Science Foundation Grant 7257. Drs. Gerald Crabtree, Neil Clipstone, Yuryi Usachev, and Chi-Wing Chow provided reagents used in this study.

*A.V. and A.H. contributed equally to this work.

Correspondence should be addressed to Michal Hetman, Kentucky Spinal Cord Injury Research Center, University of Louisville, 511 South Floyd Street, MDR616, Louisville, KY 40292. E-mail: michal.hetman@louisville.edu.

DOI:10.1523/JNEUROSCI.4873-09.2009

 0270-6474/09/2915331-10$15.00/0

Influx of calcium is critical for the neuronal responses to NMDAR stimulation, including survival (Nakanishi, 1992). In addition, NMDAR-mediated protection has been proposed to involve transcriptional regulation of gene expression (Marini and Paul, 1992; Gonzalez-Zulueta et al., 2000; Hardingham et al., 2002; Lee et al., 2005; Papadia et al., 2005, 2008). The identified transcriptional regulatory events that contribute to NMDAR-dependent antiapoptotic response include cAMP response element-binding protein (CREB)/nuclear factor κB (NFκB)-mediated upregulation of the neurotrophin BDNF, CCAAT/enhancer-binding protein (c/EBP)-mediated, or AP1-mediated upregulation of antioxidant enzymes Sesn2 or Srxn1, and suppression of the pro-oxidant protein Txbp1 by inhibiting Foxo (Lipsky et al., 2001; Hardingham et al., 2002; Papadia et al., 2008). Although NR2B has been implicated in regulation of Sesn2, Srxn1, and Txbp1 (Papadia et al., 2008), its contribution to regulation of other NMDAR-dependent survival genes including *bdnf* has not been yet reported. Because BDNF and NR2B provide major survival signals during forebrain development, their mutual regulation offers a possibility for a prosurvival positive feedback loop. Such regulatory interaction is predicted by modeling studies of extracellular signal-dependent survival of developing neurons (Deppmann et al., 2008).

The nuclear factors of activated T-cells (NFATs) represent a family of at least five transcription factors, all of one of which are regulated by the Ca^{2+}-activated protein phosphatase-2B/calcineurin (PP2B) (Crabtree and Olson, 2002; Hogan et al., 2003). The PP2B-regulated NFAT isoforms including the neuron-

expressed NFATc4/NFAT3 establish partially redundant pathways coupling calcium signaling to the nuclear transcription (Graef et al., 1999; Benedito et al., 2005; Bradley et al., 2005; Seybold et al., 2006; Vihma et al., 2008; Nguyen et al., 2009). In cultured cortical or hippocampal neurons, NFAT-driven transcription is regulated by the L-type voltage-gated calcium channels, basal NMDAR activity, and BDNF (Graef et al., 1999; Groth and Mermelstein, 2003). In cultured rat cerebellar granule neurons (CGNs), NFATc4 has been implicated in antiapoptotic effects of depolarizing concentrations of KCl (Benedito et al., 2005). However, the NFAT role in NMDAR-mediated neuronal responses including survival of developing cortical neurons has not been reported before this study. Therefore, we set out to (1) determine the mediators of the NMDAR-stimulated NFAT-driven transcription, (2) evaluate its role in NMDAR-mediated neuronal survival, and (3) identify which of NMDAR-regulated survival genes are targeted by NFAT.

Materials and Methods

Materials. The following plasmids have been described previously: pON260 (Cherrington and Mocarski, 1989); hemagglutinin (HA) or green fluorescent protein (GFP) -tagged expression vectors for wild type (wt) NFATc4 cloned in pBJ5 or enhanced GFP (EGFP) mammalian expression vectors, respectively (Graef et al., 1999); expression vector for wtNFATc1 cloned in pBJ5 plasmid (Beals et al., 1997); NFAT–luciferase reporter plasmid (Graef et al., 1999); the flag-tagged wt and R474A/N475A/T541G NFATc4 expression plasmids (Yang and Chow, 2003); EF1αLacZ β-galactosidase (β-gal) expression vector and CRE–luciferase reporter plasmid (Impey et al., 1998); rBDNF IV 4.5–chloramphenicol acetyltransferase (CAT) containing a fragment of the rat BDNF promoter IV (from −4100 through 285 relative to the transcription start) cloned 5′ to a chloramphenicol acetyltransferase reporter gene in pBLCAT2 (Shieh et al., 1998); dominant-negative p53 expression vector cytomegalovirus–p53–DD (Shaulian et al., 1992); pSUPER vector (Brummelkamp et al., 2002); and pSuper-based small interfering hairpin RNA (shRNA) constructs targeting GFP and MKL1 (Kalita et al., 2006). The 5xSRF–luciferase reporter was purchased from Stratagene. The pcDNA3-based expression vector for GFP-tagged wt NFATc3 was kindly provided by Dr. Yuriy Usachev (University of Iowa, Iowa City, IA). The following antibodies and reagents were obtained from commercial sources: rabbit polyclonal anti-GFP (MBL); rabbit polyclonal anti-β-gal (MP Biomedicals); the Texas-Red- or HRP-conjugated goat antibodies to rabbit IgG (Calbiochem); BDNF (Alomone Labs); tacrolimus (FK506; A.G. Scientific); tetrodotoxin (TTX) (Ascent Scientific); and NMDA, dizocilpine maleate (MK801 [(+)-5-methyl-10,11-dihydro-5*H*-dibenzo [a,d] cyclohepten-5,10-imine maleate]), ifenprodil, Ro-25-6981 [*R*-(*R*,*S*)-α-(4-hydroxyphenyl)-β-methyl-4-(phenylmethyl)-1-piperidine propranol], DL-amino-5-phosphonovalerate (APV), LY294002 [2-(4-morpholinyl)-8-phenyl-1(4*H*)-benzopyran-4-one], U0126 [1,4-diamino-2,3-dicyano-1,4-bis(*o*-aminophenylmercapto)butadiene], and Hoechst 33258 (Sigma or Calbiochem).

Cell culture and transfection. Cortical neurons were prepared from newborn Sprague Dawley rats at postnatal day 0 as described previously (Habas et al., 2006). The same methodology was used to culture mouse cortical neurons isolated from the previously reported NFAT–luciferase transgenic mice that were bred on the FVBN background (Wilkins et al., 2004). Briefly, culture medium was basal medium Eagle supplemented with 10% heat-inactivated bovine calf serum (Hyclone), 35 mM glucose, 1 mM L-glutamine, 100 U/ml penicillin, and 0.1 mg/ml streptomycin. Cytosine arabinoside (2.5 μM) was added to cultures on the second day after seeding [day *in vitro* 2 (DIV2)] to inhibit the proliferation of non-neuronal cells. Cells were used for experiments on DIV6–DIV7 unless indicated otherwise. Transient transfections were performed on DIV3–DIV4 using the Lipofectamine 2000 reagent (Invitrogen) as described previously (Hetman et al., 2002). Electroporation of freshly dissociated newborn rat cortical neurons was conducted using a rat neuron nucleofection reagent kit (Amaxa).

Animal treatment. Sprague Dawley rats were housed with their siblings under a 12 h light/dark cycle and with *ad libitum* access to water and food. All animals were treated in accordance with the guidelines of the National Institutes of Health and the University of Louisville *Guidelines for the Care and Use of Laboratory Animals*. MK801 and ifenprodil were dissolved in sterile saline and administered as a single subcutaneous injection at P7. To collect the tissues for RNA extraction, rats were killed with CO_2.

Cultured neuron treatments. LY294002, MK801, ifenprodil, Ro-25-6981, FK506, and U0126 were dissolved in dimethylsulfoxide (DMSO). Bicuculline/4AP, APV, NMDA, and TTX were dissolved in culture media and saline, respectively. BDNF was diluted in PBS containing 0.1% bovine serum albumin. BDNF or NMDA were added 30 min before LY294002. NMDAR blockers or FK506, U0126, or TTX were added 30 min before NMDAR or synaptic activity stimulations. Drug treatments were performed in regular culture media containing 10% bovine calf serum. The final concentration of DMSO in the medium was 0.2–0.4%.

Design and cloning of shRNA and reporter plasmids. To generate NFATc4 shRNA constructs, we selected two sequences corresponding to nucleotides 564–582 (shNFATc4-N) and 2306–2324 (shNFATc4-C) of rat NFATc4, both of which were validated previously as suitable small interfering RNA targets (Benedito et al., 2005). Comparison of mouse, rat, and human mRNA sequences demonstrated that the NFATc4-N target sequence was completely conserved between these species, whereas the NFATc4-C target sequence was unique for rodents. Oligonucleotides were designed (shNFATc4-N, gatccccgggacggctctcctagagattttcaagagaaatctctaggagagccgtccctttttggaaa; NFATc4-C, gatccccggcggaggaagcgcagtccttcaagagaggactgcg-cttcctccgccttttttggaaa) together with their complementary counterparts, followed by annealing and subcloning into pSUPER vector digested with BglII and HindIII (Oligoengine). Also, the NFATc3 shRNAs (shNFATc3) constructs were prepared in a similar way after selecting the target regions using the shRNA design freeware (http://sonnhammer.cgb.ki.SE/). The shNFATc3-1 targets nucleotide sequence 113–131 of rat NFATc3, AGATGATTGTGCATCCATT, which is rodent/human conserved; shNFATc3-2 targets nucleotide sequence 1243–1261 of rat NFATc3, CATCTTCATTACCTCCATT, which is rodent specific. The shNFATc3 consisted of an equimolar mix of shNFATc3-1 and shNFATc3-2. The hBDNF IV–luciferase plasmid was constructed by placing a fragment of the human BDNF promoter IV 5′ from a luciferase reporter gene in pGL4.15 vector (Promega). The fragment included position −205 through 337 relative to the major transcription start site (Pruunsild et al., 2007). Site-directed mutagenesis was used to introduce base substitutions in the composite NFAT/MEF2 consensus site at positions 140–156: wild type, 5′*ATTTCCA*CTATCAAATA3′; mutant, 5′*AT-TggCACgc*TCAAATA3′ (base substitutions in the *NFAT*/MEF2 binding element are in lowercase).

Reporter gene assays. Luciferase and β-gal activities were assayed using commercial assay kits (Promega); CAT protein levels were determined using ELISA (Roche Diagnostics). For experiments with transiently transfected reporter plasmids, neurons were cultured on 24-well plates (5×10^5 per well) and transfected with Lipofectamine 2000; transcriptional activity was determined as a luciferase activity or CAT expression normalized to β-gal activity and compared with unstimulated controls. In experiments with neurons from the NFAT–luciferase reporter mouse line, luciferase activity was normalized against the total protein concentration.

RNA analysis. RNA was isolated from 2–5 $\times 10^6$ cells or from newborn rat tissues using TRI Reagent (Sigma). The remaining DNA was removed by digestion with DNase I (Promega), and RNA was reverse transcribed with AMV First-Strand cDNA Synthesis kit (Invitrogen) in the presence of random hexamers. For quantitative real time (qRT)-PCR, RT^2 Real-Time SYBR Green mix (SuperArray Bioscience Corporation) and the $\Delta\Delta$CT method of quantification were applied. The reference RNA was 18S rRNA. The qRT-PCR primers were as follows: 18S (sense, gttggtttt-cggaactgaggc; antisense, gtcggcatcgtttatggtcg), NFATc1 (sense, agatggt-gctgtctggccataact; antisense, tgcggaaaggtggtatctcaacca), NFATc2 (sense, tcacagctgagtccaaggttgtgt; antisense, agcatgttaggctggctcttgtct), NFATc3 (sense, tggcatcaacagtatggacctgga; antisense, tttaccacaaggagaagtgggcct), NFATc4 (sense, atcactggcaagatggtggctaca; antisense, agcttcaggattccagca-

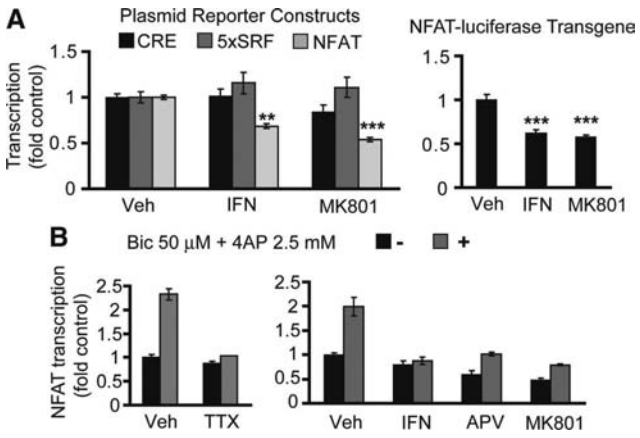

Figure 1. Regulation of NFAT-driven transcription by NMDAR. ***A***, At DIV4, rat cortical neurons were transfected with the indicated reporter plasmids and EF1αLacZ (0.2 + 0.125 μg of plasmid DNA/5 × 10^5 cells, respectively). Forty-eight hours after transfection, cells were treated for 6 h with 10 μM ifenprodil (IFN), 10 μM MK801, or vehicle (Veh, 0.2% DMSO). Cortical neurons from newborn transgenic mice carrying an NFAT-driven luciferase reporter gene underwent the same pharmacological treatment at DIV7. A specific decrease of NFAT-driven transcription after ifenprodil or MK801 treatments suggests NFAT dependence on the basal NR2B NMDAR activity. ***B***, Rat cortical neurons were transfected as in ***A***. To enhance synaptic activity, bicuculline/4AP (50 μM + 2.5 mM, Bicc/4AP) was applied for 16 h at DIV6. After blocking neuronal electrical activity with 1 mM TTX, bicuculline/4AP failed to activate NFAT-driven transcription. In addition, the synaptic activity-induced NFAT-driven transcription was reduced after blocking NR2B NMDAR. In ***A***, data represent means ± SEM of triplicate determinations from at least three independent experiments; in ***B***, triplicate determinations from sister cultures ± SD are depicted. $^{**}p < 0.01$; $^{***}p < 0.001$. Results similar to those in ***B*** were obtained in at least two independent experiments.

cagtca), BDNF (sense, gagaaagtcccggtatcaaa; antisense, ccagccaattctcttttt), alivin (sense, aaacctgtctaaggtgcctgggaa; antisense, gttgttgtggcgaacaatcagggt), and L1 (sense, tctgcttcatcaaacgcagcaagg; antisense, attgtcactgtactcgccgaaggt). For reverse-transcriptase-PCR, the qRT-PCR primers for NFATc1-4 were applied together with glyceraldehyde-3-phosphate dehydrogenase (GAPDH) primers (sense, catcaccatcttccaggagc; antisense, ctaagcagttggtggtgc).

Immunofluorescence and Western blot analysis. Transfected cells were detected by immunostaining with the rabbit antibody against β-gal using standard immunofluorescence methodology. For Western blot analysis, cortical neurons were washed twice with PBS and lysed in SDS-PAGE sample buffer. SDS-PAGE and blotting with the anti-GFP antibody were performed according to standard procedures.

Quantification of apoptosis. Cell nuclei were visualized with Hoechst 33258. The transfected, β-gal-positive cells with uniformly stained nuclei were scored as viable. The transfected cells displaying condensed or fragmented nuclei were scored as apoptotic. At least 200 cells were evaluated for each condition in each independent experiment.

Statistical analysis. Statistical analysis of the data was performed using one-way ANOVA, followed by *post hoc* comparisons.

Results

To determine whether the NMDARs regulate NFAT-driven transcription, we evaluated effects of NR2B-selective or nonselective NMDAR antagonists on the transiently transfected luciferase reporter gene whose promoter contained five repeats of the consensus NFAT binding sites from the 5′ regulatory region of the human *Il-2* gene. At DIV7, a 6 h treatment with either NR2B-selective ifenprodil or the nonselective dizocilpine (MK801) reduced NFAT activity by 35 or 45%, respectively (vehicle controls vs ifenprodil or MK801, $p < 0.01$ or <0.001, respectively) (Fig. 1*A*). The effects of dizocilpine were similar to those of ifenprodil (ifenprodil vs MK801, $p > 0.05$) (Fig. 1*A*). In contrast, neither ifenprodil nor dizocilpine affected CRE- or serum response factor (SRF)-mediated transcription (Fig. 1*A*). In cortical neurons, which were isolated from newborn NFAT–luciferase transgenic mice, ifenprodil or dizocilpine also lowered NFAT-mediated transcription (vehicle controls vs ifenprodil or MK801, $p < 0.001$, respectively) (Fig. 1*A*). Either drug induced similar decrease of NFAT activity (ifenprodil vs MK801, $p > 0.05$) (Fig. 1*A*). Thus, NR2B-mediated regulation of NFAT-driven transcription occurred at the levels of episomal plasmid- or chromatin-integrated NFAT reporter genes.

Although in some experiments, low prosurvival concentrations (1–15 μM) of NMDA moderately increased endogenous NFAT activity, increasing synaptic activity with the 16 h bicuculline + 4AP treatment consistently stimulated NFAT-driven transcription (data not shown and Fig. 1*B*). Moreover, that effect was sensitive to NR2B-selective or nonselective NMDAR blockade (Fig. 1*B*). Therefore, our results indicate that, at least in cultured rat cortical neurons, NFAT-driven transcription is regulated by the NR2B NMDAR.

To determine which NFATc isoforms may be regulated by NMDAR and contribute to NMDAR-mediated neuronal survival, we studied their expression in cultured rat cortical neurons and in developing rat cortex. In DIV7 cultures, mRNAs for NFATc1, NFATc2, NFATc3, and NFATc4 were detected (Fig. 2*A*). However, significant temporal differences were observed in relative abundance of those mRNAs during cortical development *in vivo*. Expression of NFATc1 mRNA increased 3.5-fold at P7 compared with P1 ($p < 0.001$) (Fig. 2*B*). It remained elevated at P21 (P21 vs P1, $p < 0.05$; P21 vs P7, $p > 0.05$) (Fig. 2*B*). NFATc2 mRNA levels were 6- or 11-fold higher at P7 or P21 than at P1, respectively (P7 or P21 vs P1, $p < 0.001$; P21 vs P7, $p < 0.001$) (Fig. 2*B*) NFATc3 mRNA levels were similar at P1 and P7 but declined by half at P21 (P1 vs P7, $p > 0.05$; P21 vs P7, $p < 0.05$) (Fig. 2*C*). At P7, cortical NFATc4 mRNA levels were at least twofold higher than at P1 or P21 ($p < 0.05$) (Fig. 2*C*). Thus, the relatively higher expression of NFATc3 and NFATc4 at P7 than P21 overlaps with the period of the predominant cortical presence of NR2B NMDAR and the NMDAR-dependent cortical neuron survival (Ikonomidou et al., 1999; Cull-Candy and Leszkiewicz, 2004). Consequently, we focused our additional studies on these two members of the NFAT family.

To determine NFATc3/c4 responsiveness to NMDAR stimulation, DIV4 neurons were cotransfected with an expression plasmid for either NFAT together with the NFAT–luciferase reporter plasmid. After 48 h, cells were stimulated with 10 μM NMDA for 6 h. The transcriptional activity of the overexpressed NFATs increased in response to NMDA treatment (9.2- or 5.8-fold of unstimulated controls for NFATc3 or NFATc4, respectively) (Fig. 3*A*). In addition, the NMDA-mediated NFATc3/c4 activation was disrupted by the NMDAR antagonists, including the NR2B-selective ifenprodil and Ro-25-6981, as well as the nonselective MK801 and APV (Fig. 3*A*). NMDA stimulation induced nuclear translocation of the EGFP-tagged NFATc3/c4 (Fig. 3*B* and data not shown). This translocation was abolished by the PP2B inhibitor FK506 but not by the MKK1/2 inhibitor U0126 (Fig. 3*B* and data not shown). However, either inhibitor reduced the NMDAR-

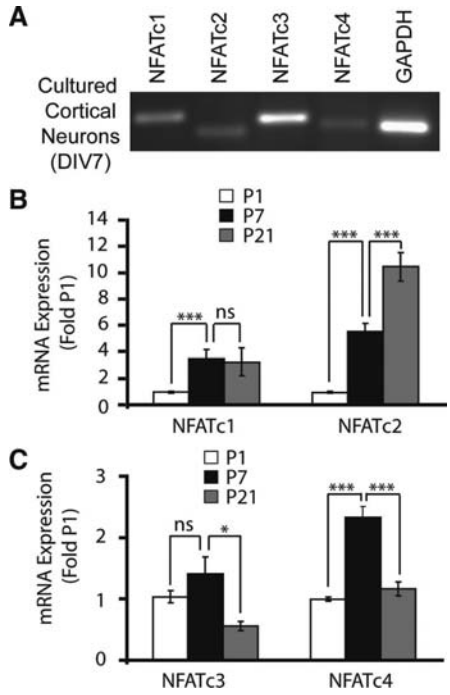

Figure 2. NFAT isoform expression in cultured rat cortical neurons and in developing rat cortex. ***A***, Reverse transcription-PCR analysis of NFAT isoform mRNA expression in cultured rat cortical at DIV7. GAPDH mRNA levels were also determined. ***B***, ***C***, The qRT-PCR was used to determine the NFAT isoform mRNA levels in developing rat neocortex at P1, P7, and P21. The 18S rRNA levels were used for normalizations. Note that expression of NFATc3 and NFATc4 peaks at P7 and declines at P21, overlapping with the maximum expression of the NR2B NMDAR and the survival dependence of cortical neurons on NMDAR (Sheng et al., 1994; Ikonomidou et al., 1999). In ***B*** and ***C***, each data point represents six to seven animals ± SEM. $*p < 0.05$; $***p < 0.001$.

mediated transcriptional activation of the overexpressed NFATc3/c4 (Fig. 3*C*). Also, NMDA failed to activate the R474A/N475A/T541G mutant form of NFATc4 that is deficient in interactions with the transcription factors AP1 and c/EBP (Yang and Chow, 2003). For instance, in cortical neurons stimulated with 10 μM NMDA for 6 h, activities of the overexpressed wt or the R474A/N475A/T541G mutant NFATc4 were 3.35 ± 0.32-fold or 1.2 ± 0.11-fold of the unstimulated controls, respectively. Thus, as in the case of other NFATc3/c4-activating stimuli, NMDAR-mediated activation of NFATc3/4 required PP2B-dependent nuclear translocation, ERK1/2 activation, and interactions with other partner transcription factor(s) (Crabtree and Olson, 2002; Hogan et al., 2003).

To further determine the NFATc3/c4 contributions to NFAT-driven transcription in cortical neurons, we used shRNA plasmids targeting these NFAT isoforms. The shNFATc4-N plasmid targeted a sequence in the 5′ coding region of the NFATc4 mRNA that was used before for a successful knockdown of rat NFATc4 (Benedito et al., 2005). The shNFATc3 consisted of a pool of two shRNAs that were designed to target rat NFATc3. The shNFATc3/c4 disrupted activity of their respective targets in NMDAR-stimulated cortical neurons (Fig. 4*A*,*B*). Additional validation experiments using NMDAR-stimulated neurons and evaluating effects of (1) shNFATc3 on activation of the overexpressed NFATc4, (2) shNFATc4-N on activation of the overexpressed NFATc1, and (3) shNFATc4-N on activation of the endogenous CRE-driven transcription, demonstrated that neither shRNA reduced NMDAR activity (supplemental Fig. 1, available at www.jneurosci.org as supplemental material). Also, shNFATc4-N reduced levels of the overexpressed NFATc4 (supplemental Fig. 1*D*, available at www.jneurosci.org as supplemental material). Therefore, these results indicate efficient knockdown of NFATc3 or NFATc4 using shNFATc3 or shNFATc4-N, respectively.

To assess contributions by NFATc3/c4 to the NMDAR-mediated increase of NFAT-driven transcription, we selected bicuculine/4AP synaptic stimulation protocol that resulted in NR2B NMDAR-dependent activation of NFAT (Fig. 1*B*). Cortical neurons that received shNFATc3 or shNFATc4 displayed reduced activation of NFAT-driven transcription in response to an 8 h bicuculine/4AP treatment. In neurons receiving control shRNA (shGFP), there was a 3.5-fold activation of NFAT-driven transcription that declined to 2- or 2.4-fold of unstimulated controls after NFATc3 or NFATc4 knockdown, respectively (shGFP vs shNFATc3 or shNFATc4, $p < 0.01$ or $p < 0.001$, respectively) (Fig. 4*C*). Hence, NMDAR regulates activity of endogenous NFATc3/c4.

Because the NR2B NMDAR-regulated NFATc3/4 are expressed in the cortex during the period when NMDAR antagonists induce cortical neuron apoptosis (Fig. 2*C*) (Ikonomidou et al., 1999), NFATc3/c4 may promote neuronal survival by suppressing apoptosis. Indeed, in cultured cortical neurons, inhibition of NFATc4 induced apoptosis as indicated by nuclear chromatin condensation (Fig. 5*A*). Thus, in neurons transfected with a control shRNA that targeted GFP, 15, 24, and 30% apoptosis were present at 48, 72, and 96 h after transfection, respectively (Fig. 5*B*). At each of these time points, neurons that were transfected with shNFATc4-N displayed significantly more apoptosis (20, 45, and 52%, respectively) (Fig. 5*B*). To ensure that this proapoptotic effect is not caused by off-target effects of the shNFATc4-N, we also tested another shRNA construct that targeted a 3′ coding region of the rodent NFATc4 mRNA (shNFATc4-C). The shNFATc4-C induced cortical neuron apoptosis whose extent and kinetics were similar to those in shNFATc4-N-receiving cells (Fig. 5*B*,*C*). Conversely, knockdown of NFATc3 did not induce neuronal apoptosis (Fig. 5*B*,*C*). Therefore, at least under culture conditions, NFATc4 but not NFATc3 is required for cortical neuron survival.

To determine whether NFATc4 contributes to NMDAR-dependent survival, DIV4 cortical neurons were transfected with shNFATc4-N or shGFP. At 48 h after transfection, cells were exposed for 24 h to 30 μM LY294002, which is a drug inhibitor of the phosphatidylinositol-3-kinase (PI3K). We have reported previously that such treatment induces cortical neuron apoptosis that can be suppressed by NR2B stimulation with moderate concentrations of exogenous NMDA (Habas et al., 2006). In concert with our published results, in shGFP- or shNFATc4-transfected neurons, LY294002 increased apoptosis from 21 to 45% or 30 to 65%, respectively ($p < 0.01$) (Fig. 6). In shGFP-receiving neurons, cotreatment with LY294002 and 10 μM NMDA reduced apoptosis from 45 to 25% ($p < 0.05$) (Fig. 6). In contrast, shNFATc4-N prevented the NMDA neuroprotection against LY294002 (65 or 54% apoptosis with 0 or 10 μM NMDA, respectively, $p > 0.05$) (Fig. 6). We also performed similar experiments to evaluate whether shNFATc3 affected NMDAR-dependent neuroprotection of PI3K-inhibited neurons. Unexpectedly, we observed a neuroprotective effect of shNFATc3 (A. Vashishta and M. Hetman, unpublished observation). Although analysis of NFATc3 contribution to NMDAR-dependent survival was not

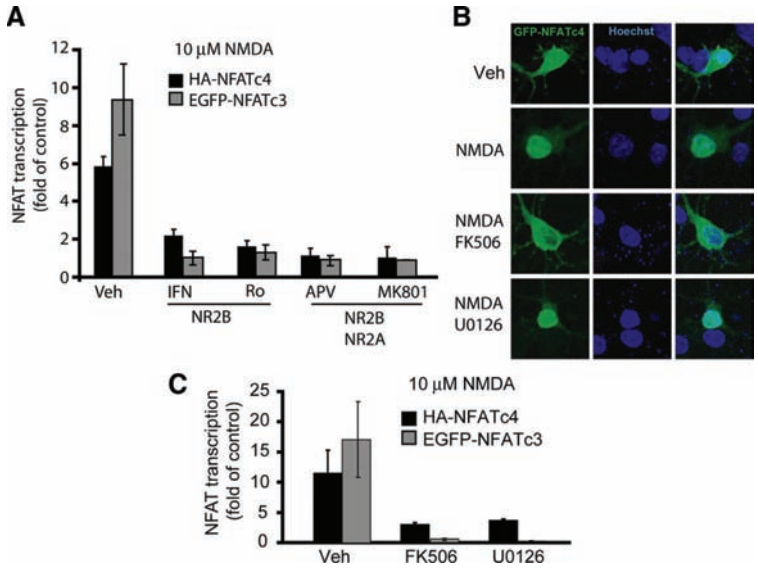

Figure 3. Regulation of NFATc3/c4 by the NR2B NMDAR. ***A***, The DIV4 cortical neurons were cotransfected with NFAT–luciferase reporter plasmid, EF1αLacZ, and wild-type NFATc3 or NFATc4 (0.2 + 0.125 + 0.2 μg of plasmid DNA/5 × 10^5 cells, respectively). Forty-eight hours after transfection, cells were treated with NMDA for 6 h in the presence of the NMDAR inhibitors: 10 μM ifenprodil (IFN), 0.5 μM Ro-25-6981 (Ro), 100 μM APV, or 10 μM MK801. Vehicle control was 0.2% DMSO (Veh). NFATc3/c4 activation by exogenous NMDA required NR2B. ***B***, The DIV4 cortical neurons were cotransfected with the expression plasmid for wild-type NFATc4 that was tagged with GFP (0.4 μg of plasmid DNA/5 × 10^5 cells). Forty-eight hours after transfection, cells were treated with NMDA in the presence of the PP2B inhibitor FK506 or the ERK1/2 pathway blocker U0126 for 6 h. The *z*-stack confocal images of GFP–NFATc4 revealed NMDAR-mediated nuclear translocation of NFATc4. This translocation was blocked by PP2B but not extracellular signal-regulated kinase inhibition. Similar results were obtained in three independent experiments using either GFP–NFATc3 or GFP–NFATc4. ***C***, Forty-eight hours after transfection that was performed as in ***A***, cells were treated with NMDA in the presence of FK506 or U0126 for 20 h as indicated. NMDAR-mediated activation of NFATc3/c4 was antagonized by blocking either PP2B or the ERK1/2 pathway. In ***A*** and ***C***, averages ± SD of triplicate determinations from sister cultures are shown. Similar results were obtained in at least two independent experiments.

possible because of the shNFATc3-mediated rescue of LY294002-treated neurons, the latter activity suggests that, at least during PI3K inhibition, NFATc3 induces rather than prevents apoptosis. Although the proapoptotic activity of NFATc3 is under current investigation (Vashishta and Hetman, unpublished observation), our results indicate specific requirement of NFATc4 for moderate NMDAR activity to protect against neuronal apoptosis.

Because the major function of NFATs is regulation of gene transcription, it is likely that NFATc4 provides antiapoptotic neuroprotection by mediating the NMDAR-induced increases in survival gene expression. Thus, we analyzed the 5′ regulatory regions of several previously identified NMDAR-regulated antiapoptotic survival genes for the presence of the NFAT consensus binding site core 5′WGGAAAW3′, with W being A or T (Hogan et al., 2003). The search included genomic sequences from human, mouse, and rat (if available) to verify the evolutionary conservation of the NFAT regulatory elements. Several putative NFAT binding sites were found in the 5′ regulatory regions of *alivin*, *l1*, and *bdnf* genes. Six of eight alternative *bdnf* promoters contain evolutionary conserved NFAT elements. Therefore, alivin, L1, and BDNF may be regulated by the NR2B-responsive NFATc4.

To further evaluate this possibility, we determined the effects of NFATc4 knockdown on the basal mRNA levels of alivin, L1, and BDNF. Four days after electroporating shNFATc4-N, mRNA levels of endogenous NFATc4 or BDNF declined to 20 or 60% of those in neurons receiving the control shRNA, respectively ($p < 0.01$) (Fig. 7). In contrast, mRNAs of alivin or L1 were unaffected by shNFATc4. Consistent with NFAT contribution to regulation of BDNF expression, a 24 h treatment with the 0.2 μg/ml PP2B inhibitor FK506 reduced BDNF mRNA levels to 58 ± 2.7% untreated controls ($p < 0.01$). These results indicate that, in cultured rat cortical neurons, NFATc4 regulates BDNF mRNA levels.

At least in rodents, transcriptional regulation of BDNF promoter IV provides a major coupling between BDNF expression and neuronal activity/NMDAR (Hong et al., 2008). Therefore, we tested a possibility that NFATc4 regulates promoter IV. Compared with its wild-type counterpart, the mutant promoter IV with disruption of the conserved NFAT/MEF2 composite site at position 140–156 (relative to the major transcription start site of human *bdnf* exon IV) had greatly reduced basal transcriptional activity and diminished responsiveness to NMDAR stimulation (Fig. 8*A*). We also evaluated effects of manipulating NFATc4 on the NMDAR-mediated activation of the promoter IV. In neurons that were stimulated with 10 μM NMDA for 20 h, overexpression of NFATc4 increased promoter IV activation, whereas shNFATc4-N-mediated knockdown of NFATc4 reduced promoter IV activation (Fig. 8*B*). Analysis of five independent experiments revealed that the NMDAR-mediated activation of promoter IV was enhanced by 40 ± 9.5% or reduced by 25 ± 3.65% in NFATc4- or shNFATc4-transfected neurons, respectively ($p < 0.001$). These results indicate that NFATc4 contributes to activation of BDNF promoter IV.

The NR2B NMDAR appears as a major NMDAR subtype that, during moderate stimulation, activates NFATc4 (Figs. 1, 3). Therefore, we tested the effects of selective NR2B inhibition on expression of candidate NFATc4-regulated survival genes in cortices of P7 rat pups or in cultured cortical neurons. At P7, single systemic injections of NMDAR antagonists induced apoptotic cell death of cortical neurons, indicating their critical dependence on NMDAR activity (Ikonomidou et al., 1999). Three hours after administering the nonselective MK801 (10 mg/kg, s.c.) or the NR2B-selective ifenprodil (20 mg/kg, s.c.), cortical levels of BDNF mRNA reached 22 or 30% of saline-treated controls ($p < 0.001$) (Fig. 9*A*). In contrast, L1 or alivin mRNA levels were significantly reduced in response to MK801 but not ifenprodil (42%, $p < 0.05$ or 34%, $p < 0.001$, respectively) (Fig. 9*A*). Also, in DIV7 cultured cortical neurons, either NR2B-selective or nonselective NMDAR blockade reduced BDNF mRNA levels (Fig. 9*B*). Although, the nonselective MK801 appeared more effective than the NR2B-selective ifenprodil or Ro-25-6981, these differences were not significant (MK801 vs ifenprodil or Ro-25-6981, $p > 0.05$). Thus, in P7 cortex or in cultured cortical neurons, moder-

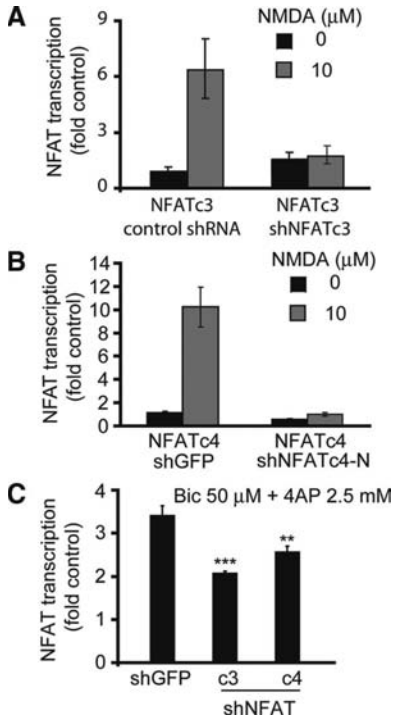

Figure 4. The shRNA-mediated inhibition of NFATc3/c4 reduces activation of NFAT-driven transcription in synaptically stimulated cortical neurons. ***A***, ***B***, DIV4 cortical neurons were cotransfected with expression plasmids for the GFP-tagged NFATc3 or the HA-tagged NFATc4 together with the NFAT–luciferase reporter, the β-gal expression plasmid EF1αLacZ, and the shNFATc3 or shNFATc4-N (0.2 + 0.2 + 0.125 + 1.1 μg of plasmid DNAs/5 $\times$ 10^5 cells, respectively). Control shRNAs included shRNA expression plasmids targeting SRF coactivator MKL1 (control shRNA for shNFATc3) or GFP (shGFP, used as a control for shNFATc4-N). Two days after transfection, cells were stimulated with 10 μM NMDA for 20 h. The shNFATc3 or shNFATc4 inhibited NMDAR-mediated activation of their respective targets. These results together with data from additional validation studies (supplemental Fig. 1, available at www.jneurosci.org as supplemental material) suggest that shNFATc3 or shNFATc4 specifically inhibited NFATc3 or NFATc4, respectively. ***C***, Neurons were transfected with shRNAs as described in ***A*** and ***B*** except omission of the NFATc3/c4 expression plasmids. At 72 h after transfection, cells were stimulated with bicuculline/4AP (50 μM + 2.5 mM, Bic/4AP) for 8 h. The synaptic activity-mediated increase of NFAT-driven transcription was reduced by shNFATc3 or shNFATc4-N. Because synaptic activity-mediated stimulation of NFAT is NMDAR dependent, these results indicate a role for NMDAR in regulating endogenous NFATc3/c4 in rat cortical neurons. In ***A*** and ***B***, averages $\pm$ SD of triplicate determinations from sister cultures are depicted. Similar results were obtained in at least two independent experiments. In ***C***, data represent averages $\pm$ SEM from six sister cultures in two independent experiments. $^{**}p < 0.01$; $^{***}p < 0.001$.

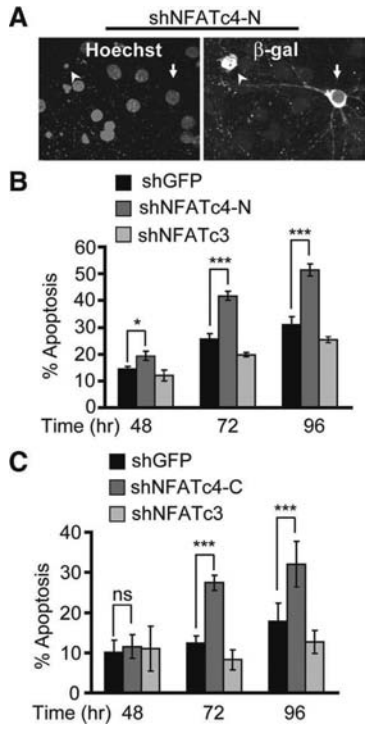

Figure 5. Cortical neuron apoptosis in response to NFATc4 knockdown. The DIV4 cortical neurons were cotransfected with control shRNA (shGFP), shNFATc4-N, or shNFATc4-C together with the β-gal expression plasmid pON260 (1.0 + 0.2 μg of plasmid DNA/5 $\times$ 10^5 cells, respectively). The shNFATc3 was used as an additional control. ***A***, Representative micrographs of shNFATc4-N-transfetced neurons at 96 h after transfection. Immunofluorescence for β-gal was used to identify transfected neurons. Counterstaining with Hoechst 33258 revealed the noncondensed chromatin of live cells (arrow) or chromatin condensation accompanying apoptosis (arrowhead). ***B***, ***C***, The shNFATc4-N or the shNFATc4-C but not shNFATc3 induced cortical neuron apoptosis. Data represent duplicate determinations from at least three independent experiments $\pm$ SEM. $^{*}p < 0.05$; $^{**}p < 0.01$; $^{***}p < 0.001$; $^{ns}p > 0.05$.

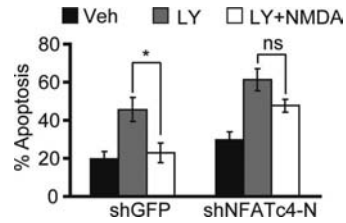

Figure 6. Requirement of NFATc4 for the NMDA-induced neuroprotection. DIV4 cortical neurons were cotransfected with control shRNA (shGFP) or shNFATc4-N together with a β-gal expression plasmid pON260 (1.0 + 0.2 μg of plasmid DNA/5 $\times$ 10^5 cells, respectively). Forty-eight hours later, cells were exposed to 30 μM PI3K inhibitor LY294002 (LY) or vehicle (Veh, 0.2% DMSO). In addition, cells were treated with 10 μM NMDA as indicated. After 24 h, LY294002 increased apoptosis in shGFP- or shNFATc4-transfected neurons. In shGFP-transfected neurons, NMDA suppressed the apoptotic response to LY294002. After NFATc4 knockdown, NMDA-mediated neuroprotection was removed. Data represent four independent experiments $\pm$ SEM; $^{*}p < 0.05$; $^{ns}p > 0.05$.

ate activity of NR2B NMDAR contributes to the regulation of BDNF mRNA levels. This is consistent with the role of NR2B in driving NFAT-mediated transcription and the contribution of the latter to BDNF expression.

If BDNF is among the survival targets of NFATc4, one could expect that its supplementation could protect against apoptotic toxicity of the shNFATc4. Thus, cortical neurons were transfected with shNFATc4-N or shGFP used as a control. Forty-eight hours after transfection, cells were treated with 0 or 10 ng/ml BDNF. After the next 24 h, apoptosis analysis revealed 15 or 28% apoptotic neurons that received shGFP or shNFATc4, respectively ($p < 0.01$) (Fig. 10*A*). BDNF lowered apoptosis of shNFATc4-N-transfected neurons from 28 to 12% ($p < 0.001$) (Fig. 10*A*). In contrast, 10 μM NMDA, which similarly to BDNF protected against PI3K inhibition (Hetman et al., 2002), failed to

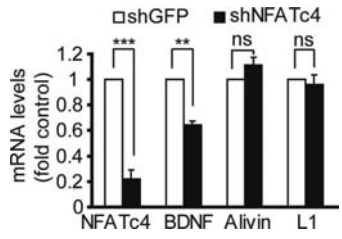

Figure 7. NFATc4 as a regulator of BDNF expression. Freshly isolated cortical neurons were electroporated with control shRNA (shGFP) or shNFATc4-N together with DN-p53 that was added to reduce electroporation toxicity (2.5 + 0.5 μg of plasmid DNA/8 $\times$ 10^6 cells, respectively). Four days later, RNA was isolated and expression of NFATc4 as well as its NMDAR-responsive candidate target genes including *bdnf*, *alivin*, and *l1* was determined using qRT-PCR. rRNA levels (18S) were used for normalizations. The shNFATc4-N significantly reduced NFATc4 and BDNF mRNA levels. Average of three independent experiments are presented. $^{**}p < 0.01$; $^{***}p < 0.001$; $^{ns}p > 0.05$. Error bars are SEM.

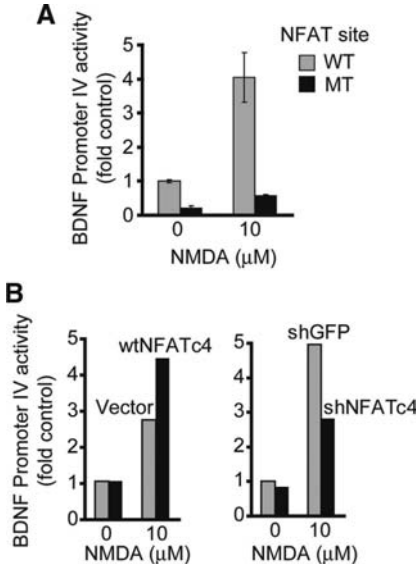

Figure 8. NFATc4 regulation of the NMDA-responsive BDNF promoter IV. ***A***, DIV4 cortical neurons were cotransfected with the β-gal expression plasmid EF1αLacZ and either the wild-type (WT) or mutant (MT) form of human BDNF promoter IV–luciferase reporter construct (0.125 + 0.2 μg of plasmid DNAs/5 $\times$ 10^5 cells, respectively). The mutation consisted of four substitutions inactivating the composite binding sites for NFAT/MEF2 that is fully conserved between primates and rodents (positions 140–156 from the major transcription start site of exon 4). Two days after transfection, cells were stimulated with 10 μM NMDA for 20 h. Disruption of the NFAT/MEF site inhibited NMDA-induced activation of the BDNF promoter IV. Data $\pm$ SD are averages of triplicate sister cultures; similar trends were observed in three independent experiments. ***B***, DIV4 cortical neurons were cotransfected with expression plasmids for NFATc4 or shNFATc4-N together with the rat BDNF promoter IV–CAT reporter construct and the β-gal expression plasmid EF1αLacZ (0.2 or 1.1 + 0.2 + 0.125 μg of plasmid DNAs/5 $\times$ 10^5 cells, respectively). The control plasmids included the empty NFATc4 expression vector pBJ5 (vector) and the shNFATc4-N control shGFP. NMDA stimulation was as in ***A***. In ***B***, data from a representative experiment are shown. Analysis of five independent experiments revealed that the wt-NFATc4 enhanced NMDA-mediated promoter IV activation by 40 $\pm$ 9.5% and the shNFATc4 reduced the activation by 25 $\pm$ 3.65% ($p < 0.001$).

suppress shNFATc4-induced apoptosis (data not shown). These results are consistent with the notion that BDNF maps downstream of the NMDAR-regulated antiapoptotic transcription factor NFATc4 (Fig. 10*B*).

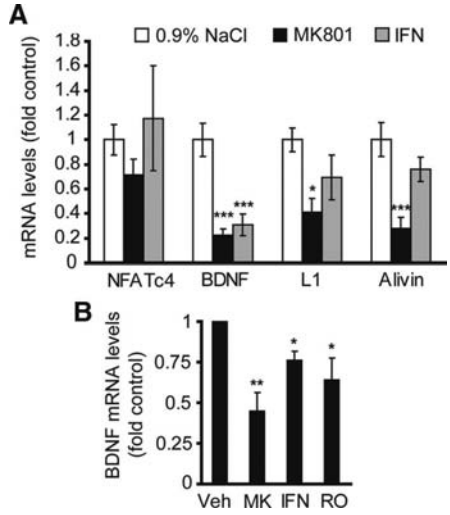

Figure 9. Role of the NR2B in maintenance of BDNF mRNA expression. ***A***, P7 rat pups received single subcutaneous injections of 0.9% NaCl (vehicle control), 10 mg/kg MK801, or 20 mg/kg ifenprodil (IFN). After 3 h, expression of the candidate NMDAR-regulated NFAT target genes was analyzed by qRT-PCR. MK801 or IFN reduced BDNF expression, whereas alivin and l1 declined only in response to MK801. Hence, NR2B appears critical for maintenance of BDNF expression in developing rat cortex. ***B***, In DIV7 cortical neurons, 24 h treatments with 10 μM MK801 (MK), 10 μM ifenprodil (IFN), or 0.5 μM Ro-25-6981 (RO) lowered BDNF mRNA levels. Veh, Vehicle. In ***A***, three animals were treated for each data point; in ***B***, data represent three independent experiments. $^{*}p < 0.05$; $^{**}p < 0.01$; $^{***}p < 0.001$. Error bars are SEM.

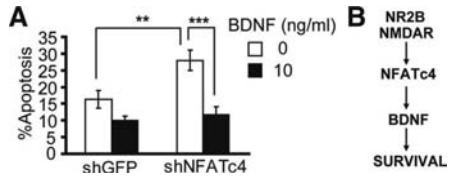

Figure 10. Rescue of shNFATc4-transfected neurons by exogenous BDNF. ***A***, Cortical neurons were transfected as in Figure 5. After 48 h, cells were treated with BDNF for the next 24 h. The shNFATc4-induced apoptosis was suppressed by BDNF. Data from three independent experiments $\pm$ SEM are depicted. $^{**}p < 0.01$; $^{***}p < 0.001$. ***B***, Our results support a model of NR2B-activated survival networks, in which BDNF maps downstream of NFATc4.

Discussion

In this study, we demonstrated that, in cortical neurons, NFATc4 contributes to the NR2B NMDAR-activated antiapoptotic gene expression program. We also identified BDNF as one of the NFATc4-regulated neuroprotective genes.

NFATc4 was expressed in both cultured rat cortical neurons and developing rat cortex in which its expression overlapped with the period of survival dependence on NMDAR activity. Although NFATc1 and NFATc2 were also expressed in developing cortex, only NFATc3 demonstrated an NFATc4-like temporal overlap with NMDAR-dependent cortical neuron survival. Therefore, the NMDAR-NFATc3/c4 signaling may serve development-specific roles, including regulation of neuronal survival and/or differentiation.

The NMDAR-mediated regulation of NFATc3/c4 involved calcineurin/PP2B-dependent nuclear translocation, ERK1/2 activity, and interactions with a partner transcription factor of yet unknown identity. Requirement of PP2B and ERK1/2 is consis-

tent with the activation mechanism that regulates all calcium-dependent isoforms of NFAT in various cell types responding to diverse stimuli (Crabtree and Olson, 2002; Hogan et al., 2003). Conversely, cell type determines the nature of the NFAT partner(s), including representatives of such transcription factor families as MEF2, AP1, Foxo, or inducible cAMP early repressor (ICER) (Crabtree and Olson, 2002; Hogan et al., 2003). Although identification of the NFATc3/c4 partner in NR2B-stimulated cortical neurons will be a subject of our future research, it is tempting to speculate that NFATc4 may synergize with the anti-apoptotic MEF2s or be antagonized by the proapoptotic ICER or Foxo family members (Brunet et al., 1999; Mao et al., 1999; Gaudilliere et al., 2002; Jaworski et al., 2003).

The shRNA-mediated knockdown of NFATc4 but not NFATc3 induced cortical neuron apoptosis. Also, shNFATc4 antagonized NR2B NMDAR-mediated neuroprotection. Therefore, NFATc4 is required for the NR2B-dependent cortical neuron survival. Although survival promoting links between glutamate signaling and the NFATc4 have not been demonstrated before this study, proapoptotic effects of NFATc4 inhibition have been reported in cultured CGNs (Benedito et al., 2005). Conversely, overexpression of active NFATc2/NFAT1 protected CGNs against trophic/neuronal activity deprivation (Benedito et al., 2005). Thus, NFATc4 may underlie neuronal activity/neurotransmitter-mediated survival in various neuronal populations throughout the CNS. However, as exemplified by the joint recruitment of NFATc3/c4 during metamphetamine-induced adult neuronal death (Jayanthi et al., 2005), other NFAT isoforms may cooperate with NFATc4 to support survival of developing neurons.

Although detailed analysis of forebrain development in NFATc4 knock-out mice has not been reported, these animals appeared normal likely attributable to functional compensation by other NFAT isoforms (Graef et al., 2001). Indeed, only double inactivation of NFATc3 and NFATc4 revealed NFAT requirement for axonal growth (Graef et al., 2003). Unfortunately, these double knock-out mice cannot be used to study glutamate-dependent survival in developing forebrain as they die *in utero* before forebrain appears (Graef et al., 2003). In concert with our results indicating that the NFATc4 mediates NMDA-dependent survival but is dispensable for the antiapoptotic effects of BDNF (A. Habas and M. Hetman, unpublished observations), neurotrophin survival response of cultured sensory neurons was not compromised by triple knock-out of NFATc4/c3/c2 (Graef et al., 2003). Therefore, the prosurvival recruitment of NFATc4 may require neuronal activity/neurotransmission and, as such, occur during synaptogenesis but not at the earlier stages of development.

In addition to its role as an antiapoptotic transducer of physiological survival signals in developing neurons, NFAT-driven transcription may also contribute to injury-induced neuronal death (Jayanthi et al., 2005; Luoma and Zirpel, 2008; Sama et al., 2008). Therefore, NFAT-driven transcription may either support or antagonize neuronal survival. The cell type and/or the character of the NFAT activating stimulus and/or its signaling context likely determine the opposite survival outcomes of NFAT activation. Finally, different NFATc isoforms may engage in contradictory regulations of neuronal survival.

Although antiapoptotic effects of NFATc4 may involve regulation of multiple antiapoptotic and proapoptotic genes, we have identified *bdnf* as one of the survival-promoting targets of NFAT. Thus, inhibition of NFATc4 or NR2B NMDAR reduced BDNF expression. Moreover, disruption of the composite NFAT/MEF2 site in the NMDAR-regulated BDNF promoter IV reduced its basal activity as well as responsiveness to NMDA. Conversely, enhancement or reduction of NFATc4 levels increased or decreased NMDA activation of promoter IV, respectively. Finally, exogenous BDNF protected against NFATc4 knockdown (Fig. 10), which by itself did not affect BDNF neuroprotection against several proapoptotic stimuli (Habas and Hetman, unpublished observations). These results are in agreement with previous studies that demonstrated requirement of BDNF for neuroprotective effects of the NMDAR (Marini and Paul, 1992; Bhave et al., 1999; Chen et al., 1999). In addition, they add NFATc4 to the list of BDNF transcriptional regulators in NMDAR-stimulated cortical neurons.

Consistent with BDNF importance for brain development and adult brain plasticity, the *bdnf* gene structure analysis revealed complex regulation of its expression (Aid et al., 2007; Pruunsild et al., 2007). Transcription of rodent BDNF is controlled by at least eight alternative promoters (Aid et al., 2007). In rodent cerebral cortex or in cultured rat or mouse cortical neurons, BDNF promoter IV (formerly known as promoter III) is the major target for neuronal activity modulation of BDNF transcription (Shieh et al., 1998; Tao et al., 1998; Aid et al., 2007; Hong et al., 2008). Also, its activity increases postnatally overlapping with the period of neuronal survival dependence on NMDAR (Aid et al., 2007). In the BDNF promoter IV region, we identified at least one potential NFAT binding site that is conserved between rodents and primates. NFAT may also bind to NFκB sites, and one of them has been suggested to activate promoter IV in NMDA-stimulated CGNs (Lipsky et al., 2001; Hogan et al., 2003). Thus, NFATc4 effects on BDNF promoter IV activity may be through direct interactions with DNA and the transcription machinery. CREB binding to the promoter IV has been shown recently to underlie the major component of the NMDAR-mediated BDNF upregulation in cortical neurons (Hong et al., 2008). Although these results identified CREB as a necessary component for NMDA-induced BDNF transcription, they did not rule out significant contributions by other transcription factors. In fact, it has been shown that CREB may be instrumental for promoter IV recruitment of such calcium-regulated transcriptional regulators as CREB binding protein or the NFAT partner MEF2D (Hong et al., 2008). Because the consensus NFAT site at the position 140 of promoter IV partially overlaps with a consensus site for a potential NFAT partner, MEF2, it is tempting to speculate that NFATc4 and MEF2D interact to regulate BDNF transcription. The non-CREB regulators of promoter IV may be either corequired for its activation by NMDAR and/or determine the maximum levels of the activation.

Besides NMDAR and neuronal activity, BDNF expression is stimulated by the BDNF itself (Groth and Mermelstein, 2003). Because BDNF induction by BDNF was sensitive to PP2B inhibition and because NFATc4 overexpression increased BDNF mRNA levels, it has been proposed that NFATc4 regulates BDNF (Groth and Mermelstein, 2003). By using the NFAT-specific loss-of-function approach, our study adds a piece of critical evidence to support that notion.

Our results indicate that stimulation of BDNF expression plays a role in NR2B NMDAR-mediated cortical neuron survival. Similar observations have been reported for the neuronal activity- and/or NMDAR-dependent survival of cultured rat cortical neurons or CGNs (Marini and Paul, 1992; Ghosh et al., 1994; Bhave et al., 1999; Chen et al., 1999). In addition to promoting survival, BDNF contributes to other key events in the developing nervous system, including morphogenesis or induction of apo-

ptosis (Huang and Reichardt, 2001; Miller and Kaplan, 2001). It remains to be tested whether the NMDAR–NFATc4–BDNF pathway plays a role in these processes. Although inhibition of NMDAR/BDNF cascade is implicated in the pathogenesis of fetal alcohol syndrome, NFATc4 hypoactivity plays a role in pathogenesis of Down syndrome (Bhave et al., 1999; Ikonomidou et al., 2000; Arron et al., 2006). Thus, disruption of the NMDAR–NFATc4 signaling may contribute to genetically or environmentally induced developmental brain disorders that produce mental retardation.

Interestingly, of the three NMDAR-regulated survival genes investigated in this study, only BDNF responded to both NR2B-selective NMDAR blockade and NFATc4 knockdown. Conversely, antiapoptotic cell adhesion molecules alivin and L1 were sensitive to nonselective NMDAR inhibition but not to NR2B NMDAR blocker ifenprodil or shNFATc4. These results suggest specificity of NFATc4 involvement in mediating the effects of NR2B NMDAR stimulation. Likewise, CREB-mediated transcription has been proposed to be preferentially activated by the NR2A receptors (Hardingham et al., 2002). Therefore, NMDAR isoform-specific recruitment of nonoverlapping transcription factors may underlie the differences in gene expression programs that were reported after activation of different NMDAR pools. Alternatively, regulation of NFATc4 may engage various subtypes of NMDAR dependent on the period of nervous system development. After the maturation-associated switch of the synaptic NMDAR from NR2B to NR2A (Cull-Candy and Leszkiewicz, 2004), the synaptic activity-regulated NFATc4 may also alter its NMDAR subtype dependence.

In summary, we identified a novel survival signaling pathway that suppresses apoptosis of developing cortical neurons. This pathway consists of the NR2B NMDAR, the transcription factor NFATc4, and the neurotrophin BDNF. Given the broad developmental impact of both NMDAR and BDNF, it is possible that NMDAR–NFATc4–BDNF signaling affects not only neuronal survival but also other key steps of neuronal differentiation, including synaptogenesis.

References

Aid T, Kazantseva A, Piirsoo M, Palm K, Timmusk T (2007) Mouse and rat BDNF gene structure and expression revisited. J Neurosci Res 85:525–535.

Arron JR, Winslow MM, Polleri A, Chang CP, Wu H, Gao X, Neilson JR, Chen L, Heit JJ, Kim SK, Yamasaki N, Miyakawa T, Francke U, Graef IA, Crabtree GR (2006) NFAT dysregulation by increased dosage of DSCR1 and DYRK1A on chromosome 21. Nature 441:595–600.

Beals CR, Sheridan CM, Turck CW, Gardner P, Crabtree GR (1997) Nuclear export of NF-ATc enhanced by glycogen synthase kinase-3. Science 275:1930–1934.

Benedito AB, Lehtinen M, Massol R, Lopes UG, Kirchhausen T, Rao A, Bonni A (2005) The transcription factor NFAT3 mediates neuronal survival. J Biol Chem 280:2818–2825.

Bhave SV, Ghoda L, Hoffman PL (1999) Brain-derived neurotrophic factor mediates the anti-apoptotic effect of NMDA in cerebellar granule neurons: signal transduction cascades and site of ethanol action. J Neurosci 19:3277–3286.

Bradley KC, Groth RD, Mermelstein PG (2005) Immunolocalization of NFATc4 in the adult mouse brain. J Neurosci Res 82:762–770.

Brummelkamp TR, Bernards R, Agami R (2002) A system for stable expression of short interfering RNAs in mammalian cells. Science 296:550–553.

Brunet A, Bonni A, Zigmond MJ, Lin MZ, Juo P, Hu LS, Anderson MJ, Arden KC, Blenis J, Greenberg ME (1999) Akt promotes cell survival by phosphorylating and inhibiting a Forkhead transcription factor. Cell 96:857–868.

Chen S, Mantei N, Dong L, Schachner M (1999) Prevention of neuronal cell death by neural adhesion molecules L1 and CHL1. J Neurobiol 38:428–439.

Cherrington JM, Mocarski ES (1989) Human cytomegalovirus iel transactivates the α promoter-enhancer via an 18-base-pair repeat element. J Virol 63:1435–1440.

Crabtree GR, Olson EN (2002) NFAT signaling: choreographing the social lives of cells. Cell 109:S67–S79.

Cull-Candy SG, Leszkiewicz DN (2004) Role of distinct NMDA receptor subtypes at central synapses. Sci STKE 2004:re16.

Deppmann CD, Mihalas S, Sharma N, Lonze BE, Niebur E, Ginty DD (2008) A model for neuronal competition during development. Science 320: 369–373.

Gaudilliere B, Shi Y, Bonni A (2002) RNA interference reveals a requirement for myocyte enhancer factor 2A in activity-dependent neuronal survival. J Biol Chem 277:46442–46446.

Ghosh A, Carnahan J, Greenberg ME (1994) Requirement for BDNF in activity-dependent survival of cortical neurons. Science 263:1618–1623.

Gonzalez-Zulueta M, Feldman AB, Klesse LJ, Kalb RG, Dillman JF, Parada LF, Dawson TM, Dawson VL (2000) Requirement for nitric oxide activation of p21(ras)/extracellular regulated kinase in neuronal ischemic preconditioning. Proc Natl Acad Sci U S A 97:436–441.

Graef IA, Mermelstein PG, Stankunas K, Neilson JR, Deisseroth K, Tsien RW, Crabtree GR (1999) L-type calcium channels and GSK-3 regulate the activity of NF-ATc4 in hippocampal neurons. Nature 401:703–708.

Graef IA, Chen F, Chen L, Kuo A, Crabtree GR (2001) Signals transduced by Ca^{2+}/calcineurin and NFATc3/c4 pattern the developing vasculature. Cell 105:863–875.

Graef IA, Wang F, Charron F, Chen L, Neilson J, Tessier-Lavigne M, Crabtree GR (2003) Neurotrophins and netrins require calcineurin/NFAT signaling to stimulate outgrowth of embryonic axons. Cell 113:657–670.

Groth RD, Mermelstein PG (2003) Brain-derived neurotrophic factor activation of NFAT (nuclear factor of activated T-cells)-dependent transcription: a role for the transcription factor NFATc4 in neurotrophin-mediated gene expression. J Neurosci 23:8125–8134.

Habas A, Kharebava G, Szatmari E, Hetman M (2006) NMDA neuroprotection against a phosphatidylinositol-3 kinase inhibitor, LY294002 by NR2B-mediated suppression of glycogen synthase kinase-3beta-induced apoptosis. J Neurochem 96:335–348.

Hardingham GE (2006) Pro-survival signalling from the NMDA receptor. Biochem Soc Trans 34:936–938.

Hardingham GE, Fukunaga Y, Bading H (2002) Extrasynaptic NMDARs oppose synaptic NMDARs by triggering CREB shut-off and cell death pathways. Nat Neurosci 5:405–414.

Hetman M, Kharebava G (2006) Survival signaling pathways activated by NMDA receptors. Curr Top Med Chem 6:787–799.

Hetman M, Hsuan SL, Habas A, Higgins MJ, Xia Z (2002) ERK1/2 antagonizes glycogen synthase kinase-3beta-induced apoptosis in cortical neurons. J Biol Chem 277:49577–49584.

Hogan PG, Chen L, Nardone J, Rao A (2003) Transcriptional regulation by calcium, calcineurin, and NFAT. Genes Dev 17:2205–2232.

Hong EJ, McCord AE, Greenberg ME (2008) A biological function for the neuronal activity-dependent component of Bdnf transcription in the development of cortical inhibition. Neuron 60:610–624.

Huang EJ, Reichardt LF (2001) Neurotrophins: roles in neuronal development and function. Annu Rev Neurosci 24:677–736.

Ikonomidou C, Bosch F, Miksa M, Bittigau P, Vöckler J, Dikranian K, Tenkova TI, Stefovska V, Turski L, Olney JW (1999) Blockade of NMDA receptors and apoptotic neurodegeneration in the developing brain. Science 283:70–74.

Ikonomidou C, Bittigau P, Ishimaru MJ, Wozniak DF, Koch C, Genz K, Price MT, Stefovska V, Hörster F, Tenkova T, Dikranian K, Olney JW (2000) Ethanol-induced apoptotic neurodegeneration and fetal alcohol syndrome. Science 287:1056–1060.

Impey S, Smith DM, Obrietan K, Donahue R, Wade C, Storm DR (1998) Stimulation of cAMP response element (CRE)-mediated transcription during contextual learning. Nat Neurosci 1:595–601.

Jaworski J, Mioduszewska B, Sánchez-Capelo A, Figiel I, Habas A, Gozdz A, Proszynski T, Hetman M, Mallet J, Kaczmarek L (2003) Inducible cAMP early repressor, an endogenous antagonist of cAMP responsive element-binding protein, evokes neuronal apoptosis *in vitro*. J Neurosci 23:4519–4526.

Jayanthi S, Deng X, Ladenheim B, McCoy MT, Cluster A, Cai NS, Cadet JL (2005) Calcineurin/NFAT-induced up-regulation of the Fas ligand/Fas

death pathway is involved in methamphetamine-induced neuronal apoptosis. Proc Natl Acad Sci U S A 102:868–873.

Kalita K, Kharebava G, Zheng JJ, Hetman M (2006) Role of megakaryoblastic acute leukemia-1 in ERK1/2-dependent stimulation of serum response factor-driven transcription by BDNF or increased synaptic activity. J Neurosci 26:10020–10032.

Lee B, Butcher GQ, Hoyt KR, Impey S, Obrietan K (2005) Activity-dependent neuroprotection and cAMP response element-binding protein (CREB): kinase coupling, stimulus intensity, and temporal regulation of CREB phosphorylation at serine 133. J Neurosci 25:1137–1148.

Lipsky RH, Xu K, Zhu D, Kelly C, Terhakopian A, Novelli A, Marini AM (2001) Nuclear factor kappaB is a critical determinant in *N*-methyl-D-aspartate receptor-mediated neuroprotection. J Neurochem 78:254–264.

Luoma JI, Zirpel L (2008) Deafferentation-induced activation of NFAT (nuclear factor of activated T-cells) in cochlear nucleus neurons during a developmental critical period: a role for NFATc4-dependent apoptosis in the CNS. J Neurosci 28:3159–3169.

Mao Z, Bonni A, Xia F, Nadal-Vicens M, Greenberg ME (1999) Neuronal activity-dependent cell survival mediated by transcription factor MEF2. Science 286:785–790.

Marini AM, Paul SM (1992) *N*-methyl-D-aspartate receptor-mediated neuroprotection in cerebellar granule cells requires new RNA and protein synthesis. Proc Natl Acad Sci U S A 89:6555–6559.

Miller FD, Kaplan DR (2001) Neurotrophin signalling pathways regulating neuronal apoptosis. Cell Mol Life Sci 58:1045–1053.

Nakanishi S (1992) Molecular diversity of glutamate receptors and implications for brain function. Science 258:597–603.

Nguyen T, Lindner R, Tedeschi A, Forsberg K, Green A, Wuttke A, Gaub P, Di Giovanni S (2009) NFAT-3 is a transcriptional repressor of the growth-associated protein 43 during neuronal maturation. J Biol Chem 284:18816–18823.

Oppenheim RW (1991) Cell death during development of the nervous system. Annu Rev Neurosci 14:453–501.

Papadia S, Stevenson P, Hardingham NR, Bading H, Hardingham GE (2005) Nuclear Ca^{2+} and the cAMP response element-binding protein family mediate a late phase of activity-dependent neuroprotection. J Neurosci 25:4279–4287.

Papadia S, Soriano FX, Léveillé F, Martel MA, Dakin KA, Hansen HH, Kaindl A, Sifringer M, Fowler J, Stefovska V, McKenzie G, Craigon M, Corriveau R, Ghazal P, Horsburgh K, Yankner BA, Wyllie DJ, Ikonomidou C, Hardingham GE (2008) Synaptic NMDA receptor activity boosts intrinsic antioxidant defenses. Nat Neurosci 11:476–487.

Pruunsild P, Kazantseva A, Aid T, Palm K, Timmusk T (2007) Dissecting the human BDNF locus: bidirectional transcription, complex splicing, and multiple promoters. Genomics 90:397–406.

Sama MA, Mathis DM, Furman JL, Abdul HM, Artiushin IA, Kraner SD, Norris CM (2008) Interleukin-1beta-dependent signaling between astrocytes and neurons depends critically on astrocytic calcineurin/NFAT activity. J Biol Chem 283:21953–21964.

Seybold VS, Coicou LG, Groth RD, Mermelstein PG (2006) Substance P initiates NFAT-dependent gene expression in spinal neurons. J Neurochem 97:397–407.

Shaulian E, Zauberman A, Ginsberg D, Oren M (1992) Identification of a minimal transforming domain of p53: negative dominance through abrogation of sequence-specific DNA binding. Mol Cell Biol 12:5581–5592.

Sheng M, Cummings J, Roldan LA, Jan YN, Jan LY (1994) Changing subunit composition of heteromeric NMDA receptors during development of rat cortex. Nature 368:144–147.

Shieh PB, Hu SC, Bobb K, Timmusk T, Ghosh A (1998) Identification of a signaling pathway involved in calcium regulation of BDNF expression. Neuron 20:727–740.

Snider WD (1994) Functions of the neurotrophins during nervous system development: what the knockouts are teaching us. Cell 77:627–638.

Tao X, Finkbeiner S, Arnold DB, Shaywitz AJ, Greenberg ME (1998) Ca^{2+} influx regulates BDNF transcription by a CREB family transcription factor-dependent mechanism. Neuron 20:709–726.

Vihma H, Pruunsild P, Timmusk T (2008) Alternative splicing and expression of human and mouse NFAT genes. Genomics 92:279–291.

Wilkins BJ, Dai YS, Bueno OF, Parsons SA, Xu J, Plank DM, Jones F, Kimball TR, Molkentin JD (2004) Calcineurin/NFAT coupling participates in pathological, but not physiological, cardiac hypertrophy. Circ Res 94:110–118.

Yang TT, Chow CW (2003) Transcription cooperation by NFAT.C/EBP composite enhancer complex. J Biol Chem 278:15874–15885.

MANUSCRIPT

Pruunsild P, Sepp M, Orav E, Koppel I, Timmusk T.
Identification of *cis*-elements and transcription factors regulating neuronal activity-dependent transcription of human *BDNF* gene

Title Page

Journal Section: Cellular & Molecular

Title: Identification of *cis*-elements and transcription factors regulating neuronal activity-dependent transcription of human *BDNF* gene

Abbreviated title: Activity-dependent h*BDNF* transcription

Authors and authors' address: Priit Pruunsild, Mari Sepp, Ester Orav, Indrek Koppel and Tõnis Timmusk

Institute of Gene Technology, Tallinn University of Technology, Estonia

Corresponding authors: Tõnis Timmusk,

Institute of Gene Technology, Tallinn University of Technology, Akadeemia tee 15, 12618, Tallinn, Estonia. e-mail: tonis.timmusk@ttu.ee and

Priit Pruunsild, Institute of Gene Technology, Tallinn University of Technology, Akadeemia tee 15, 12618, Tallinn, Estonia. e-mail: priit.pruunsild@ttu.ee

Number of figures and tables: 7 figures

Contents of supplemental material: 1 table and 3 figures

Number of pages: 39

Number of words for

abstract: 216

introduction: 499

discussion: 1594

Key words: calcium-dependent transcription, neuronal activity, promoter, bHLH-PAS, CREB, DREAM

Acknowledgements: We thank Enn Jõeste from North Estonian Regional Hospital, Tallinn, for collaboration and Epp Väli for technical assistance. This work was supported by Wellcome Trust (Grant 067952), Estonian Ministry of Education and Research (Grant 0140143), Estonian Enterprise (Grant EU27553).

Abstract

Brain derived neurotrophic factor (BDNF) is an important mediator of activity-dependent functions of the nervous system and its expression is dysregulated in several neuropsychiatric disorders. Regulation of rodent *BDNF* neuronal activity-dependent transcription has been relatively well characterized. Here, we have studied regulation of human *BDNF* (h*BDNF*) transcription by membrane depolarization of cultured mouse or rat primary cortical neurons expressing h*BDNF* gene or transfected with h*BDNF* promoter constructs, respectively. We identified an asymmetric E-box-like element, PasRE, in h*BDNF* promoter I and demonstrate that binding of this element by bHLH-PAS transcription factors ARNT2 and NPAS4 is crucial for neuronal activity-dependent transcription from promoter I. We show that binding of CREB to the cAMP/Ca^{2+}-response element (CRE) in h*BDNF* promoter IV is critical for activity-dependent transcription from this promoter and that USF transcription factors also contribute to the activation by binding to the upstream stimulatory factor binding element (UBE) in h*BDNF* promoter IV. However, we report that full induction of h*BDNF* exon IV mRNA transcription is dependent on ARNT2 and NPAS4 binding to a PasRE in promoter IV. Finally, we demonstrate that CRE and PasRE elements in h*BDNF* promoter IX are required for the induction of this promoter by neuronal activity. Taken together, this study has identified the *cis*-elements and transcription factors regulating neuronal activity-dependent transcription of human *BDNF* gene.

Introduction

Neuronal activity-responsive transcription is an important component in development and in adaptive functions of the nervous system. Neuronal activity leads to expression of about 300 genes (Lin et al., 2008), including *BDNF*, one of the major mediators of activity-dependent functions (Poo, 2001). BDNF was first described to support survival of embryonic sensory neurons (Barde et al., 1982). Currently, BDNF is implicated in survival and differentiation of several neuronal populations and in regulation of synaptic plasticity, LTP, learning, memory and neurogenesis (Ernfors et al., 1994; Jones et al., 1994; Patterson et al., 1996; Lyons et al., 1999; Hall et al., 2000; Binder and Scharfman, 2004). Moreover, neuronal activity-dependent transcription of *BDNF* has been shown to be essential for development of cortical inhibition (Hong et al., 2008).

Regulation of *BDNF* has been thoroughly studied in rodents. Rat *BDNF* (r*BDNF*) gene was first described to have four promoters driving expression of transcripts containing different 5' exons spliced to a single coding exon (Timmusk et al., 1993). To date it has been found that rodent *BDNF* (rod*BDNF*) contains nine exons (Aid et al., 2007) and several regulators of calcium-dependent up-regulation have been identified. Foremost, r*BDNF* promoter IV (pIV) is up-regulated via CREB (alias CREB1) binding to a cAMP/Ca^{2+}-response element (CRE) (Shieh et al., 1998; Tao et al., 1998). This is modulated by USF-s and CaRF binding to an E-box element and a CaRE1 element, respectively (Tao et al., 2002; Chen et al., 2003a). Additionally, MeCP2, BHLHB2 and NFkB have been shown to regulate rodent pIV (Chen et al., 2003b; Jiang et al., 2008). However, CRE plays a central role because knock-in mutation of CRE blocks mouse *BDNF* (m*BDNF*) pIV activity-responsiveness *in vivo* (Hong et al., 2008). Exon I of r*BDNF* is also induced by neuronal activity (Timmusk et al., 1993). CREB, USF-s, MEF2D and NFkB have been implicated in mediating the induction (Tabuchi et al., 2002; Lubin et al., 2007; Flavell et al., 2008). Additionally, NPAS4 has been shown to bind pI and pIV of m*BDNF* (Lin et al., 2008), but the binding sites were not specified. Finally, *BDNF* exon IXa transcripts are also up-regulated whereas levels of mRNAs with other 5' exons are elevated to a lesser extent or not influenced by neuronal activity (Koppel et al., 2009).

Decreased *BDNF* expression has been documented in neurodegenerative diseases and in cognitive, mood and anxiety disorders (Binder and Scharfman, 2004). To enable studying human *BDNF* (h*BDNF*) transcription, h*BDNF* gene structure was described. Similarly to rod*BDNF*, multiple 5' exons are spliced to a single coding exon in human and altogether the h*BDNF* gene contains 11 exons and nine promoters (Pruunsild et al., 2007). Importantly, there are two human-specific exons in h*BDNF* and additionally, the locus comprises a non-coding antisense gene that is absent in rodents (Pruunsild et al., 2007). Although much is known about regulation of rod*BDNF*, regulation of h*BDNF* by neuronal-activity has been poorly studied. Here, we identify *cis*-elements and transcription factors involved in h*BDNF* transcriptional activation by membrane depolarization of cultured cortical neurons.

Materials and Methods

Primary neuron cultures. All animal procedures were carried out in compliance with the local ethics committee. Primary neuron cultures from human *BDNF*-BAC mice, line C3 (Koppel et al., 2009), were generated from P0 mouse brains and the rat primary neuron cultures for luciferase assays were generated from E21 rat embryo brains (Sprague–Dawley). Briefly, the cortices, together with hippocampi, were dissected and cells were dissociated with 0.25 % trypsin (Gibco), treated with 0.05% DNase I (Roche) and the cell suspension was plated on poly-L-lysine-coated dishes in Neurobasal A medium (Gibco) with B27 supplement (Gibco), penicillin (PAA, 100 U/ml), streptomycin (PAA, 0,1 mg/ml) and 1 mM L-glutamine (PAA). Mitotic inhibitor 5-fluoro-2′-deoxyuridine (Sigma) was added to the medium (10 μM) at 2 DIV. For modeling neuronal activity by activation of voltage-sensitive calcium channels, final concentration of 25 mM KCl was added to the medium at 7 DIV (mouse primary neurons) and *BDNF* gene expression was analyzed by RT-qPCR using RNA isolated at indicated time points. Transfection and KCl treatment of rat primary neurons are specified in *DNA transfection and luciferase assay* section of Materials and Methods. Amaxa nucleofection with GFP or dominant negative ARNT2 (delTAD-ARNT2) and NPAS4 (delTAD-NPAS4) coding constructs was performed with the Amaxa Rat Neuron Nucleofector Kit (Lonza).

Briefly, 10^7 E19 rat primary neurons were electroporated with 5 ug of indicated plasmid using the pre-defined program O-003 of the Nucleofector II (Lonza) according to the manufacturer's instructions. Nucleofected neurons were treated with KCl at 5 DIV and endogenous rat *BDNF* transcript levels were measured by RT-qPCR using RNA isolated at indicated time points.

DNA constructs and mutagenesis. h*BDNF* promoter regions and r*BDNF* pI were amplified from human genomic DNA and rat genomic DNA, respectively, using Expand High Fidelity PCR System (Roche). All *BDNF* promoters were cloned into the pGL4.15[luc2P/Hygro] (Promega) in front of firefly luciferase coding sequence. For normalization of the luciferase assays promoter of human *EF1alpha* was cloned into the pGL4.83[hRlucP/Puro] in front of Renilla luciferase. Mutagenesis was performed using complementary primers against the target sequence containing the respective mutation (listed in Supplementary Table S1) with Phusion High-Fidelity DNA Polymerase (Finnzymes) according to manufacturer's instructions. After 25 cycles of PCR the samples were treated with the DpnI restriction enzyme (Fermentas) to degrade the WT template plasmid and transformed into TOP10 competent cells (Invitrogen). All promoter sequences were verified by sequencing and are shown in Supplementary Figures 1 and 2. Full length coding regions of human CREB1, USF1, USF2, ARNT2, NPAS4, SIM2 and DREAM family members were amplified from human cDNA using Phusion High-Fidelity DNA Polymerase (Finnzymes) (primers listed in Supplementary Table S1) and cloned into the pcDNA3.1 vector (Invitrogen). The viral transcription activator domain VP16 was obtained from the vector pACT (Promega). The delTAD-ARNT2 and delTAD-NPAS4 constructs expressing ARNT2 and NPAS4 proteins without C-terminal transcription activator domains were generated by removing the 3' part of cDNAs. In human ARNT2, DNA sequence downstream of the ClaI (Bsu15I, Fermentas) restriction site was removed and in human NPAS4, DNA sequence downstream of the more 5' located XmnI (PdmI, Fermentas) restriction site of two XmnI sites was removed, creating constructs coding for ARNT2 amino acids 1 - Arg402 and NPAS4 amino acids 1 - Glu348.

DNA transfection and luciferase assays. Rat primary neurons were transfected at 6-7 DIV with *BDNF*promoter/pGL4.15[luc2P/Hygro] plasmids using Lipofectamine 2000 transfection reagent (Invitrogen) according to manufacturer's instructions. 1 µg/2 µl ratio of DNA/Lipofectamine and 0.5

µg DNA per 0.75 cm² well of a 48-well cell culture plate was used. The effector protein pcDNA3.1 expression constructs were cotransfected in 1:1 ratio with the *BDNF* promoter construct where indicated. For normalization, p*EF1alpha*/pGL4.83[luc2P/Hygro] (1/100 of *BDNF* promoter construct quantity) was cotransfected. At 8-9 DIV neuronal membranes were depolarized by addition of 25 mM KCl to the medium and luciferase assays were performed with the Dual-Glo Luciferase Assay System (Promega) using cell lysates prepared at indicated time points. At least three independent experiments were performed. For presentation of data in relative luciferase units (RLUs), the background signals from untransfected neurons were subtracted from signals obtained from transfected cells and the firefly luciferase signal values were normalized to *EF1alpha* promoter-dependent Renilla luciferase signals. All data were log-transformed and autoscaled using the data of the longest WT promoter in case of *cis*-element mapping, data of the pRC co-transfected WT promoter in case of effector overexpression analyses and using all data in case of induction time-course analyses. Means and standard deviations (SD) were calculated and t-tests for analyses of statistical significance were performed. For graphical representation, the data were back-transformed to the original scale. Error bars represent upper and lower limits back-transformed as mean + SD and mean – SD, respectively.

RNA isolation and RT-qPCR. Total RNA from primary neurons or HEK293 cells was purified using RNeasy Micro kit (Qiagen) as recommended by the manufacturer. First-strand cDNAs were synthesized from 500-2000 ng of total RNA with Superscript III reverse transcriptase (Invitrogen) according to manufacturer's recommendations using oligo(dT) primers. The cDNA was used for quantitative PCR with the qPCR Core kit for SYBR® Green I No Rox (Eurogentec) and LightCycler 2.0 (Roche). At least three independent experiments were performed and each sample was measured in triplicates with primers targeting the respective transcript. Expression of the housekeeping gene *HPRT1* was used for normalization. All primers used are listed in Supplementary Table S1. The data were log-transformed, autoscaled, means and standard deviations (SD) were calculated and t-tests were performed. Then, the data were back-transformed into the original scale. Error bars represent upper and lower limits back-transformed as mean + SD and mean – SD, respectively. For quantitative measurement of *BDNF* exon I to exon IV ratio with qPCR, human exon I and exon IV PCR products were cloned together in tail-to-tail orientation in one plasmid construct and the respective mouse PCR

products in another construct. Plasmid template standard curves spanning at least five orders of magnitude were generated with the same 10-fold serial dilutions with exactly 1:1 ratio of template for h*BDNF* or m*BDNF* exon I and IV qPCR primers, respectively. These directly comparable plasmid standard curves were used to quantify the relative abundance of *BDNF* exon I transcripts compared to exon IV transcripts in control untreated h*BDNF*-BAC mice primary neurons and neurons depolarized 8h with KCl. Three independent experiments were used for calculations. Error bars represent SD.

Electrophoretic mobility shift assay (EMSA). Neuronal lysates were prepared for EMSA as follows. The cells on 10 cm dish were washed with PBS and scraped in 200 µl of ice cold sonication buffer (20 mM HEPES-KOH pH 7.9, 25% glycerol, 0.5 M KCl, 1.5 mM $MgCl_2$, 0.4 mM EDTA, 5 mM DTT, 1 mM EGTA, 0.5 mM PMSF and protease inhibitors (Roche Complete Protease Inhibitor Cocktail). After sonication the lysates were centrifuged at maximum speed for 10 min in table-top centrifuge at 4 °C, the pellet was discarded and the lysates were stored in –80 °C. The *in vitro* translated proteins were produced using TnT Quick Coupled Transcription/Translation System (Promega) according to manufacturer's instructions using unlabeled methionine. Oligos used in EMSA assays were radioactively labeled with T4 polynucleotide kinase (Fermentas) according to manufacturer's instructions. For oligo binding reaction 10 µg of protein in 15 µl reaction buffer (10 mM HEPES-KOH pH 7.9, 10% glycerol, 0.1 mM EDTA, 8 mM $MgC1_2$ and 1 mM dithiothreitol) containing 0.2 µg of poly(dI-dC) was preincubated 10 min on ice. For obtaining the ARNT2-NPAS4 shift the reaction buffer contained 10 mM Tris-HCl pH 7.5, 50 mM NaCl, 1 mM EDTA, 1 mM dithiothreitol, 5% glycerol and 0,02% β-ME and 1 µg of poly(dI-dC) was added. Then, 0.15 pmol of radioactively labeled oligonucleotide was added and incubated 20 min at RT. For DNA competition, 10-fold excess of unlabeled double-stranded oligonucleotide was added 5 min before the probe. Where indicated, protein lysate was incubated with 0.5 µg of respective antibody (ab) in reaction buffer prior to incubation with the radioactively-labeled probe. The ab-s used were rabbit anti-CREB1 (Millipore cat# 06-863), rabbit anti-phospho-CREB1(Ser133) (Millipore cat# 06-519), rabbit anti-USF1 (Cemines cat# HLH230), rabbit anti USF2 (Cemines cat# HLH240), rabbit anti-ARNT2 (Santa Cruz Biotechnology, cat# sc-5581X) and rabbit anti-NPAS4 (Aviva Systems Biology, cat#

ARP32556_P050). The DNA-protein complexes were resolved in 5% nondenaturing polyacrylamide gel and visualized by autoradiography.

Western Blot. Proteins were separated by 8% SDS-PAGE and transferred to polyvinylidene fluoride membrane (Millipore). For blotting, membranes were blocked in 5% skim milk and 0.05% Tween 20 in PBS for 30 min at RT. Next, membranes were incubated with the respective primary ab for 1 h and then with secondary ab for 1 hour at RT. Three washing steps with 0.05% Tween 20 in PBS followed both incubations. Primary ab-s were diluted in 5% skim milk and 0.05% Tween 20 in PBS as follows: rabbit anti-NPAS4 (Aviva Systems Biology, cat# ARP32556_P050) 1:2000, rabbit anti-ARNT2 (Santa Cruz Biotechnology, cat# sc-5581X) 1:5000, rabbit anti-CREB1 (Millipore cat# 06-863) 1:2000, mouse anti-V5 (Invitrogen cat# R960-25) 1:5000, mouse anti-VP16 (clone 2GV-4) (Eurogentec) 1:5000. The HRP-conjugated goat anti-mouse or anti-rabbit IgG secondary ab-s (Pierce) were diluted 1:5000. Chemiluminescent signal was detected using SuperSignal West Femto Chemiluminescent Substrate (Pierce).

Chromatin immunoprecipitation (ChIP). For ChIP with HEK293 cells, cells grown on 10 cm dishes were transfected with plasmids coding V5-tagged or untagged proteins, as indicated, by LipoD293 DNA In Vitro Transfection Reagent (Signagen) according to manufacturer's instructions. 1 µg/2 µl ratio of DNA/LipoD293 and 5 µg DNA per 10 cm cell culture dish was used. Crosslinking with 1% formaldehyde was performed for 10 min 24h post-transfection. Crosslinking reaction was quenched by the addition of 1/10th volume of 1.25 M glycine to the medium and the cells were washed twice with 1x PBS. Cells were lysed with lysis buffer (1% SDS, 10 mM EDTA, 50 mM Tris-HCl, pH 8.0, with protease inhibitors). Then, the lysate was sonicated to obtain 200 bp - 1000 bp fragments of genomic DNA and insoluble material was spun down for 5 minutes at maximum speed in a table-top centrifuge. For ChIP with human postmortem parietal cortex samples, frozen tissue was chopped into small pieces with a razor blade and inserted into 1x PBS. Crosslinking was performed with final concentration of 1% formaldehyde for 15 min at RT and quenched by adding glycine to a final concentration of 0.125 M. The samples were transferred on ice and washed twice with 1x PBS. Dounce homogenizer was used to disaggregate the tissue. Cells were lysed with lysis buffer (0.5% NP40, 85 mM KCl, 5 mM PIPES pH 8.0, with protease inhibitors) on ice for 15 minutes. Then, nuclei

were pelleted and resuspended in nuclei lysis buffer (1% SDS, 10 mM EDTA, 50 mM Tris-HCl, pH 8.0, with protease inhibitors) and incubated on ice for 20 min. The lysate was sonicated as described for ChIP with HEK cells. Anti-V5 agarose (Sigma) or protein A sepharose (GE Healthcare) for HEK293 or tissue ChIP, respectively (both 40 µl of 50% slurry per reaction), was pre-absorbed with 200 µg/ml BSA and 10 µg/ml sheared salmon sperm DNA by rotating overnight at 4°C in dilution buffer (1% Triton X-100, 150 mM NaCl, 2 mM EDTA, 20 mM Tris-HCl, pH 8.0, with protease inhibitors). For HEK293 ChIP, anti-V5 agarose was then added to the lysate that was diluted 1:9 with dilution buffer and the samples were rotated for 6 h at 4°C. For tissue ChIP the lysate was diluted 1:9 with dilution buffer and incubated with rabbit anti-CREB1 (Millipore cat# 06-863), rabbit anti-ARNT2 (Santa Cruz Biotechnology, cat# sc-5581X) ab, both 1:1000, or without ab, overnight at 4°C and then the pre-absorbed protein A sepharose was added for two hours. The following steps for both ChIP experiments were as follows. Agarose- or sepharose-chromatin complexes were washed 3 times with wash buffer (1% Triton X-100, 0.1% SDS, 150 mM NaCl, 2 mM EDTA, 20 mM Tris-HCl, pH 8.0, with protease inhibitors) and once with final wash buffer (1% Triton X-100, 0.1% SDS, 500 mM NaCl, 2 mM EDTA, 20 mM Tris-HCl, pH 8.0, with protease inhibitors). The immune complexes were eluted 3 times by addition of 50 µl elution buffer (1% SDS and 100 mM $NaHCO_3$) and the eluates of the same sample were combined. Cross-links were reversed by incubating the eluates with 200 mM NaCl at 65°C overnight. DNA was purified with QIAquick PCR Purification Kit (Qiagen) and analyzed by qPCR with the qPCR Core kit for SYBR® Green I No Rox (Eurogentec) and LightCycler 2.0 (Roche). Three independent experiments were performed and each sample was measured in triplicate with primers detecting the indicated genomic regions (Supplementary Table S1). For HEK293 ChIP the data was normalized to the levels of the respective target in input DNA. All data were log-transformed, autoscaled, means and standard deviations (SD) were calculated and t-tests for analyses of statistical significance were performed. For graphical representation, the data were back-transformed into the original scale. The error bars represent upper and lower limits back-transformed as mean + SD and mean – SD, respectively.

Results

Human *BDNF* exon I and IV transcripts are up-regulated in primary cortical neurons by KCl depolarization

Bacterial artificial chromosome (BAC) transgenic mice with the human *BDNF* gene generated in our group beforehand (Koppel et al., 2009) were used to determine whether h*BDNF* expression is up-regulated in response to neuronal activity in cultured primary cortical neurons. Depolarization of primary neuronal membranes with KCl treatment was used as the model of neuronal activity. Primary neurons cultured 7 days in vitro (DIV) were treated with 25 mM KCl and the levels of the transgenic human and endogenous mouse *BDNF* mRNAs were measured by RT-qPCR. In addition, neurons were treated with KCl for different time periods to compare the time courses of up-regulation between m*BDNF* and h*BDNF* mRNAs. Firstly, the results showed that total h*BDNF* mRNA, measured with primers detecting all of the h*BDNF* transcripts, was up-regulated in these neurons similarly to the endogenous total m*BDNF* (Fig. 1A). However, m*BDNF* mRNA levels were elevated more than the transgenic h*BDNF* mRNA levels (Fig. 1A). Next, we analyzed the up-regulation of different *BDNF* exon-specific transcripts. As evidenced by Figure 1B, both h*BDNF* and m*BDNF* exon I and exon IV containing transcripts were the most up-regulated *BDNF* mRNAs by neuronal depolarization. h*BDNF* exon I and IV transcripts reached to approximately 120- and 27-fold higher levels, respectively, and m*BDNF* exon I and IV transcripts approximately 230- and 32-fold higher levels, respectively, than the levels of these transcripts in untreated neurons (Fig. 1B). The time courses of induction of h*BDNF* and m*BDNF* exon I containing transcripts were similar – after 2h of KCl treatment the levels of exon I mRNAs were about 10 % of full induction that was reached by 4h and 8h, respectively (Fig. 1B). Although not statistically significant, the induction time course of exon IV transcripts differed to some extent between m*BDNF* and h*BDNF* – m*BDNF* exon IV mRNA levels reached near to the maximum already after 2h of KCl treatment whereas h*BDNF* exon IV levels were about half of maximum after 2h and continued to rise also after 4h of KCl treatment (Fig. 1B). With a slightly weaker rise in levels compared to m*BDNF* exon IV transcripts, m*BDNF* transcripts with exon IX as the 5' exon (IX-5')

were also induced (Fig. 1B). Interestingly, the levels of m*BDNF* IX-5' mRNA were considerably more elevated than the respective h*BDNF* mRNA levels (Fig. 1B). Both h*BDNF* and m*BDNF* exon II and VI transcript levels were also elevated in response to KCl treatment, but the induction was by far weaker than the induction of exon I and exon IV transcripts, respectively (Fig. 1B). Therefore, as *BDNF* exons are divided into clusters in the genome (Timmusk et al., 1993; Pruunsild et al., 2007), it is plausible that exon I is the major activity regulated exon in the first cluster and exon IV is the major activity-regulated exon in the second cluster. Of note, expression of transcripts containing other 5' exons of h*BDNF* was undetectable in cultured neurons from h*BDNF*-BAC mice. Collectively, these data show that h*BDNF* transcripts are up-regulated in response to depolarization of primary neurons and that rodent neurons can be used as a model for studying neuronal activity-dependent regulation of h*BDNF* promoters.

Provided that induction of both h*BDNF* and m*BDNF* exon I transcripts was particularly strong, we measured the relative abundance of exon I transcripts compared to exon IV transcripts in transgenic mouse primary neurons before and after KCl-depolarization. For that we cloned the human exon I and exon IV PCR products together in one plasmid construct and the respective mouse PCR products in another construct, which enabled us to use the dilution series of these plasmids as reference for calculating the ratio of exon I to exon IV mRNA. The results showed that h*BDNF* exon I transcripts reached to comparable levels with exon IV transcript levels upon depolarization of neurons (Fig. 1C). m*BDNF* exon I transcript levels were elevated to approximately 60% of mouse exon IV transcript levels (Fig. 1C). We detected a significant difference in the ratio of exon I to exon IV mRNAs transcribed from h*BDNF* compared to m*BDNF* in uninduced cells: while the levels of mouse exon I transcripts were approximately 20-fold lower compared to the levels of mouse exon IV transcripts, the human exon I mRNAs were only 4-fold less abundant than human exon IV mRNAs (Fig. 1C). Considering this and that the r*BDNF* exon I mRNAs have been reported to constitute less than 5% of total *BDNF* mRNAs in the adult rat cortex (Timmusk et al., 1994), whereas exon I transcripts in adult human parietal cortex have been found to be half as abundant as exon IV mRNAs (Garzon and Fahnestock, 2007), we conclude that *BDNF* exon I transcripts could represent a relatively larger proportion of total *BDNF* mRNAs in human brain than in rodent brain.

Next, we cloned the promoter regions of h*BDNF* major exons and the human-specific 5' exon Vh in front of luciferase reporter and analyzed their ability to induce luciferase activity in response to KCl-depolarization in rat primary neurons. We used rat neurons because in majority of previous studies that have determined the regulatory elements for rodent *BDNF*, rat primary neuronal cultures have been used (Shieh et al., 1998; Tao et al., 1998; Tabuchi et al., 2002; Chen et al., 2003b; Chen et al., 2003a). Our results showed that h*BDNF* promoters I and IV, that were induced approximately 7- and 6-fold, respectively, were the most up-regulated *BDNF* promoters by KCl treatment (Fig. 1D). In addition, pIX was induced approximately 1.7-fold, which was statistically significant ($P<0.05$; n=3; t-test), whereas pII 1.2-fold induction was not ($P>0.05$; n=3; t-test; Fig. 1D). pVh was not induced and pVI activity was reduced upon depolarization (Fig. 1D).

Human *BDNF* promoter I is induced by neuronal activity primarily by bHLH-PAS transcription factor ARNT2-NPAS4 heterodimer

Tabuchi et al. have reported that a CRE-like element contributes to the activity-mediated activation of rat *BDNF* pI (Tabuchi et al., 2002). In order to test if this element is also involved in h*BDNF* pI regulation we generated reporter constructs containing the h*BDNF* pI linked to luciferase reporter gene with or without mutation in the orthologous CRE-like element. We mutated the CRE correspondingly to the mutation used previously for the rat pI (Tabuchi et al., 2002). The results showed that mutating the CRE-like element in h*BDNF* pI did not significantly affect the induction of h*BDNF* pI. Both wild-type (WT) h*BDNF* pI and h*BDNF* pI with mutated CRE were induced nearly 6.5-fold (Fig. 2A). Next, by removing half of the promoter we generated h*BDNF* pI 5' and 3' constructs that contained the 5' or the 3' transcription start site (TSS), respectively. As demonstrated in Figure 2B, the 5' region of h*BDNF* pI was significantly more induced (24-fold) than the 3' region of h*BDNF* pI (2-fold). This indicated that the region responsible for the induction of h*BDNF* pI upon neuronal activity is localized to the 5' half of the cloned promoter. The CRE-like element resides in this half, but mutation in the CRE did not alter the induction of h*BDNF* pI 5' (Fig. 2B). To map the *cis*-element that was needed for the induction we generated several 5'-deletion constructs. We found

that deleting the region from -242 to -166 bp upstream of the TSS1 almost abolished h*BDNF* pI up-regulation (Fig. 2B). Bioinformatic analysis indicated that this region contains two potential *cis*-elements that could regulate calcium-dependent activation. First, there is an AP1-like element known to bind FOS and JUN proteins (TCACTCA; Fig2. C; Morgan and Curran, 1991), and second, an asymmetric E-box-like element (CACGAC, named PasRE here, Fig. 2C) that has been shown to bind bHLH-PAS factors (Ooe et al., 2004). Notably, the E-box-like element is situated in reverse orientation on the complementary DNA strand compared to previously published data on such elements (Ooe et al., 2004). We mutated these elements and analyzed the effect of the mutations on pI depolarization-induced up-regulation. Mutation of the AP1-like element (m1) did not affect induction, whereas mutation of the asymmetric E-box-like element (m2) reduced the induction from 24-fold to 5-fold (Fig. 2B). Collectively, these results indicate that the proximal promoter region sufficient for induction of h*BDNF* exon I transcription by neuronal activity is located between -242 and +25 bp relative to the TSS1 and that the novel E-box-like element is the most important activity-responsive *cis*-element in this region. Also, the results argue that the NFkB binding sites described for the r*BDNF* pI (Lubin et al., 2007) and the distally located enhancer bound by MEF2D in mice (Flavell et al., 2008) are dispensable for induction of the h*BDNF* pI as the orthologous sites of h*BDNF* reside outside the h*BDNF* pI 5'SphI promoter construct. However, we cannot rule out possible induction-modulating role of these sites.

The transcription factors (TF-s) binding the region responsible for the induction of h*BDNF* pI were determined by electrophoretic mobility shift assays (EMSA). We used two different oligonucleotides and protein lysates of untreated primary rat neurons or neurons treated for 30 min or 2h with KCl. First, we confirmed that the region in h*BDNF* pI orthologous to the r*BDNF* pI region that has previously been shown to bind CREB1 and USF proteins (Tabuchi et al., 2002), also bound CREB1 and USF1 (oligo pI CRE; Fig. 2D). Second, when we used the region of the h*BDNF* pI containing the AP1-like and the asymmetric E-box-like element (oligo pI AP1/PasRE) we detected a strong signal of mobility shift only when lysate from neurons treated 2h with KCl was used (Fig. 2D). In addition, we verified with mutated oligos that the protein complex that shifted this oligo was bound to the asymmetrical E-box-like element (Fig. 2D). Ooe et al. have shown that bHLH-PAS factor NPAS4-

ARNT2 dimers bind such elements and that they bind with the highest affinity to the sequence identical to the one we mapped in h*BDNF* pI (Ooe et al., 2004 and Fig. 2C). Moreover, it has been demonstrated that NPAS4 protein is expressed in primary cortical neurons only after KCl treatment (Lin et al., 2008). Therefore, we used NPAS4 and ARNT2 antibodies and *in vitro* synthesized ARNT2 and NPAS4 to verify that the complex that binds to the h*BDNF* pI *cis*-element responsible for the depolarization-induced induction contains ARNT2-NPAS4. The results showed that ARNT2 ab blocked formation of the complex and NPAS4 ab weakened considerably the intensity of the shifted complex in EMSA (Fig. 2D). *In vitro* synthesized ARNT2 and NPAS4 proteins were able to generate a shift of the pI AP1/PasRE oligo only when added together to the reaction (Fig. 2D) indicating they bind the h*BDNF* promoter as a dimer. Unlabeled oligo with mutated E-box-like sequence could not out-compete the labeled oligo whereas unlabeled oligo with mutated AP1-like element abolished the shift obtained with the labeled WT pI AP1/PasRE oligo (Fig. 2D). Moreover, addition of ARNT2 ab completely lost the formation of *in vitro* synthesized ARNT2-NPAS4 complex (Fig. 2D). Of note, the detected complexes did not contain FOS or JUN proteins since the respective ab-s did not change the intensity or mobility of oligo shifts (data not shown). Combined, these data showed that the asymmetric E-box-like element responsible for the activity-dependent induction of h*BDNF* pI binds the ARNT2-NPAS4 dimer and therefore we named the element PasRE (bHLH-PAS factor response element).

To confirm these findings we transfected the h*BDNF* pI 5'-luciferase construct into rat primary neurons together with constructs coding for different effector proteins. Our experiments demonstrated that excess of CREB1 in primary neurons was not sufficient to enhance either basal or KCl-induced activity of h*BDNF* pI (Fig. 2E). Overexpression of constitutively active CREB1 (VP16-CREB; Barco et al., 2002) was able to increase h*BDNF* pI activity in uninduced cells but not in depolarized cells (Fig. 2E). These results, together with the EMSA results and our observation that the CRE-like element mutation lowers basal activity of h*BDNF* pI to 65% or 28% of WT promoter basal activity in pI 5' or pI construct context, respectively (Supplementary Fig. 3A and B), indicate that CREB1 binds to h*BDNF* pI, but most probably does not regulate its neuronal activity-dependent induction. Tabuchi *et al*. have described that the r*BDNF* pI CRE-like element is overlapping with a USF-binding element

(UBE; Tabuchi et al., 2002). We found that although not conserved in human (Fig. 2C), the orthologous sequence was bound by USF1 in EMSA (Fig. 2D). To study whether USF proteins could regulate h*BDNF* pI, we overexpressed USF1 and -2 fused to VP16 in neurons. The viral transcription activation domain VP16-USF fusion constructs instead of WT USF constructs were used to get a strong and clear activation of the promoter upon USF binding. We saw a small but statistically significant increase in h*BDNF* pI activity only in uninduced neurons ($P<0.05$, n=3; t-test; Fig. 2E). The KCl-induced levels were slightly reduced in these neurons (Fig. 2E), suggesting that the USF proteins are not involved in h*BDNF* pI activity-dependent regulation. Conversely, the strongest increase in KCl-induced pI activity was obtained when ARNT2 and NPAS4 together were overexpressed, reaching to about 3-fold higher levels than that seen for the empty vector control (pRC, Fig. 2E). NPAS4 overexpression could also significantly increase the activity of h*BDNF* pI, whereas ARNT2 overexpression decreased the activity (Fig. 2E). NPAS4 overexpression enhanced pI activity in uninduced state most likely because ARNT2, as the bHLH-PAS general factor (Kewley et al., 2004), was expressed in uninduced cells (Keith et al., 2001) and NPAS4 addition allowed heterodimer formation. In contrast, ARNT2 overexpression did not enhance KCl-induced pI activity probably because the balance in the levels of ARNT2 and NPAS4 was disrupted leading to potential formation of ARNT2 homodimers. ARNT2 homodimer formation has been demonstrated before by Ooe et al. (Ooe et al., 2004). To strengthen the evidence that bHLH-PAS factors were responsible for h*BDNF* pI induction we overexpressed the bHLH-PAS transcriptional repressor SIM2 that has been shown to interfere with ARNT2-NPAS4-mediated transcriptional activation (Ooe et al., 2004). As can be seen in Fig. 2E, SIM2 could effectively impede the rise of pI activity, indicating that bHLH-PAS TF-s were involved in h*BDNF* pI up-regulation (Fig. 2E). Furthermore, we deleted the C-terminal transactivation domains (TAD) of ARNT2 (Hirose et al., 1996) and NPAS4 (Ooe et al., 2004) to generate constructs coding for delTAD-ARNT2 and delTAD-NPAS4 that would act as dominant negative bHLH-PAS factors similar to the IPAS protein (Makino et al., 2001). By co-expressing delTAD-ARNT2 and delTAD-NPAS4 proteins we were able to reduce depolarization-mediated induction of h*BDNF* pI by 8-fold compared to pRC transfected cells (Fig. 2E). Overexpression of delTAD-NPAS4 alone also significantly reduced depolarization-induced activity of pI (Fig. 2E).

However, delTAD-ARNT2 alone did not affect pI induction (Fig. 2E). Taken together, these results show that KCl-mediated activation of h*BDNF* pI in cortical neurons is dependent on the novel *cis*-regulatory element PasRE and bHLH-PAS TF ARNT2-NPAS4 dimer that binds the PasRE.

To answer the question whether the predominant role of ARNT2 and NPAS4 in inducing neuronal activity-dependent up-regulation of *BDNF* pI is human-specific, we cloned the rat *BDNF* pI region corresponding to h*BDNF* pI 5' in front of the luciferase reporter and analyzed the effect of CREB1 and ARNT2-NPAS4 overexpression on this promoter. Our experiments demonstrated that excess of CREB1 in primary neurons was sufficient to significantly enhance only the basal activity, but not KCl-induced activity of r*BDNF* pI (Fig. 2F). With ARNT2 and NPAS4 overexpression, on the other hand, there was strong increase in r*BDNF* pI activity both in uninduced and KCl-treated neurons compared to the control pRC transfected cells (Fig. 2F). Relying on these results we suggest that, similarly to h*BDNF* pI, neuronal activity-dependent up-regulation of r*BDNF* pI is predominantly mediated by ARNT2-NPAS4 dimer and not by CREB1.

CREB, ARNT2-NPAS4 and USF-s are the key factors required for activation of human *BDNF* promoter IV by neuronal activity

To analyze the molecular mechanism of h*BDNF* pIV KCl-induced activation, we generated h*BDNF* pIV-luciferase constructs with mutations in the corresponding *cis*-elements that have been shown to regulate r*BDNF* pIV in response to neuronal activity (reviewed in Greer and Greenberg, 2008). In addition, we mutated a novel element upstream of the described CaRE, UBE and CRE with strong resemblance to the PasRE that we found to be important for the induction of h*BDNF* pI by neuronal activity (TTCGTG; Fig. 3A). In h*BDNF* pIV, the PasRE element is located in the same orientation as has been shown before for *Drebrin* promoter (Ooe et al., 2004).

Luciferase assays were performed similarly to h*BDNF* pI analyses. As demonstrated in Figure 3B, mutation in the CRE-element orthologous to the CRE described for the r*BDNF* pIV (Shieh et al., 1998; Tao et al., 1998) almost abolished the depolarization-induced up-regulation of h*BDNF* pIV activity. In addition, mutation in the novel PasRE element decreased the induction of the promoter

from approximately 6-fold to 2-fold, indicating that in h*BDNF* pIV this element is also needed for responsiveness to neuronal activity (Fig. 3B). The UBE mutation reduced induction, but was statistically less significant than the effect of the PasRE mutation (Fig. 3B). The effect of CaRE mutation was not significant and the effect of the mutation in the binding site for BHLHB2 had an opposite effect compared to the results obtained by Jiang et al. for the rat pIV (Fig.3B; Jiang et al., 2008). The mutations in the binding sites for NFkB (Jiang et al., 2008) and NFAT (Vashishta et al., 2009) did not affect KCl-mediated induction of pIV (Fig. 3B). This data showed that the most important *cis*-regulatory elements required for the induction of h*BDNF* pIV are CRE, PasRE and UBE.

Next, we conducted EMSA experiments to verify that the h*BDNF* pIV CRE and UBE are bound by CREB1 and USF, respectively, and to identify whether the novel PasRE element in pIV is also bound by the ARNT2-NPAS4 dimer as was pI PasRE. The results obtained with the UBE and CRE *cis*-elements containing h*BDNF* pIV oligonucleotide (pIV UBE/CRE) showed that the oligo was bound by similar protein complexes when untreated or KCl-treated primary neuron lysates were used (Fig. 3C). Addition of WT or mutated oligos confirmed that the UBE and CRE elements were bound and the complexes were verified to contain USF1 or CREB1 proteins using ab-s against USF1, USF2, CREB1 and pSer133-CREB1 (Fig. 3C). Notably, CREB1 containing complexes were detected as two separate bands with slower and faster mobility. The anti-CREB1 ab shifted only the slower-migrating complex and the anti-pSer133-CREB1 ab shifted both of the complexes (Fig. 3C). In addition, the USF1 containing complex was detected as a partially overlapping band with the CREB1 containing faster-migrating complex (Fig. 3C). Finally, *in vitro* synthesized CREB1 and USF1 and -2 proteins could shift the h*BDNF* pIV UBE/CRE oligo, whereas USF1 binding was considerably stronger than USF2 binding (Fig. 3C). When h*BDNF* pIV PasRE containing oligo was used, mobility shift pattern highly similar to that obtained with the h*BDNF* pI AP1/PAS oligo was seen - a strong signal was observed only when lysates of neurons treated 2h with KCl were used (Fig. 3C), suggesting that this PasRE element was also bound by ARNT2-NPAS4 dimer. Moreover, the complex migrated with the same speed in the gel as *in vitro* synthesized ARNT2-NPAS4 complex (Fig. 3C). The complex was bound to the PasRE element since it could be out-competed with the WT but not with PasRE mutated

unlabeled oligo and contained ARNT2 as the shift could be abolished with the anti-ARNT2 ab (Fig. 3C). Of note, there was a faster migrating complex that we were unable to identify (Fig. 3C).

We performed transient transfection experiments with h*BDNF* pIV-luciferase constructs and USF, CREB1, ARNT2 and NPAS4 expression constructs to confirm the results obtained with EMSA. In addition, because several elements were involved in human pIV induction, we used mutated promoter constructs to show specificity of effects. USF-VP16 overexpression elevated uninduced as well as KCl-induced levels of h*BDNF* pIV driven luciferase activity in primary neurons (Fig. 3D) and this effect was lost when UBE mutated h*BDNF* pIV-luciferase construct was used (Fig. 3D). In contrast to h*BDNF* pI, on which CREB1 overexpression had no effect (Fig. 2E), KCl-induction of h*BDNF* pIV was significantly enhanced by overexpression of CREB1 since induction of h*BDNF* pIV was increased from approximately 7-fold in pRC transfected neurons to about 15-fold in CREB1 transfected neurons (Fig. 3E). VP16-CREB1 overexpression enhanced both uninduced and depolarization-induced h*BDNF* pIV activity (Fig. 3E). These effects were lost when CRE mutated pIV was used (Fig. 3E). The effect of ARNT2 and NPAS4 overexpression on h*BDNF* pIV was similar to that seen for h*BDNF* pI – when ARNT2 and NPAS4 were overexpressed together, pIV activity measured from uninduced neurons was 3.5-fold higher and pIV activity measured from KCl-induced neurons was 4-fold higher than the respective activities obtained from pRC transfected cells (Fig. 3F). NPAS4 alone also significantly enhanced pIV activity, whereas ARNT2 overexpression had no effect (Fig. 3F). Although not statistically significant, overexpression of the bHLH-PAS transcriptional repressor SIM2 reduced depolarization-dependent induction of pIV activity (Fig. 3F). Interestingly, the dominant-negative forms of ARNT2 and NPAS4 (delTAD-ARNT2 and delTAD-NPAS4, respectively) did not lower the depolarization-induced h*BDNF* pIV driven luciferase activity, but instead, enhanced the uninduced levels and by that lowered the fold induction of pIV (Fig. 3F), indicating that the PasRE element in h*BDNF* pIV might recruit a repressor in the uninduced state. The effects seen with SIM2, delTAD-ARNT2 and delTAD-NPAS4 constructs were not as clear as seen for promoter I most probably because of more complex regulation of pIV compared to pI. Lastly, ARNT2-NPAS4 overexpression did not enhance PasRE mutated h*BDNF* pIV activity, showing that the effect of ARNT2-NPAS4 co-expression on WT h*BDNF* pIV was specifically dependent on the

novel PasRE element (Fig. 3F). Notably, one study has suggested transcriptional repressor DREAM (Carrion et al., 1999) to be involved in the regulation of CREB1-dependent m*BDNF* exon IV mRNA expression (Fontan-Lozano et al., 2009). However, we did not detect involvement of DREAM proteins in the regulation of h*BDNF* pIV in rat cultured cortical neurons with EMSA, using ab-s specific for the DREAM family members (Supplementary Fig. 3C), or with luciferase reporter assays, using WT as well as Ca^{2+}-insensitive EF-hand mutant DREAM constructs and constructs coding for other DREAM family members (Pruunsild and Timmusk, 2005) with mutated EF-hand motifs (Supplementary Fig. 3D). Collectively, with these experiments we showed that CREB1, ARNT2-NPAS4 and USF bind to CRE, PasRE and UBE elements in the h*BDNF* pIV, respectively, and are the central factors required for activation of h*BDNF* pIV by KCl-mediated membrane depolarization.

CRE mediates initiation and PasRE enhancement of human *BDNF* promoter IV induction by neuronal activity

Next, we studied the role of the novel PasRE element in the activity-responsive regulation of h*BDNF* pIV more thoroughly. It has been shown that CREB1-dependent r*BDNF* pIV transcription is induced rapidly after depolarization of neuronal membranes (Shieh et al., 1998; Tao et al., 1998). The novel PasRE element, on the other hand, is bound by the ARNT2-NPAS4 complex in which the NPAS4 protein has to be synthesized by neurons after the initial depolarizing signal (Lin et al., 2008). Moreover, our EMSA results showed that ARNT2-NPAS4 DNA binding was detectable only after 2h of KCl treatment. To control the hypothesis that CREB1, through activation by phosphorylation, is the initial target of depolarization induced pathways on *BDNF* pIV and subsequently ARNT2-NPAS4 dimer enhances the transcriptional activity, we studied induction of h*BDNF* pIV driven luciferase activity in rat primary neurons transfected with h*BDNF* pIV constructs over the time course of 1 to 10 hours after addition of 25 mM KCl. The results shown in Figure 4 revealed that the CRE element is crucial for induction of h*BDNF* pIV by neuronal activity. While the WT h*BDNF* pIV was induced 5.5-fold, mutation in the CRE element nearly abolished induction by KCl-mediated depolarization (Fig 4). Mutating the PasRE element allowed h*BDNF* pIV activation with identical kinetics compared

to the WT promoter (Fig. 4). However, 3h after KCl addition mutation in the PasRE caused a significant decrease in further induction of pIV activity and 10h after KCl addition the PasRE mutated h*BDNF* pIV was approximately 2-fold less induced than WT h*BDNF* pIV (Fig 4). These results argue that the CRE element in h*BDNF* pIV is needed for initiating transcription by neuronal depolarization and the PasRE element is necessary for enhancing further the transcriptional activity driven by h*BDNF* pIV.

Partially overlapping PasRE and CRE-like elements regulate human *BDNF* promoter IX induction

In a previous study, our group has demonstrated that in addition to exon I and IV, kainic acid treatment of transgenic mice carrying the h*BDNF* gene induces expression of human as well as endogenous m*BDNF* IX-5' mRNAs (Koppel et al., 2009). Furthermore, here we found that although h*BDNF* pIX promoter region of about 1200 bp was induced considerably less than pI and pIV in response to KCl treatment, the induction was statistically significant ($P<0.05$; n=3; t-test; Fig. 1D). Therefore, to map the inducible promoter region, we generated 5' and 3' deletion constructs of the promoter and used these constructs in luciferase assays. The results indicated that the region responsible for the neuronal activity-regulated induction locates to the 3' part of the cloned h*BDNF* pIX as the 5' part of the promoter was not induced and the 3' region sustained inducibility (Fig. 5A). With 5'-deletions, we reduced the inducible region to a 112 bp fragment of h*BDNF* pIX (Fig. 5A), where we identified an asymmetric E-box-like element (CTCGTG) partially overlapping with a CRE-like element (TGACAGCA) (Fig. 5B). Mutations in these elements (mut) eliminated inducibility of the 112bp h*BDNF* pIX by KCl depolarization (Fig. 5A). With EMSA analyses we detected CREB1 and USF binding to the pIX DNA region responsible for KCl-induction as shown by supershift experiments with respective ab-s using lysates of uninduced neurons (Fig. 5C). With lysates from neurons treated for 2h with KCl, an additional slower-migrating band was detected (Fig 5C). Anti-ARNT2 ab eliminated formation of this complex indicating that the complex contained ARNT2. Usage of 10-fold excess of either WT or mutated unlabeled oligos showed that the protein complexes

were binding the partially overlapping PasRE and CRE-like sites (Fig. 5C). Of note, the intensities of the obtained signals in EMSA assays with h*BDNF* oligo pIX PasRE/CRE-like were much weaker than the signals acquired with h*BDNF* pI and pIV oligonucleotides.

Next, we analyzed if the TF-s detected in EMSA regulate the activity of h*BDNF* pIX-luciferase construct when overexpressed in neurons. USF-VP16 was found not to influence the activity of h*BDNF* pIX (data not shown). Overexpression of CREB1 enhanced the induction and overexpression of VP16-CREB1 enhanced both the uninduced and induced levels of h*BDNF* pIX driven luciferase activity (Fig. 5D). ARNT2 overexpression did not enhance, whereas overexpression of NPAS4 alone or with ARNT2 enhanced the induced luciferase levels by 2- or 3-fold, respectively (Fig. 5D). SIM2 reduced the induced levels of pIX activity, whereas overexpression of delTAD-ARNT2 together with delTAD-NPAS4 slightly increased uninduced levels and abolished induction of h*BDNF* pIX-dependent luciferase activity (Fig. 5D). Altogether the results show that: a) KCl-induced activation of h*BDNF* pIX is weak compared to induction of pI and pIV and b) activation of h*BDNF* pIX is mediated by ARNT2-NPAS4 and CREB1 binding to the PasRE and CRE-like elements.

Overexpression of dominant negative ARNT2-NPAS4 reduces neuronal activity-dependent transcription of endogenous rat *BDNF* exon I, IV and IX-5' mRNAs

Since all *cis*-elements except the novel PasREs that we have described here for h*BDNF* promoters have been shown before to be important for rodent *BDNF* activity-dependent induction, we chose to validate the role of the PasRE elements also at the level of endogenous rod*BDNF* regulation. For that we used overexpression of the delTAD-ARNT2 and delTAD-NPAS4 that have the ability to compete with endogenous factors by binding to *BDNF* PasRE elements and interfering with activity-regulated *BDNF* transcription. We electroporated delTAD-ARNT2 and delTAD-NPAS4 or control GFP constructs into rat primary neurons using Amaxa nucleofection and treated the cells at 5 DIV with 25 mM KCl for 2h to 8h. We analyzed the ability of delTAD-ARNT2 and delTAD-NPAS4 to hinder endogenous *BDNF* mRNA up-regulation by RT-qPCR. The results showed that the up-regulation of r*BDNF* exon I, IV and IX-5' mRNAs in the delTAD-ARNT2 and delTAD-NPAS4 expressing cells

was considerably weaker than in GFP electroporated cells (Fig. 6). In the GFP electroporated neurons exon I mRNA levels were approximately 5-fold more induced than in the delTAD-ARNT2 and delTAD-NPAS4 electroporated cells (Fig. 6). Similarly, induction of exon IV mRNA levels was 2.5-fold weaker (Fig. 6) and induction exon IX-5' mRNA levels was 3-fold weaker (Fig. 6) at the time point of 4h of KCl treatment in delTAD-ARNT2 and delTAD-NPAS4 electroporated neurons than in GFP electroporated neurons. The results of this experiment suggest that the full induction of activity-responsive transcription of endogenous r*BDNF* exon I, IV and IX-5' mRNAs is to a great extent dependent on bHLH-PAS TF-s ARNT2 and NPAS4 binding the PasRE elements.

ARNT2-NPAS4 and CREB activate endogenous human *BDNF* transcription by binding human *BDNF* promoters I and IV

We performed chromatin immunoprecipitation (ChIP) experiments to demonstrate that ARNT2-NPAS4 and CREB1 bind to PasRE and CRE elements, respectively, on endogenous *BDNF* promoters in human cells. Moreover, to demonstrate that transcription of endogenous *BDNF* is enhanced in human cells by ARNT2-NPAS4 and CREB1 we analyzed h*BDNF* mRNA expression in human embryonic kidney HEK293 cells overexpressing ARNT2, NPAS4 or CREB1.

For ChIP, either constructs coding for ARNT2-V5 or NPAS4-V5 alone or together with NPAS4 or ARNT2 coding constructs, respectively, were transfected into HEK293 cells (Fig 7A). ChIP was performed with V5-agarose enabling us to monitor whether ARNT2-V5 and NPAS4-V5 binding to DNA was enhanced by addition of the dimer partner. Also, CREB1-V5 was expressed in HEK293 cells (Fig 7A). In qPCR analyses of the immunoprecipitated DNA, we focused on h*BDNF* pI, pIV and pIX and used primers for an unrelated region on human chromosome 11 as a negative control (Chr11URR). We observed strong binding of ARNT2-V5 and NPAS4-V5 on h*BDNF* pI and pIV only when the V5-tagged proteins were expressed together with NPAS4 and ARNT2, respectively (Fig. 7B), supporting the data that ARNT2 and NPAS4 bind DNA as a dimer. In contrast, we detected very weak binding of ARNT2-V5 and NPAS4-V5 to pIX and to the control Chr11URR in all transfection combinations (Fig. 7B). CREB1-V5 was also significantly enriched on h*BDNF* pI and IV and not

bound to pIX or the unrelated control region (Fig. 7B). ARNT2-NPAS4 dimer was enriched relatively more on pI than on pIV and CREB1 was enriched relatively more on pIV (Fig. 7B). Additionally, these results suggest that ARNT2-NPAS4 and CREB1 were either not bound to pIX or the binding was under the detection limit of the experiment.

Next, we overexpressed VP16-CREB1, ARNT2, NPAS4 or ARNT2 together with NPAS4 in HEK239 cells (Fig. 7C) and measured h*BDNF* mRNA expression by RT-qPCR. As shown in Figure 7D, h*BDNF* exon I transcript levels were elevated approximately 80-fold in ARNT2-NPAS4 co-transfected cells compared to control pRC transfected cells and approximately 10-fold induction was seen upon VP16-CREB1 or NPAS4 transfection (Fig 7D). Similarly, the highest levels of exon IV transcripts were detected when ARNT2 and NPAS4 were co-transfected (Fig. 7D). VP16-CREB1 induced h*BDNF* exon IV transcription approximately 7-fold and NPAS4 approximately 2.5-fold. Notably, VP16-CREB1 induced h*BDNF* exon IV transcription relatively more than exon I transcription when the effect of ARNT2-NPAS4 on the respective transcripts is considered. In accordance to the results of the ChIP and EMSA experiments, only weak up-reguation was detected for h*BDNF* exon IX-5' transcripts. ARNT2-NPAS4 transfection elevated *BDNF* exon IX-5' mRNA levels about 2.5-fold compared to pRC transfected cells (Fig. 7D). VP16-CREB1 overexpression did not have a significant effect on h*BDNF* IX-5' transcript levels in HEK293 cells (Fig. 7D). These results imply that TF-s ARNT2, NPAS4 and CREB1 bind h*BDNF* promoters I and IV in chromatin context and enhance transcription of endogenous h*BDNF*. Also, these experiments suggest that ARNT2-NPAS4 dimer binds and induces endogenous h*BDNF* pI relatively more than pIV and CREB1, on the other hand, binds and induces endogenous h*BDNF* pIV relatively more than pI.

Finally, we performed ChIP experiments with anti-ARNT2 and anti-CREB1 ab-s and human postmortem parietal cortex samples to analyze whether ARNT2 and CREB1 bind h*BDNF* promoters in the human brain *in vivo*. With qPCR analyses of the immunoprecipitated DNA we detected significant enrichment of ARNT2 on h*BDNF* pIV and pI compared to the control Chr11URR (Fig. 7E). CREB1 was significantly enriched only on h*BDNF* pIV and not on h*BDNF* pI (Fig. 7E). ARNT2 binding to h*BDNF* pIX was also statistically significant when compared to the control Chr11URR (Fig. 7E). However, as the enrichment of the pIX region in the precipitated DNA was low relative to

the –ab control (Fig. 7E), we suggest that the detection limit of our ChIP experiment is not enough to answer whether ARNT2 binds h*BDNF* pIX *in vivo*. Detecting ARNT2 on pIX might be complicated in postmortem tissue because the ARNT2-NPAS4 complex probably binds h*BDNF* pIX with weaker affinity than it binds h*BDNF* pI and pIV as is indicated by our results with EMSA and the results of the ChIP experiments in HEK cells. Taken together, ARNT2 binds h*BDNF* pI and pIV and CREB1 binds h*BDNF* pIV in the human parietal cortex *in vivo*, which strongly supports our previous results of this study showing that ARNT2 and NPAS4 regulate neuronal activity-dependent transcription of h*BDNF* exon I and exon IV and CREB1 regulates neuronal activity-dependent transcription of h*BDNF* exon IV.

Discussion

Results presented in this study reveal several novel findings on the regulation of neuronal activity-dependent *BDNF* transcription. Firstly, exon I and IV transcripts of human *BDNF* are the most up-regulated h*BDNF* mRNAs by depolarization of primary cortical neurons. Secondly, activity-regulated induction of h*BDNF* pI depends primarily on a novel PasRE element. Thirdly, activity-regulated induction of h*BDNF* pIV depends predominantly on CRE, PasRE and UBE elements. And lastly, the novel PasRE elements in pI and pIV are conserved in human and rodents and are bound by bHLH-PAS transcription factor ARNT2-NPAS4 heterodimers.

In this study, we analyzed neuronal activity-dependent regulation of *BDNF* transcription in cultured primary cortical neurons from h*BDNF*-BAC transgenic mice (Koppel et al., 2009) and demonstrated that exon I and IV transcripts are the most up-regulated *BDNF* mRNAs by membrane depolarization in both human and mouse *BDNF* genes. Our results showed that there was a slight difference in the time course of up-regulation between h*BDNF* and m*BDNF* exon IV transcripts as human transcripts accumulated with a delay compared to respective mouse transcripts. Human exon IX-5' transcripts were considerably less up-regulated than the respective mouse transcripts and in addition, the ratio of exon I to exon IV transcripts in uninduced cells was significantly higher for human *BDNF* than for mouse *BDNF*. These results raise the possibility that dissimilarities might exist

in the regulation of *BDNF* gene between mouse and human *in vivo*. However, two important aspects should be considered. First, we used rodent cells to study h*BDNF* regulation. Therefore, one might ask how accurately these results mirror the regulation of *BDNF* in human. Second, the results could be influenced by the fact that all regulatory sequences of h*BDNF* might not be present in the BAC construct (Koppel et al., 2009). It is recognized that differences in *cis*-regulatory elements rather than *trans*-acting factors explain many of the inter-species variations in gene regulation (Wilson and Odom, 2009). Moreover, human regulatory elements or a human chromosome have been shown to direct human-specific gene expression and TF binding in transgenic mice (Prabhakar et al., 2008; Wilson et al., 2008). Therefore, we believe it is plausible to use rodent neurons as a tool for studying regulation of a human gene. On the other hand, we admit that the h*BDNF* transgene could be missing regulatory elements. For example, the antisense *BDNF* (Pruunsild et al., 2007) or the distal 5' region that has been found to influence h*BDNF* expression *in vivo* (Gray et al., 2006). Nevertheless, in principle, depolarization of mouse primary neurons activated h*BDNF* transcription and therefore, rodent primary neurons are credible for h*BDNF* promoter studies.

We showed that the CRE-like element that has been described for the rat pI (Tabuchi et al., 2002) was not the regulator of activity-dependent induction of h*BDNF* pI. Instead, we found that a novel element upstream of the CRE-like element was responsible for the up-regulation of h*BDNF* pI. However, we propose that this effect is not human-specific. According to our results on the regulation of the r*BDNF* pI, CREB overexpression in primary neurons significantly enhances basal but not depolarization-induced levels of pI activity. Excess of ARNT2 and NPAS4 in cells, on the other hand, drastically increases both uninduced as well as induced levels of r*BDNF* pI activity. Moreover, the data of Tabuchi et al. shows that deletion of the CRE-like element in r*BDNF* pI decreases the basal activity of the promoter, whereas deletion of a region upstream of the CRE specifically reduces fold induction of r*BDNF* pI upon depolarization (Tabuchi et al., 2002). Thus, CREB or a related factor is regulating the basal activity of *BDNF* pI, but the TF-s contributing most significantly to the activity-induced activation of *BDNF* pI are bHLH-PAS TF-s ARNT2 and NPAS4 that bind the novel activity regulated *cis*-element named PasRE here. bHLH-PAS proteins regulate many crucial physiological and developmental processes (Kewley et al., 2004). Our result that they regulate h*BDNF* pI is

supported by previous studies that have shown that: a) a region upstream of the CRE-like element is involved in activity-dependent regulation of rat pI (Tabuchi et al., 2002); b) NPAS4 binds DNA in the pI region of m*BDNF* (Lin et al., 2008); c) NPAS4 forms a heterodimer preferably with ARNT2 in brain (Ooe et al., 2009); d) ARNT2-NPAS4 dimer has the highest affinity to a DNA sequence identical to the PasRE element in h*BDNF* pI (Ooe et al., 2004); and e) m*BDNF* levels are reduced in NPAS4 knock-out mice (Lin et al., 2008).

Our data showing that the CRE element is fundamental for the induction of h*BDNF* pIV is in accordance with the finding that CRE mutation in the m*BDNF* pIV loses its inducibility *in vivo* (Hong et al., 2008). Additionally, our results indicated that a novel PasRE element contributes to the depolarization induced up-regulation of pIV by significantly enhancing activity of the promoter. While initial induction of PasRE mutated pIV upon KCl depolarization was identical to the WT promoter, significant decrease in induction was detected from 3h onward. This is in good agreement with the data presented by Lin et al. that the NPAS4 protein, shown here to bind *BDNF* PasREs as a heterodimer with ARNT2, is produced in primary cultured neurons after depolarization of neuronal membranes (Lin et al., 2008). Moreover, we found that EMSA shift by ARNT2-NPAS4 heterodimer was detectable only with lysates of depolarized neurons. Interestingly, the predominant rise of both human and mouse *BDNF* exon I transcript levels took place later after KCl addition than the major rise in *BDNF* exon IV transcript levels as was shown here using primary neurons from h*BDNF*-BAC mice. This supports the finding that NPAS4 accumulation is needed for induction of pI. pIV, on the other hand, is induced by CREB as an immediate-early promoter. One might argue also that in the h*BDNF*-BAC mouse neurons h*BDNF* exon IV transcript levels were elevated more slowly than the respective mouse transcripts due to relatively bigger role of the PasRE element compared to the CRE element in h*BDNF* pIV. Proving this suggestion needs additional experiments though.

The mutation in the UBE of h*BDNF* pIV decreased induction of pIV by half, suggesting involvement of USF proteins, which was confirmed by EMSA and luciferase assays. Conversely, we saw only modest effect on induction when the CaRE element in the h*BDNF* pIV was mutated. Recently it was reported that CaRF is dispensable for induction of m*BDNF* exon IV expression (McDowell et al., 2010). Considering this, we suggest that CaRF is not one of the major contributors

to the depolarization induced up-regulation of h*BDNF* pIV activity in cortical neurons. Also, we showed here that mutations in NFkB or NFAT sites had no effect and mutation in BHLHB2 binding site had induction-decreasing effect on h*BDNF* pIV activation by depolarization, respectively. These results differed from the results described earlier (Jiang et al., 2008; Vashishta et al., 2009), but could be explained by use of glutamate receptor agonists instead of KCl-mediated depolarization for modeling neuronal activation in previous studies. In addition, we found that, at least in primary neurons, the DREAM family TF-s do not contribute to activity-dependent regulation of h*BDNF* pIV as has been proposed for m*BDNF* pIV (Fontan-Lozano et al., 2009). Again, further experiments are needed to elucidate these issues.

Here we also showed that up-regulation of h*BDNF* pIX was modest, being induced only about two-fold upon KCl treatment of primary neurons. Nevertheless, we identified partially overlapping CRE-like and PasRE elements in the region responsible for activity-dependent induction of h*BDNF* pIX. As can be suggested from our ChIP assay results, human pIX was induced less than pI and pIV by neuronal activity probably because of weaker binding of CREB and ARNT2-NPAS4 to pIX. Interestingly, the activity-regulated *cis*-elements described here for the human pIX are not conserved in rodents. However, we found that induction of endogenous rat exon IX-5' transcription was partly dependent on bHLH-PAS factors. This is conceivable though, because only one-third of TF binding events take place on an aligned site in an orthologous promoter between human and mouse (Odom et al., 2007) suggesting another PasRE location in rod*BDNF* pIX.

Transcriptional regulation of rod*BDNF* has been used as a model for studying neuronal activity-responsive gene expression (reviewed in Greer and Greenberg, 2008). Our analysis of h*BDNF* regulation showed that, in general, activity-dependent up-regulation of *BDNF* promoters is similar between human and rodent. Importantly, the role of PasRE elements in h*BDNF* promoters was described here. Because these elements had not been studied in rat beforehand we confirmed that the usage of PasREs in *BDNF* is conserved also in rodents since we could interfere with the induction of endogenous r*BDNF* by overexpressing dominant-negative forms of ARNT2 and NPAS4 proteins. We validated the findings obtained in rodent cells by showing with ChIP experiments that endogenous h*BDNF* PasRE elements are bound by overexpressed ARNT2-NPAS4 in human cells. Furthermore,

we demonstrated that these *cis*-elements are bound by endogenous ARNT2 in human brain, implying that the *BDNF* PasRE sites are active in human brain *in vivo*. It is significant that PasRE elements regulate h*BDNF* since ARNT2 has been found to be a key TF in the hippocampus, where it is potentially crucial for synaptic plasticity (Valen et al., 2009), and both ARNT2 as well as NPAS4 have been demonstrated to be neuroprotective TF-s, which could be good therapeutic targets (Drutel et al., 1999; Hester et al., 2007; Zhang et al., 2009). Altogether, our study specifies the *cis*-elements and transcription factors regulating neuronal activity-dependent transcription of human *BDNF* and provides insight into the molecular mechanisms impairment of which might be one of the causes for diseases and disorders with altered *BDNF* expression.

References

Aid T, Kazantseva A, Piirsoo M, Palm K, Timmusk T (2007) Mouse and rat BDNF gene structure and expression revisited. J Neurosci Res 85:525-535.

Barco A, Alarcon JM, Kandel ER (2002) Expression of constitutively active CREB protein facilitates the late phase of long-term potentiation by enhancing synaptic capture. Cell 108:689-703.

Barde YA, Edgar D, Thoenen H (1982) Purification of a new neurotrophic factor from mammalian brain. Embo J 1:549-553.

Binder DK, Scharfman HE (2004) Brain-derived neurotrophic factor. Growth Factors 22:123-131.

Carrion AM, Link WA, Ledo F, Mellstrom B, Naranjo JR (1999) DREAM is a Ca2+-regulated transcriptional repressor. Nature 398:80-84.

Chen WG, West AE, Tao X, Corfas G, Szentirmay MN, Sawadogo M, Vinson C, Greenberg ME (2003a) Upstream stimulatory factors are mediators of Ca2+-responsive transcription in neurons. J Neurosci 23:2572-2581.

Chen WG, Chang Q, Lin Y, Meissner A, West AE, Griffith EC, Jaenisch R, Greenberg ME (2003b) Derepression of BDNF transcription involves calcium-dependent phosphorylation of MeCP2. Science 302:885-889.

Drutel G, Heron A, Kathmann M, Gros C, Mace S, Plotkine M, Schwartz JC, Arrang JM (1999) ARNT2, a transcription factor for brain neuron survival? Eur J Neurosci 11:1545-1553.

Ernfors P, Lee KF, Jaenisch R (1994) Mice lacking brain-derived neurotrophic factor develop with sensory deficits. Nature 368:147-150.

Flavell SW, Kim TK, Gray JM, Harmin DA, Hemberg M, Hong EJ, Markenscoff-Papadimitriou E, Bear DM, Greenberg ME (2008) Genome-wide analysis of MEF2 transcriptional program reveals synaptic target genes and neuronal activity-dependent polyadenylation site selection. Neuron 60:1022-1038.

Fontan-Lozano A, Romero-Granados R, del-Pozo-Martin Y, Suarez-Pereira I, Delgado-Garcia JM, Penninger JM, Carrion AM (2009) Lack of DREAM protein enhances learning and memory and slows brain aging. Curr Biol 19:54-60.

Garzon DJ, Fahnestock M (2007) Oligomeric amyloid decreases basal levels of brain-derived neurotrophic factor (BDNF) mRNA via specific downregulation of BDNF transcripts IV and V in differentiated human neuroblastoma cells. J Neurosci 27:2628-2635.

Gray J, Yeo GS, Cox JJ, Morton J, Adlam AL, Keogh JM, Yanovski JA, El Gharbawy A, Han JC, Tung YC, Hodges JR, Raymond FL, O'Rahilly S, Farooqi IS (2006) Hyperphagia, severe obesity, impaired cognitive function, and hyperactivity associated with functional loss of one copy of the brain-derived neurotrophic factor (BDNF) gene. Diabetes 55:3366-3371.

Greer PL, Greenberg ME (2008) From synapse to nucleus: calcium-dependent gene transcription in the control of synapse development and function. Neuron 59:846-860.

Hall J, Thomas KL, Everitt BJ (2000) Rapid and selective induction of BDNF expression in the hippocampus during contextual learning. Nat Neurosci 3:533-535.

Hester I, McKee S, Pelletier P, Thompson C, Storbeck C, Mears A, Schulz JB, Hakim AA, Sabourin LA (2007) Transient expression of Nxf, a bHLH-PAS transactivator induced by neuronal preconditioning, confers neuroprotection in cultured cells. Brain Res 1135:1-11.

Hirose K, Morita M, Ema M, Mimura J, Hamada H, Fujii H, Saijo Y, Gotoh O, Sogawa K, Fujii-Kuriyama Y (1996) cDNA cloning and tissue-specific expression of a novel basic helix-loop-

helix/PAS factor (Arnt2) with close sequence similarity to the aryl hydrocarbon receptor nuclear translocator (Arnt). Mol Cell Biol 16:1706-1713.

Hong EJ, McCord AE, Greenberg ME (2008) A biological function for the neuronal activity-dependent component of Bdnf transcription in the development of cortical inhibition. Neuron 60:610-624.

Jiang X, Tian F, Du Y, Copeland NG, Jenkins NA, Tessarollo L, Wu X, Pan H, Hu XZ, Xu K, Kenney H, Egan SE, Turley H, Harris AL, Marini AM, Lipsky RH (2008) BHLHB2 controls Bdnf promoter 4 activity and neuronal excitability. J Neurosci 28:1118-1130.

Jones KR, Farinas I, Backus C, Reichardt LF (1994) Targeted disruption of the BDNF gene perturbs brain and sensory neuron development but not motor neuron development. Cell 76:989-999.

Keith B, Adelman DM, Simon MC (2001) Targeted mutation of the murine arylhydrocarbon receptor nuclear translocator 2 (Arnt2) gene reveals partial redundancy with Arnt. Proc Natl Acad Sci U S A 98:6692-6697.

Kewley RJ, Whitelaw ML, Chapman-Smith A (2004) The mammalian basic helix-loop-helix/PAS family of transcriptional regulators. Int J Biochem Cell Biol 36:189-204.

Koppel I, Aid-Pavlidis T, Jaanson K, Sepp M, Pruunsild P, Palm K, Timmusk T (2009) Tissue-specific and neural activity-regulated expression of human BDNF gene in BAC transgenic mice. BMC Neurosci 10:68.

Lin Y, Bloodgood BL, Hauser JL, Lapan AD, Koon AC, Kim TK, Hu LS, Malik AN, Greenberg ME (2008) Activity-dependent regulation of inhibitory synapse development by Npas4. Nature 455:1198-1204.

Lubin FD, Ren Y, Xu X, Anderson AE (2007) Nuclear factor-kappa B regulates seizure threshold and gene transcription following convulsant stimulation. J Neurochem 103:1381-1395.

Lyons WE, Mamounas LA, Ricaurte GA, Coppola V, Reid SW, Bora SH, Wihler C, Koliatsos VE, Tessarollo L (1999) Brain-derived neurotrophic factor-deficient mice develop aggressiveness and hyperphagia in conjunction with brain serotonergic abnormalities. Proc Natl Acad Sci U S A 96:15239-15244.

Makino Y, Cao R, Svensson K, Bertilsson G, Asman M, Tanaka H, Cao Y, Berkenstam A, Poellinger L (2001) Inhibitory PAS domain protein is a negative regulator of hypoxia-inducible gene expression. Nature 414:550-554.

McDowell KA, Hutchinson AN, Wong-Goodrich SJ, Presby MM, Su D, Rodriguiz RM, Law KC, Williams CL, Wetsel WC, West AE (2010) Reduced cortical BDNF expression and aberrant memory in Carf knock-out mice. J Neurosci 30:7453-7465.

Morgan JI, Curran T (1991) Stimulus-transcription coupling in the nervous system: involvement of the inducible proto-oncogenes fos and jun. Annu Rev Neurosci 14:421-451.

Odom DT, Dowell RD, Jacobsen ES, Gordon W, Danford TW, MacIsaac KD, Rolfe PA, Conboy CM, Gifford DK, Fraenkel E (2007) Tissue-specific transcriptional regulation has diverged significantly between human and mouse. Nat Genet 39:730-732.

Ooe N, Saito K, Kaneko H (2009) Characterization of functional heterodimer partners in brain for a bHLH-PAS factor NXF. Biochim Biophys Acta 1789:192-197.

Ooe N, Saito K, Mikami N, Nakatuka I, Kaneko H (2004) Identification of a novel basic helix-loop-helix-PAS factor, NXF, reveals a Sim2 competitive, positive regulatory role in dendritic-cytoskeleton modulator drebrin gene expression. Mol Cell Biol 24:608-616.

Patterson SL, Abel T, Deuel TA, Martin KC, Rose JC, Kandel ER (1996) Recombinant BDNF rescues deficits in basal synaptic transmission and hippocampal LTP in BDNF knockout mice. Neuron 16:1137-1145.

Poo MM (2001) Neurotrophins as synaptic modulators. Nat Rev Neurosci 2:24-32.

Prabhakar S, Visel A, Akiyama JA, Shoukry M, Lewis KD, Holt A, Plajzer-Frick I, Morrison H, Fitzpatrick DR, Afzal V, Pennacchio LA, Rubin EM, Noonan JP (2008) Human-specific gain of function in a developmental enhancer. Science 321:1346-1350.

Pruunsild P, Timmusk T (2005) Structure, alternative splicing, and expression of the human and mouse KCNIP gene family. Genomics 86:581-593.

Pruunsild P, Kazantseva A, Aid T, Palm K, Timmusk T (2007) Dissecting the human BDNF locus: bidirectional transcription, complex splicing, and multiple promoters. Genomics 90:397-406.

Shieh PB, Hu SC, Bobb K, Timmusk T, Ghosh A (1998) Identification of a signaling pathway involved in calcium regulation of BDNF expression. Neuron 20:727-740.

Zhang SJ, Zou M, Lu L, Lau D, Ditzel DA, Delucinge-Vivier C, Aso Y, Descombes P, Bading H (2009) Nuclear calcium signaling controls expression of a large gene pool: identification of a gene program for acquired neuroprotection induced by synaptic activity. PLoS Genet 5:e1000604.

Tabuchi A, Sakaya H, Kisukeda T, Fushiki H, Tsuda M (2002) Involvement of an upstream stimulatory factor as well as cAMP-responsive element-binding protein in the activation of brain-derived neurotrophic factor gene promoter I. J Biol Chem 277:35920-35931.

Tao X, Finkbeiner S, Arnold DB, Shaywitz AJ, Greenberg ME (1998) Ca2+ influx regulates BDNF transcription by a CREB family transcription factor-dependent mechanism. Neuron 20:709-726.

Tao X, West AE, Chen WG, Corfas G, Greenberg ME (2002) A calcium-responsive transcription factor, CaRF, that regulates neuronal activity-dependent expression of BDNF. Neuron 33:383-395.

Timmusk T, Belluardo N, Persson H, Metsis M (1994) Developmental regulation of brain-derived neurotrophic factor messenger RNAs transcribed from different promoters in the rat brain. Neuroscience 60:287-291.

Timmusk T, Palm K, Metsis M, Reintam T, Paalme V, Saarma M, Persson H (1993) Multiple promoters direct tissue-specific expression of the rat BDNF gene. Neuron 10:475-489.

Valen E, Pascarella G, Chalk A, Maeda N, Kojima M, Kawazu C, Murata M, Nishiyori H, Lazarevic D, Motti D, Marstrand TT, Tang MH, Zhao X, Krogh A, Winther O, Arakawa T, Kawai J, Wells C, Daub C, Harbers M, Hayashizaki Y, Gustincich S, Sandelin A, Carninci P (2009) Genome-wide detection and analysis of hippocampus core promoters using DeepCAGE. Genome Res 19:255-265.

Vashishta A, Habas A, Pruunsild P, Zheng JJ, Timmusk T, Hetman M (2009) Nuclear factor of activated T-cells isoform c4 (NFATc4/NFAT3) as a mediator of antiapoptotic transcription in NMDA receptor-stimulated cortical neurons. J Neurosci 29:15331-15340.

Wilson MD, Odom DT (2009) Evolution of transcriptional control in mammals. Curr Opin Genet Dev 19:579-585.

Wilson MD, Barbosa-Morais NL, Schmidt D, Conboy CM, Vanes L, Tybulewicz VL, Fisher EM, Tavare S, Odom DT (2008) Species-specific transcription in mice carrying human chromosome 21. Science 322:434-438.

Figure legends

Figure 1. Characterization of neuronal activity-dependent h*BDNF* mRNA expression in primary neurons and determination of activity-induced h*BDNF* promoters. **A**, Cortical neurons from BAC-transgenic mice with h*BDNF* inserted in the genome were used for studying h*BDNF* regulation in response to neuronal activity modeled by KCl-depolarization. 7 DIV neurons were treated with 25 mM KCl for the time indicated and both endogenous m*BDNF* and transgenic h*BDNF* levels were measured by RT-qPCR using species-specific primers for the coding region of *BDNF* exon IX. mRNA levels are shown as fold induced levels over levels of total *BDNF* in untreated neurons (CNTR). **B**, The same neurons as in A were used to study changes in expression levels of *BDNF* transcripts with indicated 5' exons upon KCl treatment by RT-qPCR using species-specific primers. mRNA levels at each time point are shown as fold induced levels over levels of respective transcripts in untreated neurons. The data in A and B are obtained from three independent experiments with triplicate measurements and normalized to *HPRT1* expression. **C**, The same neurons as in A were used to measure the ratio of *BDNF* exon I to exon IV mRNA for both h*BDNF* and m*BDNF* gene in untreated neurons and in neurons treated 8h with KCl. For quantification, plasmid serial dilutions with exactly 1:1 ratio of exon I and IV PCR templates of h*BDNF* or m*BDNF*, respectively, were used. Results of three independent experiments with triplicate measurements are shown. **D**, Rat primary neurons transfected with the indicated h*BDNF* promoter-dependent firefly luciferase (FFluc) construct and h*EF1alpha* promoter-dependent renilla luciferase (hRluc) construct, were treated with 25 mM KCl for 8h and luciferase activities were measured. Data are represented as fold induced promoter activities over activities measured from untreated control neurons for each h*BDNF* promoter. Results

of at least three independent experiments with duplicate measurements normalized to hRluc activities are shown. Statistical significance denoted by asterisks is relative to respective untreated control in A and B, and between the bars indicated with lines in C and D. (***, P<0.001; **, P<0.01; *, P<0.05; NS, not significant; t-test)

Figure 2. h*BDNF* pI neuronal activity-regulated induction depends on ARNT2-NPAS4 heterodimer. **A**, Rat primary neurons transfected with wild type (WT) or cAMP/Ca^{2+}-response element-like element mutated (CREm) h*BDNF* pI-dependent FFluc construct and h*EF1alpha* promoter-dependent hRluc construct, were treated with 25 mM KCl and luciferase activities were measured. **B**, Rat primary neurons transfected with indicated derivative of the WT h*BDNF* pI-dependent FFluc construct shown in A and h*EF1alpha* promoter-dependent hRluc construct, were treated with 25 mM KCl and luciferase activities were measured. Data are represented as fold induced promoter activities over activities measured from untreated control neurons both in A and B. Numbers in the schematic representations of the promoters indicate nucleotide positions relative to the most 5' transcription start site (TSS1) of h*BDNF* exon I. TSS2, 3' transcription start site of h*BDNF* exon I. 5', 5' part of h*BDNF* pI; 3', 3' part of h*BDNF* pI; SphI and E31I, SphI and Eco31I restriction sites used to generate 5' deletion constructs of h*BDNF* pI; m1 and m2, mutations in the AP1-like and asymmetric E-box-like (named PasRE here) *cis*-regulatory DNA elements, respectively. **C**, Alignment of the region responsible for neuronal activity-dependent induction of h*BDNF* pI and the region containing the CRE-like element in h*BDNF* pI with respective sequences in the rat promoter. Numbers indicate nucleotide positions relative to the TSS1 of h*BDNF* exon I. AP1-like, binding site for activator protein 1 complex; PasRE, asymmetric E-box-like bHLH-PAS TF response element; UBE, USF binding element. Note that 4 of the 6 nucleotides defined by Tabuchi and colleagues as critical for USF binding in the rat pI (boxed) are not conserved in human. **D**, EMSA showing CREB1 and USF complexes binding to the h*BDNF* pI CRE oligo and bHLH-PAS TF ARNT2-NPAS4 dimer binding to the pI AP1/PasRE oligo. Addition of 10-fold excess (10x) of respective unlabeled oligonucleotide or addition of antibody (ab) to the reaction is indicated above the panel. Lysate used in the reaction is indicated below the panel where CNTR designates untreated neurons, 30 min KCl and 2h KCl

designate KCl treated neurons and *in vitro* designates *in vitro* synthesized proteins. SS, supershift generated by the addition of ab. Representative image of at least three independent experiments is shown. **E**, Rat primary neurons transfected with h*BDNF* pI 5'-dependent FFluc construct and h*EF1alpha* promoter-dependent hRluc construct together with empty vector control (pRC) or a construct coding the indicated protein, were left untreated (CNTR) or were treated for 8h with 25 mM KCl and luciferase activities were measured. VP16, a viral transcription activator domain fused to the respective protein where indicated. delTAD represents deletion of the transcription activator domain. **F**, Rat primary neurons transfected with r*BDNF* pI-dependent FFluc construct and h*EF1alpha* promoter-dependent hRluc construct together with empty vector control (pRC) or a construct coding the indicated protein, were left untreated (CNTR) or were treated for 8h with 25 mM KCl and luciferase activities were measured. Promoter activities in E and F are presented in RLUs (specified in Materials and Methods) relative to the promoter activity measured from untreated pRC transfected neurons that was arbitrarily set as 1. Results of at least three independent experiments with duplicate measurements are shown in A, B, E and F. Statistical significance denoted by asterisks is relative to pI 5' construct fold induction in B and relative to promoter activity in pRC transfected untreated control or pRC transfected KCl treated neurons, respectively, in E and F. (***, $P<0.001$; **, $P<0.01$; *, $P<0.05$; NS, not significant; t-test)

Figure 3. h*BDNF* pIV neuronal activity-regulated induction depends on CREB, ARNT2-NPAS4 and USF-s. **A**, Alignment of the region responsible for neuronal activity-dependent induction of h*BDNF* pIV and downstream regions containing *cis*-elements mutated in this study with respective sequences in the rat promoter. PasRE, bHLH-PAS TF response element; CaRE, CaRF binding element; UBE, USF binding element; CRE, cAMP/Ca^{2+} response element; BHLHB2-RE, NFkB-RE and NFAT-RE designate response elements for the respective TF-s. **B**, Rat primary neurons transfected with wild type (WT) h*BDNF* pIV or PasRE, CaRE, UBE, CRE, BHLHB2-RE, NFkB-RE or NFAT-RE mutated h*BDNF* pIV-dependent FFluc construct and h*EF1alpha* promoter-dependent hRluc construct, were treated with 25 mM KCl and luciferase activities were measured. Data are represented as fold induced promoter activities over activities measured from untreated control neurons. Numbers in A and in the

schematic representation of the promoter in B, indicate nucleotide positions relative to the most 5' transcription start site (TSS1) of h*BDNF* exon IV. **C**, EMSA showing USF and CREB1 complexes binding to the pIV UBE/CRE oligo and bHLH-PAS TF ARNT2-NPAS4 dimer binding to the pIV PasRE oligo. Addition of unlabeled oligo or ab to the reaction and the lysates used are designated as in Figure 2D. Representative image of at least three independent experiments is shown. **D**, Rat primary neurons transfected with WT or UBEm h*BDNF* pIV-dependent FFluc construct and h*EF1alpha* promoter-dependent hRluc construct together with empty vector control (pRC) or constructs coding USF1 and USF2 fused to VP16 domain, were left untreated (CNTR) or were treated for 8h with 25 mM KCl and luciferase activities were measured. **E**, Rat primary neurons transfected with WT or CREm h*BDNF* pIV-dependent FFluc construct and h*EF1alpha* promoter-dependent hRluc construct together with pRC or a construct coding CREB1 or CREB1 fused to VP16, were left untreated or were treated for 8h with 25 mM KCl and luciferase activities were measured. **F**, Rat primary neurons transfected with WT or PasREm h*BDNF* pIV-dependent FFluc construct and h*EF1alpha* promoter-dependent hRluc construct together with pRC or with a construct coding the indicated protein, were left untreated or were treated for 8h with 25 mM KCl and luciferase activities were measured. Promoter activities in D, E and F are presented in RLUs relative to the promoter activity measured from untreated pRC transfected neurons that was arbitrarily set as 1. Results of at least three independent experiments with at least duplicate measurements are shown in B, D, E and F. Statistical significance denoted by asterisks is relative to WT construct fold induction in B and between the bars indicated with lines in D, E and F. (***, $P<0.001$; **, $P<0.01$; *, $P<0.05$; NS, not significant; t-test)

Figure 4. CRE is needed for initiation and PasRE for enhancement of h*BDNF* pIV induction by neuronal activity. Rat primary neurons transfected with WT or with CRE or PasRE mutated h*BDNF* pIV-dependent FFluc construct and h*EF1alpha* promoter-dependent hRluc construct, were treated with 25 mM KCl and luciferase activities were measured at time points from 1h to 10h after KCl addition. Data at different time points are represented as fold induced promoter activities over activities measured from untreated control neurons. Results of three independent experiments with

duplicate measurements normalized to hRluc levels are shown. Statistical significance denoted by asterisks is relative to WT construct fold induction at respective time point. (***, P<0.001; **, P<0.01; *, P<0.05; t-test)

Figure 5. PasRE and CRE-like elements regulate h*BDNF* pIX induction. **A**, Rat primary neurons transfected with h*BDNF* pIX-dependent FFluc construct or indicated derivative thereof and h*EF1alpha* promoter-dependent hRluc construct, were treated with 25 mM KCl and luciferase activities were measured. Data are represented as fold induced promoter activities over activities measured from untreated control neurons. Numbers in the schematic representations of the promoters indicate nucleotide positions relative to the 3' transcription start site (TSS2) of h*BDNF* exon IX. TSS1, 5' transcription start site in h*BDNF* exon IX. 5', 5' part of h*BDNF* pIX; 3', 3' part of h*BDNF* pIX; NdeI, NdeI restriction site used to generate the pIX 3' NdeI construct. 3' 112bp, h*BDNF* pIX-luciferase construct with minimal KCl inducible sequence. mut, mutations in the PasRE and CRE-like elements. **B**, Alignment of the region responsible for neuronal activity-dependent induction of h*BDNF* pIX with the respective region in the rat promoter. Numbers indicate nucleotide positions relative to the TSS2 of h*BDNF* exon IX. **C**, EMSA showing CREB1, USF and ARNT2-NPAS4 containing complexes binding to the PasRE and CRE-like element containing oligo pIX PasRE/CRE-like. Addition of unlabeled oligo or ab to the reaction and the lysates used are designated as in Figure 2D. Representative image of three independent experiments is shown. **D**, Rat primary neurons transfected with 3' 112bp h*BDNF* pIX-dependent FFluc construct and h*EF1alpha* promoter-dependent hRluc construct together with pRC or with a construct coding the indicated protein, were left untreated or were treated for 8h with 25 mM KCl and luciferase activities were measured. Promoter activities are presented in RLUs relative to the promoter activity measured from untreated pRC transfected neurons that was arbitrarily set as 1. Results of at least three independent experiments with duplicate measurements are shown. Statistical significance denoted by asterisks is between the bars indicated by lines in A and relative to promoter activity in pRC transfected untreated control or pRC transfected KCl treated neurons, respectively, in D. (***, P<0.001; **, P<0.01; *, P<0.05; t-test)

Figure 6. Dominant negative ARNT2-NPAS4 interfere with neuronal activity-dependent transcription of endogenous rat *BDNF* exon I, IV and IX-5' mRNAs. Control GFP coding construct or a construct coding ARNT2 without the transactivation domain (delTAD-ARNT2) together with a construct coding NPAS4 without the transactivation domain (delTAD-NPAS4), were electroporated into rat primary neurons. At 5 DIV neurons were treated with 25 mM KCl for the time indicated and mRNA levels of rat endogenous *BDNF* exon I, IV and IX-5' transcripts were measured with RT-qPCR. mRNA levels are shown as fold induced levels over levels of the respective transcript in untreated neurons. The data is from two independent experiments measured in triplicates and normalized to *HPRT1* expression levels.

Figure 7. ARNT2-NPAS4 and CREB bind endogenous h*BDNF* promoters and activate h*BDNF* transcription. **A**, Western blot showing ARNT2-V5, NPAS4-V5 or combination of ARNT2-V5 with NPAS4 and NPAS4-V5 with ARNT2, and CREB1-V5 expression in HEK293 cells transfected with the respective constructs. Protein expression was verified with anti-NPAS4, anti-ARNT2, anti-CREB1 and anti-V5 ab-s. **B**, Chromatin immunoprecipitation (ChIP) experiment with anti-V5 ab using the same cell lysates as described in A, demonstrating ARNT2-NPAS4 heterodimer and CREB1 binding to endogenous h*BDNF* pI and pIV. The data is represented as fold enrichment of immunoprecipitated DNA from cells overexpressing the indicated proteins over empty vector pRC transfected cells. Results from three independent experiments measured in triplicates and normalized to the levels of the respective target in input DNA are shown. Statistical significance denoted by asterisks is relative to enrichment values of Chr11URR obtained from each transfection. **C**, Western blot showing VP16-CREB1 or ARNT2-V5, NPAS4-V5 or combination of ARNT2-V5 with NPAS4-V5 expression in HEK293 cells transfected with the respective constructs. Protein expression was verified with anti-VP16 and anti-V5 ab-s. **D**, RT-qPCR analyses showing h*BDNF* exon I, IV or IX-5' transcript expression in HEK293 cells described in C. The data is presented as fold change in *BDNF* transcript levels in indicated protein overexpressing cells compared to levels of the respective transcript in control pRC transfected cells. Results of three independent experiments measured in triplicates and normalized to the levels of *HPRT1* mRNA levels are shown. Statistical significance

denoted by asterisks is relative to mRNA levels in pRC transfected cells. **E**, ChIP experiment with anti-CREB1 or anti-ARNT2 ab using postmortem human parietal cortex lysates, demonstrating CREB1 binding to endogenous h*BDNF* pIV and ARNT2 binding to endogenous h*BDNF* pI and pIV. The data is represented as enrichment of ab immunoprecipitated DNA relative to –ab control precipitated DNA. Statistical significance denoted by asterisks is relative to enrichment values of Chr11URR obtained with the indicated ab. Results with three independent tissue samples measured in triplicates are shown. Immunoprecipitated DNA was analyzed by qPCR with primers amplifying fragments of indicated genomic regions in B and E. pI, h*BDNF* pI; pIV, h*BDNF* pIV; pIX, h*BDNF* pIX; and Chr11URR, unrelated region in human chromosome 11 serving as a negative control. (***, $P<0.001$; **, $P<0.01$; *, $P<0.05$; t-test)

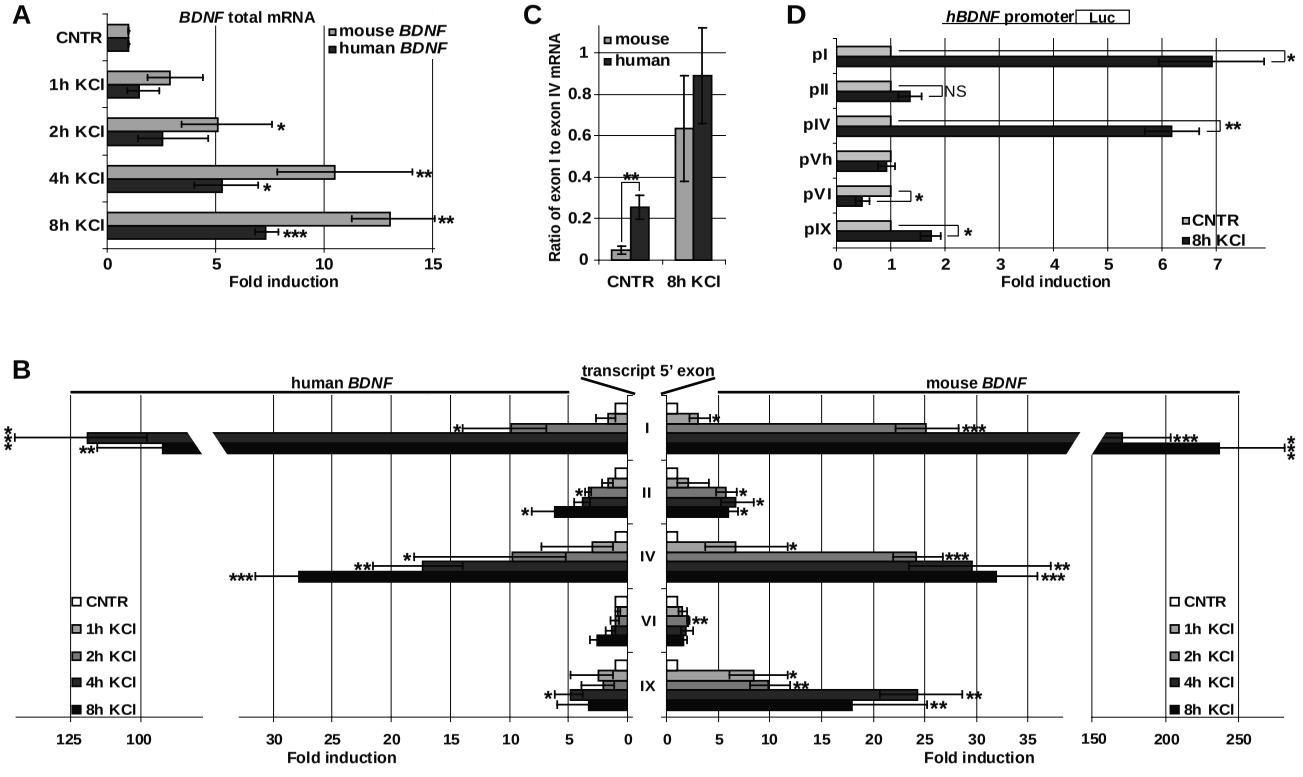
A
BDNF total mRNA
mouse BDNF
human BDNF
CNTR
1h KCl
2h KCl
4h KCl
8h KCl
Fold induction
C
mouse
human
Ratio of exon I to exon IV mRNA
CNTR
8h KCl
D
hBDNF promoter
Luc
pI
pII
pIV
pVh
pVI
pIX
NS
CNTR
8h KCl
Fold induction
B
human BDNF
transcript 5' exon
mouse BDNF
I
II
IV
VI
IX
CNTR
1h KCl
2h KCl
4h KCl
8h KCl
Fold induction
Fold induction

Figure 1

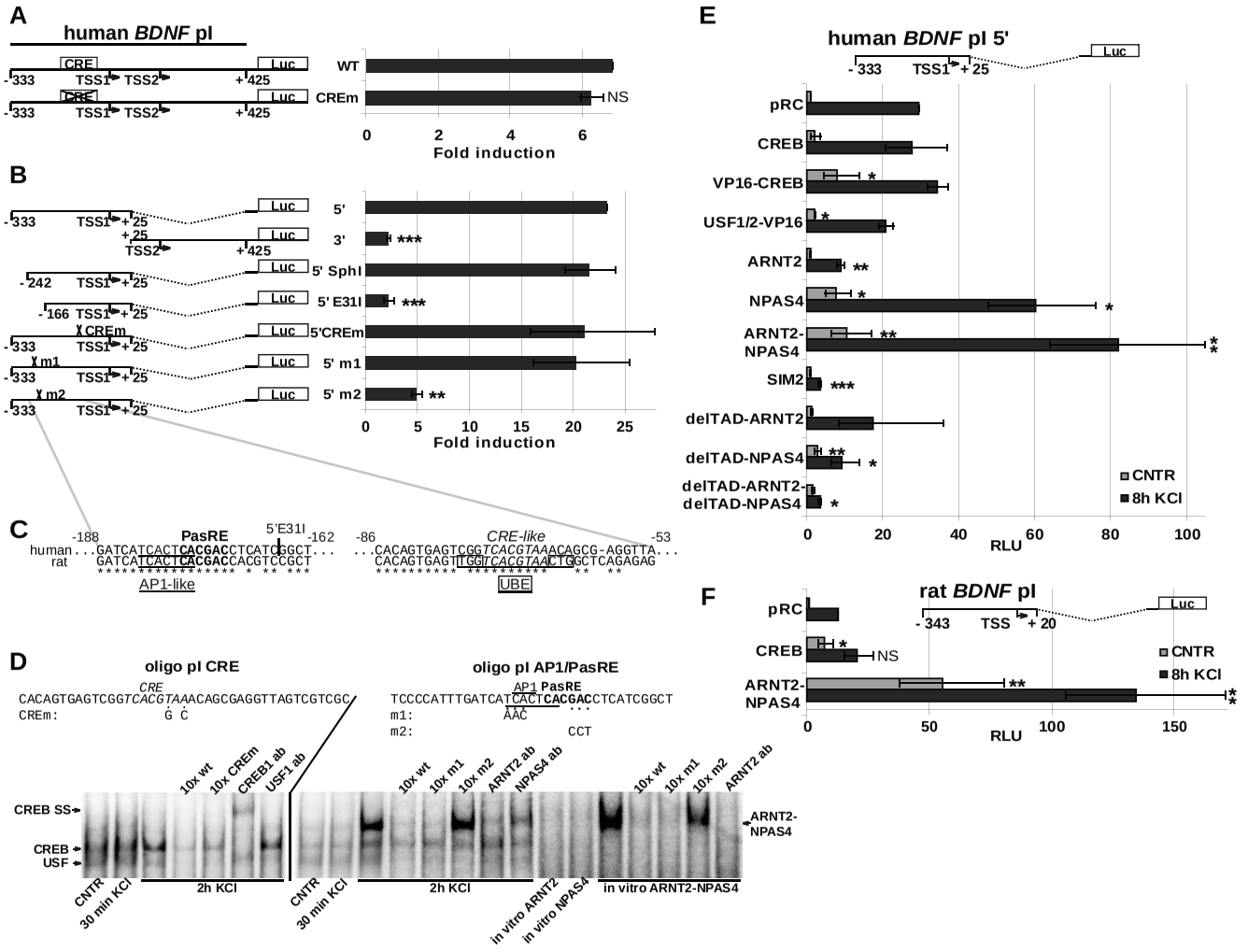
A
human BDNF pI
CRE
Luc
-333
TSS1
TSS2
+425
WT
CREm
NS
0
2
4
6
Fold induction
B
5'
3'
***
5' SphI
5' E31I
5'CREm
5' m1
5' m2
**
-242
-166
+25
0
5
10
15
20
25
C
-188
PasRE
5'E31I
-162
-86
CRE-like
-53
human ...GATCATCACTCACGACCTCATCGGCT...
rat GATCATCACTCACGACCACGTCCGCT
...CACAGTGAGTCGGTCACGTAAACAGCG-AGGTTA...
CACAGTGAGTTGGTCACGTAACTGGCTCAGAGAG
AP1-like
UBE
D
oligo pI CRE
CRE
CACAGTGAGTCGGTCACGTAAACAGCGAGGTTAGTCGTCGC
CREm: G C
oligo pI AP1/PasRE
AP1 PasRE
TCCCCATTTGATCATCACTCACGACCTCATCGGCT
m1: AAC
m2: CCT
10x wt
10x CREm
CREB1 ab
USF1 ab
10x m1
10x m2
ARNT2 ab
NPAS4 ab
CREB SS
CREB
USF
ARNT2-NPAS4
CNTR
30 min KCl
2h KCl
in vitro ARNT2
in vitro NPAS4
in vitro ARNT2-NPAS4
E
human BDNF pI 5'
pRC
CREB
VP16-CREB
USF1/2-VP16
ARNT2
NPAS4
ARNT2-NPAS4
SIM2
delTAD-ARNT2
delTAD-NPAS4
delTAD-ARNT2-delTAD-NPAS4
CNTR
8h KCl
RLU
0
20
40
60
80
100
F
rat BDNF pI
-343
TSS
+20
NS
150
50

Figure 2

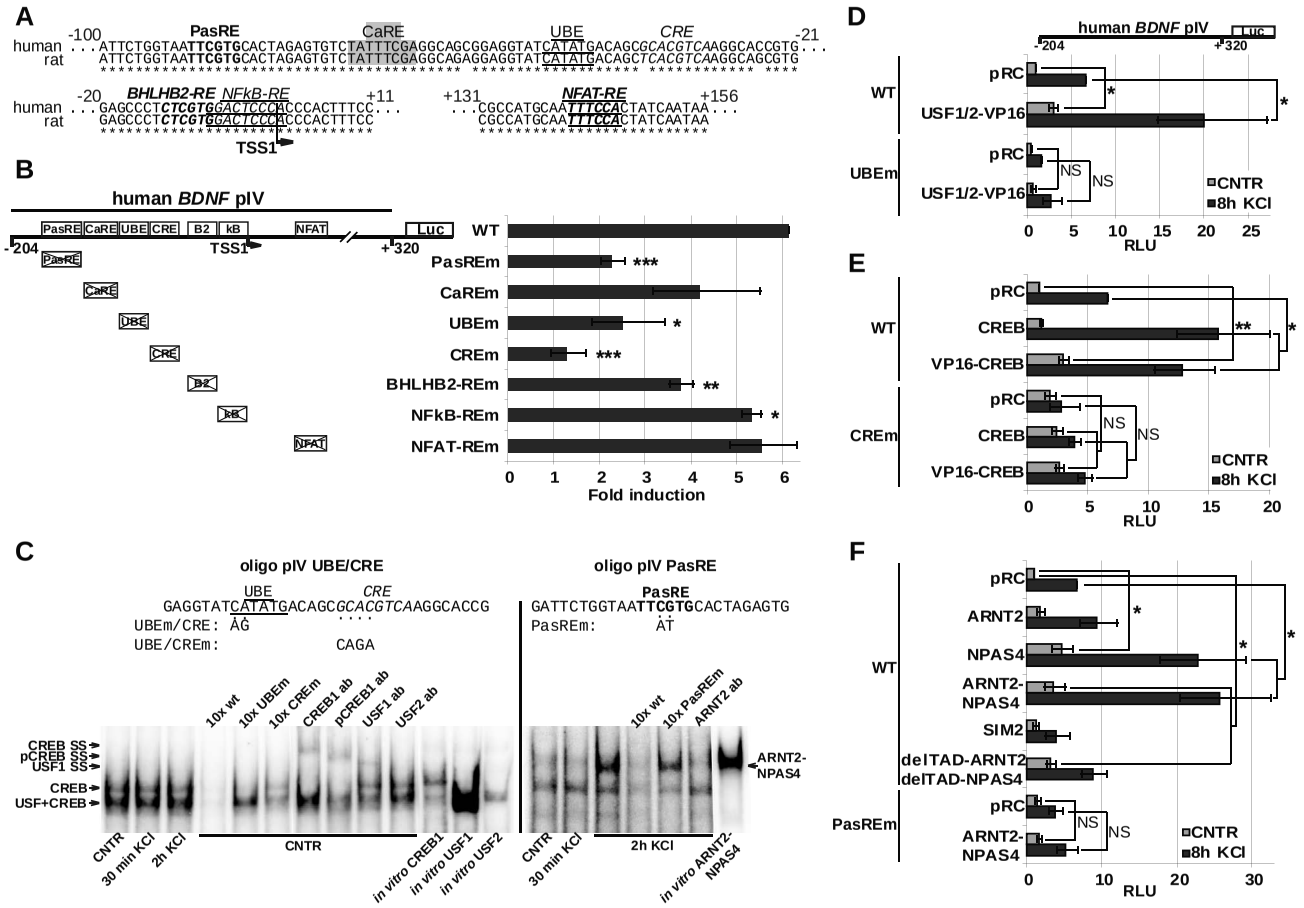
A
PasRE
CaRE
UBE
CRE
human
rat
BHLHB2-RE
NFkB-RE
NFAT-RE
TSS1
B
human BDNF pIV
Luc
WT
PasREm
CaREm
UBEm
CREm
BHLHB2-REm
NFkB-REm
NFAT-REm
Fold induction
C
oligo pIV UBE/CRE
oligo pIV PasRE
UBEm/CRE:
UBE/CREm:
PasREm:
CREB SS
pCREB SS
USF1 SS
CREB
USF+CREB
ARNT2-NPAS4
CNTR
30 min KCl
2h KCl
in vitro CREB1
in vitro USF1
in vitro USF2
in vitro ARNT2-NPAS4
D
pRC
USF1/2-VP16
NS
CNTR
8h KCl
RLU
E
CREB
VP16-CREB
CREm
F
ARNT2
NPAS4
ARNT2-NPAS4
SIM2
delTAD-ARNT2
delTAD-NPAS4
PasREm

Figure 3

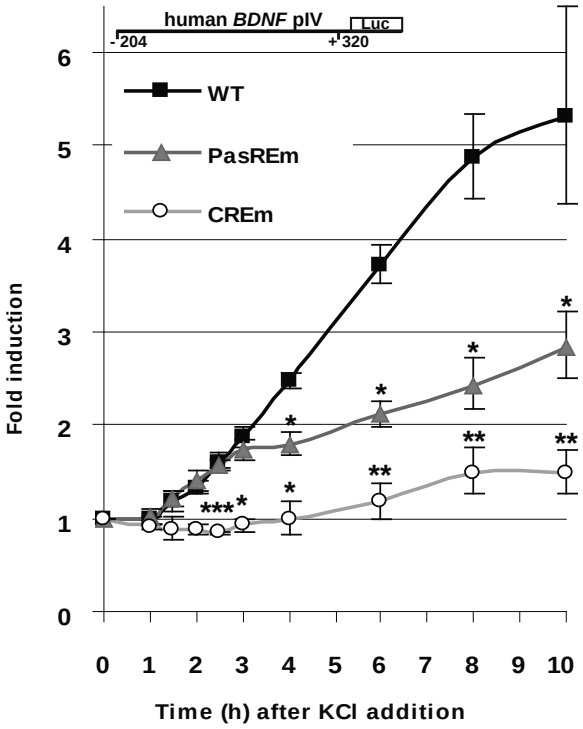
human *BDNF* pIV
Luc
-204
+320
WT
PasREm
CREm
Fold induction
Time (h) after KCl addition
0
1
2
3
4
5
6
7
8
9
10
*
**
***

Figure 4

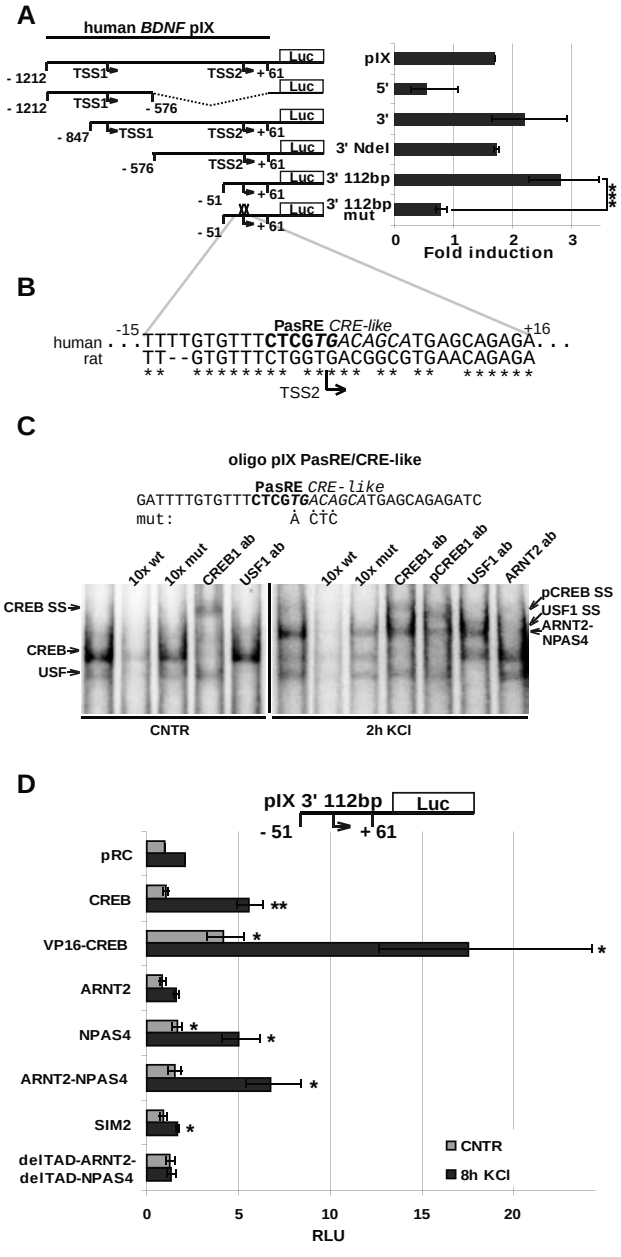
A
human BDNF pIX
Luc
- 1212
TSS1
TSS2
+61
- 576
- 847
- 51
pIX
5'
3'
3' NdeI
3' 112bp
3' 112bp mut
***
0
1
2
3
Fold induction
B
PasRE CRE-like
-15
+16
human ...TTTTGTGTTTCTCGTGACACAGCATGAGCAGAGA...
rat TT--GTGTTTCTGGTGACGGCGTGAACAGAGA
TSS2
C
oligo pIX PasRE/CRE-like
PasRE CRE-like
GATTTTGTGTTTCTCGTGACACAGCATGAGCAGAGATC
mut: A C C
10x wt
10x mut
CREB1 ab
USF1 ab
pCREB1 ab
ARNT2 ab
CREB SS
CREB
USF
pCREB SS
USF1 SS
ARNT2-NPAS4
CNTR
2h KCl
D
pIX 3' 112bp
Luc
- 51
+ 61
pRC
CREB
VP16-CREB
ARNT2
NPAS4
ARNT2-NPAS4
SIM2
delTAD-ARNT2-delTAD-NPAS4
CNTR
8h KCl
0
5
10
15
20
RLU

Figure 5

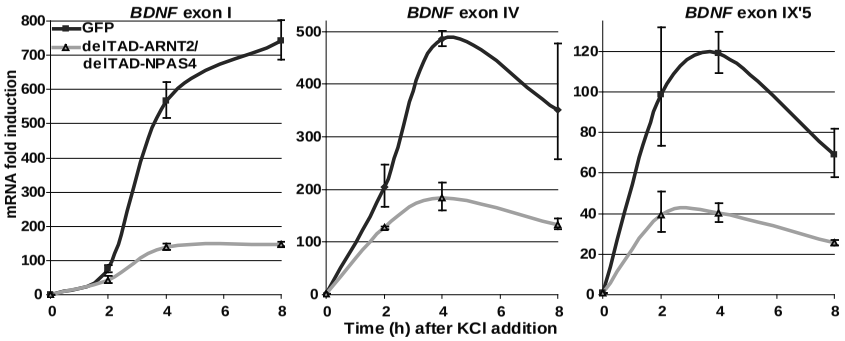
BDNF exon I
BDNF exon IV
BDNF exon IX'5
GFP
delTAD-ARNT2/
delTAD-NPAS4
mRNA fold induction
Time (h) after KCl addition

Figure 6

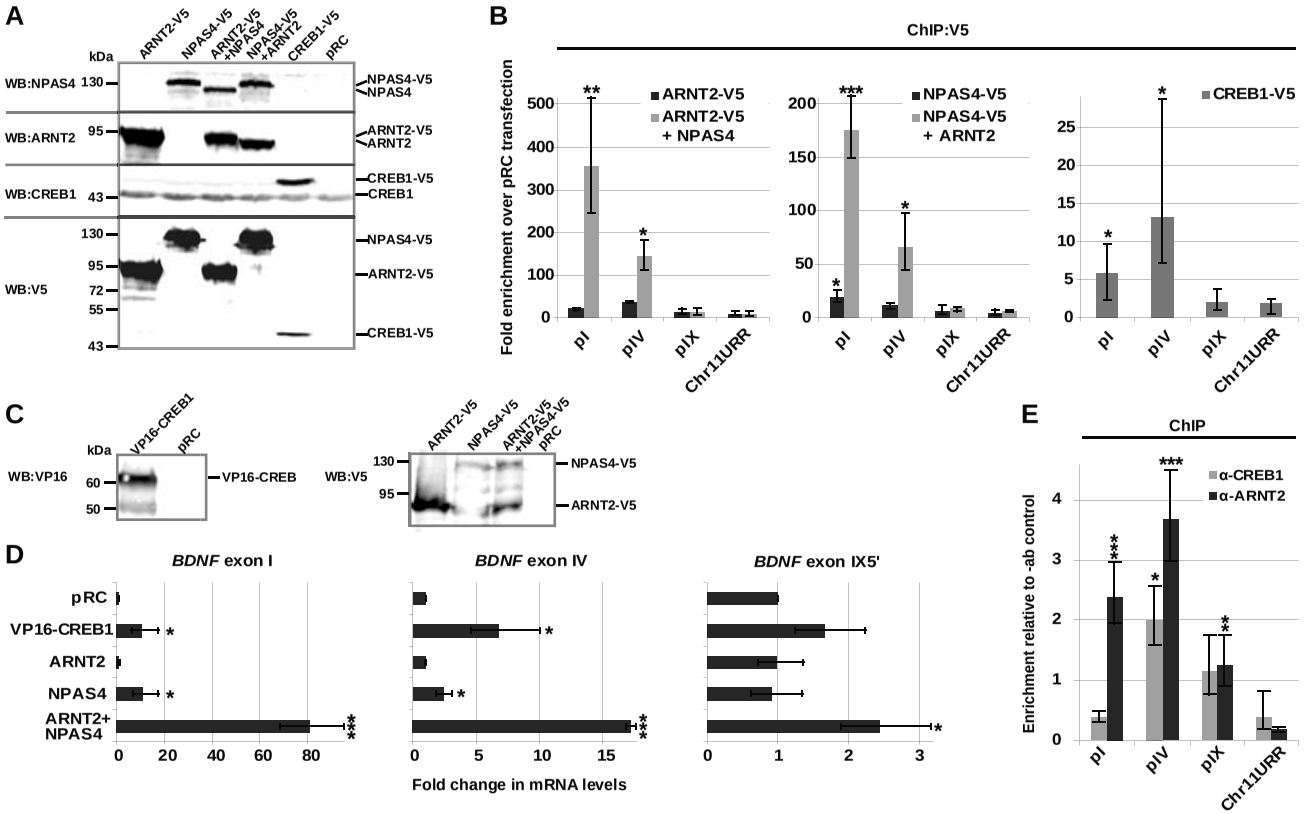
A
ARNT2-V5
NPAS4-V5
ARNT2-V5 +NPAS4
NPAS4-V5 +ARNT2
CREB1-V5
pRC
kDa
WB:NPAS4
130
NPAS4-V5
NPAS4
WB:ARNT2
95
ARNT2-V5
ARNT2
WB:CREB1
43
CREB1-V5
CREB1
WB:V5
130
95
72
55
43
NPAS4-V5
ARNT2-V5
CREB1-V5
B
ChIP:V5
Fold enrichment over pRC transfection
ARNT2-V5
ARNT2-V5 + NPAS4
NPAS4-V5
NPAS4-V5 + ARNT2
CREB1-V5
pI
pIV
pIX
Chr11URR
C
VP16-CREB1
pRC
kDa
WB:VP16
60
50
VP16-CREB
ARNT2-V5
NPAS4-V5
ARNT2-V5 +NPAS4-V5
pRC
WB:V5
130
95
NPAS4-V5
ARNT2-V5
D
BDNF exon I
BDNF exon IV
BDNF exon IX5'
pRC
VP16-CREB1
ARNT2
NPAS4
ARNT2+ NPAS4
Fold change in mRNA levels
E
ChIP
Enrichment relative to -ab control
α-CREB1
α-ARNT2
pI
pIV
pIX
Chr11URR

Figure 7

Supplementary Table S1. Primers used in the study.

	PCR product	sense primer	antisense primer
expression	Mouse total BDNF	GGCCCAACGAAGAAAACCAT	AGCATCACCCGGGAAGTGT
	Human total BDNF	CATCCGAGGACAAGGTGGCTTGG	GTCCTCATCCAACAGCTCTTCTATC
	mBDNF exon I	TTGAAGCTTTGCGGATATTGCG	AAGTTGCCTTGTCCGTGGAC
	mBDNF exon II	TGGTATACTGGGTTAACTTTGGGAAA	AAGTTGCCTTGTCCGTGGAC
	mBDNF exon IV	GAAATATATAGTAAGAGTCTAGAACCTTG	AAGTTGCCTTGTCCGTGGAC
	mBDNF exon VI	GCTTTGTGTGGACCCTGAGTTC	AAGTTGCCTTGTCCGTGGAC
	mBDNF exon IX-5′	GGACTATGCTGCTGACTTGAAAGGA	GAGTAAACGGTTTCTAAGCAAGTG
	hBDNF exon I	CAGCATCTGTTGGGGAGACGAGA	ATGGGGGCAGCCTTCATGCA
	hBDNF exon II	ATGCAAGTGTTTATCTCCAGGATCT	CCAAGCCACCTTGTCCTCGGATG
	hBDNF exon IV	GAAGTCTTTCCCGGAGCAGCT	ATGGGGGCAGCCTTCATGCA
	hBDNF exon VI	GAGCCAGAATCGGAACCAC	ATGGGGGCAGCCTTCATGCA
	hBDNF exon IX-5′	AACCTTGACCCTGCAGAATGGCCT	GATGGTCATCACTCTTCTCACCT
	rat BDNF exon I	AACAAGACACATTACCTTCCAGCAT	CTCTTCTCACCTGGTGGAACATT
	rat BDNF exon IV	GCTGCCTTGATGTTTACTTTGA	GCAACCGAAGTATGAAATAACC
	rat BDNF exon IX-5′	GGACTATGCTGCTGACTTGAAAGGA	GAGTAAACGGTTTCTAAGCAAGTG
	mouse and rat HPRT1	CAGTCCCAGCGTCGTGATTA	AGCAAGTCTTTCAGTCCTGTC
mutagenesis	hBDNF pI CREm	CACAGTGAGTCGGTCACGGACACAGCGAGGTTAGTCGTCGC	GCGACGACTAACCTCGCTGTGTCCGTGACCGACTCACTGTG
	hBDNF pI m1	TCCCCATTTGATCAAACCTCACGACCTCATCGGCT	AGCCGATGAGGTCGTGAGGTTTGATCAAATGGGGA
	hBDNF pI m2	TCCCCATTTGATCATCACTCACCCTCTCATCGGCT	AGCCGATGAGAGGGTGAGTGATGATCAAATGGGGA
	hBDNF pIV PasREm	GATTCTGGTAATTATTGCACTAGAGTG	CACTCTAGTGCAATAATTACCAGAAT
	hBDNF pIV CaREm	TTCGTGCACTAGAGTGTAAATTTCAGAGGCAGCGGAG	CTCCGCTGCCTCGAAATTTACACTCTAGTGCACGAA
	hBDNF pIV UBEm	CGAGGCAGCGGAGGTATAGTATGACAGCGCACGTCA	TGACGTGCGCTGTCATACTATACCTCCGCTGCCTCG
	hBDNF pIV CREm	CGGAGGTATCATATGACAGCCAGCTGCAAGGCACCGTGGAGCCCTCTCG	CGAGAGGGCTCCACGGTGCCTTGCAGCTGGCTGTCATATGATACCTCCG
	hBDNF pIV BHLHB2-REm	GCACCGTGGAGCCCTCTACTGGACTCCCACCCACTT	AAGTGGGTGGGAGTCCAGTAGAGGGCTCCACGGTGC
	hBDNF pIV NFkB-REm	GAGCCCTCTCGTGGACTAACACCCACTTTCCCATTC	GAATGGGAAAGTGGGTGTTAGTCCACGAGAGGGCTC
	hBDNF pIV NFAT-REm	TCCGCCATGCAATTGGCACTATCAATAATT	AATTATTGATAGTGCCAATTGCATGGCGGA
	hBDNF pIX mut	GATTTTGTGTTTCTCGAGCTCGCATGAGCAGAGATC	GATCTCTGCTCATGCGAGCTCGAGAAACACAAAATC
cloning	FL hARNT2	CACCATGGCAACCCCGGCGGCGGTCAAC	CCGCAGCTACTCAGAAAACGG
	FL hNPAS4	CACCATGTACCGCTCCACCAAGGG	TTCAAAACGTTGGTTCCCCTCC
	FL hSIM2	CACCATGAAGGAGAAGTCCAAGAATGCG	GTCACCTCCCGTTGGTGATGATG
	FL hCREB1	CACCATGACCATGGAATCTGGAGCCGAG	CCAAATTAATCTGATTTGTGGCAGTAAAGG
	FL hUSF1	CACCATGAAGGGGCAGCAGAAAACAGC	CCCATAGTTAGTTGCTGTCATTCTTG
	FL hUSF2	CACCATGGACATGCTGGACCC	CGTCACTGCCGGGTGCCCT
	FL hDREAM	CACCATGCAGCCGGCTAAG	CTAGATGACATTCTCAAACAGCTGC
	FL hKChIP1	CACCATGGGGGCCGTCATGGGCAC	TTACATGACATTTTGAAACAGCTGG
	FL hKChIP2	CACCATGCGGGGCCAGGGCCGCAAG	CTAGATGACATTGTCAAAGAGCTGC
	FL hKChIP4	CACCATGAATGTGAGGAGGGTGGAAAG	TTAAATCACATTTTCAAAGAGCTGC
ChIP	hBDNF pI	TCACGACCTCATCGGCTGGA	GACGACTAACCTCGCTGTTT
	hBDNF pIV	CTGGTAATTCGTGCACTAGAGT	CACGAGAGGGCTCCACGGT
	hBDNF pIX	CACTTGCAGTTGTTGCTTA	GGCTTCAAGTTCTCCTTCTTCCCA
	hChr11URR	GTCATGAGGGCTCCACTCTTA	AAGGGCAAAGAGGGCAACAGA

785 bp of human BDNF promoter I cloned into pGL4.15

>humanBDNFpI

CTAGTGGCTCGCCTTGGTGCCTCTCGCCTAGTCATCAGTACCTAAGAGGAAAAGGGAAAGTTGTTGGGCTGGTTCGCGCTTCGACGATGCAGA
TGTTCCCAAGGACAAGTCACTTACTCGCCCCCCTCCCCCCAGTCCCCATTTGATCATCACTCACGACCTCATCGGCTGGAGACCCTTAGTCATG
ATGGGGGAGGGGGAGGGGCACGAACTTTTCTAAGAAGTTTCCTTTTTTTACCCAGAGAGTCACAGTGAGTCGGTCACGTAAACAGCGAGGTTAG
TCGTCGCCGTTGCCGCCCCCCACCCCCTCCCTGCTGCGCTTTTCTGGTATTTATTATTAAAGCGGTAGTCTGCGGCGCTGATAAGCAACAAGTT
CCCCAGCGGTCTTCCCGCCCTAGCCTGACAAGGCGAAGGTTTTCTTACCTGGCGACAGGGAAATCTCCCGAGCCGAATTCAGCTTCGCCGGAGC
CCCAGGTGTGACCTGCGTAGTGGGCAAGGGAGCGGTGTGCAGGCTGAGTTTTTTTTTTACAGGGGTACCCTGAAACTCCTCACTTTCTCTGGGA
ACTTTCAGTGCCAGGACCCAGTAACGGGCGGTTAGAAGGCAGCCCTAGGAAACACCTGCTACATAGCAGGGCAGTTGGGCAATCATTGGTAACC
TCGCTCATTCATTAGAATCACGTAAGAACTCAAAAGGAAACGTGTCTCTCGGAGTGAGGGCGTTTGCGTAAATCTATAGGTTTTTCGACATCGA
TGCCAGTTGCTTTGTCTTCTGTAGTCGCCAAGG

753 bp of human BDNF promoter II cloned into pGL4.15

>humanBDNFpII

TGCTTGTCTGTCAGCAGTCTTGCATTCTATTCTTTTCCTTAATGTGTATGGTGTATGATCATATTCTATGATTTATATGTGGGCATGTAATTGA
CATTTGCAAGGGGGTTAATTTCCATCTAAAAACAATAATGCTGTTAGAGGTTGGGGTTAGGGGGTGGAGTGGGGGTAAGGGTGGGGTAAAGACT
GGGAGTTTAGGTGTAGATGGGGGGTGGGGTTGGGGGGAGAGAAATAAGTCAGAAGTGCATATCACCGGTAATGGGTAATCCTCTCGTAGAAGAA
AAGGTTCTCATCAACATGTGATCAACTATTAACAGGATGGCTTTGGCAAAGCCATCCGCACGTGACAAACCGTAAGGAAGTGGAAGAAACCGTC
TAGAGCAATATCAAGTATCACTTAATTAGAGATTTTTAAGCCTTTTCCTCCTGCTGTGCCGGGTGTGTAATCCGGGCGATAGGAGTCCATTCAG
CACCTTGGACAGAGCCAACGGATTTGTCCGAGGTGGCGGTACCCCCAGGTAGTCTTCTTGGCCCCGCTGTAAAGCCAACCCTGTGTCGCCCTTA
AAAAGCGTCTTTTCTGAGGTTCGGCTCACACTGAGATCGGGGCTGGAGAGAGAGTCAGATTTTGGAGCGGAGCGTTTGGAAAGCGAGCCCCAGT
TTGGTCCCCTCATTGAGCTCGCTGAAGTTGGCTTCCTAGCGGTGTAGGCTGGAATAGACTCTTGGCAAGCTCCGGGTTGGTATACTGGGTTAAC
T

524 bp of human BDNF promoter IV cloned into pGL4.15

>humanBDNFpIV

TGTGTTTGCTGGGGCTGGAAGTGAAAACATCTGCAAAAGCATGCAATGCCTTGGAACGGAACTCTTCTAATAAAAGATGTATCATTTTAAATGC
GCTGAATTTTGATTCTGGTAATTCGTGCACTAGAGTGTCTATTTCGAGGCAGCGGAGGTATCATATGACAGCGCACGTCAAGGCACCGTGGAGC
CCTCTCGTGGACTCCCACCCACTTTCCCATTCACCGCGGAGAGGGCTGCTCTCGCTGCCGCTCCCCCCGGCGAACTAGCATGAAATCTCCCTGC
CTCTGCCGAGATCAAATGGAGCTTCTCGCTGATGGGGTGCGAGTATTACCTCCGCCATGCAATTTTCCACTATCAATAATTTAACTTCTTTGCTG
CAGAACAGAAGGAGTACATACCGGGCACCAAAGACTCGCGCCCCCTCCCCCCTTTAATTAAGCGAAGGGAACGTGAAAAAATAATAGAGTGTGG
GAGTTTTGGGGGCCGAAGTCTTTCCCGGAGCAGCTGCCTTGATGGTTACTTTGAC

CTACTG — BHLHB2-RE — NFkB-RE — GGACTAACA — NFAT-RE — TTGGCA

200 bp of human BDNF promoter Vh cloned into pGL4.15

>humanBDNFpVh

TCGCGTTCGCAAGCTCCGTAGTGCAGGAAGGTGCGGGAAGGTGTGTCTGTGGCCCGGGAAACGCACGCCCTCTCCCAGAGAACTTGGGTGCTGG
GATGGGGAGGAAGGGGAGAGTTGAAAGCTAGGGGAGCGAGACCTCGGGGCGTGCGATTCTCACTCGCTCCCTCCCGCCCCAGCGCCCACAGCCG
GGGTTTCTGCAG

607 bp of human BDNF promoter VI cloned into pGL4.15

>humanBDNFpVI

GAGGGCGCGGGACGCGGGGTTCCCCGGGGCTGAGGCTGGGGCTGGAACACCCCTCGAAGCCGCGGGCGTCCTGTCCAAGGCGCCCCAGGAGGGC
GCAGGACTCGCAGGGCGATGTCGCGGGGCCCTAGGGGAGGAGGTGAGGACAGGCCCCGGGGGAGCGGGGAGTTCCGGGCGCCCCTCGGTTCCCC
GCGCGAGGAAAAGACGCGGCGTTCCCTTTAAGCGGCCGCCTCGAACGGGTATCGGTAGCGCGGGCGAGCGGGGAGCGGGGGGCGGGGGGCGGGG
GGGGGCGGCGCCGTTTGACCAATCGAAGCTCAACCGAAGAGCTAAATAATGTCTGACCCGGGCGCAAGGCGCAGCCTGGAGCTCCGGGTCCCCG
CCGCTGCCGCCGCCGGCCGGGCGCACCCGCCCGCTCGCTGTCCCGCGCACCCCGTAGCGCCTCGGGCTCCCGGGCCGGACAGAGGAGCCAGC
CCGGTGCGCCCCTCCACCTCCTGCTCGGGGGGCTTTAATGAGACACCCACCGCTGCTGTGGGGCCGGCGGGGAGCAGCACCGCGACGGGGACCG
GGGCTGGGCGCTGGAGCCAGAATCGGAACCACGATGTGACTCC

1273 bp of human BDNF promoter IX cloned into pGL4.15

>humanBDNFpIX

AATTCAGTAAAACTTCATGGGCAGAAACACAGTTCCTTTTCCTACTTATTTGGATATCATGATGGCCATTGCATGTATGTGTCTTTTTTGTAAGT
CCATGCCTCAGAACTGAGAAGTAGGAATAAAATTAGGGTCAGGGCTGGGGATGCTACTCTTTGCTGCTGAAAACACAATGCTTCAGGTAAGTG
ATTCTGAAGTCCTTCACCACCTGACGGTAACCTTGGGTTGGTCCATAGGTATGTTTTCATTTTGCTTGTTCATCCATTTTAATTGGCTTCCTAG
AGCATGCTTGTAGATGTAGAGCCAAATTTAGAGTAGAGCAACCCTCTGGCAAACAGGAAGAGATTAATTTTGTGGTATGCTTTTAAGGGACTTC
CCAGGAAACTTCAAAAGCAGAAAAAGAAGCACTAGCTGCCTATTCCAAAATGTGTAAAACACCACTCAGCTTTTTAAAAGTAGGATAAACTCAG
AGCGCGCGCACACGCGCGCGCGCACACACACACACACACACACAGAGAGAACATCTCTAGTAAAAAGAAAAGTTGAGCTTTCTTAGCTAGATGT
GTGTATTAGCCAGAAAAAGCCAAGGAGTGAAGGGTTTTAGAGAACTGGAGGAGATAAAGTGGAGTCTGCATATGGGAGGCATTTGAAATGGACT
TAAATGTCTTTTTAATGCTGACTTTTTCAGTTTTCTCCTTACCAGACACATTGTTTTCATGACATTAGCCCCAGGCATAGACACATCATTAAAA
TGAACATGTCAAAAAATGATTTCTGTTTAGAAATAAGCAAAACATTTTCAGTTGTGACCACCCAGGTGTAGAATAAAGAACAGTGGAATTGGGA
GCCCTGAGTTCTAACATAAACTTTCTTCATGACATAAGGCAAGTCTTCTATGGCCTTTGGTTTCCTTACCTGTAAAACAGGATGGCTCAATGAA
ATTATCTTTCTTCTTTGCTATAATAGAGTATCTCTGTGGGAAGAGGAAAAAAAAAGTCAATTTAAAGGCTCCTTATAGTTCCCCAACTGCTGTT
TTATTGTGCTATTCATGCCTAGACATCACATAGCTAGAAAGGCCCATCAGACCCCTCAGGCCACTGCTGTTCCTGTCACACATTCCTGCAAAGG
ACCATGTTGCTAACTTGAAAAAAATTACTATTAATTACACTTGCAGTTGTTGCTTAGTAACATTTATGATTTTGTGTTTCTCGTGACAGCATGA
GCAGAGATCATTAAAAATTAAACTTACAAAGCTGCTAAAGTGGGAAGAAGG

start of pIX3'112bp

end of pIX5'/start of pIX3'NdeI

start of pIX3'

PasRE — CRE-like — mut — CTCGAGCTCGCA

Supplementary Figure 1

350 bp of rat BDNF promoter I* cloned into pGL4.15
>ratBDNFpI
CTAGTGGCTCGCCCGGGTGCCTCTCGCCTAGTCATCAGTCCCTAAGAGGAAAAGGGAAAGTTGTGGGGCTGATGC
GCTCTTCGATTCACGCAGTTGTTCCCTAGAACAAGTCACTCCTGCTCCATCACCCCTCCCCCCCCATTTGATCAT
CACTCACGACCACGTCCGCTGGAGACCCTTAGTCATGGTGGGGGAGGGGCACGAACTTTTCTAAGAAGTTTCCTT
TTTACCAAGGGAGTCACAGTGAGTTGGTCACGTAACTGGCTCAGAGAGGCTGCCCTGGCCCCCTCCCCTCGCCCC
CTCCCCGCTGCGCTTTTCTGGTATTCTTATTAAAGCGGTAGCCGGCTGGT

*lacks a 13 bp insert compared to the Nov. 2004 (Baylor 3.4/rn4) BLAT rat genome assembly; similar to the mouse and human BDNF pI in that respect

Supplementary Figure 2

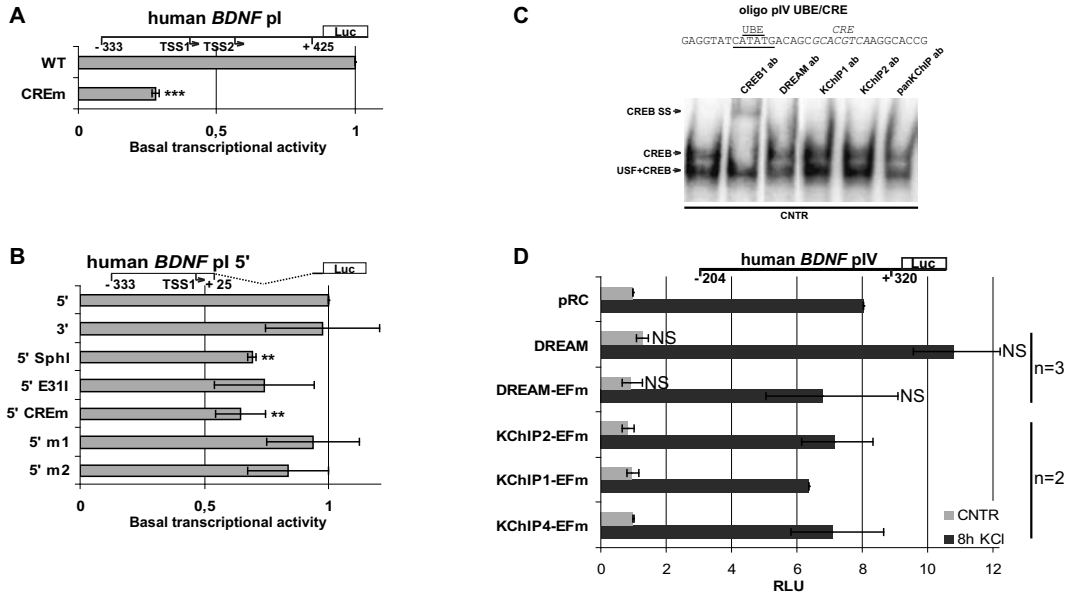

Supplementary Figure 3

Supplementary Figure legends

Supplementary Figure 1. h*BDNF* promoter sequences cloned in front of the firefly luciferase in this study. The relevant TF binding sites and the nucleotides changed in mutated constructs (dots) are indicated. E31I, SphI and NdeI, designate the Eco31I, SphI and NdeI restriction sites used to generate h*BDNF* pI and pIX derivatives. Arrows above the sequence denote 5' ends of respective cloned construct. TSS and arrows below the sequence indicate transcription start sites.

Supplementary Figure 2. r*BDNF* promoter I sequence cloned in front of the firefly luciferase in this study.

Supplementary Figure 3. **A**, Basal levels of h*BDNF* pI and h*BDNF* pICREm promoter-dependent luciferase activities in uninduced cultured neurons. Luciferase activities were measured from rat primary neurons transfected with wild type (WT) or cAMP/Ca^{2+}-response element-like element mutated (CREm) h*BDNF* pI-dependent FFluc construct and h*EF1alpha* promoter-dependent hRluc construct. Promoter activity measured from h*BDNF* pI transfected neurons normalized to h*EF1alpha* promoter activity was arbitrarily set as 1. **B,** Basal levels of h*BDNF* pI 5', h*BDNF* pI 3', h*BDNF* pI 5' SphI, h*BDNF* pI 5' E31I, h*BDNF* pI 5'CREm, h*BDNF* pI 5'm1 and h*BDNF* pI 5'm2 promoter-dependent luciferase activities in uninduced cultured neurons. Luciferase activities were measured from rat primary neurons transfected with the indicated construct and h*EF1alpha* promoter-dependent hRluc construct. Promoter activity measured from h*BDNF* pI 5' transfected neurons normalized to h*EF1alpha* promoter activity was arbitrarily set as 1. Results of at least three independent experiments with duplicate measurements are shown in A and B. Statistical significance denoted by asterisks is relative to the WT pI construct in A and relative to pI 5' promoter activity in B. (***, $P<0.001$; **, $P<0.01$; t-test). **C**, EMSA showing that the DREAM family TF-s do not bind to the h*BDNF* pIV UBE/CRE oligo. The pIV CRE containing oligo was used because transcriptional repressor DREAM (Carrion et al., 1999) has been proposed to be involved in the regulation of CREB1-dependent m*BDNF* exon IV mRNA expression (Fontan-Lozano et al., 2009). Addition of ab to the reaction and the lysate used are designated as in Figure 2D of the main article. ab-s used: rabbit anti-CREB1 (Millipore cat# 06-863); anti-Calsenilin/DREAM/KChIP3 K+ channel, clone K66/38; anti-KChIP1

K+ channel, clone K55/7, anti-KChIP2 K+ channel, clone K60/73; and anti-Pan-KChIP, clone K55/82 (all mouse monoclonal, NeuroMab Antibodies Incorporated). Representative image of two independent experiments is shown. sc-9142 DREAM(FL-214) ab was also used, but supershift or loss of shift was not observed (data not shown). **D**, Rat primary neurons transfected with h*BDNF* pIV-dependent FFluc construct and h*EF1alpha* promoter-dependent hRluc construct together with empty vector control (pRC) or construct coding WT DREAM or DREAM with Ca^{2+}-insensitive EF-hand motifs (EFm; Carrion et al., 1999) or DREAM gene family members (Pruunsild and Timmusk, 2005) with Ca^{2+}-insensitive EF-hand motifs, were left untreated (CNTR) or were treated for 8h with 25 mM KCl and luciferase activities were measured. The EF-hand mutations in all of the DREAM family members were generated according to Carrion et al., 1999. Promoter activities are presented in RLUs relative to the promoter activity measured from untreated pRC transfected neurons that was arbitrarily set as 1. Results of three independent experiments with duplicate measurements are shown for DREAM and DREAM-EFm constructs and results of two independent experiments are shown for other DREAM gene family protein-EFm constructs. NS, statistically not significant relative to promoter activity in pRC transfected untreated control or pRC transfected KCl treated neurons, respectively (t-test).

Supplementary References

Carrion AM, Link WA, Ledo F, Mellstrom B, Naranjo JR (1999) DREAM is a Ca2+-regulated transcriptional repressor. Nature 398:80-84.

Fontan-Lozano A, Romero-Granados R, del-Pozo-Martin Y, Suarez-Pereira I, Delgado-Garcia JM, Penninger JM, Carrion AM (2009) Lack of DREAM protein enhances learning and memory and slows brain aging. Curr Biol 19:54-60.

Pruunsild P, Timmusk T (2005) Structure, alternative splicing, and expression of the human and mouse KCNIP gene family. Genomics 86:581-593.

CURRICULUM VITAE

Name:	Priit Pruunsild
Date and place of birth:	06.10.1980, Tartu, Estonia
Nationality:	Estonian
Citizenship:	Estonian
Contact information:	Department of Gene Technology, Tallinn University of Technology, Akadeemia tee 15, 12618 Tallinn, Tel: +372 620 4444, e-mail: priit.pruunsild@ttu.ee

Education:
2005 - Department of Gene Technology, Tallinn University of Technology (PhD student)
2003 - 2005 Department of Gene Technology, Tallinn University of Technology (MSc)
1999 - 2003 Institute of Molecular and Cell Biology, University of Tartu (BSc)
1988 - 1999 Miina Härma Secondary School, Tartu

Employment:
2007 - Department of Gene Technology, Tallinn University of Technology, researcher
2005 - 2007 Department of Gene Technology, Tallinn University of Technology, engineer
2003 - 2004 Department of Molecular Genetics, National Institute of Chemical Physics and Biophysics, engineer

Dissertations supervised:
Ester Orav, Master's Degree, 2010, (sup) Tõnis Timmusk, Priit Pruunsild, TrkB signalling responsive cis-elements in human BDNF gene, Department of Gene Technology, Tallinn University of Technology
Martin Kask, Master's Degree, 2009, (sup) Tõnis Timmusk, Priit Pruunsild, Promoter characterization and expression analysis of human CTNNA1 and CTNNA2 novel isoforms, Department of Gene Technology, Tallinn University of Technology
Hanna Vihma, Master's Degree, 2007, (sup) Tõnis Timmusk, Priit Pruunsild, Structure, Alternative Splicing and Expression of Human and Mouse NFAT Genes, Department of Gene Technology, Tallinn University of Technology

Research experience:
Analysis of gene structure, expression and regulation in neuronal cells
Publications:

Vashishta, A; Habas, A; **Pruunsild, P**; Zheng, J.J., Timmusk, T.; Hetman, M. (2009). Nuclear Factor of Activated T cells isoform c4 (NFATc4/NFAT3) as a mediator of anti-apoptotic transcription in NMDA receptor-stimulated cortical neurons. Journal of Neuroscience, 29, 15331 - 15340.

Karpova, N.; Lindholm, J.; **Pruunsild, P**.; Timmusk, T.; Castrén, E. (2009). Long-lasting behavioural and molecular alterations induced by early postnatal fluoxetine exposure are restored by chronic fluoxetine treatment in adult mice. European Neuropsychopharmacology, 19, 97 - 108.

Kairisalo M, Korhonen L, Sepp M, **Pruunsild P**, Kukkonen JP, Kivinen J, Timmusk T, Blomgren K, Lindholm D. 2009 NF-kappaB-dependent regulation of brain-derived neurotrophic factor in hippocampal neurons by X-linked inhibitor of apoptosis protein. European Journal of Neuroscience Sep;30(6):958-66.

Koppel, I.; Aid-Pavlidis, T.; Jaanson, K.; Sepp, M.; **Pruunsild, P**.; Palm, K.; Timmusk, T. (2009). Tissue-specific and neural activityregulated expression of human BDNF gene in BAC transgenic mice. BMC Neuroscience, 10, 68

Vihma, H.; **Pruunsild, P**.; Timmusk, T. (2008). Alternative splicing and expression of NFAT genes in human and mouse . Genomics, 92, 279 - 291.

Timmusk, T.; Koppel, I.; **Pruunsild, P**.; Sepp, M.; Tamme, R. (2007). Neurotroofsed tegurid. Eesti Arst, 86, 614 - 621. Estonian

Uvarov, P.; Ludwig, A.; Markkanen, M.; **Pruunsild, P**.; Kaila, K.; Delpire, E.; Timmusk, T.; Rivera, C.; Airaksinen, M.S. (2007). A Novel N-terminal Isoform of the Neuronal K-Cl Cotransporter KCC2. Journal of Biological Chemistry, 282, 30570 - 30576.

Francks, C.; Maegawa, S.; Lauren, J.; Abrahams, B.S.; Velayos-Baeza, A.; Medland, S.E.; Colella, S.; Groszer, M.; McAuley, E.Z.; Caffrey, T.M.; Timmusk, T.; **Pruunsild, P**.; Koppel, I.; Lind, P.A.; Matsumoto-Itaba, N.; Nicod, J.; Xiong, L.; Joober, R.; Enard, W.; Krinsky, B.; Nanba, E.; Richardson, A.J.; Riley, B.P.; Martin, N.G.; Strittmatter, S.M.; Moller, H.J.; Rujescu, D.; St Clair, D.; Muglia, P.; Roos, J.L.; Fisher, S.E.; Wade-Martins, R.; Rouleau, G.A.; Stein, J.F.; Karayiorgou, M.; Geschwind, D.H.; Ragoussis, J.; Kendler, K.S.; Airaksinen, M.S.; Oshimura, M.; Delisi, L.E.; Monaco, A.P. (2007). LRRTM1 on chromosome 2p12 is a maternally suppressed gene that is associated paternally with handedness and schizophrenia. Molecular Psychiatry, 12, 1129 - 1139.

Pruunsild Priit, Kazantseva Anna, Aid Tamara, Palm Kaia, Timmusk Tõnis (2007). Dissecting the human BDNF locus: bidirectional transcription, complex splicing, and multiple promoters. Genomics, 90, 397 - 406.

Uvarov, P; **Pruunsild, P**.; Timmusk, T.;Airaksinen, M.S. (2005). Neuronal K+/Cl- co-transporter (KCC2) transgenes lacking neurone restrictive silencer element recapitulate CNS neuronespecific expression and developmental up-regulation of endogenous KCC2 gene. Journal of Neurochemistry, 1144 - 1155.

Pruunsild, P.; Timmusk, T (2005). Structure, alternative splicing and expression of the human and mouse KCNIP gene family. Genomics, 86, 581 - 593.

Horak, R.; Ilves, H.; **Pruunsild, P**.; Kuljus, M.; Kivisaar, M. (2004). The ColR-ColS two-component signal transduction system is involved in regulation of Tn4652 transposition in Pseudomonas putida under starvation conditions. Molecular Microbiology, 54, 795 - 807.

ELULOOKIRJELDUS

Nimi:	Priit Pruunsild
Sünniaeg ja -koht:	06.10.1980, Tartu, Eesti
Rahvus:	Eestlane
Kodakondsus:	Eesti
Kontaktandmed:	Geenitehnoloogia Instituut, Tallinna Tehnikaülikool, Akadeemia tee 15, 12618 Tallinn, Tel: +372 620 4444, e-kiri: priit.pruunsild@ttu.ee

Hariduskäik:
2005 - Geenitehnoloogia Instituut, Tallinna Tehnikaülikool (PhD üliõpilane)
2003 - 2005 Geenitehnoloogia Instituut, Tallinna Tehnikaülikool (MSc)
1999 - 2003 Molekulaar- ja Rakubioloogia Instituut, Tartu Ülikool (BSc)
1988 - 1999 Miina Härma Gümnaasium, Tartu

Teenistuskäik:
2007 - Geenitehnoloogia Instituut, Tallinna Tehnikaülikool, teadur
2005 - 2007 Geenitehnoloogia Instituut, Tallinna Tehnikaülikool, insener
2003 - 2004 Molekulaargeneetika laboratoorium, Keemilise ja bioloogilise füüsika instituut, insener

Juhendatud lõputööd:
Ester Orav, magistritöö, 2010, (juh) Tõnis Timmusk, Priit Pruunsild, TrkB signalling responsive cis-elements in human BDNF gene (TrkB signaalist sõltuvad cis-elemendid inimese BDNF geenis), Geenitehnoloogia Instituut, Tallinna Tehnikaülikool
Martin Kask, magistritöö, 2009, (juh) Tõnis Timmusk, Priit Pruunsild, Promoter characterization and expression analysis of human CTNNA1 and CTNNA2 novel isoforms (Inimese CTNNA1 ja CTNNA2 uute isovormide promootorite iseloomustamine ja avaldumise analüüs), Geenitehnoloogia Instituut, Tallinna Tehnikaülikool
Hanna Vihma, magistritöö, 2007, (juh) Tõnis Timmusk, Priit Pruunsild, Structure, Alternative Splicing and Expression of Human and Mouse NFAT Genes (NFAT geenide struktuur, alternatiivne splaissing ja ekspressioon inimeses ja hiires), Geenitehnoloogia Instituut, Tallinna Tehnikaülikool

Teadustöö põhisuund:
Geenide struktuur, avaldumine ja regulatsioon närvirakkudes

Teadusüllitised:

Vashishta, A; Habas, A; **Pruunsild, P**; Zheng, J.J., Timmusk, T.; Hetman, M. (2009). Nuclear Factor of Activated T cells isoform c4 (NFATc4/NFAT3) as a mediator of anti-apoptotic transcription in NMDA receptor-stimulated cortical neurons. Journal of Neuroscience, 29, 15331 - 15340.

Karpova, N.; Lindholm, J.; **Pruunsild, P**.; Timmusk, T.; Castrén, E. (2009). Long-lasting behavioural and molecular alterations induced by early postnatal fluoxetine exposure are restored by chronic fluoxetine treatment in adult mice. European Neuropsychopharmacology, 19, 97 - 108.

Kairisalo M, Korhonen L, Sepp M, **Pruunsild P**, Kukkonen JP, Kivinen J, Timmusk T, Blomgren K, Lindholm D. 2009 NF-kappaB-dependent regulation of brain-derived neurotrophic factor in hippocampal neurons by X-linked inhibitor of apoptosis protein. European Journal of Neuroscience Sep;30(6):958-66.

Koppel, I.; Aid-Pavlidis, T.; Jaanson, K.; Sepp, M.; **Pruunsild, P**.; Palm, K.; Timmusk, T. (2009). Tissue-specific and neural activityregulated expression of human BDNF gene in BAC transgenic mice. BMC Neuroscience, 10, 68

Vihma, H.; **Pruunsild, P**.; Timmusk, T. (2008). Alternative splicing and expression of NFAT genes in human and mouse . Genomics, 92, 279 - 291.

Timmusk, T.; Koppel, I.; **Pruunsild, P**.; Sepp, M.; Tamme, R. (2007). Neurotroofsed tegurid. Eesti Arst, 86, 614 - 621. Eesti keeles

Uvarov, P.; Ludwig, A.; Markkanen, M.; **Pruunsild, P**.; Kaila, K.; Delpire, E.; Timmusk, T.; Rivera, C.; Airaksinen, M.S. (2007). A Novel N-terminal Isoform of the Neuronal K-Cl Cotransporter KCC2. Journal of Biological Chemistry, 282, 30570 - 30576.

Francks, C.; Maegawa, S.; Lauren, J.; Abrahams, B.S.; Velayos-Baeza, A.; Medland, S.E.; Colella, S.; Groszer, M.; McAuley, E.Z.; Caffrey, T.M.; Timmusk, T.; **Pruunsild, P**.; Koppel, I.; Lind, P.A.; Matsumoto-Itaba, N.; Nicod, J.; Xiong, L.; Joober, R.; Enard, W.; Krinsky, B.; Nanba, E.; Richardson, A.J.; Riley, B.P.; Martin, N.G.; Strittmatter, S.M.; Moller, H.J.; Rujescu, D.; St Clair, D.; Muglia, P.; Roos, J.L.; Fisher, S.E.; Wade-Martins, R.; Rouleau, G.A.; Stein, J.F.; Karayiorgou, M.; Geschwind, D.H.; Ragoussis, J.; Kendler, K.S.; Airaksinen, M.S.; Oshimura, M.; Delisi, L.E.; Monaco, A.P. (2007). LRRTM1 on chromosome 2p12 is a maternally suppressed gene that is associated paternally with handedness and schizophrenia. Molecular Psychiatry, 12, 1129 - 1139.

Pruunsild Priit, Kazantseva Anna, Aid Tamara, Palm Kaia, Timmusk Tõnis (2007). Dissecting the human BDNF locus: bidirectional transcription, complex splicing, and multiple promoters. Genomics, 90, 397 - 406.

Uvarov, P; **Pruunsild, P**.; Timmusk, T.;Airaksinen, M.S. (2005). Neuronal K+/Cl- co-transporter (KCC2) transgenes lacking neurone restrictive silencer element recapitulate CNS neuronespecific expression and developmental up-regulation of endogenous KCC2 gene. Journal of Neurochemistry, 1144 - 1155.

Pruunsild, P.; Timmusk, T (2005). Structure, alternative splicing and expression of the human and mouse KCNIP gene family. Genomics, 86, 581 - 593.

Horak, R.; Ilves, H.; **Pruunsild, P**.; Kuljus, M.; Kivisaar, M. (2004). The ColR-ColS two-component signal transduction system is involved in regulation of Tn4652 transposition in Pseudomonas putida under starvation conditions. Molecular Microbiology, 54, 795 – 807.

DISSERTATIONS DEFENDED AT TALLINN UNIVERSITY OF TECHNOLOGY ON *NATURAL AND EXACT SCIENCES*

1. **Olav Kongas**. Nonlinear dynamics in modeling cardiac arrhytmias. 1998.

2. **Kalju Vanatalu**. Optimization of processes of microbial biosynthesis of isotopically labeled biomolecules and their complexes. 1999.

3. **Ahto Buldas**. An algebraic approach to the structure of graphs. 1999.

4. **Monika Drews**. A metabolic study of insect cells in batch and continuous culture: application of chemostat and turbidostat to the production of recombinant proteins. 1999.

5. **Eola Valdre**. Endothelial-specific regulation of vessel formation: role of receptor tyrosine kinases. 2000.

6. **Kalju Lott**. Doping and defect thermodynamic equilibrium in ZnS. 2000.

7. **Reet Koljak**. Novel fatty acid dioxygenases from the corals *Plexaura homomalla* and *Gersemia fruticosa.* 2001.

8. **Anne Paju**. Asymmetric oxidation of prochiral and racemic ketones by using sharpless catalyst. 2001.

9. **Marko Vendelin**. Cardiac mechanoenergetics *in silico*. 2001.

10. **Pearu Peterson**. Multi-soliton interactions and the inverse problem of wave crest. 2001.

11. **Anne Menert**. Microcalorimetry of anaerobic digestion. 2001.

12. **Toomas Tiivel**. The role of the mitochondrial outer membrane in *in vivo* regulation of respiration in normal heart and skeletal muscle cell. 2002.

13. **Olle Hints**. Ordovician scolecodonts of Estonia and neighbouring areas: taxonomy, distribution, palaeoecology, and application. 2002.

14. **Jaak Nõlvak**. Chitinozoan biostratigrapy in the Ordovician of Baltoscandia. 2002.

15. **Liivi Kluge**. On algebraic structure of pre-operad. 2002.

16. **Jaanus Lass**. Biosignal interpretation: Study of cardiac arrhytmias and electromagnetic field effects on human nervous system. 2002.

17. **Janek Peterson**. Synthesis, structural characterization and modification of PAMAM dendrimers. 2002.

18. **Merike Vaher**. Room temperature ionic liquids as background electrolyte additives in capillary electrophoresis. 2002.

19. **Valdek Mikli**. Electron microscopy and image analysis study of powdered hardmetal materials and optoelectronic thin films. 2003.

20. **Mart Viljus**. The microstructure and properties of fine-grained cermets. 2003.

21. **Signe Kask**. Identification and characterization of dairy-related *Lactobacillus*. 2003.

22. **Tiiu-Mai Laht**. Influence of microstructure of the curd on enzymatic and microbiological processes in Swiss-type cheese. 2003.

23. **Anne Kuusksalu**. 2–5A synthetase in the marine sponge *Geodia cydonium*. 2003.

24. **Sergei Bereznev**. Solar cells based on polycristalline copper-indium chalcogenides and conductive polymers. 2003.

25. **Kadri Kriis**. Asymmetric synthesis of C_2-symmetric bimorpholines and their application as chiral ligands in the transfer hydrogenation of aromatic ketones. 2004.

26. **Jekaterina Reut**. Polypyrrole coatings on conducting and insulating substracts. 2004.

27. **Sven Nõmm**. Realization and identification of discrete-time nonlinear systems. 2004.

28. **Olga Kijatkina**. Deposition of copper indium disulphide films by chemical spray pyrolysis. 2004.

29. **Gert Tamberg**. On sampling operators defined by Rogosinski, Hann and Blackman windows. 2004.

30. **Monika Übner**. Interaction of humic substances with metal cations. 2004.

31. **Kaarel Adamberg**. Growth characteristics of non-starter lactic acid bacteria from cheese. 2004.

32. **Imre Vallikivi**. Lipase-catalysed reactions of prostaglandins. 2004.

33. **Merike Peld**. Substituted apatites as sorbents for heavy metals. 2005.

34. **Vitali Syritski**. Study of synthesis and redox switching of polypyrrole and poly(3,4-ethylenedioxythiophene) by using *in-situ* techniques. 2004.

35. **Lee Põllumaa**. Evaluation of ecotoxicological effects related to oil shale industry. 2004.

36. **Riina Aav**. Synthesis of 9,11-secosterols intermediates. 2005.

37. **Andres Braunbrück**. Wave interaction in weakly inhomogeneous materials. 2005.

38. **Robert Kitt**. Generalised scale-invariance in financial time series. 2005.

39. **Juss Pavelson**. Mesoscale physical processes and the related impact on the summer nutrient fields and phytoplankton blooms in the western Gulf of Finland. 2005.

40. **Olari Ilison**. Solitons and solitary waves in media with higher order dispersive and nonlinear effects. 2005.

41. **Maksim Säkki**. Intermittency and long-range structurization of heart rate. 2005.

42. **Enli Kiipli**. Modelling seawater chemistry of the East Baltic Basin in the late Ordovician–Early Silurian. 2005.

43. **Igor Golovtsov**. Modification of conductive properties and processability of polyparaphenylene, polypyrrole and polyaniline. 2005.

44. **Katrin Laos**. Interaction between furcellaran and the globular proteins (bovine serum albumin β-lactoglobulin). 2005.

45. **Arvo Mere**. Structural and electrical properties of spray deposited copper indium disulphide films for solar cells. 2006.

46. **Sille Ehala**. Development and application of various on- and off-line analytical methods for the analysis of bioactive compounds. 2006.

47. **Maria Kulp**. Capillary electrophoretic monitoring of biochemical reaction kinetics. 2006.

48. **Anu Aaspõllu.** Proteinases from *Vipera lebetina* snake venom affecting hemostasis. 2006.

49. **Lyudmila Chekulayeva**. Photosensitized inactivation of tumor cells by porphyrins and chlorins. 2006.

50. **Merle Uudsemaa**. Quantum-chemical modeling of solvated first row transition metal ions. 2006.

51. **Tagli Pitsi**. Nutrition situation of pre-school children in Estonia from 1995 to 2004. 2006.

52. **Angela Ivask**. Luminescent recombinant sensor bacteria for the analysis of bioavailable heavy metals. 2006.

53. **Tiina Lõugas**. Study on physico-chemical properties and some bioactive compounds of sea buckthorn (*Hippophae rhamnoides* L.). 2006.

54. **Kaja Kasemets**. Effect of changing environmental conditions on the fermentative growth of Saccharomyces cerevisae S288C: auxo-accelerostat study. 2006.

55. **Ildar Nisamedtinov**. Application of ^{13}C and fluorescence labeling in metabolic studies of Saccharomyces spp. 2006.

56. **Alar Leibak**. On additive generalisation of Voronoï's theory of perfect forms over algebraic number fields. 2006.

57. **Andri Jagomägi**. Photoluminescence of chalcopyrite tellurides. 2006.

58. **Tõnu Martma**. Application of carbon isotopes to the study of the Ordovician and Silurian of the Baltic. 2006.

59. **Marit Kauk**. Chemical composition of $CuInSe_2$ monograin powders for solar cell application. 2006.

60. **Julia Kois**. Electrochemical deposition of $CuInSe_2$ thin films for photovoltaic applications. 2006.

61. **Ilona Oja Açik**. Sol-gel deposition of titanium dioxide films. 2007.

62. **Tiia Anmann**. Integrated and organized cellular bioenergetic systems in heart and brain. 2007.

63. **Katrin Trummal**. Purification, characterization and specificity studies of metalloproteinases from *Vipera lebetina* snake venom. 2007.

64. **Gennadi Lessin**. Biochemical definition of coastal zone using numerical modeling and measurement data. 2007.

65. **Enno Pais**. Inverse problems to determine non-homogeneous degenerate memory kernels in heat flow. 2007.

66. **Maria Borissova**. Capillary electrophoresis on alkylimidazolium salts. 2007.

67. **Karin Valmsen**. Prostaglandin synthesis in the coral *Plexaura homomalla*: control of prostaglandin stereochemistry at carbon 15 by cyclooxygenases. 2007.

68. **Kristjan Piirimäe**. Long-term changes of nutrient fluxes in the drainage basin of the gulf of Finland – application of the PolFlow model. 2007.

69. **Tatjana Dedova**. Chemical spray pyrolysis deposition of zinc sulfide thin films and zinc oxide nanostructured layers. 2007.

70. **Katrin Tomson**. Production of labelled recombinant proteins in fed-batch systems in *Escherichia coli*. 2007.

71. **Cecilia Sarmiento**. Suppressors of RNA silencing in plants. 2008.

72. **Vilja Mardla**. Inhibition of platelet aggregation with combination of antiplatelet agents. 2008.

73. **Maie Bachmann**. Effect of Modulated microwave radiation on human resting electroencephalographic signal. 2008.

74. **Dan Hüvonen**. Terahertz spectroscopy of low-dimensional spin systems. 2008.

75. **Ly Villo**. Stereoselective chemoenzymatic synthesis of deoxy sugar esters involving *Candida antarctica* lipase B. 2008.

76. **Johan Anton**. Technology of integrated photoelasticity for residual stress measurement in glass articles of axisymmetric shape. 2008.

77. **Olga Volobujeva**. SEM study of selenization of different thin metallic films. 2008.

78. **Artur Jõgi**. Synthesis of 4'-substituted 2,3'-dideoxynucleoside analogues. 2008.

79. **Mario Kadastik**. Doubly charged Higgs boson decays and implications on neutrino physics. 2008.

80. **Fernando Pérez-Caballero**. Carbon aerogels from 5-methylresorcinol-formaldehyde gels. 2008.

81. **Sirje Vaask**. The comparability, reproducibility and validity of Estonian food consumption surveys. 2008.

82. **Anna Menaker**. Electrosynthesized conducting polymers, polypyrrole and poly(3,4-ethylenedioxythiophene), for molecular imprinting. 2009.

83. **Lauri Ilison**. Solitons and solitary waves in hierarchical Korteweg-de Vries type systems. 2009.

84. **Kaia Ernits**. Study of In_2S_3 and ZnS thin films deposited by ultrasonic spray pyrolysis and chemical deposition. 2009.

85. **Veljo Sinivee**. Portable spectrometer for ionizing radiation "Gammamapper". 2009.

86. **Jüri Virkepu**. On Lagrange formalism for Lie theory and operadic harmonic oscillator in low dimensions. 2009.

87. **Marko Piirsoo**. Deciphering molecular basis of Schwann cell development. 2009.

88. **Kati Helmja**. Determination of phenolic compounds and their antioxidative capability in plant extracts. 2010.

89. **Merike Sõmera**. Sobemoviruses: genomic organization, potential for recombination and necessity of P1 in systemic infection. 2010.

90. **Kristjan Laes**. Preparation and impedance spectroscopy of hybrid structures based on $CuIn_3Se_5$ photoabsorber. 2010.

91. **Kristin Lippur**. Asymmetric synthesis of 2,2'-bimorpholine and its 5,5'-substituted derivatives. 2010.

92. **Merike Luman**. Dialysis dose and nutrition assessment by an optical method. 2010.

93. **Mihhail Berezovski**. Numerical simulation of wave propagation in heterogeneous and microstructured materials. 2010.

94. **Tamara Aid-Pavlidis**. Structure and regulation of BDNF gene. 2010.

95. **Olga Bragina**. The role of Sonic Hedgehog pathway in neuro- and tumorigenesis. 2010.

96. **Merle Randrüüt**. Wave propagation in microstructured solids: solitary and periodic waves. 2010.

97. **Marju Laars**. Asymmetric organocatalytic Michael and aldol reactions mediated by cyclic amines. 2010.

98. **Maarja Grossberg**. Optical properties of multinary semiconductor compounds for photovoltaic applications. 2010.

99. **Alla Maloverjan**. Vertebrate homologues of Drosophila fused kinase and their role in Sonic Hedgehog signalling pathway. 2010.